Cross Species Identification of Genetic Factors that Determine Fruit Surface Characteristics

by

Justin Graham Lashbrooke

Dissertation presented for the degree of
Doctor of Philosophy (Science)

at
Stellenbosch University
Institute for Wine Biotechnology, Faculty of AgriSciences

Supervisor: Prof. Asaph Aharoni
Co-supervisor: Dr. Fabrizio Costa
Co-supervisor: Prof. Melané Vivier

December 2015

Declaration

By submitting this dissertation electronically, I declare that the entirety of the work contained therein is my own, original work, that I am the sole author thereof (save to the extent explicitly otherwise stated) that reproduction and publication thereof by Stellenbosch University will not infringe any third party rights and that I have not previously in its entirety or in part submitted it for obtaining any qualification.

Date: 03/09/15

Summary

The plant cuticle is a typically waxy layer that covers the entire above ground part of higher plants and performs a number of important roles in vegetative organs and during fruit development and ripening, including protection from a range of abiotic and biotic stresses. This complex hydrophobic layer consists of a cutin matrix of predominantly fatty acids embedded with long chain waxes, synthesized in (and secreted from) the epidermal cells. Suberin, an aliphatic polymer which is higher in phenolic content than cutin and less elastic, may be formed due to wounding and/or cuticle damage. While the synthesis and transport of cutin and wax have been investigated for a number of decades, there are still steps in these pathways that are yet to be elucidated. In the case of suberin biosynthesis, much less has been described. The understanding of the regulatory mechanisms for these processes has only recently received attention, and has already proven to be an area of significant interest for plant scientists, particularly with regard to the interaction between the regulation of epidermal cell identity and cuticle development. In terms of fruit production the cuticle can be linked to many quality parameters, especially postharvest storage. This is particularly true for apple, a crop dependent on a long shelf life. Apple is also susceptible to the formation of a cuticle failure disorder known as russet. Apple russet results from micro-cracking of the cuticle and the formation of a corky suberized layer. During normal growth suberin can be found in potato tubers, roots, bark, and seed coat. However, on most fruit, suberin is typically an undesirable consumer trait, and in the case of apples can have a negative impact on the postharvest storage.

In this work, the current understanding of plant cuticles is built upon with particular emphasis on fleshy fruit cuticle assembly and the regulation of the biosynthetic pathways generating its constituents. Research goals focused on identifying and characterizing genetic factors involved in fruit surface formation, particularly with regard to cuticle biosynthesis. Further attention is paid to understanding the regulatory mechanisms of cuticular pathways, including the emerging concept of co-regulation of epidermal cell differentiation and cuticle biosynthesis. Tomato and apple were the species in which these investigations were focused. This was due to the fact that tomato is seen as a model species for fruit surface biology research, while the applied aspects of apple surface research have far reaching impact.

To examine the relationship between epidermal cell development and cuticle assembly in the context of fruit surface the tomato *SlMIXTA-like* gene was investigated. MIXTA/MIXTA-like proteins, initially described in snapdragon petals, are regulators of epidermal cell differentiation. In an effort to understand these processes in fruit, tomato was transgenically silenced for *SlMIXTA-like* expression. Plants displayed defects in the patterning of conical epidermal cells of fruit, and also showed altered postharvest water loss and resistance to pathogens. Transcriptome and cuticular lipids profiling, coupled with comprehensive microscopy, revealed significant modifications to cuticle assembly and suggested SlMIXTA-like to regulate cutin biosynthesis. Candidate genes acting downstream of *SlMIXTA-like* included oxidases, transferases and transporters involved in cutin synthesis and assembly. As part of a larger regulatory network of epidermal cell patterning and L1-layer identity, it was found that SlMIXTA-like acts downstream of the cutin biosynthesis regulator SlSHN3 and possibly co-operates with homeodomain-leucine zipper IV transcription factors. Hence, SlMIXTA-like is a positive regulator of both cuticle and conical epidermal cell formation in tomato fruit, acting as a mediator of the tight association between fruit cutin polymer formation, cuticle assembly and epidermal cell patterning.

While russeting may occur in apples after cuticle damage, it is also a heritable trait, and therefore is to some extent under genetic control. In order to identify genetic factors controlling cuticle biosynthesis in apple (and thus preventing russet), a QTL-mapping survey was performed on a full-sib population. Two genomic regions located on chromosome 2 and 15 that could be associated with russeting were identified. Apples with compromised cuticles were identified through a novel and high throughput tensile analysis of the skin, while histological analysis confirmed cuticle failure in a subset of the progeny. Additional genomic investigation of the determined QTL regions identified a set of underlying genes involved in cuticle biosynthesis. Candidate gene expression profiling by qRT-PCR on a subset of the progeny highlighted the specific expression pattern of a *SHN1*/*WIN1* transcription factor (termed *MdSHN3*) on chromosome 15. The *MdSHN3* transcription factor displayed extremely low expression in lines with improper cuticle formation suggesting it to be a fundamental regulator of cuticle biosynthesis in apple fruit, and thus necessary for the prevention of suberized fruit surfaces (russet).

In an effort to gain a greater understanding of the mechanisms underlying suberin biosynthesis in fruit, and in plants in general, transgenic tomato were generated

with compromised cutin formation. This was achieved via the transcriptional silencing of *SlDCR*, an orthologue to *AtDCR* which was previously identified as a key step in cutin biosynthesis in *Arabidopsis*. Silencing of this BAHD acyltransferase resulted in an almost total elimination of the major monomer from the fruit cutin (C16-9,10-dihydroxy fatty acid), and the plants developed fruit with a suberized surface. This provided an excellent opportunity for transcriptome and chemical characterization of the suberization process in fleshy fruit. In parallel an apple clone that developed a russeted fruit surface was identified, and characterized. A large scale comparative transcriptomic analysis of these tomato and apple mutants was performed, generating a list of candidate genes for suberin deposition. Increasing the comparison to include data mined from literature resulted in the elucidation of a multi-species gene expression signature for suberin biosynthesis, and allowed for the identification and characterization of novel genetic elements, including those involved in the regulation of suberin formation and its deposition. Of these genetic elements, *MYB107*, was demonstrated to be a positive regulator of suberin accumulation in *Arabidopsis* seed coat.

In totality this study has produced a greater understanding of genetic mechanisms governing cuticle biosynthesis, particularly in developing fruit. This was achieved primarily through the functional characterization of regulatory elements (MIXTA-like, SHN3 and MYB107 transcription factors) controlling the synthesis of cutin and suberin matrices. Additionally the DCR enzyme was demonstrated to be a crucial step in fruit cutin biosynthesis. Finally the intricate relationship between epidermal cell development and cuticle biosynthesis has been further highlighted.

Opsomming

Die plant kutikula is 'n tipiese wasagtige laag wat die hele bogrondse deel van hoër plante dek en voer 'n aantal belangrike rolle in vegetatiewe organe en tydens die ontwikkeling en rypwording vrugte, insluitend die beskerming van 'n verskeidenheid van abiotiese en biotiese stres. Hierdie komplekse hidrofobiese laag bestaan uit 'n cutin matriks van oorwegend vetsure ingesluit met lang ketting wasse, gesintetiseer in (en afgeskei van) die epidermale selle. Suberien, 'n alifatiese polimeer wat hoër in fenoliese inhoud as cutin en minder elasties, kan gevorm word as gevolg van gewond en/of skade kutikula. Terwyl die sintese en vervoer van cutin en was reeds ondersoek vir 'n aantal dekades, is daar nog stappe in hierdie paaie wat nog beantwoord word. In die geval van suberien biosintese, veel minder is al beskryf. Die begrip van die regulerende meganismes vir hierdie prosesse het eers onlangs ontvang aandag en het reeds bewys dat 'n oppervlakte van beduidende belang vir plant wetenskaplikes, veral met betrekking tot die interaksie tussen die regulering van epidermale sel identiteit en kutikula ontwikkeling. In terme van die vrugte produksie kan die kutikula gekoppel word aan baie kwaliteit parameters, veral na-oes stoor. Dit is veral waar vir appel, 'n gewas afhanklik van 'n lang raklewe. Apple is ook vatbaar vir die vorming van 'n kutikula mislukking siekte bekend as rooibruin. Apple rooibruin resultate van mikro-krake van die kutikula en die vorming van 'n Corky suberized laag. Gedurende normale groei suberien kan gevind word in moere, wortels, bas, en saadhuid. Maar op die meeste vrugte, suberien is tipies 'n ongewenste eienskap verbruiker, en in die geval van appels kan 'n negatiewe impak op die oes stoor het.

In hierdie werk, is die huidige begrip van plant cuticles gebou op met spesifieke klem op vlesige vrugte kutikula vergadering en die regulering van die biosintetiese weë genereer sy bestanddele. Navorsing doelwitte gefokus op die identifisering en karakterisering van genetiese faktore wat betrokke is in die vorming vrugte oppervlak, veral met betrekking tot kutikula biosintese. Verdere aandag word aan die begrip van die regulerende meganismes van kutikulêre paaie, insluitend die opkomende konsep van mede-regulering van epidermale seldifferensiasie en kutikula biosintese. Tamatie en appel was die spesies in wat hierdie ondersoeke is gefokus. Dit was as gevolg van die feit dat tamatie is gesien as 'n model vir spesie vrugte oppervlak biologie navorsing, terwyl die toegepaste aspekte van appel oppervlak navorsing verreikende impak.

Om die verhouding tussen epidermale sel ontwikkeling en kutikula vergadering in die konteks van die vrugte te ondersoek oppervlak die tamatie *SlMIXTA-like* gene ondersoek. MIXTA/MIXTA-like proteïene, aanvanklik beskryf in leeubekkies kroonblare, is reguleerders van epidermale seldifferensiasie. In 'n poging om hierdie prosesse in vrugte te verstaan, was tamatie transgenically stilgemaak vir *SlMIXTA-like* uitdrukking. Plante vertoon gebreke in die patroon van koniese epidermisselle van die vrugte, en het ook getoon veranderde oes water verlies en weerstand teen patogene. Transkriptoom en kutikulêre lipiede profilering, tesame met 'n omvattende mikroskopie, geopenbaar beduidende veranderinge aan die gemeente kutikula en voorgestel SlMIXTA-like om cutin biosintese reguleer. Kandidaat gene optree stroomaf van *SlMIXTA-like* ingesluit oxidases, transferases en karweiers betrokke in cutin sintese en die gemeente. As deel van 'n groter netwerk van regulerende epidermale sel patrone en L1-laag identiteit, is daar gevind dat SlMIXTA-like handelinge stroomaf van die cutin biosintese reguleerder SlSHN3 en moontlik werk saam met homeodomain-leucine rits IV transkripsie faktore. Dus, SlMIXTA-like is 'n positiewe reguleerder van beide kutikula en koniese epidermale sel vorming in tamatie vrugte, wat as 'n bemiddelaar van die stywe assosiasie tussen vrugte cutin polimeer vorming, kutikula vergadering en epidermale sel patrone.

Terwyl skilverruwing mag voorkom in appels na kutikula skade, is dit ook 'n oorerflike eienskap, en daarom is tot 'n mate onder genetiese beheer. Ten einde genetiese faktore beheer kutikula biosintese in die appel (en dus die voorkoming van rooibruin) identifiseer, is 'n QTL-kartering opname uitgevoer op 'n full-sib bevolking. Twee genoom gebiede geleë op chromosoom 2 en 15 wat kan geassosieer word met skilverruwing is geïdentifiseer. Appels met verswakte cuticles is geïdentifiseer deur 'n roman en 'n hoë deurset trek ontleding van die vel, terwyl histologiese analise bevestig kutikula mislukking in 'n subset van die nageslag. Bykomende genomiese ondersoek van die bepaal QTL streke geïdentifiseer is 'n stel van onderliggende gene betrokke by kutikula biosintese. Kandidaat geenuitdrukking profiele deur QRT-PCR op 'n subset van die nageslag beklemtoon die spesifieke uitdrukking patroon van 'n *SHN1*/*WIN1* transkripsie faktor (genoem *MdSHN3*) op chromosoom 15. Die *MdSHN3* transkripsie faktor vertoon uiters lae uitdrukking in lyne met onbehoorlike kutikula vorming daarop dui dit 'n fundamentele reguleerder van kutikula biosintese in die appel vrugte, en dus nodig is vir die voorkoming van suberized vrugte oppervlaktes (rooibruin) wees.

In 'n poging om 'n beter begrip van die meganismes onderliggend suberien biosintese in vrugte te kry, en in plante in die algemeen, is transgeniese tamatie gegenereer met verswakte cutin vorming. Dit is bereik deur middel van die transkripsionele swye van *SlDCR*, 'n orthologue om *AtDCR* wat voorheen geïdentifiseer as 'n belangrike stap in cutin biosintese in *Arabidopsis*. Swye van hierdie BAHD acyltransferase gelei tot 'n byna totale uitwissing van die groot monomeer van die vrugte cutin (C16-9,10-dihydroxy vetsuur), en die plante ontwikkel vrugte met 'n suberized oppervlak. Dit verskaf 'n uitstekende geleentheid vir transkriptoom en chemiese karakterisering van die suberization proses vlesige vrugte. In parallel 'n appel kloon dat 'n russeted vrugte oppervlak ontwikkel is geïdentifiseer, en wat gekenmerk word. A groot skaal vergelykende transcriptomic ontleding van hierdie tamatie en appel mutante is uitgevoer, wat 'n lys van kandidaat gene vir suberien afsetting. Die verhoging van die vergelyking in te sluit data ontgin uit die literatuur het gelei tot die toeligting van 'n multi-spesie geenuitdrukking handtekening vir suberien biosintese en toegelaat word vir die identifisering en karakterisering van nuwe genetiese elemente, insluitend diegene wat betrokke is by die regulering van suberien vorming en sy afsetting. Van hierdie genetiese elemente, *MYB107*, is gedemonstreer om 'n positiewe reguleerder van suberien opeenhoping in Arabidopsis saadhuid wees.

In totaliteit het hierdie studie 'n groter begrip van genetiese meganismes regerende kutikula biosintese, veral in ontwikkelende vrugte geproduseer. Dit is bereik deur middel van die funksionele hoofsaaklik karakterisering van regulatoriese elemente (MIXTA-like, SHN3 en MYB107 transkripsie faktore) die beheer van die sintese van cutin en suberien matrikse. Daarbenewens is die DCR ensiem gedemonstreer belangrike stap in vrugte cutin biosintese wees. Ten slotte word die ingewikkelde verhouding tussen epidermale sel ontwikkeling en kutikula biosintese is verder uitgelig.

This thesis is dedicated to my uncle, James Alexander Corbet McGregor

Biographical Sketch

Justin Lashbrooke was born in 1983 in Cape Town, South Africa. He matriculated from Wynberg Boys' High School before beginning tertiary studies at Stellenbosch University. There he earned a Bachelor's degree in Science (B.Sc.), majoring in Microbial Biotechnology. Subsequently he began research on carotenoid metabolism in grapevine under the guidance of Dr. Philip Young and Prof. Melané Vivier. This work was performed at the Institute for Wine Biotechnology at Stellenbosch University, and led to the completion of an M.Sc. in Wine Biotechnology in March 2010. In October, later that year, he left South Africa and began a Ph.D. under the collaborative guidance of Prof. Asaph Aharoni at the Weizmann Institute of Science (Israel) and Dr. Fabrizio Costa at Fondazione Edmund Mach (FEM, Italy). The work presented here was performed during the next five years as part of that collaboration.

Acknowledgements

The last five years have been a truly life changing period and one that I shall always cherish. The experience would not have been possible without the many people who assisted me, not only academically, but also during my stay in Israel and Italy. The friendships and memories I have made will last a life time, while my academic growth over this period is unquantifiable. I wish to thank all of you who opened up your hearts and lives to me during my time in your lab, your country or your home. Because of the huge number of people who have touched my life over the last five years I apologize for anybody whom I have left out, this was certainly done without intention.

Firstly, to my parents, who without requiring very much explanation have unconditionally supported me as I plunged deeper and deeper into an academic career. Mum and Dad, I am so grateful for all the love and all the opportunities you have given me. All the sacrifice and all the kindness and all the little things and the not so little things you have done that have led me to this place. It's impossible to quantify, but I will always be endlessly thankful. I love you so very much. It was particularly special having you to visit in Israel and Italy. Showing you around, travelling together and sharing my life a little with you was wonderful!

To my supervisors, who guided me through this work. Melané, thank you for listening (and caring) about my desire to travel, and then sending me off on this amazing journey. You have introduced me to a world that I absolutely love, and I will be eternally grateful. Although we didn't work together as much as we hoped, I am sure we will have many opportunities to collaborate in the future. Asaph, arriving in Israel, and more specifically your lab was a radical change for me, but such a wonderful change. Your never ending passion for science is inspirational, and something I hope, at least to some degree, to emulate. The stimulating and hard working environment you have created made for a very productive time full of fascinating work and people. I will remember fondly your enthusiasm and excitement when I showed you a new result, and the time spent with you looking through endless lists of genes spotting the interesting ones. Thank you for all the opportunities and experiences I had in your lab. It was a time I shall not forget, and will forever impact the way I approach science. Fabrizio, you welcomed me to another strange new world, first in the refurbished cow sheds, and then in the "Palace". Thank you for providing calm and level headed thinking

to an over excited student. You successfully imparted the value of long term thinking and helped me to visualise a completed thesis with a coherent story. Your dedication and hard work have been a wonderful example to me. Thank you for all your efforts and time you have invested in me over the last few years.

To my lab colleagues, who have enriched my days, taught me so many new things and inspired me to keep on pushing. There are so many of you! Avital, when I first arrived in Israel you met me at airport, and drove me in to work, and began introducing me to cuticle biology. This work owes so much to those first few months of supervision, and I am extremely grateful for your efforts. Sagit, without you Asaph's lab would be a sadder place. The warmth, care and thought you show, especially for the foreign students, is remarkable. I know I am not alone in feeling incredibly lucky to have you looking after me during my stay. Thank you so much. Louise, Shelly, Prashant, Sergey, Illana, Max, Dario, Pablo, Pathy, Terry and the rest who made every day a pleasure to go to work.

And my new friends, I hope we'll see each other soon. Maybe it's time for a trip to South Africa? Maor, how many discussions about absolutely everything did we have over a beer and a cigarette after work? We must have solved all the world's problems many times over. I will always remember Florentine fondly. Sam, Guy, Oren, and Salva the last few years in Tel Aviv would have been so empty without you - so many adventures and good times! Alex, what a great partner in all things sport related. Finding a mate like you is really special, thanks for all the jols. Dan, your support and guidance when I felt like things were falling apart was so needed. Thank you so much for everything. Laura, Jaap, Pana, thanks for all the fun times shared in Trento. We must have explored every pub there! Antonio, Chida, my flat mates at various times, thanks for putting up with me. Oshry, Tali, Uwe, Lee, Rebecca, Nir, Elisabeta, Anjte, Alessandro, Tomas, Nada, Marco and Sara thanks for the friendship and good times. You made my life outside the lab a very happy time. Then, my mates from South Africa, who came to visit me during my travels. It was so good to have a bit of home come and find me. Sloth, Bob, Rich, Champ, Mosey, Smith, Jens and Gunther, thanks guys so much. Your visits were just a refreshing change and exactly what I needed.

To my family, both back home in South Africa and my extended English family. What a pleasure it was to come home to all the love and interest after being away. Your support and encouragement has been amazing. Bruce, Menna, Anna, Luca, Kit, Sam and

the rest of the Peckham team, thanks so much for having me to stay at Talfourd Road so easily during my stay in Europe. It was so wonderful to have a place nearby to be able to visit and to be able to call home.

And to my sweet Manu. Your support and love these last few months as I battle to complete everything has been amazing and I'm so grateful. But even more than that has been your love these past few years. So many wonderful memories of moments shared in Italy, Israel and now South Africa. I love you so much. I'm so lucky to have you in my life and I can't wait for our next chapter together.

Finally to the institutions who provided financial support for me to perform this research. The Foundazione Edmund Mach who granted me a fellowship for the majority of my PhD studies. And the Aharoni and Vivier labs which supported me after this fellowship expired. Further specific funding agencies connected to the various sections of the thesis are highlighted in each chapter.

Preface

This dissertation is presented as a compilation of six separate chapters. Chapters 1 and 6 introduce and summarize, respectively, the overall themes and findings of the entire thesis. The remaining chapters form the bulk of the thesis and comprise of a literature review (Chapter 2) and the results of the research performed (Chapters 3 to 5). These chapters have been submitted to, or published in, various scientific journals. They are presented here in the style and format of the corresponding journal, and each can be seen as a separately introduced, self-contained work.

Chapter 1 **General Introduction and Research Aims**

Chapter 2 **Literature Review**
Scratching the Surface of Fleshy Fruit: The Biosynthesis, Assembly, Regulation and Role of the Cuticular Layer

Chapter 3 **Research Results**
The Tomato *MIXTA-like* Transcription Factor Coordinates Fruit Epidermis Conical Cell Development and Cuticular Lipid Biosynthesis and Assembly

Chapter 4 **Research Results**
Genome Investigation Suggests *MdSHN3*, an APETALA2-domain Transcription Factor, to be a Positive Regulator of Apple Fruit Cuticle Formation and an Inhibitor of Russet Development

Chapter 5 **Research Results**
MYB107 and MYB9 are Members of a Multi-species Clade of Transcription Factors Regulating Suberin Formation

Chapter 6 **General Discussion and Concluding Remarks**

Appendices **Supplemental Materials**

I hereby declare that I was the primary contributor with respect to the experimental design, data acquisition and analysis, and the writing of the multi-author manuscripts presented in the research chapters (Chapters 3, 4 and 5). My supervisors, Prof. Asaph Aharoni and Dr Fabrizio Costa were involved in the conceptual design of the research presented in Chapter 3 and 5, and Chapter 4 respectively. Secondary authors of the manuscripts presented in Chapter 3 and 5 acquired specific experimental data. Where relevant, any technical assistance is acknowledged in the specific research chapters.

Contents

Chapter 1

General Introduction and Research Aims

This chapter serves to broadly introduce the themes covered in this thesis, as well as to outline the aims of the research undertaken. In an effort to maintain consistency, the chapter is written in the style of *Journal of Experimental Botany*.

1.1 Introduction

Many of the surface features of land plants have their origins about 450 million years ago during the colonisation of terrestrial environments by the aquatic ancestors of modern plants. The formation of specialised epidermal cells and a waxy waterproofing layer, named the plant cuticle, allowed early land plants to survive in the relatively dry atmosphere (Riederer and Schreiber, 2001). This has resulted in a huge variety of specialised epidermal cells such as trichomes and stomata existing across plant species and their organs. Many of these cells are involved in the regulation of transpiration, or contribute to pathogen defence, amongst other roles. The plant cuticle also shows significant diversity amongst species and organs, but can generally be described as a lipophilic layer that covers all aerial plant surfaces and regulates water movement into, and out of, the plant (Pollard *et al.*, 2008; Riederer and Schreiber, 2001; Schreiber, 2010). The importance of the cuticle is evidenced by its ubiquitous presence in all living land plants, from bryophytes to angiosperms, and has been argued as being one of the most important adaptations of terrestrial evolution (Martin and Rose, 2014). While chiefly responsible for plant water-proofing, as the plant's outermost layer, the cuticle is also the primary interaction point for the plant and its environment. This has resulted in a number of adaptations to minimise other abiotic and biotic stresses, such as the incorporation of metabolites with anti-microbial and anti-oxidant properties (Adato *et al.*, 2009; Brendolise *et al.*, 2011; Domínguez *et al.*, 2011; Domínguez *et al.*, 2009; Mintz-Oron *et al.*, 2008). Finally the cuticle also provides mechanical support to developing plant organs and prevents organ fusions. While the composition of the cuticle varies from species to species and organ to organ, it is typically comprised of an ester bonded matrix of fatty acids embedded with unbound waxes (Kolattukudy, 2001). These components are synthesised in, and secreted from, the epidermal cells. Due to the evolutionary and physical connections between the plant epidermal layer and the cuticle their developmental and regulatory mechanisms are intrinsically linked and represent an increasingly interesting avenue of study (Oshima *et al.*, 2013; Shi *et al.*, 2013).

1.2 Fruit Surface

The surface structure plays a major role in the development of fleshy fruit and the maintenance of the fruit quality properties. In addition, it is essential for fruit

postharvest management, impacting shelf life, storage and transport. The majority of these features are determined by the fruit cuticle. The cuticle of developing fleshy fruit not only regulates water movement, but is adapted to maintain its integrity coping with the increase in turgor pressure during fruit development and expansion (Domínguez *et al.*, 2011; Domínguez *et al.*, 2012). It therefore is a significant contributor to the structural support of the fruit. The fruit cuticle also plays a substantial role in protection of the fruit from environmental stresses, both biotic and abiotic (Adato *et al.*, 2009; Mintz-Oron *et al.*, 2008), impacting quality and fruit loss during agricultural production. Further, the fruit cuticle, together with various epidermal cell morphologies, influences the attraction of agents of seed dispersal (Martin and Glover, 2007). The cuticle can therefore be seen as a feature of the plant that is of both fundamental interest and also critically important to agricultural practices and productivity.

While a number of the steps in the biosynthesis of the plant cuticle have been elucidated, the majority of this work has been performed in non-fruit species (Franke *et al.*, 2005; Pollard *et al.*, 2008; Schreiber, 2010). However, working with fruit species has a number of advantages, including having more relevance to the fruit agricultural industry, fruit cuticles are thicker and more easily isolated than cuticle from other organs. Due to the availability of a high quality annotated tomato genome and the relative ease with which transgenic tomato can be generated, tomato is increasingly becoming the model of choice for cuticle research (Adato *et al.*, 2009; Isaacson *et al.*, 2009; Shi *et al.*, 2013; Wang *et al.*, 2011; Yeats *et al.*, 2012). Noteworthy gaps in our understanding of cuticle biosynthesis include the transport of monomers to the cell membrane, and the polymerisation of the matrix, while we are only beginning to understand the regulatory mechanisms controlling fruit cuticle deposition (Isaacson *et al.*, 2009; Shi *et al.*, 2013). Other economically important fruit species including apple and grape have received considerably less attention with regard to the functional characterisation of genes involved in determining fruit surface characteristics. This is largely due to the fact that they are inherently less amenable to these types of study due to long life cycles and lack of functional genomic tools. However, interesting work making use of classical genetic approaches and large-scale transcriptomic analyses is increasingly possible in these species. Further, the direct impact of the cuticle on fruit quality in apple and grape makes understanding its formation in these species highly relevant.

1.3 Research Rationale and Aims

The broad aim of this study was to identify and characterise novel genetic factors that influence the formation and morphology of fruit surface. Elucidation of these processes is not only fundamentally interesting but can and does impact applied aspects of fruit production. Of particular interest were factors conserved across multiple species, which can be considered central to these processes in general. As the cuticle can be considered a major contributor to fruit quality this aspect was the primary focus, however the relationship between cuticle formation and epidermal cell development was also investigated. In this regard the MIXTA/MIXTA-like family has been previously identified as an interesting clade potentially involved in this regulatory network (Brockington *et al.*, 2013; Mintz-Oron *et al.*, 2008; Noda *et al.*, 1994). This family of transcription factors are known regulators of epidermal cell differentiation in a variety of plant species, but their role in fleshy fruit formation has not been investigated. *How does this gene family influence epidermal development and cuticle biosynthesis in fruit?* With regard to cuticle formation in fruit, one of the major commercial fruit crops affected by cuticle performance is apple. But there is very little knowledge specifically relating to cuticle biosynthesis in apple. *What are the crucial genetic factors underlying cuticle formation in apple?* One of the more striking defects caused by cuticle failure in apple is the formation of russet, a corky suberized surface. Suberization however is not limited to apple and is present as a wounding response in many fleshy fruits. *What genetic mechanisms are at work during suberin formation in fruit?*

As highlighted earlier, tomato provides a very useful model for fruit surface research. By making use of the ever increasing suite of functional genomic tools available to researchers, characterisation of specific genes is possible. Due to recent results suggesting the involvement of a tomato *MIXTA-like* gene in fruit cuticle formation (Mintz-Oron *et al.*, 2008; Shi *et al.*, 2013) this gene was selected as a candidate for further study. In addition, significant attention was also given to factors affecting apple fruit surface formation. This was made possible by the existence of a large collection of apple cultivars (including those displaying russet), as well an apple cross population showing a variety of surface phenotypes, growing in the experimental orchard of the Foundazione Edmund Mach (Northern Italy). Finally, the increase in availability, and use of, large scale transcriptomic techniques allows for this type of analysis to be performed in order to promote novel gene discovery. In order to answer

the research questions posed, while keeping in mind the resources available, the following specific research objectives were defined:

i. Identify and characterize a *MIXTA*/*MIXTA-like* gene from tomato. Create transgenic tomato lines silenced for *SlMIXTA-like* expression. Analyse tomato fruit from these lines particularly in regard to epidermal cell differentiation and cuticle formation via a variety of transcriptomic, molecular, chemical and cytological methods.

ii. Quantify the fruit cuticle performance for an apple population showing a variety of surface phenotypes and perform a QTL-mapping survey. Confirm potential involvement of candidate genes via phylogenetic and expression analysis.

iii. Perform parallel large scale transcriptomic analysis of tomato and apple fruit displaying a suberized surface, and perform a comparative genomic analysis in order to identify conserved candidates. Perform relevant functional characterisation of identified candidates.

1.4 References

Adato A, Mandel T, Mintz-Oron S, Venger I, Levy D, Yativ M, Domínguez E, Wang Z, De Vos RC, Jetter R, Schreiber L, Heredia A, Rogachev I, Aharoni A. 2009. Fruit-surface flavonoid accumulation in tomato is controlled by a SlMYB12-regulated transcriptional network. PLoS Genet **5**, 823-851.

Brendolise C, Yauk YK, Eberhard ED, Wang M, Chagne D, Andre C, Greenwood DR, Beuning LL. 2011. An unusual plant triterpene synthase with predominant α-amyrin-producing activity identified by characterizing oxidosqualene cyclases from Malus × domestica. FEBS J **278**, 2485-2499.

Brockington SF, Alvarez-Fernandez R, Landis JB, Alcorn K, Walker RH, Thomas MM, Hileman LC, Glover BJ. 2013. Evolutionary analysis of the MIXTA gene family highlights potential targets for the study of cellular differentiation. Mol Biol Evol **30**, 526-540.

Domínguez E, Cuartero J, Heredia A. 2011. An overview on plant cuticle biomechanics. Plant Sci **181**, 77-84.

Domínguez E, Fernández MD, Hernández JC, Parra JP, España L, Heredia A, Cuartero J. 2012. Tomato fruit continues growing while ripening, affecting cuticle properties and cracking. Physiol Plant **146**, 473-486.

Domínguez E, Luque P, Heredia A. 2009. Sorption and interaction of the flavonoid naringenin on tomato fruit cuticles. J Agric Food Chem **57**, 7560-7564.

Franke R, Briesen I, Wojciechowski T, Faust A, Yephremov A, Nawrath C, Schreiber L. 2005. Apoplastic polyesters in Arabidopsis surface tissues--a typical suberin and a particular cutin. Phytochemistry **66**, 2643-2658.

Isaacson T, Kosma DK, Matas AJ, Buda GJ, He Y, Yu B, Pravitasari A, Batteas JD, Stark RE, Jenks MA, Rose JK. 2009. Cutin deficiency in the tomato fruit cuticle consistently affects resistance to microbial infection and biomechanical properties, but not transpirational water loss. Plant J **60**, 363-377.

Kolattukudy PE. 2001. Polyesters in higher plants. Adv Biochem Eng Biotechnol **71**, 1-49.

Martin C, Glover BJ. 2007. Functional aspects of cell patterning in aerial epidermis. Curr Opin Plant Biol **10**, 70-82.

Martin LB, Rose JK. 2014. There's more than one way to skin a fruit: formation and functions of fruit cuticles. J Exp Bot **65**, 4639-4651.

Mintz-Oron S, Mandel T, Rogachev I, Feldberg L, Lotan O, Yativ M, Wang Z, Jetter R, Venger I, Adato A, Aharoni A. 2008. Gene expression and metabolism in tomato fruit surface tissues. Plant Physiol **147**, 823-851.

Noda K, Glover BJ, Linstead P, Martin C. 1994. Flower colour intensity depends on specialized cell shape controlled by a Myb-related transcription factor. Nature **369**, 661-664.

Oshima Y, Shikata M, Koyama T, Ohtsubo N, Mitsuda N, Ohme-Takagi M. 2013. MIXTA-like transcription factors and WAX INDUCER1/SHINE1 coordinately regulate cuticle development in Arabidopsis and Torenia fournieri. Plant Cell **25**, 1609-1624.

Pollard M, Beisson F, Li Y, Ohlrogge JB. 2008. Building lipid barriers: biosynthesis of cutin and suberin. Trends Plant Sci **13**, 236-246.

Riederer M, Schreiber L. 2001. Protecting against water loss: analysis of the barrier properties of plant cuticles. J Exp Bot **52**, 2023-2032.

Schreiber L. 2010. Transport barriers made of cutin, suberin and associated waxes. Trends Plant Sci **15**, 546-553.

Shi JX, Adato A, Alkan N, He Y, Lashbrooke J, Matas AJ, Meir S, Malitsky S, Isaacson T, Prusky D, Leshkowitz D, Schreiber L, Granell AR, Widemann E, Grausem B, Pinot F, Rose JK, Rogachev I, Rothan C, Aharoni A. 2013. The tomato SlSHINE3 transcription factor regulates fruit cuticle formation and epidermal patterning. New Phytol **197**, 468-480.

Wang Z, Guhling O, Yao R, Li F, Yeats TH, Rose JK, Jetter R. 2011. Two oxidosqualene cyclases responsible for biosynthesis of tomato fruit cuticular triterpenoids. Plant Physiol **155**, 540-552.

Yeats T, Martin L, Viart H, Isaacson T, He Y, Zhao L, Matas A, Buda G, Domozych D, Clausen M, Rose J. 2012. The identification of cutin synthase: formation of the plant polyester cutin. Nature Chemical Biology **8**, 609-611.

Chapter 2

Literature Review

Scratching the Surface of Fleshy Fruit: The Biosynthesis, Assembly, Regulation and Role of the Cuticular Layer

This chapter has been compiled from two published manuscripts referenced below, and has been rewritten in the style of *Journal of Experimental Botany.*

Lashbrooke J, Costa F, Aharoni A (2014) Making the Surface of Fleshy Fruit: Biosynthesis, Assembly, and Role of the Cuticular Layer. In Nath P *et al* (eds.) *Fruit Ripening: Physiology, Signalling and Genomics*. Oxfordshire, UK: CABI, 81-98.

Hen-Avivi S*, Lashbrooke J*, Costa F, Aharoni A (2014) Scratching the Surface: Genetic Regulation of Cuticle Assembly in Fleshy Fruit. *Journal of Experimental Botany*, 65, 4653-4664.

*These authors contributed equally to this work

2.1 Introduction

The colonization of terrestrial environments by aquatic plants occurred approximately 450 million years ago, resulting in a number of challenges to plant survival including desiccation, increased temperature changes, and UV radiation (Bargel *et al.*, 2006; McCourt *et al.*, 2004). Evolution of a lipophilic layer covering all aerial plant parts allowed land plants to successfully overcome these new challenges. This lipophilic layer is known as the cuticular membrane or the cuticle and can be considered a major driving force towards terrestrial colonization by plants. During recent decades, intensive study has illuminated the complex network underpinning the processes associated with cuticle biosynthesis, regulation, and trafficking of its building blocks.

Briefly, the cuticular layer is a continuous hydrophobic structure, composed predominantly of two components, namely, cutin, a covalently linked macromolecular scaffold of long chain fatty acids; and wax, very long chain fatty acids and their derivatives (Kunst and Samuels, 2003; Pollard *et al.*, 2008; Samuels *et al.*, 2008; Yeats and Rose, 2013). The unpolymerized waxes are embedded in, and deposited on top of the cutin matrix which in turn is connected to the polysaccharides of the outer cell wall of the underlying epidermal cells (López-Casado *et al.*, 2007). Further, the cuticular membrane from different species and different organs may contain additional metabolites such as flavonoids and sterols (Domínguez *et al.*, 2011; Kunst and Samuels, 2003). A wide variety of cuticle structures can be found throughout the plant kingdom, which can be attributed to differences in monomer composition of the cutin and waxes as well as the inclusion of a number of secondary metabolites. All the cuticle components and building blocks are produced and secreted by the epidermal cells (Kunst and Samuels, 2003; Yeats and Rose, 2013).

As the primary barrier between the relatively dry atmosphere and the aerial parts of higher plants the cuticle can be considered as an interface between the plant and its environment. Due to the varied nature of the aerial organs found in higher plants including stems, leaves, flowers, fruits and seeds the specific function of the cuticle (as well as the structure) is relatively diverse. Typically the cuticle provides a waterproof barrier between the epidermal cells and the environment and regulates gaseous exchange. It also provides resistance against biotic and abiotic stresses such as mechanical damage caused by microorganisms and damaging UV light (Bargel *et al.*, 2006). Additionally the cuticle provides mechanical support to the plant organ and acts

as a division to prevent, or in some cases promote, the fusion of plant organs during development. Being the outermost part of the plant, the cuticle can be regarded as a detector for environmental changes and plays a role in transmitting signals to the interior of the plant (Curvers *et al*., 2010). More recently, a broader picture has emerged, as cuticle formation is understood to be tightly linked with fundamental cell developmental processes, such as organ development and cell patterning (Javelle *et al.*, 2011; Neinhuis and Barthlott, 1997; Reina-Pinto and Yephremov, 2009; Riederer and Muller, 2006; Shi *et al.*, 2013). Fleshy fruit cuticles must be specifically adapted to protect and prevent dehydration of the fruit during development and rapid fruit expansion. The cuticle must therefore be sufficiently elastic and strong enough to cope with the high forces exerted upon it as the fruit expands (Domínguez *et al*., 2012).

As for many fields of plant research, much of the work on cuticle biology has been performed in *Arabidopsis* (Nawrath, 2006; Pollard *et al.*, 2008; Samuels *et al.*, 2008). In retrospect, this may have not been the most representative model as the cutin in green tissue of *Arabidopsis* is comprised in excess of 50% dicarboxylic acids, while the majority of other plants contain less than 5% dicarboxylic acids in the cutin. However, it has been shown that *Arabidopsis* petals have a very similar cutin composition when compared to the cutin found in fleshy fruits. Specifically, both fleshy fruits and *Arabidopsis* flowers contain high levels of 10,16-dihydroxypalmitic acid (10,16-DHPA) (Li-Beisson *et al*., 2009). Other models commonly used include maize, which has been the model of choice in the study of wax composition during phase transition (Sturaro *et al*., 2005), and more recently tomato (*Solanum lycopersicum*) which is used as a model for the cuticle of fleshy fruit (Isaacson *et al*., 2009; Matas *et al*., 2011; Mintz-Oron *et al*., 2008). In contrast to *Arabidopsis*, tomato fruit offer a convenient and possibly more suitable system as the cuticle is relatively thick and stomataless, providing a continuous, easy to isolate surface (Figure 1) (Franke *et al.*, 2005; Vogg *et al.*, 2004). The short life cycle, simplicity of genetic transformation, and availability of a high quality genome sequence (Consortium, 2012) further entrench tomato as the model of choice for fruit cuticle studies. These studies are able to provide an insight to processes associated with crop quality and postharvest traits as cuticular characteristics have a major impact on physiology and quality of fleshy fruit. The surface influences the outward appearance of the fruit (color, glossiness, texture, and uniformity), efficacy of postharvest treatments, storage, transport, and shelf life (Domínguez *et al.*, 2011; Isaacson *et al.*, 2009; Saladié *et al.*, 2007). Hence, knowledge regarding the regulation of surface properties and, in

turn cuticle biosynthesis, is fundamental for the improvement of a number of fruit quality traits.

This chapter will describe the current understanding of the structure and assembly of the plant cuticle in general, with specific attention being paid to fleshy fruit specific aspects. Focus will be placed on the genes and enzymes implicated in the construction of the fleshy fruit cuticle and the mechanisms of regulation controlling this assembly.

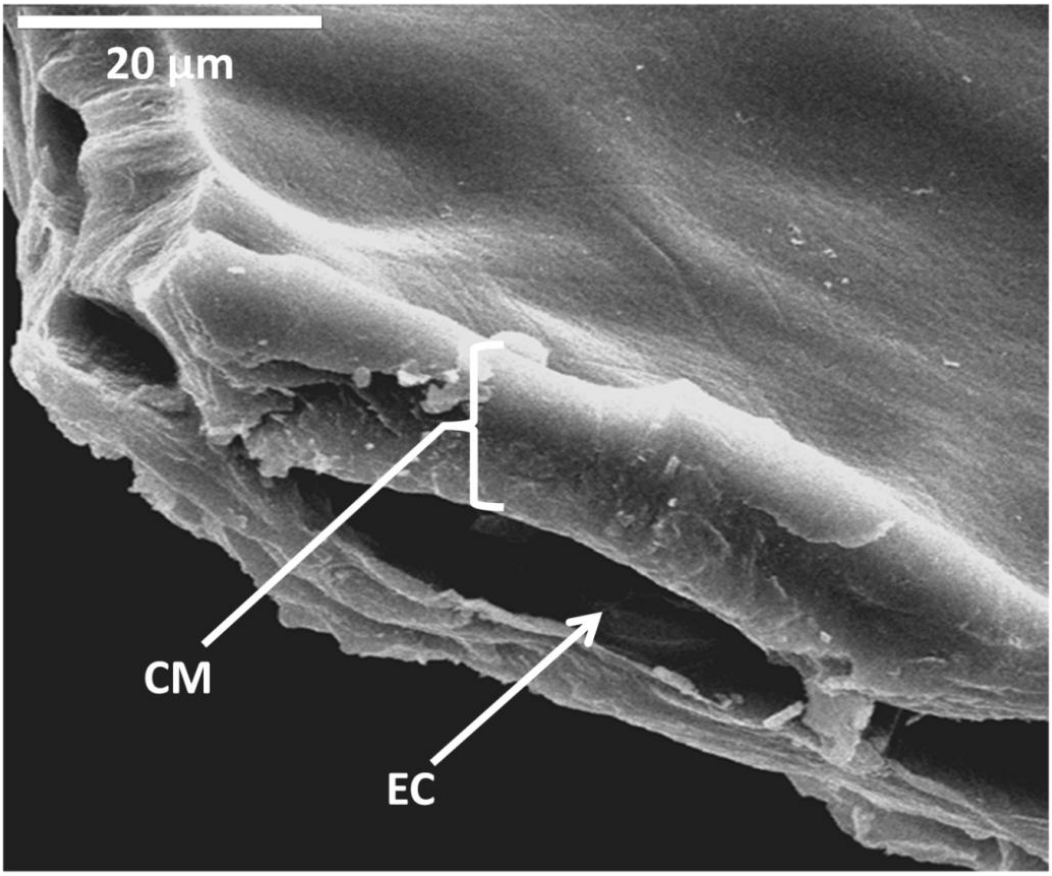

Figure 1. Scanning Electron Micrograph (SEM) of tomato fruit surface. A cross section of a ripe tomato peel (cv. *Ailsa Craig*), showing the thick cuticular membrane (CM) and an epidermal cell (EC).

2.2 Composition, Structure and Function of the Cuticle

2.2.1 General: Composition and Structure of the Cuticle

The structure and composition of the plant cuticle can vary widely between plant species, and between organs and developmental stages within a plant species. This is illustrated in the typical range of thickness (1 to 10 µm) and quantity (100 to 1000 $\mu g.cm^{-2}$) of the deposited cuticle (Riederer and Muller, 2006). The major components of

the plant cuticle are the cutin matrix and epicuticular and intracuticular waxes. In some species a non-hydrolysable polymer matrix named cutan may also be present (Pollard *et al*., 2008). The cutin is attached to the underlying epidermal cells while a thin layer of wax crystals cover the outermost surface of the cutinized layer. This hydrophobic epicuticular wax allows the plant to repel water and is thus important as a transpiration barrier. A cutinized cell wall is formed at the inner surface of the cutin where it is interconnected with the polysaccharides of the epidermal cell wall (López-Casado *et al*., 2007). The typical fatty acid monomers found in cutin are C16 and C18 *ω*-hydroxy fatty acids and glycerol. The cuticular waxes are comprised of very-long-chain saturated non-polar hydrocarbons (typically C20-C60) and their derivatives (alcohols, aldehydes, and alkanes) as well as secondary metabolites such as triterpenoids and phenylpropanoids (e.g. flavonoids) (Kunst and Samuels, 2003). The polysaccharides present in the cutin matrix are understood to be the major factor contributing to the elasticity of the matrix while the cutin provides the strength (Lopez-Casado *et al*., 2010; López-Casado *et al*., 2007).

Transmission electron microscopy (TEM) has identified six different types of cuticle fine structures, but how this relates to the molecular structure of the cutin matrix is not yet known (Riederer and Muller, 2006). This lack of knowledge of the polymer structure makes the deciphering of cutin biosynthesis an interesting but complex task. The specific monomer composition of numerous species and organs is, however, well described. The fatty acid monomers of cutin are thought to be partially polymerized into di- or triacylglycerols, which are then transported to the exterior of the cell where further polymerization may occur (Panikashvili and Aharoni, 2008). Polymerization of the *ω*-hydroxy fatty acids then results in a linear polymer. However, depending on species and organ a large percentage (up to 90% in tomato) of the *ω*-hydroxy fatty acid monomers may contain mid-chain hydroxyls (Mintz-Oron *et al*., 2008), which allow for branching of the polymer via esterification of the hydroxyls to *ω*-hydroxy fatty acids. While the involvement of glycerol in the biosynthesis of the initial cutin oligomers is reported (Chen *et al*., 2011; Li *et al*., 2007), its contribution to the cutin polymer assembly is poorly understood. It is suggested that it may lead to further branch points in the polymer via increased cross linking and subsequently a larger cutin matrix. Additionally phenolics (such as ferulates which are found in low quantities in the cutin matrix) may be able to act as branching points for fatty acids, or to allow for cross

linking within the cutin polymer or to the polysaccharide and lignin components of the cell wall (Li *et al*., 2007; Pollard *et al*., 2008).

2.2.2 The Cuticle of Developing Fleshy Fruit

The cuticle of developing fleshy fruit is adapted to maintain its integrity while the fruit rapidly expands as well as to attract agents of seed dispersal. The structure of the fruit cuticle is therefore evolved to perform these roles and to be able to withstand both biotic and abiotic stresses (Domínguez *et al*., 2012). The function played by the cuticle to reduce water loss and maintain structural support for the fruit is illustrated in the tomato *dfd* (*delayed fruit deterioration*) mutant (Saladie *et al*., 2005). Cutin deposition in this mutant continues throughout fruit development which is in contrast to the typical deposition profile which shows significant reduction at the so called "breaker" stage of fruit development. This stage of development can be characterized by the first appearance of red pigments. Fruits of *dfd* mutants therefore have significantly more cutin than normal fruits at the ripening stage. These fruit have a dramatically longer shelf life than wild type fruit and show a reduction in fruit softening. Saladie *et al*. (2005) shows that transpirational water loss is reduced and that there is elevated cellular turgor in the fruits of *dfd* mutants. A combination of increased physical support provided by the thicker cuticle and reduced water loss likely contribute to the reduction in fruit softening (Saladie *et al*., 2005).

Not only is the cuticle able to maintain its integrity and cope with the increase in turgor pressure during fruit development and ripening, but it also plays a central role in protection of the fruit from external factors. Both biotic stresses (e.g. insects and fungi) and abiotic stresses [e.g. ultraviolet (UV) radiation] must be coped with. There are a number of specialized (i.e. secondary) metabolites found in the cuticle that contribute to the protection from environmental conditions and deter potential pathogens (Mintz-Oron *et al*., 2008). High light and temperature causes an increase in the concentration of reactive oxygen species in exposed tissue and these may result in oxidative damage to the fruit. Antioxidants are therefore important metabolites in the outer layer of the fruit to moderate the potential damage. The yellow flavonoid naringenin chalcone accumulates in the epidermal cells as well as the cuticular membrane of tomato fruit (Adato *et al*., 2009; Domínguez *et al*., 2009), where it likely protects against excessive UV radiation while also serving to attract agents of seed dispersal due to their intense pigmentation. Another group of specialized metabolites

found in the tomato cuticle are pentacyclic triterpenoids. While suggested to perform a structural role in the cuticle membrane, triterpenoids also possess anti-microbial properties and contribute to the defense against fungal pathogens (Brendolise *et al*., 2011; Wang *et al*., 2011a).

2.2.3 The Inner Fruit Epidermis Contains a Cuticular Layer

An inner epidermal layer (or endoderm) containing a cuticle-like structure was first suggested in the mid-twentieth century (Kraus, 1949), but was only recently described in tomato by Mintz-Oron *et al* (2008), and further characterized by Matas *et al* (2011). This internal cuticle covers the cells of the endocarp, separating the fleshy tissue pericarp from the locular region (i.e. the placental tissue, locular tissue and seeds). The cuticle is impermeable to water during the early stages of development, but as the fruit matures, the permeability increases (Matas *et al*., 2011). The inner epidermal cuticle possesses similar properties with regards to the thicker external cuticle, and according to expression analysis also shares common routes of biosynthesis. While a number of known cuticle biosynthesis genes are found to be expressed in the endodermal cell layer there are some noteworthy exceptions such as *CYP77A*, which encodes a protein catalyzing the mid-chain hydroxylation of fatty acids (Li-Beisson *et al*., 2009), and has a 40-fold lower expression in the endodermal layer (Matas *et al*., 2011). The differences observed in expression of biosynthesis genes are reflected in the structure of the inner epidermal cuticle, which, while being structurally similar to the outer cuticle, does show marked differences. Chemical analysis of the cutin monomer composition of the inner and outer layer of tomato found the same two dominant monomers (16-hydroxypalmitic acid and 10,16-DHPA). However, while in the outer cuticle 10,16-DHPA (a mid-chain fatty acid) was the most abundant monomer, the most abundant monomer in the inner cuticle was 16-hydroxypalmitic acid (lacking mid-chain hydroxylation).

2.3 Assembly of the Cutin Polymer

The precise mechanism of cutin polymer assembly and polymerization still remains largely undescribed, while the biosynthesis of the monomers/oligomers that form the building blocks of the polymer is far better described. Cutin polymer assembly can be divided into three parts: (1) monomer/oligomer biosynthesis, (2) extracellular transport,

and (3) polymerization (see Figure 2). The order of these reactions is not completely clear and it is likely that there is some degree of overlap between the processes.

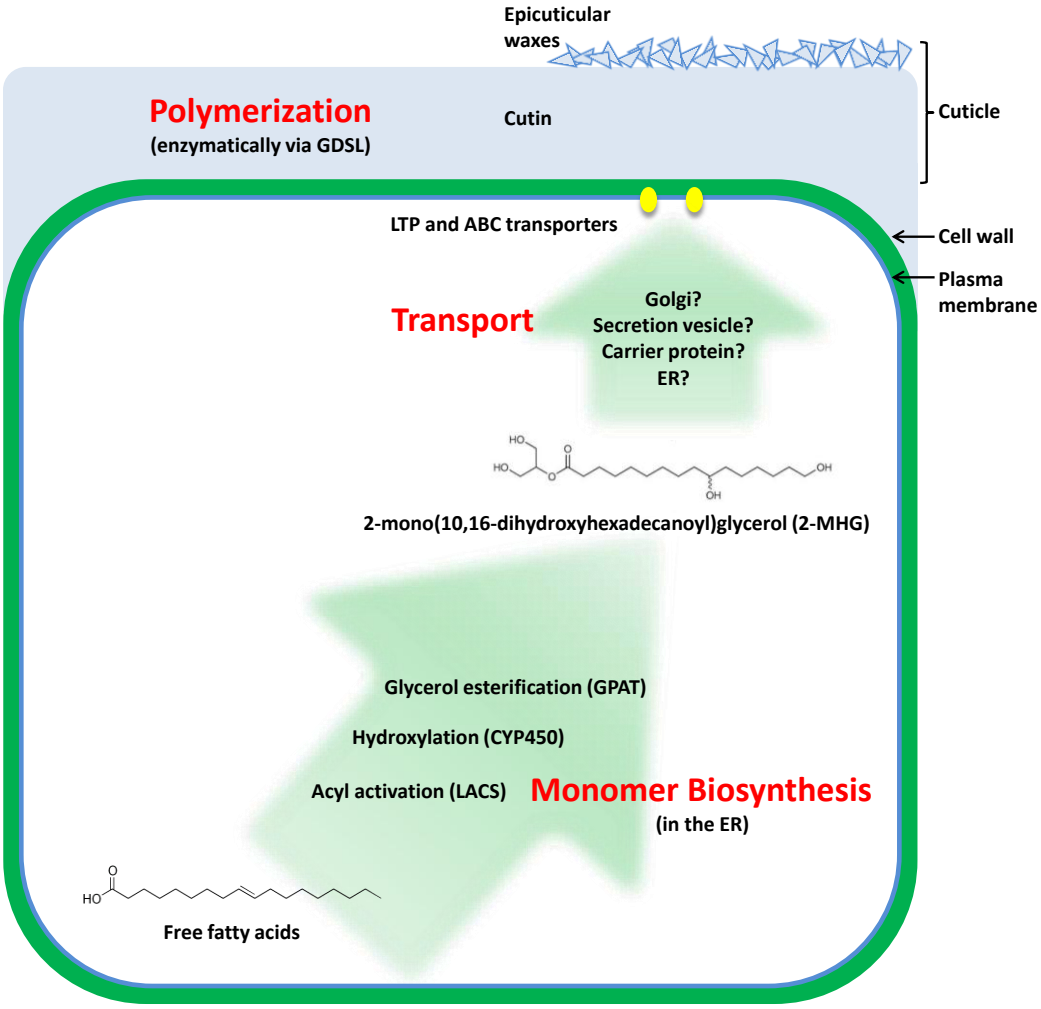

Figure 2. Schematic of proposed routes of cutin monomer and polymer biosynthesis in an epidermal plant cell. Enzymatic modifications of free fatty acids occur in the endoplasmic reticulum (ER) resulting in a variety of acylglycerols (here represented by 2-mono[10,16-dihydroxyhexadecanoyl]glycerol). Important genes in this process include long-chain acyl-CoA synthetases (LACS), cytochrome P450s (CYP450) and glycerol-3-phosphate-acyltransferases (GPAT). Acylglycerol oligomers are then transported to the exterior of the cell via ATP Binding Cassette (ABC) and Lipid Transfer Protein (LTP) transporters. It is possible that secretion vesicles and carrier proteins play additional roles in the extracellular transport of cutin. Cutin oligomers are further polymerised outside the cell by enzymes including GDSL-motif lipases.

The biosynthesis of the fatty acid monomers occurs in the plastids. Free fatty acids (FFAs) (mostly C16 and 18) undergo three major reactions on their way to incorporation into *ω*-hydroxy acylglycerols, namely, oxidation, acyl activation and acyltransferase (Chen *et al*., 2011; Li-Beisson *et al*., 2009; Tang *et al*., 2007). The sequence of these reactions is yet to be determined; however, individual knockouts in *Arabidopsis* of the genes involved in these processes results in significantly reduced

biosynthesis of acylglycerols. A possible candidate for the first reaction is the acyl activation of the FFAs through a member of the long-chain acyl-CoA synthetase (LACS) family (Bessire *et al*., 2007; Schnurr *et al*., 2004). Metabolism of acyl-CoAs may then lead to a variety of pathways such as membrane lipid biosynthesis, storage lipid biosynthesis, cuticular wax and cutin biosynthesis. Acyl-CoAs destined for cutin biosynthesis will undergo oxidation by members of the cytochrome P450 (CYP450) family (the CYP86A and CYP77A subfamilies) and transfer of the acyl chains to a glycerol-based acceptor mediated by glycerol-3-phosphate:acyl-CoA *sn*-1 acyltransferase (GPAT) (Li *et al*., 2007; Li-Beisson *et al*., 2009; Shi *et al*., 2011). CYP86 family members and CYP77A6 have been shown to be responsible for ω-hydroxylase and mid-chain hydroxylase activity, respectively. It is not known if the substrate for the P450 *ω*-hydroxylases are acyl-CoAs or acylglycerol moieties or even the non-acyl activated FFA. While P450s have been shown to act on FFAs *in vitro* this does not exclude their action on acyl-CoAs and/or acylglycerols. The P450s are not the only enzymes to be able to act on FFAs as in the case of the LACSs, which have demonstrated activity on both normal and *ω*-hydroxy FFAs. It is surely too early to assume we fully understand the metabolic pathway(s) leading to *ω*-oxidized acylglycerols.

Regardless of the order of the reactions, the resultant *ω*-hydroxy acylglycerol molecules are considered the putative structural element of lipid polymers. However, the extracellular transportation of these molecules and their subsequent polymerization raises further questions. Analysis of *Arabidopsis* mutants revealed the major role of a BAHD acyl transferase in cutin formation (Panikashvili *et al*., 2009). DCR (DEFECTIVE IN CUTICULAR RIDGES), was suggested to be required for the incorporation of 10,16-DHPA into cutin. This mid-chain *ω*-hydroxy fatty acid is the major monomer of cutin in both *Arabidopsis* flowers and the fruit of species such as tomato (Mintz-Oron *et al*., 2008), cherry (Peschel *et al*., 2007) and gooseberry (Kolattukudy, 2001). DCR mutants in *Arabidopsis* displayed almost undetectable levels of 10,16-DHPA in their flowers and leaves, and were susceptible to salinity, osmotic, and water deprivation stress (Panikashvili *et al*., 2009). DCR seems likely to carry out partial polymerization of the cutin monomers. Some possible mechanisms of action for DCR have been suggested: (i) it may catalyze the acylation of aromatics or hydroxy fatty acids with the CoA of 10,16-DHPA or (ii) the acylation of cutin dimers or trimers using aromatic or aliphatic CoAs or the CoA of 10,16-DHPA (Panikashvili *et al*., 2009; Rani *et al*., 2010). These reactions could result in linear and branched chains of 10,16-DHPA. Panikashvili *et al*. (2010)

localized the DCR protein to the cytosol suggesting that polymerization of cutin commences inside the cell.

While partial polymerization seems to occur in the cell, the extent of this polymerization is yet to be determined. The degree of intracellular polymerization will have a direct effect on the extracellular transport, and the mechanisms capable of this process. The waxes embedded in the cutin matrix have been shown to be transported to the apoplast by ATP-dependent ATP-binding cassette (ABC) transporters (Bird *et al*., 2007; Panikashvili and Aharoni, 2008). However, the strict substrates of these transporters are yet to be discovered. Of particular interest is the level of cutin polymerization that occurs before transport and therefore what degree of oligomerized cutin is accepted by ABC transporters. If monomers are exclusively transported out of the cell the entire cutin matrix must be polymerized extracellularly. It is likely that there are multiple routes for extracellular transport depending on the specific monomer or the degree of intracellular polymerization. Highly polymerized molecules would likely require transport via vesicles. Studies in *Arabidopsis* have showed that ABC transporters are at least partially responsible for cutin and wax monomer transport (Bessire *et al*., 2011; Bird *et al*., 2007; Panikashvili and Aharoni, 2008; Panikashvili *et al*., 2007; Panikashvili *et al*., 2011; Pighin *et al*., 2004).

One such ABC transporter that was characterized by Panikashvili *et al*. (2011) is ABCG13. *Arabidopsis* mutants for *abcg13* showed flower specific phenotypes including fusion of flower organs and abnormal epidermal cell development (Panikashvili *et al*., 2011). These phenotypes are likely the result of the significant reduction in cutin seen in *abcg13* flowers. The first ABC transporter characterized for wax transport was ECERIFERUM5 (CER5) (Pighin *et al*., 2004). *Arabidopsis cer5* mutants showed a reduced deposition of stem cuticular wax. Electron microscope analysis found that wax inclusions had formed in the cytoplasm of the epidermal cells, indication wax biosynthesis was normal, but the extracellular transport was defective. The CER5 gene was found to encode an ABC transporter (ABCG12) specific for wax monomers (Pighin *et al*., 2004).

Arabidopsis ABCG11 and ABCG32 mutants also show a reduced deposition of cutin (Bessire *et al*., 2011; Panikashvili *et al*., 2007). Analysis of the *permeable cuticle 1* (*pec1*) mutant of *Arabidopsis* revealed the role ABCG32 plays in cuticular lipids transport (Bessire *et al*., 2011). The *pec1* mutation was mapped to the *ABCG32* gene, a member of the *PLEIOTROPIC DRUG RESISTANCE* gene family. The *pec1* mutants

displayed phenotypes associated with cuticle permeability, and chemical analysis of the flowers revealed a 40% reduction in both ω-hydroxylated fatty acids and 10,16-dihydroxypalmitic fatty acid. As expected for an extracellular transport protein, ABCG32 is localized to the plasma membrane of the epidermal cells, but interestingly localization occurs in a polar manner so that the proteins are found on the surface side of the epidermal cells (Bessire *et al*., 2011). Another protein implicated in the extracellular transport of cuticular lipids is the *Arabidopsis* LTPG (glycosylphosphatidylinositol-anchored lipid transfer protein) (DeBono *et al*., 2009). LTPG is able to bind lipids *in vitro* and was localized to the plasma membrane of epidermal cells in growth regions of *Arabidopsis*, while mutants for LTPG show a reduction in wax load on the stem surface (DeBono *et al*., 2009).

Once the monomers/oligomers are outside the cell, polymerization takes place through the formation of ester bonds between the monomers or oligomers. Lipases are likely candidates for driving these reactions and may be found outside the cell in the cuticular membrane. One characterized enzyme is BODYGUARD (Kurdyukov *et al*., 2006), an extracellular epidermal protein with lipase domains, while other lipase candidates are the monoacylglycerol or glycine–aspartic acid–serine-leucine (GDSL) motif lipases. *Arabidopsis* mutants for BODYGUARD in fact show an increase in cutin and wax monomers, but this is coupled with phenotypes characteristic of a plant with a deficient cuticle. It is suggested that the increase in cutin monomers is a response of the plant after sensing a disrupted cuticle, but the monomers remain unpolymerized (Kurdyukov *et al*., 2006). More recently, a GDSL from tomato (SlGDSL1) has been shown to be localized to the exterior of the cell in the cuticular membrane, where it is able to polymerize monoacylglycerol cutin monomers (Girard *et al*., 2012; Yeats *et al*., 2012; Yeats *et al*., 2014).

2.4 Genes Involved in the Biosynthesis and Assembly of the Cuticle of Fleshy Fruit

2.4.1 Building the Cutin Polymer

While the majority of the fundamental work to describe cuticle biosynthesis has been performed in *Arabidopsis*, a dry fruit bearing species, several genes have also been characterized in various fleshy fruit species, these will be discussed in this section (see Table 1). Mapping of the *cutin deficient 1* mutant gene (*cd1*) led to the identification of

SlGDSL1, a candidate for the extracellular polymerization of cutin monomers in tomato (Isaacson *et al*., 2009). The *cd1* mutants possessed a significantly thinner cuticle than that of wild-type tomato as well as a reduction in cutin monomers and in the ester bonds cross-linking the cutin matrix (Isaacson *et al*., 2009; Yeats *et al*., 2012). This was coupled with an increase in cuticle permeability and postharvest water loss. SlGDSL1 was characterized as an acyltransferase that is able to perform the polymerization of cutin monomers, specifically 2-mono(10,16-dihydroxyhexadecanoyl) glycerols (Yeats *et al*., 2012). Importantly, this protein has been localized to the exterior of the cell in tomato fruit, providing evidence for polymerization occurring after the extracellular transport of monomers and/or oligomers. This class of extracellular proteins are now classified as cutin synthases (CUS) (Yeats *et al*., 2014).

Table 1. Genes involved in cuticle biosynthesis that have been functionally characterized in fleshy fruit species.

Gene	Species	Function	References
GDSL1 (CD1)	*Solanum lycopersicum*	Extracellular polymerization of cutin monomers	(Girard *et al*., 2012; Isaacson *et al*., 2009; Yeats *et al*., 2012)
CYP86A89	*Solanum lycopersicum*	Cutin monomer biosynthesis	(Shi *et al*., 2013)
CER6 (KCS6)	*Solanum lycopersicum*	very-long-chain fatty acid elongation	(Mintz-Oron *et al*., 2008; Vogg *et al*., 2004)
TTS2	*Solanum lycopersicum*	amyrin synthase	(Wang *et al*., 2011a)
OSC1 and OSC3	*Malus domestica*	amyrin synthase	(Brendolise *et al*., 2011)
F3H	*Solanum lycopersicum*	Flavonoid biosynthesis	(Verhoeyen *et al*., 2002)
FLS	*Solanum lycopersicum*	Flavonoid biosynthesis	(Verhoeyen *et al*., 2002)
CHS	*Solanum lycopersicum*	Flavonoid biosynthesis	(Adato *et al*., 2009; Ballester *et al*., 2010; Schijlen *et al*., 2007)

CD1 – CUTIN DEFECIENT1; CER - ECERIFERUM; CHS - CHALCONE SYNTHASE; CYP - CYTOCHROME P450; F3H - FLAVANONE 3-HYDROXYLASE; FLS - FLAVONOL SYNTHASE; GDSL - GDSL-MOTIF LIPASE/HYDROLASE; TTS – TRITERPENOID SYNTHASE; OSC – OXIDOSQUALENE CYCLASE

A gene involved in the biosynthesis of fruit cutin monomers was discovered through the analysis of the tomato *cuticle deficient 3* mutant (*cd3*) (Isaacson *et al*., 2009). The mutation was mapped to SlCYP86A69, a cytochrome P450 oxidase (Shi *et al*., 2013). SlCYP86A69 shares an amino acid sequence similarity of 96% with the petunia CYP86A22, a fatty acyl-CoA *ω*-hydroxylase shown to be required for the production of *ω*-hydroxy fatty acids and the biosynthesis of cutin polymer in the petunia stigma (Han

et al., 2010). While *cd3* mutants display a strong reduction in cutin there is an insignificant change in cuticular wax composition. Chemical analyses of *slcyp86a69* mutants showed a significant reduction in all cutin monomers in the tomato fruit cuticle (Isaacson *et al*., 2009; Shi *et al*., 2013). The plants had an increased susceptibility to microbial infection as well as an increase in susceptibility to dehydration stress (Figure 3). Enzymatic assays performed with SlCYP86A89 found that the enzyme preferentially catalyzes the hydroxylation of C18:1 fatty acid to C18-hydroxyoleic acid but it was also able to hydroxylate C14 and C16 fatty acids (at a significantly lower activity) (Shi *et al*., 2013). This acyl hydroxylation is a key step in the biosynthesis of the cutin monomers, as the hydroxyl groups allow for increased branching during the subsequent polymerization reactions.

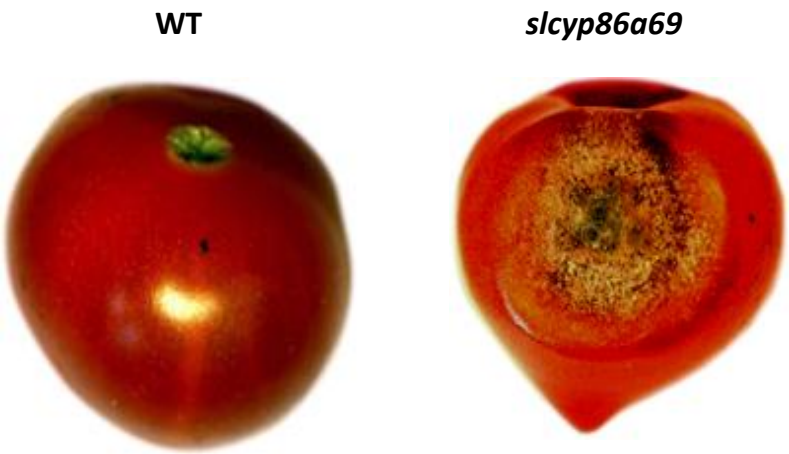

Figure 3. Responses of tomato fruit with depleted cuticle to fungal infection. Tomato fruit were inoculated with *Colletotrichum coccodes* conidia. Five days post inoculation shows the wild-type (WT) has negligible fungal growth, while the *slcyp86a69* mutant (*slcyp86a69*) has developed a severe infection (Shi *et al*., 2013).

2.4.2 Wax Associated Genes Involved in the Formation of Fleshy Fruit Cuticle

Genes involved in wax biosynthesis in fleshy fruit cuticles have been studied in a number of species although tomato is the species most investigated to date. Mutations in, or RNA interference (RNAi) knock downs of genes involved in wax biosynthesis typically lead to a greater increase in water permeability than observed in cutin mutants. The composition of the cuticular waxes of tomato is primarily made up of n-alkanes followed by triterpenoids and sterol derivatives and alkanoic acids (Schreiber, 2010).

An orthologue of the *Arabidopsis CER6* has been studied in tomato fruit, where the gene was shown to encode a *β*-ketoacyl-CoA synthase which acts as a condensing

enzyme involved in very-long-chain fatty acid elongation (Mintz-Oron *et al*., 2008; Vogg *et al*., 2004). Expression of a reporter gene driven by the upstream promoter region of *SlCER6* was localized to both the exocarp and endocarp of tomato fruit (Figure 4) (Mintz-Oron *et al*., 2008). Analysis of *slcer6* mutant tomato lines reveals that starting from the mature green stage of fruit development there is a reduction of n-alkanes with a chain length greater than C28 when compared to wild type tomato (Vogg *et al*., 2004). Substrates for the SlCER6 are therefore likely to include fatty acids with chain lengths longer than C28. This decrease in n-alkanes (n>C28) is coupled with an increase in cyclic triterpenoids and sterols, as well as an increase in the weight of the cuticle, considered to be a compensating mechanism. The triterpenoids, however, do not sufficiently compensate for the permeability of the cuticle as the mutants display a 3-8-fold increase in water loss when compared with wild type tomato. The effect of the absence of *β*-ketoacyl-CoA synthase is not limited to n-alkanes as *slcer6* lines also show a complete lack of cuticular alkene (C33, C35), aldehyde (C24, C26, C32), alkenol (C24, C26) and alkadienol (C22, C24, C26) formation, likely caused by an absence of the fatty acid precursors (Vogg *et al*., 2004).

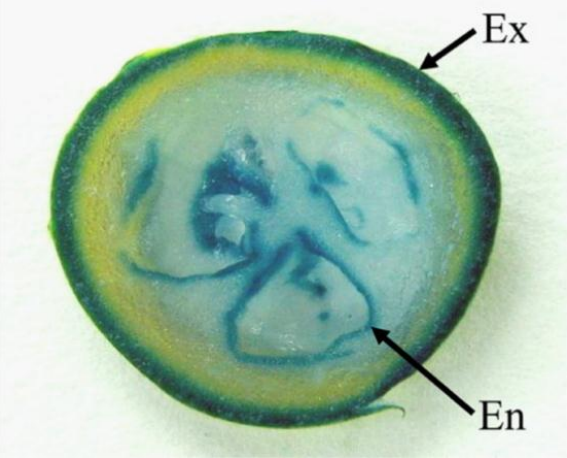

Figure 4. Expression of a GUS reporter driven by the tomato *SlCER6* promoter region. GUS expression is driven by the wax biosynthesis SlCER6 promoter and shows gene expression in the exocarp (Ex) and endocarp (En) tissues in a tomato fruit slice indicating the presence of the inner epidermal cuticular layer (Mintz-Oron *et al*., 2008).

Another tomato mutant that has shed light on the biosynthesis of fruit cuticular wax is the recessive *positional sterile* (*ps*) mutant (Leide *et al*., 2011). The *ps* phenotype is characterized by floral organ fusions (a commonly observed phenotype in plants with depleted cuticles), positional sterility and the formation of wrinkled ripe and overripe fruits. The surface area of the *ps* fruit at the fully ripe stage was approximately 33% that

seen in wild type (Leide *et al*., 2011). Chemical analysis of the cuticular wax composition of the *ps* mutants revealed a severe depletion of alkanes and aldehydes. As with the *slcer6* mutant an increase in triterpenoids and sterol derivatives was observed as well as a five- to eightfold increase in water permeability. There was however almost no effect on the cutin composition of the *ps* mutant cuticle. The observed modification of the cuticular waxes coupled with the lack of change seen in the cutin composition indicates that the *ps* mutation causes the disabling of the alkane pathway of wax biosynthesis in the fruit epidermal cells (Leide *et al*., 2011).

2.4.3 Triterpenoid Related Genes involved in Formation of the Fleshy Fruit Cuticle

In a number of fruits, including tomato, triterpenoids are found in the cuticle layer and in particular as constituents of the intracuticular waxes (Leide *et al*., 2007; Mintz-Oron *et al*., 2008). Typically they are more abundant in fruit than leaf cuticles and are suggested to be a contributing factor to the increased permeability of fruit cuticles as they have been shown to provide a less effective barrier to water transport than long chain hydrocarbons (Leide *et al*., 2007). A number of genes that code for triterpenoid synthases (TTSs) have been characterized in tomato (Wang *et al*., 2011a) and apple (Brendolise *et al*., 2011) fruit. Characterization of enzymes has been focused on the oxidosqualene cyclases (OSCs) which catalyze the first committed step of triterpenoids biosynthesis, the cyclization of epoxysqualene into various triterpene alcohol isomers. While the expression of *OSC* genes contributes significantly to the distribution of triterpenoids in plants there are additional points of control. This can be observed by the only partial correlation between expression levels and cuticular triterpenoids across tomato cultivars. Within a cultivar, however, *OSC* expression between organs correlated well with triterpenoid accumulation (Wang *et al*., 2011a).

The product specificity (or lack thereof) categorizes OSCs and determines the triterpenoid profile found in fruit waxes. The tomato TTS1 is a monofunctional *β*-amyrin, synthase while SlTTS2 is a multifunctional amyrin synthase producing predominantly *δ*-amyrin and six other terpenoid products (Wang *et al*., 2011a). The genes' major roles as the producers of cuticular triterpenoids in the fruit is illustrated in their exclusively fruit epidermal expression pattern and the fact that the combined enzyme activities correlate with all the triterpenoids present in the cuticular wax of tomato fruit (Wang *et al*., 2011a). The characterization of apple *OSC* genes led to the

discovery of the first TTS (MdOSC1) that is primarily an α-amyrin synthase (Brendolise *et al*., 2011). MdOSC1 produces both α-amyrin and β-amyrin in a 5:1 ratio. The fact that α-amyrin is the precursor to ursolic acid, the major terpenoic acid found in the cuticular wax of apple fruit, indicates the importance of MdOSC1 in wax terpenoid biosynthesis in apple. Additional apple TTS encoding genes identified include *MdOSC2* and *MdOSC3*. MdOSC3 shares a greater than 99% amino acid identity with MdOSC1, exhibits a similar fruit peel-specific expression pattern and is thought to have the same activity (Brendolise *et al*., 2011). *MdOSC2*, however, exhibits a significantly reduced expression level and has no observed activity when assayed with epoxysqualene (Brendolise *et al*., 2011). Although the activity of MdOSC3 has not been tested it likely has the same activity as MdOSC1 due to its high homology, while *MdOSC2* is hypothesized to be a pseudogene.

2.4.4 Genes Involved in Flavonoid Accumulation in the Fleshy Fruit Cuticle

Flavonoids are typically found embedded in the cuticle of tomato fruit, but have not been found in many other fleshy fruit cuticles (Mintz-Oron *et al*., 2008). They comprise of a diverse group of polyphenolic compounds that can be divided based on their core structure, the aglycone, into chalcones, flavanones, aurones, flavonols, and anthocyanins. The diversity of flavonoids is largely the result of the activity of a number of modifying enzymes such as glycosyl-, malonyl-, acyl-, and methyl-transferases. They fulfil a number of diverse roles in plant growth and development that include pigments for the attraction of pollinators and agents of seed dispersal, pathogen resistance and protection against damage from ultraviolet light (Adato *et al*., 2009; Domínguez *et al*., 2009; Harborne and Williams, 2000). Transcript and metabolite analysis during tomato fruit development indicates that the synthesis of cuticular lipids precedes phenylpropanoid and flavonoid biosynthesis. Expression of *CHALCONE SYNTHASE* (*CHS*), *FLAVANONE- 3-HYDROLASE* (F3H), and *FLAVONOL SYNTHASE* (FLS) have all been shown to increase during ripening of tomato fruits, peaking at the breaker stage (Mintz-Oron *et al*., 2008; Schijlen *et al*., 2007; Verhoeyen *et al*., 2002). While anthocyanins contribute to red, purple, and blue pigments in many flowers and fruit other flavonoids are responsible for imparting yellow pigmentation, such as chalcones and aurones. The major contributor to tomato fruit color is the red carotenoid, lycopene, found throughout the flesh of ripe tomatoes. However, through the characterization of *chs* mutants in tomato the contribution of the yellow pigmented naringenin chalcone to the perceived fruit color has been elucidated (Adato *et al*., 2009; Schijlen *et al*., 2007).

Naringenin chalcone typically accumulates in the peel of the developing tomato, however RNAi knock down lines for *SlCHS* exhibit a colorless epidermis devoid of the yellow-colored flavonoid naringenin chalcone (Schijlen *et al.*, 2007). These tomatoes appear pink as the combination of a yellow epidermal layer and the pink flesh is required for the typical red-orange color of wild type tomatoes.

2.5 Transcription Factors Associated with Cuticle Assembly

2.5.1 The Role of Members of the APETALA2/ETHYLENE-RESPONSIVE ELEMENT BINDING PROTEIN Family

The APETALA2/ETHYLENE-RESPONSIVE ELEMENT BINDING PROTEINS (AP2/EREBP) comprise one of the largest groups of transcription factors in plants. Members of this transcription factor superfamily possess at least one AP2 DNA-binding domain. These proteins regulate diverse biological processes including hormone biosynthesis, reproduction, cell proliferation and abiotic and biotic stress responses (Gutterson and Reuber, 2004; Xu *et al.*, 2011). Several members of this family have also been demonstrated to regulate cuticle-related genes. The maize AP2-like gene *Glossy15*, (Moose and Sisco, 1996) was reported nearly 20 years ago to regulate leaf epidermal cell identity (Evans *et al.*, 1994; Moose and Sisco, 1994, 1996). Recessive mutation of *gl15* in maize results in a switch from juvenile to the adult phase earlier than in wild-type plants. Interestingly, this mutation only affects the character of the epidermis and does not have any effect on the overall vegetative morphology of the plant or on its reproductive development. Mutant *gl15* plants lack visible epicuticular wax, possess epidermal hairs and rectangular epidermal cells and have highly crenulated lateral walls; all characteristics of the adult phase which apparently occurs earlier in the mutant (Evans *et al.*, 1994; Moose and Sisco, 1994). *GL15* is therefore an example of a gene that is associated with epicuticular wax formation, while having a wide effect on the epidermal cells and the genetic program of the juvenile phase of the plant.

In Arabidopsis, the AP2-domain super family member *SHN1/WIN1* was the first to be recognized for its role in cuticular wax metabolism (Aharoni *et al.*, 2004; Broun *et al.*, 2004; Kannangara *et al.*, 2007). Overexpression of *AtSHN1/WIN1* promotes cutin biosynthesis and the rapid induction of several cutin biosynthetic genes (Kannangara *et al.*, 2007). However, while wax biosynthesis was also increased, the induction of wax-related genes was delayed and suggested to be a secondary effect. The down-regulation

of *AtSHN1/WIN1* caused significant changes in petal cutin monomer composition, together with the reduction of the total cutin content (Kannangara *et al.*, 2007). Shi *et al.* (2011) suggested an additional role in cell wall metabolism for AtSHN1 and its related proteins (i.e. AtSHN2 and AtSHN3) that is beyond the regulation of the cutin metabolic pathway. The expression of *AtSHN1/WIN1* may be further modulated by the AtNFX1-LIKE2 transcription factor (Lisso *et al*., 2012).

In some plants, cuticular wax deposition increases daily during the light period as compared to the dark (Giese, 1975; Shepherd *et al*., 1995). A recent report shows that *Decrease Wax Biosynthesis (DEWAX)*, which encodes an AP2/ERF-type transcription factor, is a transcriptional repressor of cuticular wax biosynthesis (Go *et al*., 2014). *DEWAX* was identified using microarray data for higher expression in stem epidermal peels than in whole stems; and found to be dark inducible. In addition, DEWAX was found to directly mediate the transcriptional repression of several wax related genes, including FAR6, CER1, LACS2, ACLA2, and ECR, via binding their promoters. *DEWAX* expression correlated with wax biosynthetic genes in daily dark/light cycles. The relation between DEWAX activity throughout the day with relation to other regulators of wax biosynthesis remains unclear.

Recent work investigating the role of *SHN* TFs in the fruit cuticle identified three tomato orthologues of the *AtSHN1-3* clade members (Table 2) (Shi *et al.*, 2013). The study focused on characterizing a single member (*SlSHN3*) which was highly expressed in the exocarp of mature green stage fruit, resembling expression of other cuticle-related genes (Mintz-Oron *et al.*, 2008). Silencing *SlSHN3* in tomato resulted in a dramatic reduction in cuticle formation (Figure 5A and B) (Shi *et al.*, 2013). Various other epidermis associated phenotypes such as a glossier surface and thicker as well as more sharply defined primary cell wall were also observed (Shi *et al.*, 2013). Chemical analysis showed that silencing of *SlSHIN3* reduced the amount of cutin and wax in the tomato fruit cuticle. It was suggested that besides the regulation of genes associated with cutin metabolism, *SlSHN3* possibly controls the expression of regulatory genes associated with epidermal cell patterning including tomato genes similar to *GLABRA2* and a *MIXTA* (Shi *et al.*, 2013). This and other mechanisms involved in the regulatory connection between epidermal cell differentiation and cuticle biosynthesis are discussed later in this chapter.

Table 2. Transcription factors reported to possess a cuticle related role in fleshy fruit.

Transcription factor	Role	Organism	Direct target genes[a]	Regulated genes[b]	References
SHINE3(Solyc06g065820)[c]	Cutin and wax biosynthesis and epidermal pattering	Tomato	SlMIXTA, *SlGL2a*, *SlCYP86A68*, *SlCYP86A69*, *SlGRXC11*	*SlCYP77A1*, *SlGDSLa*, *SlGDSLb/SlGDSL1*, *SlDCR*, *SlGPAT6*, *SlLACS2*, *SlHTH*, *SlSHN2*, *SlSHN3*, *SlHDG11a*, *SlANL2c*	Buxdorf *et al.*, 2014; Shi *et al.*, 2013
MYB12 (Solyc01g079620)[c] (GSVIVT01028091001)[d]	Regulation of the flavonoid pathway	Tomato Grape	*CHS*, *F3H*, *FLS*, *CHI*	*SlPDH*, *SlPAL*, *SlC3H*, *Sl4CL*, *SlCHS1*, *SlCHS2*, *SlCCR*, *SlCHI*, *SlCHI-like*, *SlF3H*, *SlF3'H*, *SlF3H-like*, *SlFLS*, *SlANS-like*, *SlRT*, *SlMYB4-like*, *SlTHM27*, *Sl3GT*	Adato *et al.*, 2009; Ballester *et al.*, 2010; Matus *et al.*, 2009; Mehrtens *et al.*, 2005
FUL1/TDR4 (Solyc06g069430)[c] and FUL2/MBP7 (Solyc03g114830)[c]	Cuticle assembly	Tomato	*ACS2*, *ACS4*, *RIN*, *FUL1*, *PSY1-a* and *PSY1-b*	n.d.	Bemer *et al.*, 2012; Shima *et al.*, 2013
VvMYB5b (GSVIVT01025452001)[d]	Triterpenoid biosynthesis	Grapevine	n.d.	n.d.	Mahjoub *et al.*, 2009
CD2 (Solyc01g091630)[c]	Cuticle assembly (cutin)	Tomato	n.d.	n.d.	Isaacson *et al.*, 2009; Nadakuduti *et al.*, 2012; Kimbara *et al.*, 2013

a Relationship demonstrated via promoter binding assays.
b Relationship demonstrated via qRT, RNA blot analysis or other expression analysis method
c Tomato Gene ID (Bombarely *et al.*, 2011).
d Grape Gene ID (Jaillon *et al.*, 2007).
n.d. not determined.
LACS - LONG-CHAIN ACYL-COA SYNTHETASE; CYP - CYTOCHROME P450; CER - ECERIFERUM; GL8 - *β* -KETOACYL-COA REDUCTASE; FAR - FATTY ACID REDUCTASE; RIN - RIPENING INHIBITOR; LCR -LACERATA; GDSL - GDSL-motif lipase/hydrolase; DCR – DEFECTIVE IN CUTICULAR RIDGES; GPAT – ACYL-CoA:GLYCEROL-3-PHOSPHATE ACYLTRANSFERASE; HTH - HOTHEAD; CD2 – CUTIN DEFECIENT2; GL2 – GLABRA2; HDG – HOMEO-DOMAIN GLABOROUS; ANL - ANTHOCYANINS; GRXC11 - GLUTAREDOXIN-C; CHS - CHALCONE SYNTHASE; CHI - CHALCONE FLAVANONE ISOMERASE; F3H - FLAVANONE 3-HYDROXYLASE; FLS - FLAVONOL SYNTHASE; PAL - PHENYLALANINE AMMONIA-LYASE; CCR - CINNAMOYL COA REDUCTASE-LIKE; RT – RHAMNOSYLTRANSFERASE; PDH - PREPHENATE DEHYDRATASE; C3H - P-COUMAROYL 3'-HYDROXYLASE; 4CL - 4-COUMARATE COA LIGASE; ANS-LIKE - ANTHOCYANIDIN SYNTHASE-LIKE; 3GT - FLAVONOID-3-O-GLUCOSYLTRANSFERASE; F3'H -FLAVONOID-3'-HYDROXYLASE.

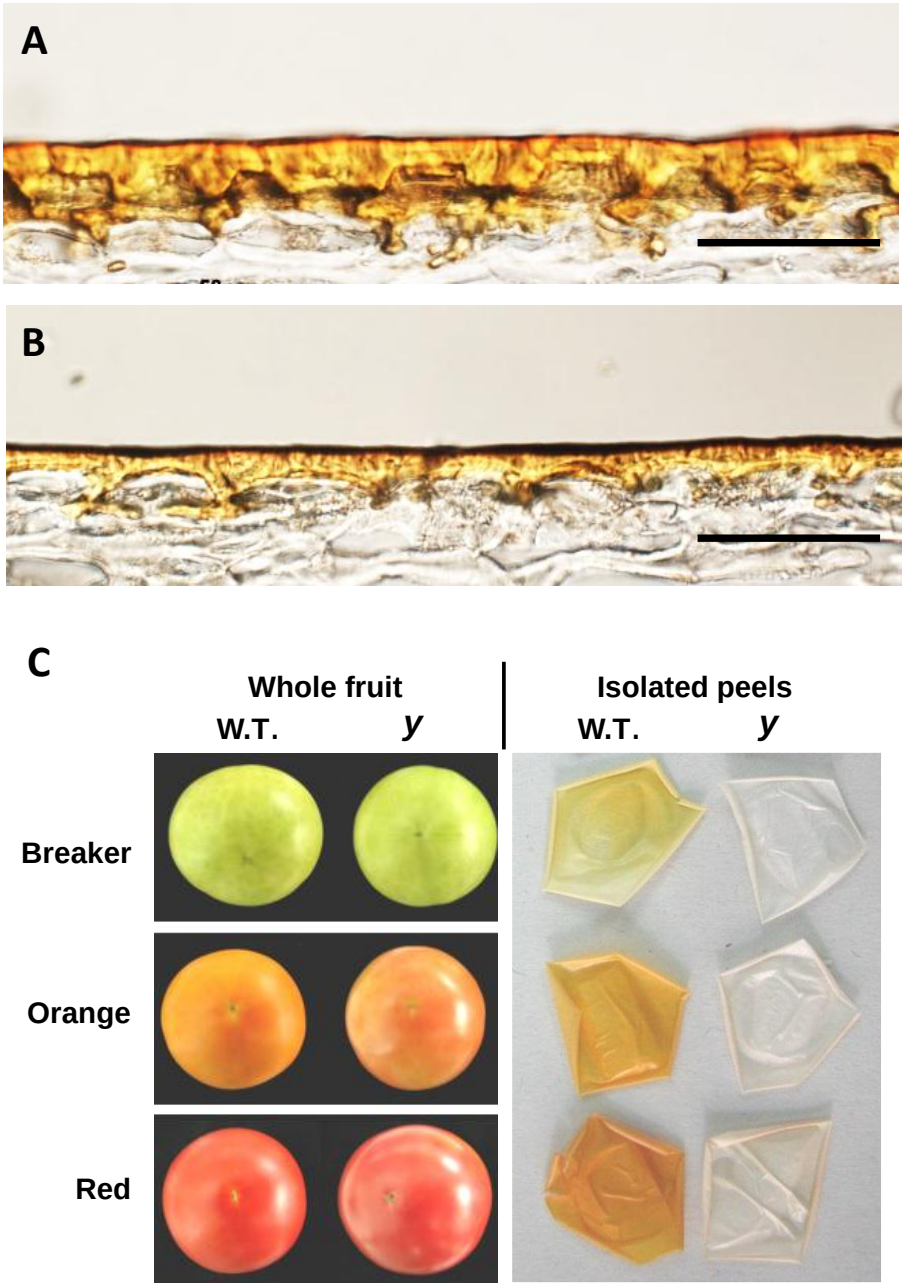

Figure 5. Transcription factors are involved in the regulation of diverse cuticular properties. Silencing of the *SlSHN3* transcription factor in tomato resulted in reduced cuticle deposition in tomato fruit as shown via light microscopy analysis of (A) wild-type and (B) *SlSHN3-RNAi* tomato peel sections (Shi *et al*., 2013). Additionally, the epidermal cells of the *SlSHN3-RNAi* tomato sections in (B) do not possess the conical shape observed in the wild-type shown in (A) (Shi *et al*., 2013). Tissue was stained with the lipid specific Sudan IV stain resulting in the cuticular membrane staining orange. Scale bar indicates 50 µm. Further, investigation of the *y* mutant phenotype demonstrated that SlMYB12 is a positive regulator of anthocyanin accumulation in tomato peels (C). Enzymatically isolated cuticles show the near absence of colour development and flavonoid accumulation during tomato development in *y* mutant peels when compared with wild-type (W.T.) ones (C) (Adato *et al.*, 2009). The *y* mutant tomato has significantly reduced *MYB12* expression. The phenotype is more strongly visible after separation of the cuticles from the fruit due to the presence of red carotenoid pigment in the underlying pericarp.

SlSHN3 was also found to be expressed in the inner epidermal layer of tomato fruit (Matas *et al.*, 2011; Shi *et al*., 2013). Matas *et al.* (2011) profiled gene expression in multiple cell types of tomato fruit, and demonstrated that a number of cuticle biosynthesis genes were expressed in the inner epidermal layer (Figure 4). The identification of *SlSHN3* expression in this cell layer as well as other known regulators of cuticle biosynthesis suggests that similar mechanisms of regulation are in operation in the inner epidermal layer as in the outer epidermal layer (Figure 6). More recently, Buxdorf *et al.* (2014) demonstrated the importance of the cuticle in tomato plant-pathogen interactions. In this study, *SlSHN3*, was shown to regulate tomato leaf cuticle biosynthesis as leaves of *SlSHN3* over expressing plants (*SlSHN3*-OE) were shiny, underdeveloped and displayed increased permeability (Buxdorf *et al.*, 2014). *SlSHN3*-OE leaves were, however, more resistant than the wild-type leaves to the necrotrophic foliar pathogen, *Botrytis cinerea*, and the biotrophic bacterial pathogen, *Xanthomonas campestris pv. vesicatoria*; while *SlSHN3*-RNAi lines appeared more sensitive. These results strengthened the previously proposed model in which increased cuticle permeability may provide the plant with increased resistance to fungal infection, possibly due to an incremental release of fungitoxic compounds (Bessire *et al.*, 2007; Chassot *et al.*, 2007).

The legume, *Medicago truncatula* Gaertn. AP2 transcription factors *WAX PRODUCTION1 (WXP1)* and *WAX PRODUCTION2 (WXP2)* were shown to have a major effect on cuticular wax accumulation when overexpressed in alfalfa (*Medicago sativa*) and *Arabidopsis*. Phylogenetic analysis showed that WXP1 is distinct from most of the known AP2 domain-containing transcription factors based on examination of their complete protein sequences. Overexpression of *WXP1* in alfalfa led to typical wax induction phenotypes, including a significant increase in cuticular wax, accumulation of wax crystals, induction of wax-related genes, reduced water loss and chlorophyll leaching and enhanced drought tolerance (Zhang *et al.*, 2005). Further work by Zhang *et al.* (2007), characterized plants with heterologous expression of *WXP1* and its paralog *WXP2* from *M. truncatula* in *Arabidopsis.* Interestingly, both genes were found to be involved in wax production, however with different morphological and cellular responses. Equally, overexpression of *WXP1* and *WXP2* led to significantly increased cuticular wax deposition, but these two genes affect wax composition differently. Cuticle permeability determined by chlorophyll leaching assays revealed no change in *WXP1* expressing plants in comparison to high permeability in the *WXP2* plants. Both

transgenic plants retained more water than the control and displayed enhanced drought tolerance. However, *WXP1* over expressing lines exhibited enhanced freezing tolerance while *WXP2* over expressing lines were more sensitive. This study highlighted the complexity of the cuticle production network, and how seemingly similar genes affect plant characteristics and survival very differently.

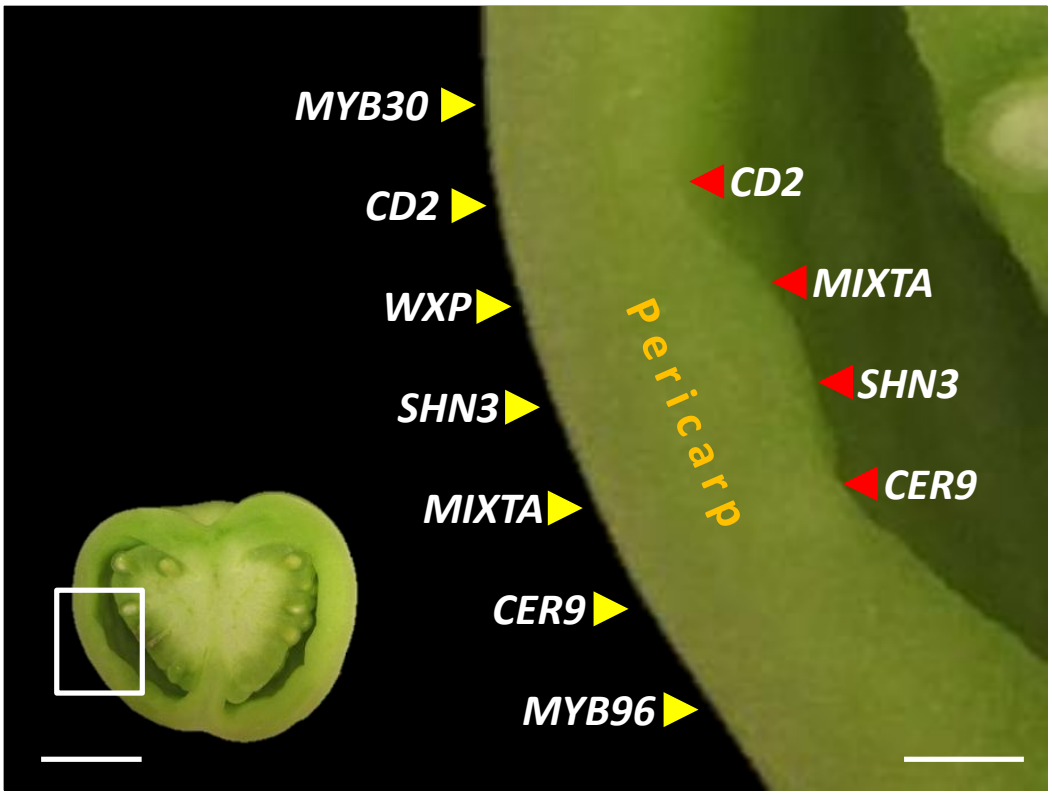

Figure 6. Transcription factors expressed in the inner and outer epidermal layers of tomato fruit. Expression profiling of five cell types of tomato fruit by Matas *et al.,* (2011) revealed a similar genetic basis for the biosynthesis of the inner- and outer- epidermal cuticular layers. A bisected tomato is shown (scale bar = 10 mm) and an enlarged area (scale bar = 1 mm) where the location of expression for transcription factors discussed in this review (or the tomato orthologue) is shown. Yellow arrows indicate outer epidermal expression; red arrows indicate inner epidermal expression. Orthologues of *GL2* (*GLABRA2*), *MYB12*, *MYB41* and *CER7* discussed here were not found to have epidermal specific expression patterns in the expression dataset generated by Matas *et al.,* (2011). *WXP – WAX PRODUCTION*; *CD2 – CUTIN DEFICIENT2; CER – ECERIFERUM.*

2.5.2 MYB Transcription Factors and the Regulation of Cuticular Wax Metabolism

Most MYB family members typically function as transcription factors and include proteins with varying numbers of MYB domain repeats, providing their ability to bind DNA (Ambawat *et al.*, 2013; Dubos *et al.*, 2010; Martin and Paz-Ares, 1997).

Although MYB transcription factors are not restricted to plants, some of those proteins function in a variety of plant-specific processes, as evidenced by their extensive functional characterization in *Arabidopsis*. MYB proteins seem to be key factors in regulatory networks controlling development, metabolism and responses to biotic and abiotic stresses (Ambawat *et al.*, 2013; Dubos *et al.*, 2010; Martin and Paz-Ares, 1997). Based on the number of MYB domains, the MYB family can be divided into four classes, 1R-, R2R3-, 3R- and 4RMYB proteins (Dubos *et al.*, 2010; Stracke *et al.*, 2001). R2R3-MYB proteins are specific to plants and are also the most abundant class in plant genomes, with more than 100 R2R3-MYB members in the genomes of dicots and monocots (Ambawat *et al.*, 2013).

As described in previous sections the cuticle of many fruit species contains secondary metabolites such as triterpenoids, sterols, alkaloids and phenylpropanoids, including flavonoids. For example, the flavonoid naringenin chalcone accumulates up to 1% dry weight of the tomato fruit cuticle (Muir *et al.*, 2001). The plant flavonoids, anthocyanins and proanthocyanidins biosynthesis pathways have been shown to be regulated by MYB-type transcription factors in several plant species (e.g. maize, petunia, snapdragon, *Arabidopsis*, tobacco, grape and apple) (Bogs *et al.*, 2007; Deluc *et al.*, 2006; Gális *et al.*, 2006; Mehrtens *et al.*, 2005; Stracke *et al.*, 2007). MYB12, an R2R3 protein, was demonstrated to play an important role in regulating the flavonoid pathway in tomato fruit (Adato *et al.*, 2009; Ballester *et al.*, 2010). Previous studies have elucidated the role of MYB12 in regulation of the flavonols production in *Arabidopsis* (Mehrtens *et al.*, 2005) and grape (*V. vinifera*) (Matus *et al.*, 2009). In tomato, the so called *y* mutant, displaying a pink fruit phenotype, showed low expression of *MYB12* that led to lack of the flavonoid pigment naringenin chalcone in the fruit cuticle (Table 2, Figure 5C). Mutation in *MYB12* was suggested to underlay the *y* fruit phenotype. The *y* mutant fruit also possessed broad effects on both primary and secondary metabolism, alterations in thickness, elasticity, cutin content and wax composition of the cuticle. However, the lack of naringenin chalcone did not have a major impact on fruit water relations (Adato *et al.*, 2009; Ballester *et al.*, 2010).

In grapevine, an R2R3-MYB transcription factor (VvMYB5b) has been suggested to act as a regulator of cuticular wax accumulation (Mahjoub *et al.*, 2009). Overexpression of *VvMYB5b* in tomato plants produced a variety of pleiotropic phenotypes, including modified leaf structure, alterations in floral morphology, and glossy fruit appearance. These phenotypes are typical of plants possessing an altered

cuticular membrane. Chemical analysis of the tomato fruit revealed a decrease in the total amyrin content, specifically *β*-amyrin, which is the precursor to oleanoic acid, the major triterpenoic acid found in grape berry cuticles (Mahjoub *et al.*, 2009). While inferring the function of transcription factors from over-expression in a heterologous system could be inaccurate, it is possible that VvMYB5b regulates similar pathways in grapevine. Further study, however, is required to identify the downstream targets of VvMYB5b in grape.

MYB family transcription factors have also been reported to act in the regulation of cuticular waxes pathways in non-fruit tissues. The MYB factor, AtMYB30, was shown to regulate very-long-chain fatty acid biosynthesis as part of the hyper-sensitive cell death response (Raffaele *et al.*, 2008). In this work, wild-type plants, *MYB30* overexpression and *MYB30* antisense plants were inoculated with a bacterial pathogen prior to microarray analyses. This experiment revealed that genes encoding the VLCFA elongase subunits are the main putative targets of MYB30. Likewise, wax related genes (*CER2* and *CER3*) expression were found up-regulated in the *MYB30* overexpression plants during pathogen infection, indicating that wax synthesis might be under MYB30 regulation. A different MYB factor, AtMYB41, was found to alter cell expansion, leaf surface permeability and cuticle deposition in response to abiotic stress (Cominelli *et al.*, 2008). Further transcriptome and metabolome analysis suggested that *AtMYB41* is involved in control of primary metabolism and in the regulation of short-term transcriptional responses to osmotic stress (Lippold *et al.*, 2009). *MIXTA*, another MYB-related protein, was reported to participate in the transcriptional control of epidermal cell shape and to affect flower color intensity in *Antirrhinum majus* petals (Noda *et al.*, 1994). Very recently, the MIXTA-like MYB transcription factors MYB106 and MYB16, were shown to also regulate cuticle development coordinately with WIN1/SHN1 in *Arabidopsis* and *Torenia fournieri* (Oshima *et al., 2013)*.

2.5.3 The Link Between MADS-box Ripening Regulators and Cuticle Formation

The MADS-box gene family can be found in animals, fungi, and plants. The function of the different MADS-protein domains includes DNA binding, protein- protein interactions, transcriptional activation or repression as well as protein complex formation (Cho *et al.*, 1999; de Folter and Angenent, 2006; Egea-Cortines *et al.*, 1999). Based on sequence conservation in the MADS domain, these transcription factors can

be grouped into two main lineages named type I (SRF-like) and type II (MEF2-like) (Alvarez-Buylla *et al.*, 2000). Plant MADS box genes are known to play a role in a myriad of developmental processes among them the regulation of floral organ identity, determination of meristem identity, root growth, ovule and female gametophyte development, flowering time, fruit ripening, as well as dehiscence (Colombo *et al.*, 2008; Giovannoni, 2004; Liu *et al.*, 2009; Ng and Yanofsky, 2001; Whipple *et al.*, 2004; Zhang and Forde, 1998).

In the framework of studying fruit ripening, several tomato MADS-box genes including *TOMATO AGAMOUS LIKE1, FRUTFULL1/TDR4 and FRUTFULL2/MBP7*) were found to be involved in the fruit ripening regulation network (Bemer *et al.*, 2012; Giménez *et al.*, 2010; Itkin *et al.*, 2009; Shima *et al.*, 2013; Vrebalov *et al.*, 2009). Recently, *FUL/TDR4* and *FUL2/MBP7* were shown to impact cuticle formation of the tomato fruit (Table 2) (Bemer *et al.*, 2012). *FUL1/2* silenced fruits showed increased water loss. While both pericarp and cuticle thickness did not differ between wild-type and transgenic lines, transcriptome analysis suggested altered lipid and cuticle metabolism in *FUL1/2* fruit. Cuticle-associated genes including a cytochrome P450-dependent fatty acid hydroxylase, a long-chain acyl-CoA synthetase family protein and a GDSL-like lipase were strongly up regulated in the *FUL1/2* transgenic fruits (Bemer *et al.*, 2012). The fact that fruit ripening regulatory genes also affect cuticle formation re-emphasizes the role of cuticle-related genes in the general developmental program of the plant.

2.5.4 The Homeodomain-leucine Zipper IV Subfamily in the L1 Layer and the Cuticle

The homeodomain-leucine zipper (HD-Zip) family of genes is a group of TFs unique to the plant kingdom. Of particular interest to cuticle research is the HD-Zip IV subfamily, whose members have been found to be specifically or preferentially expressed in the epidermal layers of many plants. HD-Zip IV TFs contain a DNA binding homeodomain as well as a START (steroidogenic acute regulatory lipid transfer) domain which likely binds regulatory lipids (Schrick *et al.*, 2004). A number of these proteins have been found to be associated with the transcriptional control of epidermal cell differentiation, anthocyanin accumulation, the regulation of lipid biosynthesis and transport and cuticle biosynthesis. The first identified HD-Zip IV factor was the *Arabidopsis* GLABRA2 (GL2) which was shown to regulate trichome and root hair development (Di Cristina *et al.*,

1996; Hülskamp *et al.*, 1994; Masucci *et al.*, 1996; Rerie *et al.*, 1994). Other characterized HD-Zip IV members in *Arabidopsis* include ANTHOCYANINLESS 2 (ANL2), ARABIDOPSIS THALIANA MERISTEM LAYER 1 (ATML1), PROTODERMAL FACTOR 2 (PDF2) and HOMEODOMAIN GLABROUS 11 (HDG11). ANL2 positively regulates anthocyanin accumulation in the epidermal cells (Kubo *et al.*, 1999), while HDG11 regulates trichome development (Nakamura *et al.*, 2006), and ATML1 and PDF2 are involved in shoot epidermal cell differentiation (Abe *et al.*, 2003; Lu *et al.*, 1996; Sessions *et al.*, 1999). ATML1 and PDF2 are expressed predominantly in the outermost layer (L1) of the shoot apical meristems and have been shown to specifically bind the L1 box sequence, suggesting a regulatory role of L1 layer-specific gene expression (Abe *et al.*, 2003). The double *pdf2-1 atml1-1 Arabidopsis* mutant fails to differentiate epidermal cells confirming the central role these transcription factors perform (Abe *et al.*, 2003).

In maize, the HD-Zip IV member, OUTER CELL LAYER 1 (OCL1), has been proposed to regulate cuticle biosynthesis (Depège-Fargeix *et al.*, 2011; Javelle *et al.*, 2010). Overexpression of *OCL1* in maize resulted in modulated expression of a number of genes involved in lipid metabolism, defense, cell envelope-related functions, and cuticle biosynthesis (Javelle *et al.*, 2010). Specifically, orthologues of the cutin and wax transporter, *AtWBC11* (white brown complex 11), and the fatty acyl-coenzyme A reductase, *AtFAR1*, were shown to be downstream targets of the OCL1 protein. Over-expression of *OCL1* led to increased expression of *ZmWBC11a* and in turn an increase in accumulation of extracellular cuticular wax compounds (Javelle *et al.*, 2010). It was also suggested that OCL1 interacts directly with the promoter of *ZmWBC11a* (Javelle *et al.*, 2010). The effect of the increase in *ZmFAR1* expression caused by *OCL1* overexpression was observed in the increase in C24 to C28 alcohols found in the cuticular wax of maize kernels.

In tomato, an HD-Zip IV member named CD2 (CUTIN DEFICIENT 2) was identified by map based cloning of cuticular mutant genes (Isaacson *et al.*, 2009). The CD2 protein showed high homology to AtANL2 and is reported to regulate cutin monomer biosynthesis (Table 2) (Isaacson *et al.*, 2009; Nadakuduti *et al.*, 2012). Expression of *CD2* was localized to the epidermal cell layer of tomato (Nadakuduti *et al.*, 2012). The *cd2* mutant displayed a variety of phenotypes including reduced anthocyanin accumulation, a lower density of glandular trichomes, an associated reduction in trichome-derived terpenes and a dramatic reduction in cutin content in the tomato fruit cuticle (Isaacson *et al.*, 2009; Nadakuduti *et al.*, 2012). Interestingly, an insignificant

change in waxes was observed and the water retention of *cd2* tomato fruit was only mildly affected, supporting the view that waxes are more important than the structural cutin polymer with respect to waterproofing. Nevertheless, an increase in stiffness and susceptibility to fungal infection was observed in the *cd2* mutant (Isaacson *et al.*, 2009).

2.6 Further Levels of Regulation 0f Cuticular Pathways

2.6.1 A Global Network of Transcriptional Regulation and Epidermal Cell Differentiation

While there exists some debate with respect to which phylum shares the closest evolutionary relationship with land plants (embryophytes), the charophytes are typically considered to be land plants' closest extant relative (McCourt *et al.*, 2004). The evolutionary divide between these mostly fresh water green algae and land plants occurred approximately 450 million years ago. While initial plant life on land likely occurred in moist environments the atmosphere was still significantly drier than life under water. The development of the cuticle together with the specialized epidermal cells such as stomata occurred concurrently as mechanisms to cope with this major change in environment. Therefore since the beginning of plant life on land the regulation mechanisms governing epidermal cell differentiation and the biosynthesis of the cuticular layer have been co-evolving. Recent studies of the transcriptional networks controlling these processes have elucidated some of the molecular mechanisms involved in the cross talk and coordination of these programs of plant development.

The transcription factors discussed in this chapter have either been directly linked to epidermal cell patterning and differentiation or form part of a gene family shown to be involved in this regulation. As highlighted above the HD-ZIP IV transcription factor family has been shown in a variety of plants to be regulating processes in epidermal cells. Examples include seed mucilage production and root cell wall biosynthesis by AtGL2 (Ishida *et al.*, 2007; Rerie *et al.*, 1994; Tominaga-Wada *et al.*, 2009); trichome development by AtHDG11 (Nakamura *et al.*, 2006) and GhHD-1 (Walford *et al.*, 2012); and control of epidermal cell fate by SlANL2 (CD2), ATML1 and AtPDF2 (Nadakuduti *et al.*, 2012; Abe *et al.*, 2003). A recent study has further elucidated the mechanism by which AtATML1 and AtPDF2 maintain epidermal cell identity (San-Bento *et al.*, 2013). The authors describe a feedback loop between the two transcription

factors and the receptor kinase ARABIDOPSIS CRINKLY4 (AtACR4) that is capable of maintaining robust epidermal cell identity post-germination via cell-cell communication.

The dual action of transcription factors involved in cuticle biosynthesis and epidermal cell differentiation has been further illustrated by the work performed on the members of the SHN1/WIN1 clade of the AP2-domain superfamily. The regulation of cuticle biosynthesis by AtSHN1 and SlSHN3 was discussed earlier; however these transcription factors have also been shown to impact epidermal cell differentiation (Aharoni *et al.*, 2004; Broun *et al.*, 2004; Shi *et al.*, 2013; Shi *et al.*, 2011). It appeared that in tomato, SlSHN3 acts relatively high up the pathway as it is able to modulate the expression of regulatory genes including the HD-ZIP IV genes *SlGL2*, *SlPDF2d* and *SlHDG11a* and the R2R3 MYB factor, *SlMIXTA-like* gene (Figure 7) (Shi *et al.*, 2013). The MIXTA-like clade of MYB transcription factors has been demonstrated to regulate conical epidermal cell formation (Baumann *et al.*, 2007; Di Stilio *et al.*, 2009; Noda *et al.*, 1994) and trichome and cotton fiber development (Gilding and Marks, 2010; Perez-Rodriguez *et al.*, 2005; Plett *et al.*, 2010; Machado *et al.*, 2009; Walford *et al.*, 2011). Recent work has shown that the AtMIXTA-like protein is also able to regulate cuticle biosynthesis (Oshima *et al.*, 2013) in *Arabidopsis*. Interestingly, in *Arabidopsis* it was shown that AtMIXTA-like regulates AtSHN (Oshima *et al.*, 2013), while in tomato the reverse appears to be the case (Shi *et al.*, 2013). This aptly illustrates the complex nature of the transcriptional relationship between epidermal cell patterning and cuticle biosynthesis.

2.6.2 Hormonal Regulation of Cuticular Wax Biosynthesis

Due to its role in the protection of the plant against abiotic stresses the plant cuticle is strongly regulated in response to environmental cues such as osmotic stress. Biosynthesis of waxes and the cutin matrix would appear to be under independent control as their synthesis and deposition is not correlated across organs or during development (Bargel *et al.*, 2006). The intra-cuticular waxes are considered to be the major element contributing to the water proofing of the plant, and wax deposition is typically increased when the plant is under various stresses such as osmotic stress (Seo *et al.*, 2011; Shepherd and Wynne Griffiths, 2006), or in organs that demand increased protection from osmotic stress, such as fleshy fruit (Leide *et al.*, 2007; Vogg *et al.*, 2004).

Osmotic stress is known to stimulate the synthesis of abscisic acid (ABA), which in turn activates a number of responses in the plant with the purpose of reducing the

stress or minimizing the damage caused (Finkelstein and Rock, 2002; Nambara and Marion-Poll, 2005; Zhu, 2002). Kosma *et al.* (2009) showed that ABA application to *Arabidopsis* plants resulted in a significant increase in the wax component of the cuticle, but observed no significant changes in cutin content. *Arabidopsis* plants overexpressing *AtMYB96* display a phenotype resembling the one of plants grown under abiotic stress conditions (Seo *et al.*, 2009). Further analysis showed that *MYB96* expression was up-regulated by drought in an ABA-dependent manner and its expression levels were positively correlated with plant resistance to water stress (Seo *et al.*, 2009). In a continuation of this work, Seo *et al.* (2011) identified genes upregulated by *AtMYB96* expression. These genes included many characterized wax biosynthetic and transport genes such as *KCS1*, *KCS2*, *KCS6*, *CER1*, *CER3*, and *WBC11*. The results suggested that *MYB96* functions as a transcription factor that regulates the entire wax metabolic network in response to ABA signaling.

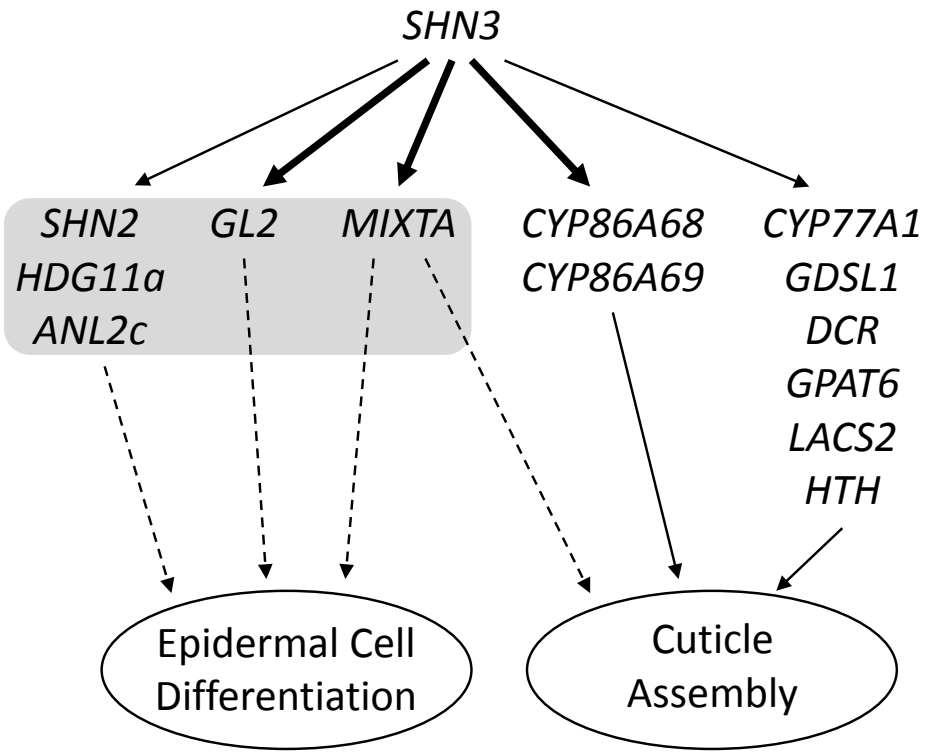

Figure 7. SlSHINE3 (SlSHN3) forms part of a transcriptional network regulating cuticle development and epidermal cell differentiation in tomato fruit. The schematic illustrates the primary role played by the SlSHN3 transcription factor in the regulation of tomato fruit surface characteristics. SlSHN3 downstream activity is mediated though the induction of a number of other transcription factors, as well as through direct action on cuticle biosynthesis genes (Shi *et al*., 2013). The grey highlight indicates downstream transcription factors; bold arrows indicate that the relationship has been characterized via a promoter binding assay (while thin arrows show relationships inferred from expression analysis); dashed lines indicate the inferred function from orthologous characterized in other species. *GL2, HDG11a* and *ANL2c* – HD-ZIP IV genes; *CYP* – cytochrome P450; *GDSL* – GSDL-motif lipase; *DCR* and *GPAT* – acyltransferases; *LACS* – long-chain acyl-CoA synthetase; *HTH* – an oxidoreductase.

ABA biosynthesis proceeds with the concomitant step of oxidative cleavage of epoxycarotenoids by NCED (9-cis-epoxycarotenoid dioxygenase) (Schwartz *et al.*, 1997). Analysis by Wang *et al.* (2011b) of an *Arabidopsis* mutant that failed to induce *NCED* expression under osmotic stress found that the plant was mutated in a gene orthologous to *BODYGUARD*, encoding a protein likely required for proper cutin polymerization (Kurdyukov *et al.*, 2006). The results of this study suggested that an improperly formed cuticle is unable to mediate a normal osmotic stress signal. This observation was confirmed after analyzing a number of additional cutin biosynthesis mutants, including *lacs2-1*, *gpat4gpat8* and *cyp86a8* which all exhibited a reduced induction of ABA in response to osmotic stress (Wang *et al.*, 2011b). Further, this effect was only observed in cutin biosynthesis mutants and not the mutants of wax biosynthesis tested, suggesting that cutin, but not wax, is required for osmotic stress response. It remains to be seen if this phenomenon occurs in fruit species as well, yet, the conserved nature of cuticle biosynthesis and regulation in general indicates that this is likely the case. The link between the cuticle and ABA biosynthesis is still unclear, although it has been suggested that epidermal cell wall or cuticle associated proteins that are necessary for proper osmotic stress sensing and signal transduction are unable to function correctly due to incorrect localization caused by the structurally defective cuticle (Wang *et al.*, 2011b).

Gibberellins have also been implicated in the regulation of cuticle biosynthesis. *Arabidopsis* plants with a mutation in *GLABRA1 (GL1)*, a gene that plays an important role in trichome development, were treated with gibberellic acid and this resulted in an increase in cuticular components (Xia *et al.*, 2010). Further, it has been observed that gibberellins are able to increase cuticle deposition in tomato (Knoche and Peschel, 2007) and apple (Barandoozi and Talaie, 2009). Gibberellins are routinely used to prevent apple russet, a disorder resulting from damaged or improperly formed cuticle. The mechanism of gibberellin induced cuticle biosynthesis has not been fully elucidated; however it seems that in *Arabidopsis* the SHN1/WIN1 transcription factor is at least partially responsible for mediating the gibberellin signal with regard to cuticle biosynthesis (Shi *et al.*, 2011). This was evident when analyzing the *Arabidopsis* gibberellin biosynthesis mutant, *ga1-3*, that displayed reduced *SHN1/WIN1* expression, while exogenous application of gibberellic acid to *ga1-3* plants increased the levels of *SHN1/WIN1* (Shi *et al.*, 2011). The reduction in *SHN1/WIN1* expression was consistent with a reduction in cutin load in *ga1-3* plants.

2.6.3 Post-Transcriptional and Epigenetic Mechanisms

While up until now most of the findings with respect to the regulation of cuticular pathways involved transcriptional regulation, some are concerned with post transcriptional mechanisms. In *Arabidopsis*, an exosomal exoribonuclease (CER7) was identified that apparently degrades mRNA(s) that code for a repressor of *CER3*, a major wax biosynthesis gene (Hooker *et al.*, 2007). Absence of *CER7* expression in *cer7* mutants resulted in reduced *CER3* expression and a concomitant reduction in stem wax. Recently two genes have been identified as potential degradation targets of CER7 namely *RNA-DEPENDENT RNA POLYMERASE1* (*RDR1*) and *SUPPRESSOR OF GENE SILENCING3* (*SGS3*) (Lam *et al.*, 2012). Both genes code for components of the RNAi-mediated gene silencing pathway, and it was therefore hypothesized that CER7 is able to degrade a small RNA species that negatively regulates the *CER3* wax biosynthesis gene (Lam *et al.*, 2012). Another gene involved in RNA processing that has been implicated in the regulation of cuticle biosynthesis is the *Arabidopsis Cap Binding Protein 20* (*AtCBP20*) (Jäger *et al*., 2011). *AtCBP20* encodes a protein that is part of a complex implicated in splicing, mRNA 3' end maturation and in the export of snRNAs from the nucleus (Jäger *et al*., 2011). *Arabidopsis cbp20* mutants are hypersensitive to ABA and display an increase in cuticle thickness as well as an increase in both trichome and stomata density (Jäger *et al*., 2011). This mutant therefore further highlights the connection between epidermal cell identity, cuticle biosynthesis and hormonal regulation and may prove interesting for further study.

Another likely component of the post-transcriptional regulatory system involved in cuticle biosynthesis is *CER9* (Lü *et al.*, 2012). This *Arabidopsis* gene encodes for an E3 ubiquitin ligase involved in the degradation of misfolded proteins in the endoplasmic reticulum. *Arabidopsis cer9* mutants show modifications in leaf and stem waxes, which, together with the fact that the biosynthesis of cuticle waxes occurs in the endoplasmic reticulum has led to the proposal that CER9 plays a role in maintaining the homeostasis of key cuticle biosynthesis genes (Lü *et al.*, 2012). Future work to identify the targets of CER9 and the small RNAs involved in CER7 mediated regulations is yet to be done. The identification of the orthologous processes in fleshy fruit will be of particular interest.

Recent work has highlighted the role of chromatin remodeling in the regulation of cuticle biosynthesis (Ménard *et al.*, 2014). The authors identified two RING E3 ligases,

namely HISTONE MONOUBIQUITINATION 1 and 2 (HUB1 and HUB2) that were required for the proper expression of the cuticle biosynthesis genes *LONG-CHAIN ACYL-CoA SYNTHASE2* (*LACS2)*, *CYP86A2*, *HOTHEAD* and *CER1*. Chromatin immunoprecipitation assays performed with *Arabidopsis* mutants *hub1-6* and *hub2-2* showed that the mutants were impaired in dynamic changes of histone H2B monoubiquitination at specific loci of *LACS2*, *CYP86A2*, *HOTHEAD* and *CER1*, resulting in the downregulation of transcription of these genes and a range of cuticle deficient phenotypes.

2.7 Conclusions

The cuticle membrane of fleshy fruit is a highly specialized and complex layer. While we have a relatively good understanding of the biosynthesis and assembly of the cuticle, we still have much to learn about the regulation of cuticle biosynthesis. Recent work however, has shown that the regulation of cuticle biosynthesis and deposition likely forms part of a global regulatory network controlling epidermal cell differentiation and response to environmental stresses. Regulation therefore occurs on multiple levels creating a complex network of not just transcription factors but also elements of post-transcriptional regulation and epigenetic effects. Together this makes the regulation of cuticle structure and function both a fascinating and challenging topic of research. It is therefore likely that regulation together with solving the final problem of cutin oligomer polymerization and transport will be a focus of future work. These lines of research are of particular interest in fleshy fruit due to the great impact the cuticle may have on fruit quality traits including resistance, appearance and texture. The mechanical failure of the fruit cuticle leads to sizable economic loss for both farmers and retailers, while conversely the fruit surface is the major feature by which the consumer is able to judge fruit quality. As our understanding of the relationship between cuticle structure and fruit surface characteristics advances we will increasingly be able to manipulate these important traits, leading to the possibility of improvement in fruit production and quality.

2.8 References

Abe M, Katsumata H, Komeda Y, Takahashi T. 2003. Regulation of shoot epidermal cell differentiation by a pair of homeodomain proteins in Arabidopsis. *Development* **130**, 635-643.

Adato A, Mandel T, Mintz-Oron S, Venger I, Levy D, Yativ M, Domínguez E, Wang Z, De Vos RC, Jetter R, Schreiber L, Heredia A, Rogachev I, Aharoni A. 2009. Fruit-surface flavonoid accumulation in tomato is controlled by a SlMYB12-regulated transcriptional network. *PLoS Genet* **5**, 823-851.

Aharoni A, Dixit S, Jetter R, Thoenes E, van Arkel G, Pereira A. 2004. The SHINE clade of AP2 domain transcription factors activates wax biosynthesis, alters cuticle properties, and confers drought tolerance when overexpressed in Arabidopsis. *Plant Cell* **16**, 2463-2480.

Alvarez-Buylla ER, Liljegren SJ, Pelaz S, Gold SE, Burgeff C, Ditta GS, Vergara-Silva F, Yanofsky MF. 2000. MADS-box gene evolution beyond flowers: expression in pollen, endosperm, guard cells, roots and trichomes. *Plant J* **24**, 457-466.

Ambawat S, Sharma P, Yadav NR, Yadav RC. 2013. MYB transcription factor genes as regulators for plant responses: an overview. *Physiol Mol Biol Plants* **19**, 307-321.

Ballester AR, Molthoff J, de Vos R, Hekkert B, Orzaez D, Fernández-Moreno JP, Tripodi P, Grandillo S, Martin C, Heldens J, Ykema M, Granell A, Bovy A. 2010. Biochemical and molecular analysis of pink tomatoes: deregulated expression of the gene encoding transcription factor SlMYB12 leads to pink tomato fruit color. *Plant Physiol* **152**, 71-84.

Barandoozi F, Talaie A. 2009. The effect of gibberellins on russeting in golden delicious apples. *Journal of Horticulture and Forestry* **1**, 61-64.

Bargel H, Koch K, Cerman Z, Neinhuis C. 2006. Structure–function relationships of the plant cuticle and cuticular waxes – a smart material?. *Functional Plant Biology* **33**, 893-910.

Baumann K, Perez-Rodriguez M, Bradley D, Venail J, Bailey P, Jin H, Koes R, Roberts K, Martin C. 2007. Control of cell and petal morphogenesis by R2R3 MYB transcription factors. *Development* **134**, 1691-1701.

Bemer M, Karlova R, Ballester AR, Tikunov YM, Bovy AG, Wolters-Arts M, Rossetto PeB, Angenent GC, de Maagd RA. 2012. The tomato FRUITFULL homologs TDR4/FUL1 and MBP7/FUL2 regulate ethylene-independent aspects of fruit ripening. *Plant Cell* **24**, 4437-4451.

Bessire M, Chassot C, Jacquat AC, Humphry M, Borel S, Petétot JM, Métraux JP, Nawrath C. 2007. A permeable cuticle in Arabidopsis leads to a strong resistance to Botrytis cinerea. *EMBO J* **26**, 2158-2168.

Bessire M, Borel S, Fabre G, Carraça L, Efremova N, Yephremov A, Cao Y, Jetter R, Jacquat AC, Métraux JP, Nawrath C. 2011. A member of the PLEIOTROPIC DRUG RESISTANCE family of ATP binding cassette transporters is required for the formation of a functional cuticle in Arabidopsis. *Plant Cell* **23**, 1958-70.

Bird D, Beisson F, Brigham A, Shin J, Greer S, Jetter R, Kunst L, Wu X, Yephremov A, Samuels L. 2007. Characterization of Arabidopsis ABCG11/WBC11, an ATP binding cassette (ABC) transporter that is required for cuticular lipid secretion. *Plant J* **52**, 485-98.

Bogs J, Jaffé FW, Takos AM, Walker AR, Robinson SP. 2007. The grapevine transcription factor VvMYBPA1 regulates proanthocyanidin synthesis during fruit development. *Plant Physiol* **143**, 1347-1361.

Bombarely A, Menda N, Tecle IY, Buels RM, Strickler S, Fischer-York T, Pujar A, Leto J, Gosselin J, Mueller LA. 2011. The Sol Genomics Network (solgenomics.net): growing tomatoes using Perl. *Nucleic Acids Res* **39**, D1149-1155.

Bowena DJ, Walton TJ. 1988. Cutin composition and biosynthesis during gibberellic acid-induced stem extension of Pisum sativum var. Meteor. *Plant Science* **55**, 115-127.

Brendolise C, Yauk YK, Eberhard ED, Wang M, Chagne D, Andre C, Greenwood DR, Beuning LL. 2011. An unusual plant triterpene synthase with predominant α-amyrin-producing activity identified by characterizing oxidosqualene cyclases from Malus × domestica. *FEBS J* **278**, 2485-99.

Broun P, Poindexter P, Osborne E, Jiang CZ, Riechmann JL. 2004. WIN1, a transcriptional activator of epidermal wax accumulation in Arabidopsis. *Proc Natl Acad Sci U S A* **101**, 4706-4711.

Buxdorf K, Rubinsky G, Barda O, Burdman S, Aharoni A, Levy M. 2014. The transcription factor SlSHINE3 modulates defense responses in tomato plants. *Plant Mol Biol* **84**, 37-47.

Chassot C, Nawrath C, Métraux JP. 2007. Cuticular defects lead to full immunity to a major plant pathogen. *Plant J* **49**, 972-980.

Chen X, Truksa M, Snyder CL, El-Mezawy A, Shah S, Weselake RJ. 2011. Three homologous genes encoding sn-glycerol-3-phosphate acyltransferase 4 exhibit different expression patterns and functional divergence in Brassica napus. *Plant Physiol* **155**, 851-65.

Cho S, Jang S, Chae S, Chung KM, Moon YH, An G, Jang SK. 1999. Analysis of the C-terminal region of Arabidopsis thaliana APETALA1 as a transcription activation domain. *Plant Mol Biol* **40**, 419-429.

Colombo M, Masiero S, Vanzulli S, Lardelli P, Kater MM, Colombo L. 2008. AGL23, a type I MADS-box gene that controls female gametophyte and embryo development in Arabidopsis. *Plant J* **54**, 1037-1048.

Cominelli E, Sala T, Calvi D, Gusmaroli G, Tonelli C. 2008. Over-expression of the Arabidopsis AtMYB41 gene alters cell expansion and leaf surface permeability. *Plant J* **53**, 53-64.

Consortium TG. 2012. The tomato genome sequence provides insights into fleshy fruit evolution. *Nature* **485**, 635-641.

Curvers K, Seifi H, Mouille G, de Rycke R, Asselbergh B, Van Hecke A, Vanderschaeghe D, Höfte H, Callewaert N, Van Breusegem F, Höfte M. 2010. Abscisic acid deficiency causes changes in cuticle permeability and pectin composition that influence tomato resistance to Botrytis cinerea. *Plant Physiol* **154**, 847-860.

De Folter S, Angenent GC. 2006. trans meets cis in MADS science. *Trends Plant Sci* **11**, 224-231.

Debono A, Yeats TH, Rose JK, Bird D, Jetter R, Kunst L, Samuels L. 2009. Arabidopsis LTPG is a glycosylphosphatidylinositol-anchored lipid transfer protein required for export of lipids to the plant surface. *Plant Cell* **21**, 1230-1238.

Deluc L, Barrieu F, Marchive C, Lauvergeat V, Decendit A, Richard T, Carde JP, Mérillon JM, Hamdi S. 2006. Characterization of a grapevine R2R3-MYB transcription factor that regulates the phenylpropanoid pathway. *Plant Physiol* **140**, 499-511.

Depège-Fargeix N, Javelle M, Chambrier P, Frangne N, Gerentes D, Perez P, Rogowsky PM, Vernoud V. 2011. Functional characterization of the HD-ZIP IV transcription factor OCL1 from maize. *J Exp Bot* **62**, 293-305.

Di Cristina M, Sessa G, Dolan L, Linstead P, Baima S, Ruberti I, Morelli G. 1996. The Arabidopsis Athb-10 (GLABRA2) is an HD-Zip protein required for regulation of root hair development. *Plant J* **10**, 393-402.

Di Stilio VS, Martin C, Schulfer AF, Connelly CF. 2009. An ortholog of MIXTA-like2 controls epidermal cell shape in flowers of Thalictrum. *New Phytol* **183**, 718-728.

Domínguez E, Luque P, Heredia A. 2009. Sorption and interaction of the flavonoid naringenin on tomato fruit cuticles. *J Agric Food Chem* **57**, 7560-7564.

Domínguez E, Cuartero J, Heredia A. 2011. An overview on plant cuticle biomechanics. *Plant Sci* **181**, 77-84.

Domínguez E, Fernández MD, Hernández JC, Parra JP, España L, Heredia A, Cuartero J. 2012. Tomato fruit continues growing while ripening, affecting cuticle properties and cracking. *Physiol Plant* **146**, 473-86.

Dubos C, Stracke R, Grotewold E, Weisshaar B, Martin C, Lepiniec L. 2010. MYB transcription factors in Arabidopsis. *Trends Plant Sci* **15**, 573-581.

Egea-Cortines M, Saedler H, Sommer H. 1999. Ternary complex formation between the MADS-box proteins SQUAMOSA, DEFICIENS and GLOBOSA is involved in the control of floral architecture in Antirrhinum majus. *EMBO J* **18**, 5370-5379.

Evans MM, Passas HJ, Poethig RS. 1994. Heterochronic effects of glossy15 mutations on epidermal cell identity in maize. *Development* **120**, 1971-1981.

Finkelstein RR, Rock CD. 2002. Abscisic Acid biosynthesis and response. *Arabidopsis Book* **1**, e0058.

Franke R, Briesen I, Wojciechowski T, Faust A, Yephremov A, Nawrath C, Schreiber L. 2005. Apoplastic polyesters in Arabidopsis surface tissues--a typical suberin and a particular cutin. *Phytochemistry* **66**, 2643-2658.

Giese BN. 1975. Effects of light and temperature on the composition of epicuticular wax of barley leaves. *Phytochemistry* **14**, 921-929.

Gilding EK, Marks MD. 2010. Analysis of purified glabra3-shapeshifter trichomes reveals a role for NOECK in regulating early trichome morphogenic events. *Plant J* **64**, 304-317.

Giménez E, Pineda B, Capel J, Antón MT, Atarés A, Pérez-Martín F, García-Sogo B, Angosto T, Moreno V, Lozano R. 2010. Functional analysis of the Arlequin mutant corroborates the essential role of the Arlequin/TAGL1 gene during reproductive development of tomato. *PLoS One* **5**, e14427.

Giovannoni JJ. 2004. Genetic regulation of fruit development and ripening. *Plant Cell* **16 Suppl**, S170-180.

Girard AL, Mounet F, Lemaire-Chamley M, Gaillard C, Elmorjani K, Vivancos J, Runavot JL, Quemener B, Petit J, Germain V, Rothan C, Marion D, Bakan B. 2012. Tomato GDSL1 is required for cutin deposition in the fruit cuticle. *Plant Cell* **24**, 3119-34.

Go YS, Kim H, Kim HJ, Suh MC. 2014. Arabidopsis Cuticular Wax Biosynthesis Is Negatively Regulated by the DEWAX Gene Encoding an AP2/ERF-Type Transcription Factor. *Plant Cell* doi:10.1105/tpc.114.123307.

Gutterson N, Reuber TL. 2004. Regulation of disease resistance pathways by AP2/ERF transcription factors. *Curr Opin Plant Biol* **7**, 465-471.

Gális I, Simek P, Narisawa T, Sasaki M, Horiguchi T, Fukuda H, Matsuoka K. 2006. A novel R2R3 MYB transcription factor NtMYBJS1 is a methyl jasmonate-dependent regulator of phenylpropanoid-conjugate biosynthesis in tobacco. *Plant J* **46**, 573-592.

Han J, Clement JM, Li J, King A, Ng S, Jaworski JG. 2010. The cytochrome P450 CYP86A22 is a fatty acyl-CoA omega-hydroxylase essential for Estolide synthesis in the stigma of Petunia hybrida. *J Biol Chem* **285**, 3986-96.

Harborne JB, Williams CA. 2000. Advances in flavonoid research since 1992. *Phytochemistry* **55**, 481-504.

Hooker TS, Lam P, Zheng H, Kunst L. 2007. A core subunit of the RNA-processing/degrading exosome specifically influences cuticular wax biosynthesis in Arabidopsis. *Plant Cell* **19**, 904-913.

Hülskamp M, Misŕa S, Jürgens G. 1994. Genetic dissection of trichome cell development in Arabidopsis. *Cell* **76**, 555-566.

Isaacson T, Kosma DK, Matas AJ, Buda GJ, He Y, Yu B, Pravitasari A, Batteas JD, Stark RE, Jenks MA, Rose JK. 2009. Cutin deficiency in the tomato fruit cuticle consistently affects resistance to microbial infection and biomechanical properties, but not transpirational water loss. *Plant J* **60**, 363-377.

Ishida T, Hattori S, Sano R, Inoue K, Shirano Y, Hayashi H, Shibata D, Sato S, Kato T, Tabata S, Okada K, Wada T. 2007. Arabidopsis TRANSPARENT TESTA GLABRA2 is directly regulated by R2R3 MYB transcription factors and is involved in regulation of GLABRA2 transcription in epidermal differentiation. *Plant Cell* **19**, 2531-2543.

Itkin M, Seybold H, Breitel D, Rogachev I, Meir S, Aharoni A. 2009. TOMATO AGAMOUS-LIKE 1 is a component of the fruit ripening regulatory network. *Plant J* **60**, 1081-1095.

Jäger K, Fábián A, Tompa G, Deák C, Höhn M, Olmedilla A, Barnabás B, Papp I. 2011. New phenotypes of the drought-tolerant cbp20 Arabidopsis thaliana mutant have changed epidermal morphology. *Plant Biol (Stuttg)* **13**, 78-84.

Jaillon O, Aury JM, Noel B, Policriti A, Clepet C, Casagrande A, Choisne N, Aubourg S, Vitulo N, Jubin C, Vezzi A, Legeai F, Hugueney P, Dasilva C, Horner D, Mica E, Jublot D, Poulain J, Bruyère C, Billault A, Segurens B, Gouyvenoux M, Ugarte E, Cattonaro F, Anthouard V, Vico V, Del Fabbro C, Alaux M, Di Gaspero G, Dumas V, Felice N, Paillard S, Juman I, Moroldo M, Scalabrin S, Canaguier A, Le Clainche I, Malacrida G, Durand E, Pesole G, Laucou V, Chatelet P, Merdinoglu D, Delledonne M, Pezzotti M, Lecharny A, Scarpelli C, Artiguenave F, Pè ME, Valle G, Morgante M, Caboche M, Adam-Blondon AF, Weissenbach J, Quétier F, Wincker P. 2007. The grapevine genome sequence suggests ancestral hexaploidization in major angiosperm phyla. *Nature* **449**, 463-467.

Javelle M, Vernoud V, Depège-Fargeix N, Arnould C, Oursel D, Domergue F, Sarda X, Rogowsky PM. 2010. Overexpression of the epidermis-specific homeodomain-leucine zipper IV transcription factor Outer Cell Layer1 in maize identifies target genes involved in lipid metabolism and cuticle biosynthesis. *Plant Physiol* **154**, 273-286.

Javelle M, Vernoud V, Rogowsky PM, Ingram GC. 2011. Epidermis: the formation and functions of a fundamental plant tissue. *New Phytol* **189**, 17-39.

Jetter R, Schäffer S. 2001. Chemical composition of the Prunus laurocerasus leaf surface. Dynamic changes of the epicuticular wax film during leaf development. *Plant Physiol* **126**, 1725-37.

Kannangara R, Branigan C, Liu Y, Penfield T, Rao V, Mouille G, Höfte H, Pauly M, Riechmann JL, Broun P. 2007. The transcription factor WIN1/SHN1 regulates Cutin biosynthesis in Arabidopsis thaliana. *Plant Cell* **19**, 1278-1294.

Kimbara J, Yoshida M, Ito H, Kitagawa M, Takada W, Hayashi K, Shibutani Y, Kusano M, Okazaki Y, Nakabayashi R, Mori T, Saito K, Ariizumi T, Ezura H. 2013. Inhibition of CUTIN DEFICIENT 2 Causes Defects in Cuticle Function and Structure and Metabolite Changes in Tomato Fruit. *Plant Cell Physiol* **54**, 1535-1548.

Knoche M, Peschel S. 2007. Gibberellins Increase Cuticle Deposition in Developing Tomato Fruit. *Plant Growth Regulation* **51**, 1-10.

Knoche M, Khanal BP, Stopar M. 2011. Russeting and Microcracking of 'Golden Delicious' Apple Fruit Concomitantly Decline Due to Gibberellin A_{4+7} Application. *Journal of American Society of Horticultural Science* **136**, 159-164.

Kosma DK, Bourdenx B, Bernard A, Parsons EP, Lü S, Joubès J, Jenks MA. 2009. The impact of water deficiency on leaf cuticle lipids of Arabidopsis. *Plant Physiol* **151**, 1918-1929.

Kolattukudy PE. 2001. Polyesters in higher plants. *Adv Biochem Eng Biotechnol* **71**, 1-49.

Kraus G. 1949. Morphologic-anatomical studies on development-conditioned changes in axis, leaf and ovary in some berry fruits. *Oesterr. Bot. Z.* **96**, 325-360.

Kubo H, Peeters AJ, Aarts MG, Pereira A, Koornneef M. 1999. ANTHOCYANINLESS2, a homeobox gene affecting anthocyanin distribution and root development in Arabidopsis. *Plant Cell* **11**, 1217-1226.

Kunst L, Samuels AL. 2003. Biosynthesis and secretion of plant cuticular wax. *Prog Lipid Res* **42**, 51-80.

Kurdyukov S, Faust A, Nawrath C, Bär S, Voisin D, Efremova N, Franke R, Schreiber L, Saedler H, Métraux JP, Yephremov A. 2006. The epidermis-specific extracellular BODYGUARD controls cuticle development and morphogenesis in Arabidopsis. *Plant Cell* **18**, 321-339.

Lam P, Zhao L, McFarlane HE, Aiga M, Lam V, Hooker TS, Kunst L. 2012. RDR1 and SGS3, components of RNA-mediated gene silencing, are required for the regulation of cuticular wax biosynthesis in developing inflorescence stems of Arabidopsis. *Plant Physiol* **159**, 1385-1395.

Leide J, Hildebrandt U, Reussing K, Riederer M, Vogg G. 2007. The developmental pattern of tomato fruit wax accumulation and its impact on cuticular transpiration barrier properties: effects of a deficiency in a beta-ketoacyl-coenzyme A synthase (LeCER6). *Plant Physiol* **144**, 1667-1679.

Leide J, Hildebrandt U, Vogg G, Riederer M. 2011. The positional sterile (ps) mutation affects cuticular transpiration and wax biosynthesis of tomato fruits. *J Plant Physiol* **168**, 871-7.

Li Y, Beisson F, Koo AJ, Molina I, Pollard M, Ohlrogge J. 2007. Identification of acyltransferases required for cutin biosynthesis and production of cutin with suberin-like monomers. *Proc Natl Acad Sci U S A* **104**, 18339-44.

Li-Beisson Y, Pollard M, Sauveplane V, Pinot F, Ohlrogge J, Beisson F. 2009. Nanoridges that characterize the surface morphology of flowers require the synthesis of cutin polyester. *Proc Natl Acad Sci U S A* **106**, 22008-13.

Lippold F, Sanchez DH, Musialak M, Schlereth A, Scheible WR, Hincha DK, Udvardi MK. 2009. AtMyb41 regulates transcriptional and metabolic responses to osmotic stress in Arabidopsis. *Plant Physiol* **149**, 1761-1772.

Lisso J, Schröder F, Schippers JH, Müssig C. 2012. NFXL2 modifies cuticle properties in Arabidopsis. *Plant Signal Behav* **7**, 551-555.

Liu J, Xu B, Hu L, Li M, Su W, Wu J, Yang J, Jin Z. 2009. Involvement of a banana MADS-box transcription factor gene in ethylene-induced fruit ripening. *Plant Cell Rep* **28**, 103-111.

Lu P, Porat R, Nadeau JA, O'Neill SD. 1996. Identification of a meristem L1 layer-specific gene in Arabidopsis that is expressed during embryonic pattern formation and defines a new class of homeobox genes. *Plant Cell* **8**, 2155-2168.

López-Casado G, Matas AJ, Domínguez E, Cuartero J, Heredia A. 2007. Biomechanics of isolated tomato (Solanum lycopersicum L.) fruit cuticles: the role of the cutin matrix and polysaccharides. *J Exp Bot* **58**, 3875-3883.

Lopez-Casado G, Salamanca A, Heredia A. 2010. Viscoelastic nature of isolated tomato (Solanum lycopersicum) fruit cuticles: a mathematical model. *Physiol Plant* **140**, 79-88.

Lü S, Zhao H, Des Marais DL, Parsons EP, Wen X, Xu X, Bangarusamy DK, Wang G, Rowland O, Juenger T, Bressan RA, Jenks MA. 2012. Arabidopsis ECERIFERUM9 involvement in cuticle formation and maintenance of plant water status. *Plant Physiol* **159**, 930-944.

Machado A, Wu Y, Yang Y, Llewellyn DJ, Dennis ES. 2009. The MYB transcription factor GhMYB25 regulates early fibre and trichome development. *Plant J* **59**, 52-62.

Mahjoub A, Hernould M, Joubès J, Decendit A, Mars M, Barrieu F, Hamdi S, Delrot S. 2009. Overexpression of a grapevine R2R3-MYB factor in tomato affects vegetative development, flower morphology and flavonoid and terpenoid metabolism. *Plant Physiol Biochem* **47**, 551-561.

Martin C, Paz-Ares J. 1997. MYB transcription factors in plants. *Trends Genet* **13**, 67-73.

Masucci JD, Rerie WG, Foreman DR, Zhang M, Galway ME, Marks MD, Schiefelbein JW. 1996. The homeobox gene GLABRA2 is required for position-dependent cell differentiation in the root epidermis of Arabidopsis thaliana. *Development* **122**, 1253-1260.

Matas AJ, Yeats TH, Buda GJ, Zheng Y, Chatterjee S, Tohge T, Ponnala L, Adato A, Aharoni A, Stark R, Fernied AR, Fei Z, Giovannoni JJ, Rose JK. 2011. Tissue- and cell-type specific transcriptome profiling of expanding tomato fruit provides insights into metabolic and regulatory specialization and cuticle formation. *Plant Cell* **23**, 3893-3910.

Matus JT, Loyola R, Vega A, Peña-Neira A, Bordeu E, Arce-Johnson P, Alcalde JA. 2009. Post-veraison sunlight exposure induces MYB-mediated transcriptional regulation of anthocyanin and flavonol synthesis in berry skins of Vitis vinifera. *J Exp Bot* **60**, 853-867.

McCourt RM, Delwiche CF, Karol KG. 2004. Charophyte algae and land plant origins. *Trends Ecol Evol* **19**, 661-666.

Mehrtens F, Kranz H, Bednarek P, Weisshaar B. 2005. The Arabidopsis transcription factor MYB12 is a flavonol-specific regulator of phenylpropanoid biosynthesis. *Plant Physiol* **138**, 1083-1096.

Mintz-Oron S, Mandel T, Rogachev I, Feldberg L, Lotan O, Yativ M, Wang Z, Jetter R, Venger I, Adato A, Aharoni A. 2008. Gene expression and metabolism in tomato fruit surface tissues. *Plant Physiol* **147**, 823-851.

Moose SP, Sisco PH. 1994. Glossy15 Controls the Epidermal Juvenile-to-Adult Phase Transition in Maize. *Plant Cell* **6**, 1343-1355.

Moose SP, Sisco PH. 1996. Glossy15, an APETALA2-like gene from maize that regulates leaf epidermal cell identity. *Genes Dev* **10**, 3018-3027.

Muir SR, Collins GJ, Robinson S, Hughes S, Bovy A, Ric De Vos CH, van Tunen AJ, Verhoeyen ME. 2001. Overexpression of petunia chalcone isomerase in tomato results in fruit containing increased levels of flavonols. *Nat Biotechnol* **19**, 470-474.

Ménard R, Verdier G, Ors M, Erhardt M, Beisson F, Shen WH. 2014. Histone H2B Monoubiquitination is Involved in the Regulation of Cutin and Wax Composition in Arabidopsis thaliana. *Plant Cell Physiol* **55**, 455-466.

Nadakuduti SS, Pollard M, Kosma DK, Allen C, Ohlrogge JB, Barry CS. 2012. Pleiotropic phenotypes of the sticky peel mutant provide new insight into the role of CUTIN DEFICIENT2 in epidermal cell function in tomato. *Plant Physiol* **159**, 945-960.

Nakamura M, Katsumata H, Abe M, Yabe N, Komeda Y, Yamamoto KT, Takahashi T. 2006. Characterization of the class IV homeodomain-Leucine Zipper gene family in Arabidopsis. *Plant Physiol* **141**, 1363-1375.

Nambara E, Marion-Poll A. 2005. Abscisic acid biosynthesis and catabolism. *Annu Rev Plant Biol* **56**, 165-185.

Nawrath C. 2006. Unraveling the complex network of cuticular structure and function. *Curr Opin Plant Biol* **9**, 281-287.

Neinhuis C, Barthlott W. 1997. Characterization and distribution of waterrepellent, self-cleaning plant surfaces. *Annals of Botany* **79**, 667-677.

Ng M, Yanofsky MF. 2001. Function and evolution of the plant MADS-box gene family. *Nat Rev Genet* **2**, 186-195.

Noda K, Glover BJ, Linstead P, Martin C. 1994. Flower colour intensity depends on specialized cell shape controlled by a Myb-related transcription factor. *Nature* **369**, 661-664.

Oshima Y, Shikata M, Koyama T, Ohtsubo N, Mitsuda N, Ohme-Takagi M. 2013. MIXTA-like transcription factors and WAX INDUCER1/SHINE1 coordinately regulate cuticle development in Arabidopsis and Torenia fournieri. *Plant Cell* **25**, 1609-1624.

Panikashvili D, Aharoni A. 2008. ABC-type transporters and cuticle assembly: Linking function to polarity in epidermis cells. *Plant Signal Behav* **3**, 806-9.

Panikashvili D, Savaldi-Goldstein S, Mandel T, Yifhar T, Franke RB, Höfer R, Schreiber L, Chory J, Aharoni A. 2007. The Arabidopsis DESPERADO/AtWBC11 transporter is required for cutin and wax secretion. *Plant Physiol* **145**, 1345-60.

Panikashvili D, Shi JX, Schreiber L, Aharoni A. 2009. The Arabidopsis DCR encoding a soluble BAHD acyltransferase is required for cutin polyester formation and seed hydration properties. *Plant Physiol* **151**, 1773-1789.

Panikashvili D, Shi JX, Schreiber L, Aharoni A. 2011. The Arabidopsis ABCG13 transporter is required for flower cuticle secretion and patterning of the petal epidermis. *New Phytol* **190**, 113–124.

Perez-Rodriguez M, Jaffe FW, Butelli E, Glover BJ, Martin C. 2005. Development of three different cell types is associated with the activity of a specific MYB transcription factor in the ventral petal of Antirrhinum majus flowers. *Development* **132**, 359-370.

Peschel S, Franke R, Schreiber L, Knoche M. 2007. Composition of the cuticle of developing sweet cherry fruit. *Phytochemistry* **68**, 1017-1025.

Pighin JA, Zheng H, Balakshin LJ, Goodman IP, Western TL, Jetter R, Kunst L, Samuels AL. 2004. Plant cuticular lipid export requires an ABC transporter. *Science* **306**, 702-704.

Plett JM, Wilkins O, Campbell MM, Ralph SG, Regan S. 2010. Endogenous overexpression of Populus MYB186 increases trichome density, improves insect pest resistance, and impacts plant growth. *Plant J* **64**, 419-432.

Pollard M, Beisson F, Li Y, Ohlrogge JB. 2008. Building lipid barriers: biosynthesis of cutin and suberin. *Trends Plant Sci* **13**, 236-246.

Raffaele S, Vailleau F, Léger A, Joubès J, Miersch O, Huard C, Blée E, Mongrand S, Domergue F, Roby D. 2008. A MYB transcription factor regulates very-long-chain fatty acid biosynthesis for activation of the hypersensitive cell death response in Arabidopsis. *Plant Cell* **20**, 752-767.

Rani, SH, Krishna, TH, Saha, S, Negi, AS. Rajasekharan, R. 2010. Defective in cuticular

ridges (DCR) of Arabidopsis thaliana, a gene associated with surface cutin formation, encodes a

soluble diacylglycerol acyltransferase. *Journal ofBiological Chemistry* **285**, 38337-38347.

Reina-Pinto JJ, Yephremov A. 2009. Surface lipids and plant defenses. *Plant Physiol Biochem* **47**, 540-549.

Rerie WG, Feldmann KA, Marks MD. 1994. The GLABRA2 gene encodes a homeo domain protein required for normal trichome development in Arabidopsis. *Genes Dev* **8**, 1388-1399.

Riederer M, Muller C (*eds*) (2006) Biology of the Plant Cuticle. *Annual Plant Reviews* 23. Blackwell, Oxford, UK.

Saladie M, Rose JKC, Watkins CB. 2005. Characterization of DFD (Delayed Fruit Deterioration): a new tomato mutant. *Acta horticulturae* 79-84.

Saladié M, Matas AJ, Isaacson T, Jenks MA, Goodwin SM, Niklas KJ, Xiaolin R, Labavitch JM, Shackel KA, Fernie AR, Lytovchenko A, O'Neill MA, Watkins CB, Rose JK. 2007. A reevaluation of the key factors that influence tomato fruit softening and integrity. *Plant Physiol* **144**, 1012-1028.

Shepherd T, Robertson GW, Griffiths DW, Birch ANE, Duncan G. 1995. Effects of environment on the composition of epicuticular wax from kale and swede. *Phytochemistry* **40,** 407-417.

Samuels L, Kunst L, Jetter R. 2008. Sealing plant surfaces: cuticular wax formation by epidermal cells. *Annu Rev Plant Biol* **59**, 683-707.

San-Bento R, Farcot E, Galletti R, Creff A, Ingram G. 2013. Epidermal identity is maintained by cell-cell communication via a universally active feedback loop in Arabidopsis thaliana. *Plant J*.

Schijlen EG, de Vos CH, Martens S, Jonker HH, Rosin FM, Molthoff JW, Tikunov YM, Angenent GC, van Tunen AJ, Bovy AG. 2007. RNA interference silencing of chalcone synthase, the first step in the flavonoid biosynthesis pathway, leads to parthenocarpic tomato fruits. *Plant Physiol* **144**, 1520-30.

Schnurr J, Shockey J, Browse J. 2004. The acyl-CoA synthetase encoded by LACS2 is essential for normal cuticle development in Arabidopsis. *Plant Cell* **16**, 629-42.

Schreiber L. 2010. Transport barriers made of cutin, suberin and associated waxes. *Trends Plant Sci* **15**, 546-53.

Schrick K, Nguyen D, Karlowski WM, Mayer KF. 2004. START lipid/sterol-binding domains are amplified in plants and are predominantly associated with homeodomain transcription factors. *Genome Biol* **5**, R41.

Schwartz SH, Tan BC, Gage DA, Zeevaart JA, McCarty DR. 1997. Specific oxidative cleavage of carotenoids by VP14 of maize. *Science* **276**, 1872-1874.

Seo PJ, Lee SB, Suh MC, Park MJ, Go YS, Park CM. 2011. The MYB96 transcription factor regulates cuticular wax biosynthesis under drought conditions in Arabidopsis. *Plant Cell* **23**, 1138-1152.

Seo PJ, Xiang F, Qiao M, Park JY, Lee YN, Kim SG, Lee YH, Park WJ, Park CM. 2009. The MYB96 transcription factor mediates abscisic acid signaling during drought stress response in Arabidopsis. *Plant Physiol* **151**, 275-289.

Sessions A, Weigel D, Yanofsky MF. 1999. The Arabidopsis thaliana MERISTEM LAYER 1 promoter specifies epidermal expression in meristems and young primordia. *Plant J* **20**, 259-263.

Shepherd T, Wynne Griffiths D. 2006. The effects of stress on plant cuticular waxes. *New Phytol* **171**, 469-499.

Shi JX, Adato A, Alkan N, He Y, Lashbrooke J, Matas AJ, Meir S, Malitsky S, Isaacson T, Prusky D, Leshkowitz D, Schreiber L, Granell AR, Widemann E, Grausem B, Pinot F, Rose JK, Rogachev I, Rothan C, Aharoni A. 2013. The tomato SlSHINE3 transcription factor regulates fruit cuticle formation and epidermal patterning. *New Phytol* **197**, 468-480.

Shi JX, Malitsky S, De Oliveira S, Branigan C, Franke RB, Schreiber L, Aharoni A. 2011. SHINE transcription factors act redundantly to pattern the archetypal surface of Arabidopsis flower organs. *PLoS Genet* **7**, e1001388.

Shima Y, Kitagawa M, Fujisawa M, Nakano T, Kato H, Kimbara J, Kasumi T, Ito Y. 2013. Tomato FRUITFULL homologues act in fruit ripening via forming MADS-box transcription factor complexes with RIN. *Plant Mol Biol* **82**, 427-438.

Stracke R, Ishihara H, Huep G, Barsch A, Mehrtens F, Niehaus K, Weisshaar B. 2007. Differential regulation of closely related R2R3-MYB transcription factors controls

flavonol accumulation in different parts of the Arabidopsis thaliana seedling. *Plant J* **50**, 660-677.

Stracke R, Werber M, Weisshaar B. 2001. The R2R3-MYB gene family in Arabidopsis thaliana. *Curr Opin Plant Biol* **4**, 447-456.

Sturaro M, Hartings H, Schmelzer E, Velasco R, Salamini F, Motto M. 2005. Cloning and characterization of GLOSSY1, a maize gene involved in cuticle membrane and wax production. *Plant Physiol* **138**, 478-89.

Tang D, Simonich MT, Innes RW. 2007. Mutations in LACS2, a long-chain acyl-coenzyme A synthetase, enhance susceptibility to avirulent Pseudomonas syringae but confer resistance to Botrytis cinerea in Arabidopsis. *Plant Physiol* **144**, 1093-103.

Tominaga-Wada R, Iwata M, Sugiyama J, Kotake T, Ishida T, Yokoyama R, Nishitani K, Okada K, Wada T. 2009. The GLABRA2 homeodomain protein directly regulates CESA5 and XTH17 gene expression in Arabidopsis roots. *Plant J* **60**, 564-574.

Verhoeyen ME, Bovy A, Collins G, Muir S, Robinson S, de Vos CH, Colliver S. 2002. Increasing antioxidant levels in tomatoes through modification of the flavonoid biosynthetic pathway. *J Exp Bot* **53**, 2099-106.

Vogg G, Fischer S, Leide J, Emmanuel E, Jetter R, Levy AA, Riederer M. 2004. Tomato fruit cuticular waxes and their effects on transpiration barrier properties: functional characterization of a mutant deficient in a very-long-chain fatty acid beta-ketoacyl-CoA synthase. *J Exp Bot* **55**, 1401-1410.

Vrebalov J, Pan IL, Arroyo AJ, McQuinn R, Chung M, Poole M, Rose J, Seymour G, Grandillo S, Giovannoni J, Irish VF. 2009. Fleshy fruit expansion and ripening are regulated by the Tomato SHATTERPROOF gene TAGL1. *Plant Cell* **21**, 3041-3062.

Walford SA, Wu Y, Llewellyn DJ, Dennis ES. 2011. GhMYB25-like: a key factor in early cotton fibre development. *Plant J* **65**, 785-797.

Walford SA, Wu Y, Llewellyn DJ, Dennis ES. 2012. Epidermal cell differentiation in cotton mediated by the homeodomain leucine zipper gene, GhHD-1. *Plant J* **71**, 464-478.

Wang Z, Guhling O, Yao R, Li F, Yeats TH, Rose JK, Jetter R. 2011a. Two oxidosqualene cyclases responsible for biosynthesis of tomato fruit cuticular triterpenoids. *Plant Physiol* **155**, 540-552.

Wang ZY, Xiong L, Li W, Zhu JK, Zhu J. 2011b. The plant cuticle is required for osmotic stress regulation of abscisic acid biosynthesis and osmotic stress tolerance in Arabidopsis. *Plant Cell* **23**, 1971-1984.

Whipple CJ, Ciceri P, Padilla CM, Ambrose BA, Bandong SL, Schmidt RJ. 2004. Conservation of B-class floral homeotic gene function between maize and Arabidopsis. *Development* **131**, 6083-6091.

Xia Y, Yu K, Navarre D, Seebold K, Kachroo A, Kachroo P. 2010. The glabra1 mutation affects cuticle formation and plant responses to microbes. *Plant Physiol* **154**, 833-846.

Xu ZS, Chen M, Li LC, Ma YZ. 2011. Functions and application of the AP2/ERF transcription factor family in crop improvement. *J Integr Plant Biol* **53**, 570-585.

Yeats T, Martin L, Viart H, Isaacson T, He Y, Zhao L, Matas A, Buda G, Domozych D, Clausen M, Rose J. 2012. The identification of cutin synthase: formation of the plant polyester cutin. *Nature Chemical Biolog,* **8**, 609-611.

Yeats TH, Rose JK. 2013. The formation and function of plant cuticles. *Plant Physiol* **163**, 5-20.

Yeats TH, Huang W, Chatterjee S, Viart HM, Clausen MH, Stark RE, Rose JK. 2014. Tomato Cutin Deficient 1 (CD1) and putative orthologs comprise an ancient family of cutin synthase-like (CUS) proteins that are conserved among land plants. *Plant J* **77**, 667-675.

Zhang H, Forde BG. 1998. An Arabidopsis MADS box gene that controls nutrient-induced changes in root architecture. *Science* **279**, 407-409.

Zhang JY, Broeckling CD, Blancaflor EB, Sledge MK, Sumner LW, Wang ZY. 2005. Overexpression of WXP1, a putative Medicago truncatula AP2 domain-containing transcription factor gene, increases cuticular wax accumulation and enhances drought tolerance in transgenic alfalfa (Medicago sativa). *Plant J* **42**, 689-707.

Zhang JY, Broeckling CD, Sumner LW, Wang ZY. 2007. Heterologous expression of two Medicago truncatula putative ERF transcription factor genes, WXP1 and WXP2, in Arabidopsis led to increased leaf wax accumulation and improved drought tolerance, but differential response in freezing tolerance. *Plant Mol Biol* **64**, 265-278.

Zhu JK. 2002. Salt and drought stress signal transduction in plants. *Annu Rev Plant Biol* **53**, 247-273.

Chapter 3

Research Results

The Tomato *MIXTA-like* Transcription Factor Coordinates Fruit Epidermis Conical Cell Development and Cuticular Lipid Biosynthesis and Assembly

This chapter has been compiled from a manuscript published in *Plant Physiology* as referenced below, and is written in the style and format of that journal.

Lashbrooke J, Adato A, Lotan O, Alkan N, Tsimbalist T, Rechav K, Fernandez-Moreno J-P, Widemann E, Grausem B, Pinot F, Granell A, Costa F, Aharoni A (2015) The Tomato MIXTA-like Transcription Factor Coordinates Fruit Epidermis Conical Cell Development and Cuticular Lipid Biosynthesis and Assembly. *Plant Physiology.* doi: 10.1104/pp.15.01145

3.1 Introduction

The epidermal layer of plants is a multifunctional and diverse tissue. Epidermal cells interact directly with the surrounding environment, and as such are involved in a number of processes, including osmotic regulation, defense and pollinator attraction (Glover, 2000; Martin and Glover, 2007; Whitney et al., 2009). In order to optimally perform these functions, cells of the epidermis are differentiated into a variety of cell types. For the above ground parts of plants this typically includes pavement cells, trichomes and stomatal guard cells. Each of these cell types may be further differentiated, resulting in a range of more subtle variations and morphological shapes. An excellent example of this subtle variation can be seen in the conical cell shape of petal epidermal cells (Whitney et al., 2009; Whitney et al., 2011). The widespread occurrence of these conical petal epidermal cells in nature has been associated with petal color, petal reflection, scent production, petal wettability and pollinator grip on the flower surface (Neinhuis and Barthlott, 1997; Riederer and Muller, 2006; Whitney et al., 2009).

One of the major evolutionary developments of land plants was the formation of the cuticular membrane (or cuticle) found to the exterior of the source of its building blocks, the epidermis layer. The cuticle provides a waterproof barrier between epidermal cells and the comparatively dry external environment (Riederer and Muller, 2006). It also plays an important role in the protection of plants against biotic and abiotic stresses such as pathogen attack and damaging UV light (Bargel et al., 2006). Recent research has highlighted the cuticle as an important element in the plant's detection and transmission of osmotic stress signals (Wang et al., 2011). The cuticle is comprised of a polymerized cutin matrix embedded with waxes (Kolattukudy, 2001). In many fleshy fruit, including *Solanum lycopersicum* (tomato), the major monomer of the cutin matrix is the C16-9/10, 16-dihydroxy fatty acid (DiHFA) (Mintz-Oron et al., 2008). A number of the enzymatic steps for the biosynthesis, extracellular transport and polymerization of the cutin matrix have been described in *Arabidopsis*, and to some extent in tomato. In short, free fatty acids (FFA) are synthesized in the chloroplast, transported to the endoplasmic reticulum, and subsequently modified. Modification includes mid- and terminal-chain hydroxylation and CoA-activation followed by transfer to a glycerol moiety. Enzymes responsible for these steps include long-chain acyl-CoA synthetases (LACSs), (Schnurr et al., 2004; Jessen et al., 2011), oxidases (CYP86A and CYP77A), (Li-Beisson et al., 2009; Pinot and Beisson, 2011; Shi et al., 2013) and

acyltransferases (GPATs and likely DCR), (Panikashvili et al., 2009; Rani et al., 2010; Yang et al., 2010; Yang et al., 2012). The resultant monoacylglycerols undergo extracellular transport and finally polymerization to form the cutin matrix. Enzymes responsible for these steps include ATP-binding-cassette (ABC) transporters (Bird et al., 2007; Bessire et al., 2011; Panikashvili et al., 2011) and cutin synthases (GDSL/CUSs and BDG (Kurdyukov et al., 2006; Girard et al., 2012; Yeats et al., 2012; Yeats et al., 2014).

Interestingly, the characterization of mutants and transgenic plants altered in cuticle assembly revealed a major effect on the patterning of epidermis cells. *Arabidopsis* mutants for *cyp77a6* and *gpat6* both exhibit a lack of cuticular nanoridges as well as petals with flatter epidermal cells (Li-Beisson et al., 2009). The lack of cuticular nanoridges was also observed in *dcr Arabidopsis* mutants (Panikashvili et al., 2009), while *Arabidopsis* mutants for genes possibly responsible for cutin synthesis, *bdg* and *gdsl*, show changes to epidermal cell shape (Kurdyukov et al., 2006). Study of transcriptional regulators further revealed a tight relationship between the cuticle and epidermal cell. It appears that a number of reported regulators of epidermal cell differentiation and cuticle biosynthesis are closely related proteins belonging to the same gene families (Hen-Avivi et al., 2014). Of particular interest in this regard are transcription factors from the SHN1/WIN1 clade of the APETELA2 (AP2)-domain superfamily, the homeodomain-leucine zipper IV (HD-ZIP IV) and R2-R3 MYB factors families. Members of the HD-ZIP IV family were shown to regulate cuticle metabolism in tomato and maize including CUTIN DEFICIENT2 (CD2), (Isaacson et al., 2009; Nadakuduti et al., 2012) and OUTER CELL LAYER1 (OCL1), (Javelle et al., 2010; Depège-Fargeix et al., 2011), respectively. Other HD-ZIP IV proteins including AtGL2 (Rerie et al., 1994; Ishida et al., 2007; Tominaga-Wada et al., 2009; Tominaga-Wada et al., 2013), AtPDF2 (Abe et al., 2003), AtHDG11 (Nakamura et al., 2006), ATML1 (Abe et al., 2003; Takada et al., 2013), and GhHD-1 (Walford et al., 2012), were demonstrated to be involved in the regulation of epidermal cell differentiation. Two members of the SHN1/WIN1 clade of transcription factors from *Arabidopsis* and tomato (AtSHN1 and SlSHN3, respectively), have been shown to be required for both cutin biosynthesis as well as epidermal cell patterning (Aharoni et al., 2004; Broun et al., 2004; Shi et al., 2011; Shi et al., 2013). Finally, members of the R2R3 MYB transcription factor superfamily, AtMYB41 and AtMYB96, have also been shown to regulate wax deposition during abiotic stress (Cominelli et al., 2008; Seo et al., 2011), although more recent results suggest that AtMYB41 likely promotes suberin biosynthesis and deposition (Kosma et al., 2014).

Members of the MYB protein family termed MIXTA or MIXTA-like were shown to be key regulators of epidermal cell differentiation across multiple plant species (Martin and Glover, 2007; Brockington et al., 2013). Orthologs of the MIXTA/MIXTA-like clade have been reported specifically to act as positive regulators of conical epidermal cell formation (Noda et al., 1994; Baumann et al., 2007; Di Stilio et al., 2009), trichome development (Perez-Rodriguez et al., 2005; Gilding and Marks, 2010; Plett et al., 2010) and cotton fiber development (Machado et al., 2009; Walford et al., 2011). Recently *Arabidopsis* MIXTA-like orthologs, AtMYB16 and AtMYB106, were demonstrated to regulate cuticle development (Oshima et al., 2013). To date however, *MIXTA/MIXTA-like* clade genes were not characterized with relation to fleshy fruit surface. In a recent work characterizing SlSHN3 activity in tomato, it was suggested that this transcription factor may exert its influence on epidermal cell patterning through HD-ZIP IV and/or MIXTA transcription factors (Shi et al., 2013). While expression of a tomato *MIXTA-like* gene (i.e. *SlMIXTA-like*) was shown earlier to be enriched in the epidermal tissue throughout tomato fruit development (Mintz-Oron et al., 2008), its functional role in tomato fruit surface was not examined.

In this work we functionally characterize the tomato *SlMIXTA-like* gene through the detailed investigation of lines with transgenically silenced *SlMIXTA-like* expression. Our findings show that SlMIXTA-like not only promotes conical epidermal cell development in tomato fruit, but is a major positive regulator of cuticular lipids, more specifically cutin monomer biosynthesis as well as cuticle assembly. This is apparent from the wide range of down-regulated cutin biosynthetic genes in tomato lines silenced for *SlMIXTA-like* expression, as well as the notable correlation between *SlMIXTA-like* expression and the deposition of cuticle. Thus, this study further advances the understanding of co-regulation between epidermal cell patterning and cuticle biosynthesis during organ formation.

3.2 Results

3.2.1 The Tomato Genome Contains a Single Expressed Member of the MIXTA/MIXTA-like Gene Family that is Predominantly Expressed in the Fruit Epidermal Layer

Analysis of the tomato genome via BLAST searches using well characterized MIXTA and MIXTA-like proteins from *Antirrhinum majus* and *Petunia hybrida* (AmMIXTA (Noda et al., 1994) and PhMYB1 (Baumann et al., 2007), respectively) as input, identified a number of potential tomato orthologs of this clade. Molecular phylogenetic analysis of the best hits revealed that the tomato genome retains seven potential orthologs to the clade containing MIXTA and MIXTA-like proteins (R2R3-MYB group 9) (Supplemental Fig. S1) (Stracke et al., 2001; Brockington et al., 2013). This group of MYB factors also includes MYB17 proteins, with which two of the tomato candidates (Solyc01g094360 and Solyc05g048830) group. These candidates can therefore be ruled out as potential MIXTA/MIXTA-like orthologs (Supplemental Fig. S1). Of the remaining five candidates, four group separately from both the MYB17 and the MIXTA/MIXTA-like branch (Solyc01g010910, Solyc04g005600, Solyc05g007690 and Solyc05g007710) and may be considered a novel group (Supplemental Fig. S1). These four genes show no expression in previously generated large scale multi-organ expression data (Itkin et al., 2013) and thus were not investigated further. The final identified candidate (Solyc02g088190) groups in the MIXTA-like branch of the phylogenetic tree (Supplemental Fig. S1). This protein termed SlMIXTA-like, shares 75% and 80% amino acid identity with the well characterized MIXTA-like epidermal cell differentiation factors, AmMYBML2 and PhMYB1, respectively (Baumann et al., 2007). A molecular phylogenetic tree for all previously characterized MIXTA and MIXTA-like proteins showed that SlMIXTA-like groups with MIXTA-like orthologs (Fig. 1A). Previous results have demonstrated that *SlMIXTA-like* has enriched transcript levels in the surface layers of fruit (Mintz-Oron et al., 2008; Shi et al., 2013). Quantitative Real Time-PCR (qRT-PCR) analysis of *SlMIXTA-like* expression in five stages of tomato fruit development in skin (epidermal enriched) and flesh tissues revealed that while expression levels were highest in the skin at the immature green stage of fruit development, expression remained high in this tissue throughout development (Mintz-Oron et al., 2008). *SlMIXTA-like* transcripts in the skin were found to be at least 16-fold higher than in flesh at all measured stages of development. Examination of publically available large-scale gene expression data for

various fruit cell-types (Matas et al., 2011), revealed that *SlMIXTA-like* expression is predominantly detected in the outer- and inner-epidermis of the fruit, albeit to a lesser extent in the latter (Fig. 1B). The inner epidermal layer of tomato fruit separates the locular region from the pericarp. A very low level of *SlMIXTA-like* expression was detected in the collenchyma tissue and none in the vasculature and parenchyma. Additionally, the expression profile of *SlMIXTA-like* across 20 tomato tissues (Itkin et al., 2013) showed that while fruit transcripts were enriched in the skin (at all 5 stages of fruit development examined), significant expression could be detected in petals, buds and pollen (Fig. 1C).

3.2.2 Silencing of *SlMIXTA-like* Results in the Flattening of Epidermal Cells and a Thinner Cuticle in Tomato Fruit

To investigate the function of *SlMIXTA-like* in tomato fruit surface development, silenced (*SlMIXTA*-RNAi) lines were generated (Fig. 2). *SlMIXTA*-RNAi tomato lines exhibited a variety of phenotypes at the vegetative stage, including retarded growth and smaller, crinkled and curled leaves (Fig. 2, B and C). Fruit of the *SlMIXTA*-RNAi plants appeared glossier than wild-type fruits, and were subsequently subject to detailed investigation.

A variety of microscopy techniques were employed to investigate the changes in the surface morphology of the tomato lines with reduced *SlMIXTA-like* expression. Initial observations by light microscopy and lipid staining (using Sudan IV stain) revealed significantly less cuticle deposition in the fruit of *SlMIXTA*-RNAi lines throughout development and what appeared to be flatter epidermal cells (Fig. 3). While in wild type tomato the cuticle frequently surrounds the entire epidermal cell (Mintz-Oron et al., 2008; Matas et al., 2011), *SlMIXTA*-RNAi fruit displayed almost no sub-epidermal staining (Fig. 3, A and B). Cryo-scanning electron microscopy (Cryo-SEM) and atomic force microscopy (AFM) confirmed the change in cell shape and a concomitant change in the surface morphology of the tomato fruit (Fig. 3, C and D). Analysis by AFM revealed a disrupted and rough micro-surface (Fig. 3D; Supplemental Fig. S3). Transmission electron microscopy (TEM) illustrated the typical conical shape of tomato fruit epidermal cells in wild-type and confirmed that lines silenced for *SlMIXTA-like* expression possessed flatter cells (Fig. 3E).

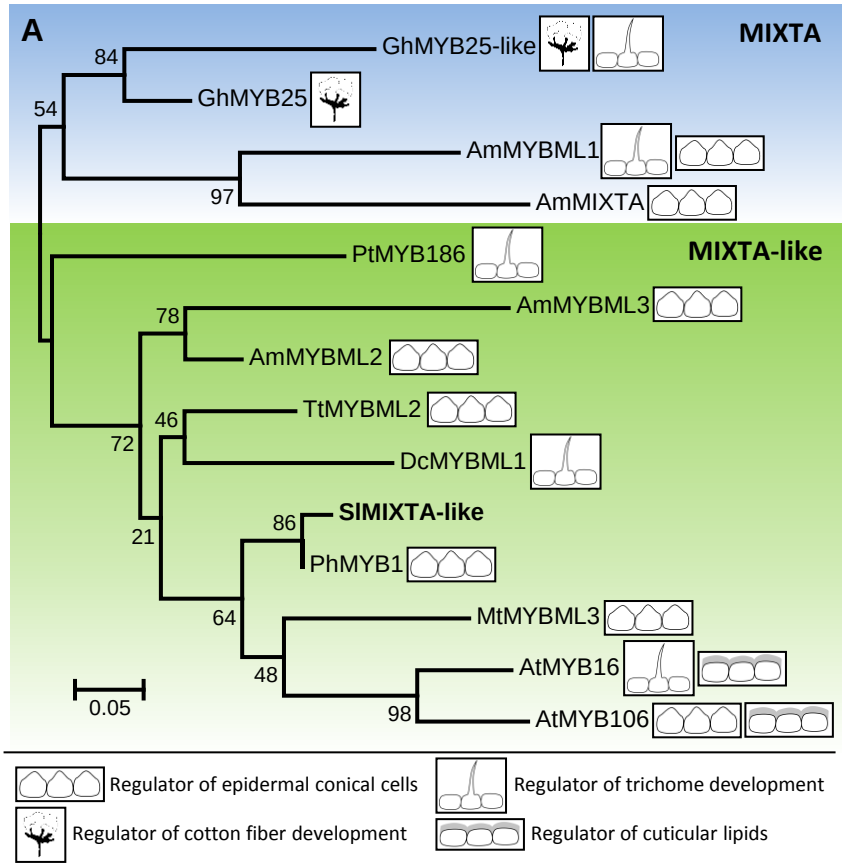

Figure 1. The tomato *MIXTA-like* gene is predominantly expressed in fruit epidermal layers. A, Molecular phylogenetic analysis of the functionally characterized members of the MIXTA/MIXTA-like protein clade are shown together with the assigned functional roles. ClustalW and the MEGA6 software were used to align the proteins and compute the neighbor-joining tree with significance percentages (bootstrap values out of 1000). The scale bar represents the relative amino acid difference. Alignments can be viewed in Supplemental Fig. S2. *Gossypium hirsuta* (Gh), *Populus trichopoda* (Pt), *Antirrhinum majus* (Am), *Solanum lycopersicum* (Sl), *Petunia hybrida* (Ph), *Medicago truncatula* (Mt), *Arabidopsis* (At), *Dendrobium crumenatum* (Dc) and *Thalictrum thalictroides* (Tt). B, An epidermal specific expression pattern is observed for the *SlMIXTA-like* gene. Normalized expression of *SlMIXTA-like* in immature green fruit tissues showed outer and inner epidermal expression (data was extracted from previously published results (Matas et al., 2011)). outepi, outer epidermis; collen, collenchyma; vascu, vascular tissue; paren, parenchyma; inepi, inner epidermis. C, Normalized expression of *SlMIXTA-like* across 20 tomato tissues highlights skin enriched expression in developing tomato fruit as well as significant expression in the petals and pollen (data extracted from previously published work (Itkin et al., 2013)). IG, immature green; MG, mature green; Br, breaker; Or, orange; Re, red; Y, young.

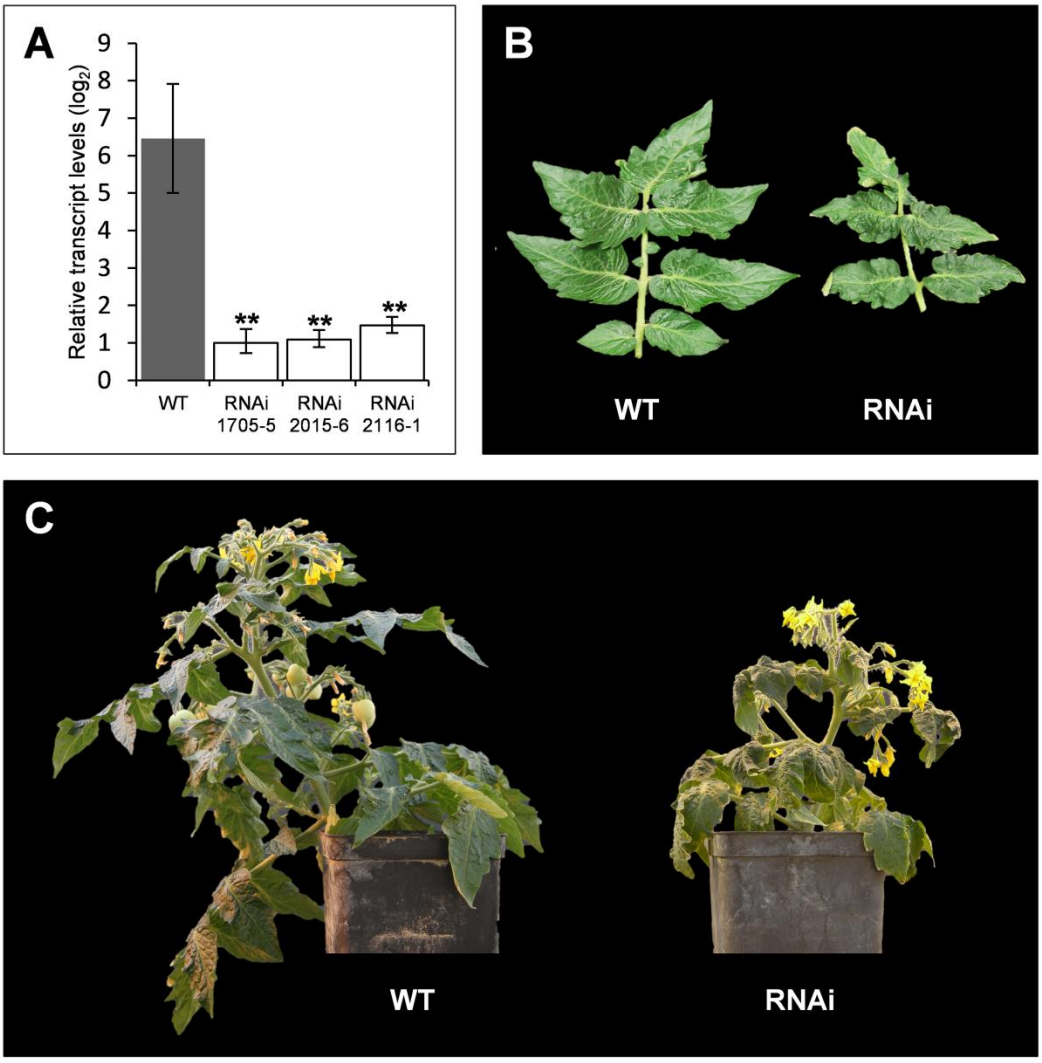

Figure 2. Growth and developmental phenotypes of tomato plants with altered *SlMIXTA-like* expression. A, Confirmation of *SlMIXTA-like* gene silencing confirmed by quantitative Real Time-PCR (qRT-PCR) analysis of transgenic tomato plants (*cv.* MicroTom). Data shows mean and standard error for three individually transformed lines. n = 3, ** = p-value < 0.01. B, Silencing of the *SlMIXTA-like* gene resulted in smaller, crinkled and curled leaves. C, Altered expression of the *SlMIXTA-like* gene in tomato results in changes to plant architecture. Lines silenced for *SlMIXTA-like* gene expression were smaller and displayed stunted growth. WT, wild type; RNAi, lines silenced for *SlMIXTA-like* expression.

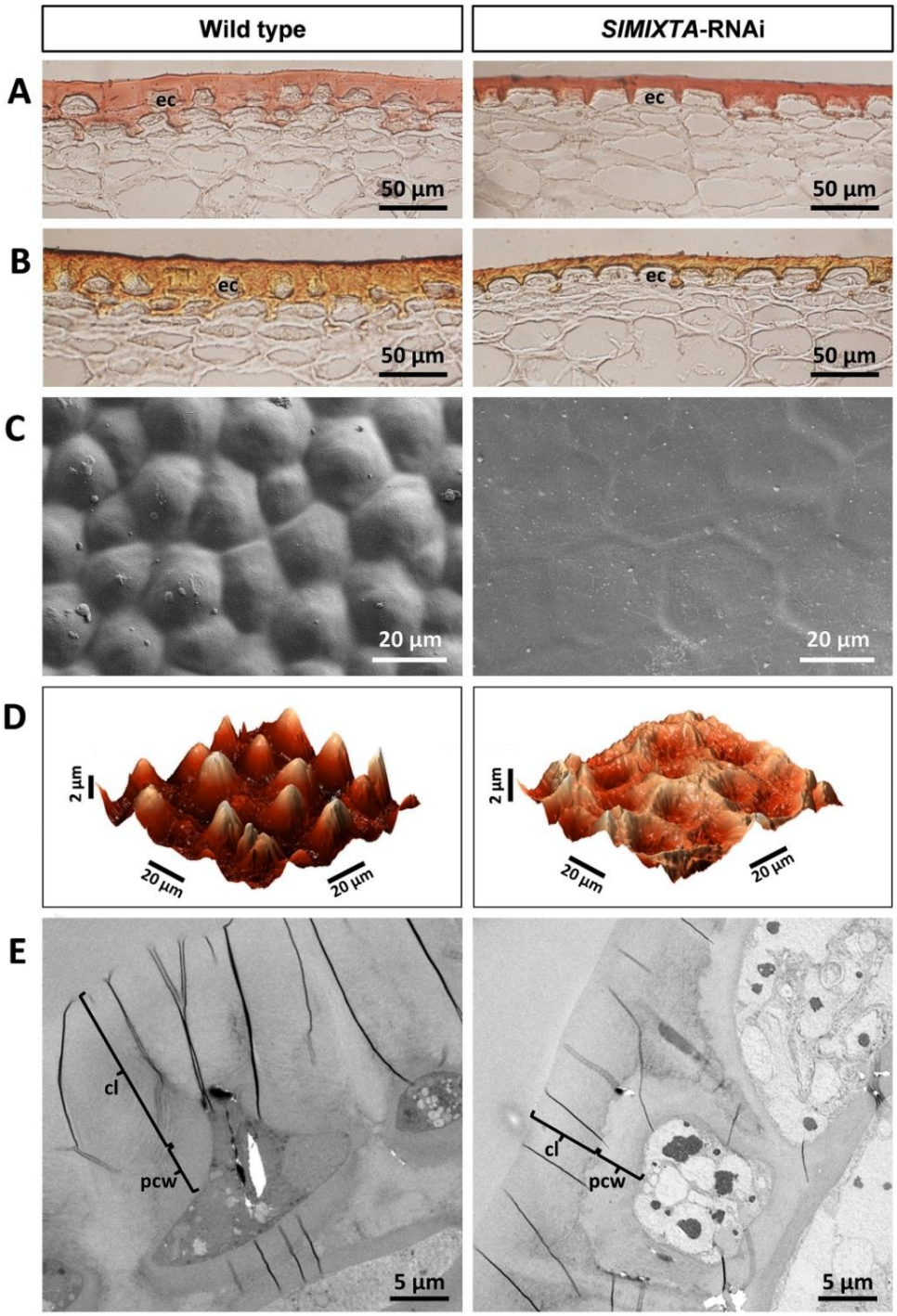

Figure 3. Epidermal cell patterning and cuticle deposition in fruit surface of *SlMIXTA-like* silenced tomato plants. A, Light microscopy observations of Sudan IV stained tomato skin sections showing reduced cuticle deposition and flatter epidermal cells at the mature green fruit stage. ec, epidermal cell. B, As in A but in the red stage of development. C, Cryo- Scanning Electron Microscopy (SEM) of the surface of tomato fruit at the mature green stage illustrates the effect of cell shape on surface morphology. Note the flat cells in the *SlMIXTA-like* silenced fruit. D, Atomic Force Microscopy (AFM) images of red, ripe tomato fruit surface displaying a flatter, more irregular and rough surface in the *SlMIXTA*-RNAi sample. Scale bars for the x- and y-axis represent 20µm, while the z-axis scale bar represents 2µm. Images are mixed light-shaded to contrast the small features on the overall large topography. E, Transmission Electron Microscopy (TEM) observations of tomato fruit epidermal cells (red fruit stage). A thinner cuticle as well as a distinct cell shape can be observed in the *SlMIXTA*-RNAi sample. pcw, primary cell wall; cl, cuticular layer.

In order to more deeply investigate cell shape, Focused Ion Beam Scanning Electron Microscopy (FIB-SEM) was employed. This technique is able to produce a three-dimensional (3D) image with the resolution typical of electron microscopy. Briefly, a biological sample is repeatedly milled (via the FIB) and then imaged (via the SEM), producing hundreds of SEM images from a few microns of tissue. These images can then be stacked (*in silico*) and the 3D structure of the observed specimen elucidated. In the case of the analysis of epidermal cells from ripe tomato fruit, wild-type fruit clearly possessed conical epidermal cells while the epidermal cells from *SlMIXTA*-RNAi lines were considerably flatter (Fig. 4; Supplemental Movie S1; Supplemental Movie S2).

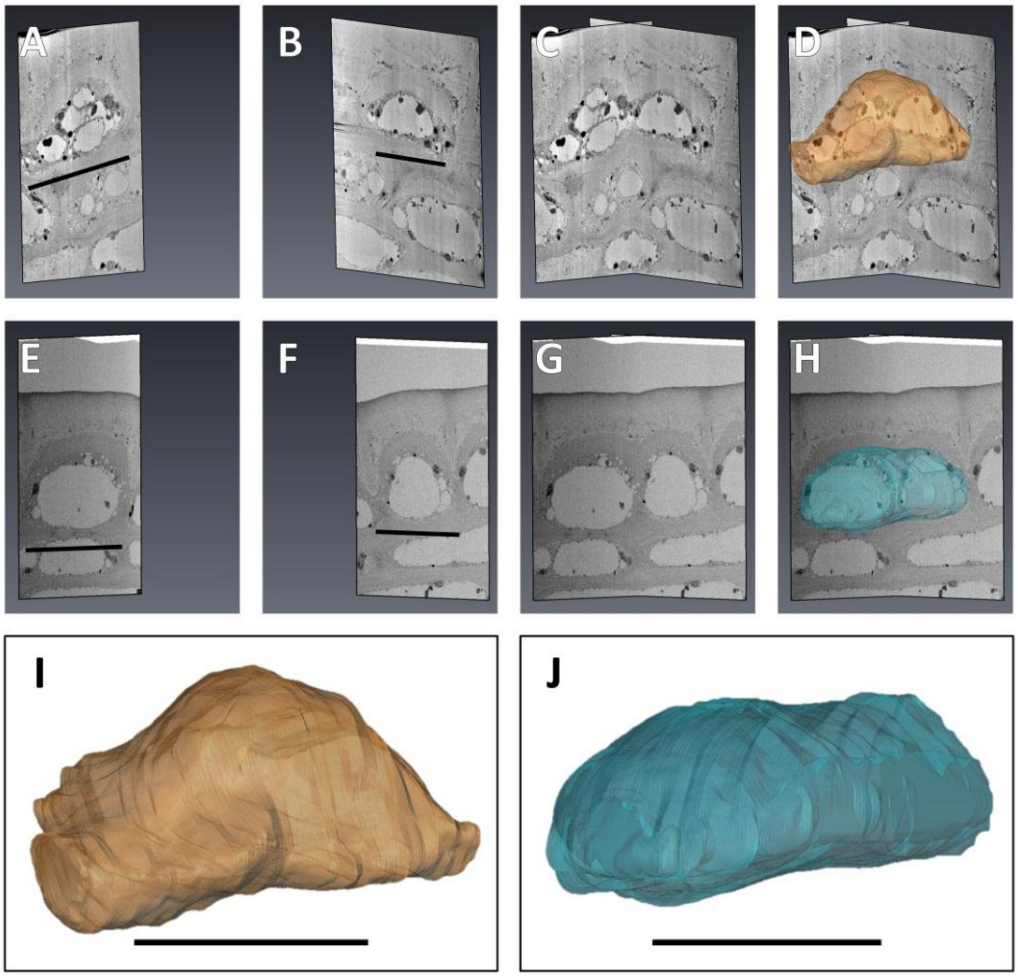

Figure 4. Three-dimensional reconstruction from Focused Ion Beam Scanning Electron Microscopy (FIB-SEM) acquisition shows that fruit of tomato lines silenced for *SlMIXTA-like* expression possess flatter epidermal cells. A, B, C and D, Images acquired from the fruit skin of wild-type tomato display conical epidermal cell shape. E, F, G, and H, Images of an epidermal cell from *SlMIXTA*-RNAi tomato fruit display a considerably flattened shape. I and J, The observations above were corroborated by *in silico* construction of three-dimensional models of epidermal cells for both wild-type (I) and *SlMIXTA*-RNAi (J). Scale bars indicate 20 µm. See also Supplemental Movie S1 and Supplemental Movie S2 for three-dimensional model construction.

3.2.3 *SlMIXTA-like* Expression is Positively Correlated with the Accumulation of Cutin Monomers in Tomato Fruit Cuticle

Analysis of enzymatically isolated cuticles from fruit altered in *SlMIXTA-like* expression revealed a positive correlation between *SlMIXTA-like* expression and cuticle mass (Table 1; Supplemental Dataset S2). Cuticles isolated from *SlMIXTA*-RNAi fruit displayed a lower mass compared to wild-type cuticles. Deeper chemical analysis via gas chromatography-mass spectrometry (GC-MS) was performed to determine which elements of the cuticle were contributing to the observed change in mass. The overall cutin monomer abundance was significantly altered in the *SlMIXTA*-RNAi lines (down 27%; Table 1). Quantification of the total cuticular waxes from the tomato lines revealed no significant change (Supplemental Table S1). The change in cutin monomers was underlined by the significant reduction of aromatics, dicarboxylic fatty acids (DFA), and mid-chain and terminal-hydroxylated fatty acids (*ω*-HFA) in the *SlMIXTA*-RNAi lines (Fig. 5; Table 1). No significant change was observed in the accumulation of the saturated fatty acids in the different genotypes examined (Table 1).

3.2.4 Silencing of *SlMIXTA-like* Results in the Down-regulation of a Wide Spectrum of Cutin Biosynthesis and Assembly Genes

Further investigation of the *SlMIXTA-like* RNAi lines identified a pertinent array of gene expression changes in the fruit skin. Global expression analysis via microarrays and quantitative real time-PCR (qRT-PCR) assays for validation revealed a considerable down-regulation of cutin biosynthesis genes in the skin of *SlMIXTA*-RNAi fruit at the mature green stage (Table 2; Supplemental Dataset S1; Supplemental Fig. S4). The mature green stage of fruit development was selected for gene expression analysis as at this stage the skin and flesh are more easily separated when compared with the earlier stages of development, and cuticle biosynthesis genes are still strongly enriched (Mintz-Oron et al., 2008). Mining the microarray data to identify genes with at least 2-fold change (p-value ≤ 0.05), generated a relatively concise list of 93 down-regulated and 153 up-regulated genes in the *SlMIXTA*-RNAi fruit skin as compared to wild-type (Supplemental Dataset S1). Gene ontology (GO) enrichment analysis of the 93 down-regulated genes revealed significant enrichment for lipid metabolism, specifically fatty acid and lignin biosynthesis (p-value < 0.01). Among the 93 down-regulated genes, 13 orthologs of genes previously functionally characterized and associated with cuticle assembly were annotated (Fig. 5; Table 2). Due to the fact that *SlSHN3* has been shown

via promotor binding assays to act upstream of *SlMIXTA-like* (Shi et al., 2013), the initial list of down-regulated genes was further extended via qRT-PCR analysis of candidates previously shown to be down-regulated in *SlSHN3*-RNAi lines (Shi et al., 2013) but not detected in the *SlMIXTA*-RNAi microarray experiment either due to not being present on the array or due to expression levels below the background of detection. In total 17 genes putatively involved in cuticle biosynthesis and assembly were identified to be down-regulated in *SlMIXTA*-RNAi lines (Table 2). It is also important to note that qRT-PCR confirmed no significant change in expression of *SlSHN3*, *SlCD2*, *SlPDF2d*, *SlDCR* and *SlCD1* (Supplemental Fig. S4).

Of the 17 cuticle-associated down-regulated genes, fourteen could be linked to various steps of cutin biosynthesis and assembly (Fig. 5). These consisted of two long chain acyl-CoA synthase coding genes (*SlLACS2* and *SlLACS4*) putatively involved in the acyl activation of fatty acids (Fig. 5). Orthologs to these genes have been demonstrated to be required for normal cuticle development in *Arabidopsis*: *AtLACS1*, *AtLACS2* and *AtLACS4* (Schnurr et al., 2004; Jessen et al., 2011). Three CYP450s were identified, *SlCYP77A1* and *SlCYP77A2* and *SlCYP86A68* (Fig. 5; Table 2). Orthologs of CYP77A have been demonstrated to be responsible for the mid-chain hydroxylation of C16 fatty acids during cutin biosynthesis (Li-Beisson et al., 2009) while CYP86A orthologs have been shown to catalyze the terminal hydroxylation of free fatty acids (Han et al., 2010; Shi et al., 2013). Another candidate for the modification of fatty acids is the down-regulated *SlHTH* gene. The *Arabidopsis* ortholog, *AtHTH*, has been shown to be crucial for the formation of dicarboxylic fatty acids (Kurdyukov et al., 2006). The final step in the biosynthesis of cutin monomers is acyl transfer of the activated fatty acid to a glycerol moiety. This reaction is catalyzed by *AtGPAT4* and *BnGPAT4* in *Arabidopsis* (Li et al., 2007) and *Brassica napus* (Chen et al., 2011), respectively. The tomato ortholog to these genes (*SlGPAT4*) was down-regulated in *SlMIXTA*-RNAi lines (Fig. 5; Table 2). The monoacylglycerols formed through the action of the enzymes described above are subsequently transported to the exterior of the cell before polymerization occurs (Pollard et al., 2008). *SlMIXTA*-RNAi lines showed down-regulation of two extracellular transporter genes: *SlABCG11* and *SlABCG32*. *SlABCG11* is orthologous to the characterized cutin and wax monomer transporter in *Arabidopsis*, *AtABCG11* (Bird et al., 2007; Panikashvili et al., 2007), while *SlABCG32* is the tomato ortholog to *AtABCG32* an extracellular transporter of cuticle components (Bessire et al., 2011). Finally, five genes potentially involved in the extracellular polymerization of the cutin matrix were found

to be down-regulated in the *SlMIXTA*-RNAi lines (Fig. 5; Table 2). Three orthologs to the tomato *CD1* gene, recently reported to be an extracellular cutin polymerase (Girard et al., 2012; Yeats et al., 2012), were also down-regulated in the *SlMIXTA*-RNAi lines (*Solyc07g049440 Solyc03g121180* and *Solyc04g081770*), as well as two *α/ß-hydrolases* (*Solyc09g075140* and *Solyc05g054330*), orthologous to the *Arabidopsis AtBDG* suggested to be an extracellular synthase required for cutin formation (Kurdyukov et al., 2006).

Table 1. Quantification of cutin monomer composition in fruit of *SlMIXTA-like* silenced lines and wild-type lines.

	Wild type		*SlMIXTA*-RNAi	
Cutin Monomers	**Average**	**SE**	**Average**	**SE**
Aromatic				
cis-Coumaric acid	0.92	0.23	0.55	0.17
trans-Coumaric acid	50.52	1.57	11.26**	3.01
Subtotal	51.44	1.44	11.81**	2.84
Saturated fatty acids (FA)				
C16:0 FA	2.84	0.14	2.45	0.21
C18:0 FA	5.51	0.26	4.89	0.2
Subtotal	8.35	0.4	7.33	0.41
Dicarboxylic fatty acids (DFA)				
C16:0 DFA	24.92	1.34	11.22**	1.14
C16-9,10 hydroxy-DFA	67.53	4.73	40.57**	4.3
Subtotal	92.46	4.78	51.79**	5.37
Mid chain hydroxylated fatty acids (HFA)				
C16-9/10,16 DiHFA	797.66	43.11	640.48**	35.58
C18-9,18 DiHFA	2.97	0.33	2.77	0.2
C18:1-9,10,18-TriHFA	1.0	0.27	0.32*	0.03
C18-9,10 DiHFA	43.69	3.72	30.18**	2.32
Subtotal	845.31	47.32	673.75**	37.7
Terminal hydroxylated fatty acids (ω HFA)				
C16:1-ω HFA	7.37	0.6	4.13**	0.93
C16-ω HFA	142.55	1.82	77.46**	6.75
Subtotal	149.91	2.28	81.59**	7.58
Epoxy fatty acids				
C18:1-9,10-epoxy-18- ω -HFA	2.34	0.24	2.38	0.07
C18-9,10-epoxy-18- ω -HFA	3.44	0.31	3.69	0.23
Subtotal	5.78	0.55	6.08	0.27
Other				
Naringenin	22.58	4.89	27.66	13.45
Naringenin dimer	23.88	0.49	13.86*	4.37
Subtotal	46.46	4.66	41.52	12.8
Unknown				
Subtotal	187.38	6.46	134.1**	19.26
Total	1387.09	53.86	1012.65**	70.94

Cutin monomers quantified after BF3 depolymerization of enzymatically isolated, dewaxed tomato fruit cuticles (red stage fruit). Concentrations (µg/cm^{-2}) shown for lines silenced for *SlMIXTA-like* (*SlMIXTA*-RNAi) and the corresponding wild type (WT). Extractions were performed on three independently transformed lines. Monomers that show significant changes (Student's *t*-test) from the wild type are indicated with an ** ($p < 0.01$), or * ($p < 0.05$).

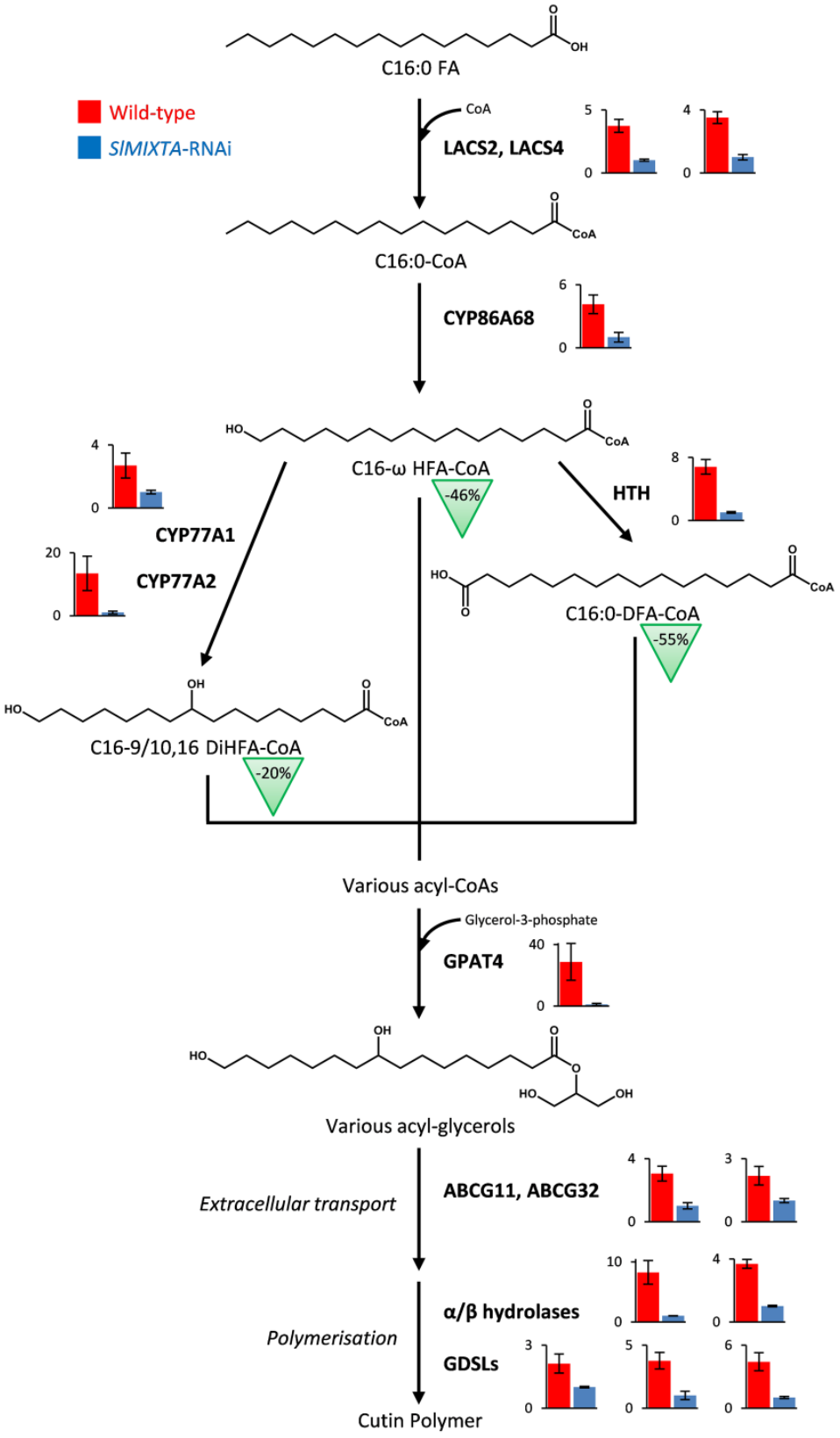

Figure 5. *SlMIXTA-like* is required for cutin biosynthesis and deposition of the cuticle. A generic cutin biosynthetic pathway using the most abundant C16 fatty acid moiety as a substrate. Transcriptomic analysis pertaining to the pathway is displayed in the form of graphs indicating relative gene expression. Values are a mean of three independently transformed lines ± standard error (n=3), see Table 2 for specific fold change values. Relative changes to major cutin monomers are also shown (green arrows; n = 3).

Table 2. Genes putatively involved in cuticle assembly showing down-regulation in the *SlMIXTA*-RNAi lines.

Gene ID	Gene Name	Putative Function	Fold-change	*p*-value	Cluster	Characterised orthologue	Reference
Solyc05g054330	α/β-hydrolase	cutin polymerisation	-7.8	0.001	IV.iib	AtBDG (At1g64670)	Kurdyukov et al. (2006a)
Solyc03g117800^{L1}	CER3	alkane biosynthesis	-7.7	0.014	IV.iia	AtCER3 (At5g57800)	Bernard et al. (2012)
Solyc08g080190^{L1}	HTH	dicarboxylic-acid biosynthesis	-6.8	0.001	IV.iia	AtHTH (At1g72970)	Kurdyukov et al. (2006b)
Solyc03g121180^{L1}	GDSL esterase/lipase	cutin polymerisation	-4.3	0.040	IV.i	SlCD1 (Solyc11g006250)	Girard et al. (2012); Yeats et al. (2012)
Solyc01g109180^{LB,L1}	LACS2	acyl activation	-3.7 (-8.3)	0.001 (0.033)	IV.iia	AtLACS2 (At1g49430)	Schnurr et al. (2004); Jessen et al. (2011)
Solyc09g075140^{LB}	α/β-hydrolase	cutin polymerisation	-3.7	0.001	IV.iia	AtBDG (At1g64670)	Kurdyukov et al. (2006a)
Solyc01g095750^{LB,L1}	LACS4	acyl activation	-3.6 (-4.3)	0.003 (0.011)	IV.iia	AtLACS4 (At4g23850)	Schnurr et al. (2004); Jessen et al. (2011)
Solyc03g019760^{LB,L1}	ABCG11	cuticular lipids transport	-3.1	0.009	IV.iia	AtABCG11 (At1g17840)	Bird et al. (2007); Panikashvili et al. (2007)
Solyc11g072990^{LB,L1}	KCS3	fatty acid elongation	-3.0	0.003	IV.iia	AtKCS3 (At1g07720)	Millar et al. (1999)
Solyc05g055400^{LB,L1}	CYP77A2	midchain fatty-acid oxidation*	-2.5 (-20.7)	0.038 (0.022)	IV.iia	AtCYP77A4 (At5g04660)	Li-Beisson et al. (2009)
Solyc06g065670^{LB,L1}	PDR4/ABCG32	cuticular lipids transport	-2.1	0.043	IV.iib	AtABGC32 (At2g26910)	Bessire et al. (2011)
Solyc04g081770^{LB,L1}	GDSL esterase/lipase	cutin polymerisation	-2.0	0.025	IV.iia	SlCD1 (Solyc11g006250)	Girard et al. (2012); Yeats et al. (2012)
Solyc01g094700^{LB,L1}	GPAT4	acyl transfer	(-38.1)	(0.013)	IV.iia	AtGPAT4 (At1g01610)	Li et al. (2007)
Solyc11g007540^{LB,L1}	CYP77A1	midchain fatty-acid oxidation*	(-13.3)	(0.045)	IV.iia	AtCYP77A4 (At5g04660)	Li-Beisson et al. (2009)
Solyc01g094750^{LB}	CYP86A68	terminal fatty-acid oxidation*	(-4.8)	(0.039)	IV.iia	SlCYP86A69 (Solyc08g081220)	Shi et al. (2013)
Solyc07g049440^{LB,L1}	GDSLa	cutin polymerisation	(-4.2)	(0.003)	IV.iia	SlCD1 (Solyc11g006250)	Girard et al. (2012); Yeats et al. (2012)
Solyc03g120620^{LB}	GL2	cuticle regulation	(-3.6)	(0.037)	IV.iia	SlCD2 (Solyc01g091630)	Isaacson et al. (2009); Nadakuduti et al. (2012)

A 2-fold change cut off and *p*-value ≤ 0.05 were used. Majority of values are derived from microarray experiment, however values in brackets are derived from quantitative real time-PCR (qRT-PCR) analysis. LB = Contains the L1-box promoter motif (Abe et al., 2001). L1 = L1 layer specific expression (Filippis et al., 2013). * = putative function confirmed in this paper.

Only two out of the 17 cuticle-associated genes down-regulated in the *SlMIXTA*-RNAi lines could putatively be linked to wax biosynthesis (*Solyc03g117800* and *Solyc11g072990*). The *Arabidopsis* ortholog of Solyc03g117800, AtCER3, has been reported to be catalyze the conversion of very long chain acyl-CoAs to very long chain alkanes (Bernard et al., 2012), while the ortholog of Solyc11g072990, AtKCS3, catalyzes the first step of fatty acid elongation (Millar et al., 1999).

3.2.5 Putative *SlMIXTA-like* Downstream Targets Display an L1 Layer-specific Enrichment

In silico promoter analysis of the genes identified to be down-regulated in *SlMIXTA*-RNAi lines revealed a significant enrichment ($p < 0.01$) for the L1-box motif -TAAATGYA- (Table 2; Supplemental Dataset S1). This motif has previously been demonstrated to be the binding site for two L1-specific HD-ZIP transcriptional regulators in *Arabidopsis*, AtPDF2 and ATML1 (Abe et al., 2003; Takada et al., 2013). In the *SlMIXTA*-RNAi lines an ortholog to these genes, *SlGL2* (*Solyc03g120620*), was demonstrated to be down-regulated (Table 2). The 93 down-regulated genes were also analyzed for their L1 layer specificity by comparison with a recently generated data set (Filippis et al., 2013). In this work 255 genes out of the 13,277 examined were identified to exhibit L1 layer-specific tomato expression. Of the reported 255 L1 layer-specific gene set, 18 genes were found to be down-regulated in the *SlMIXTA*-RNAi lines (Table 2; Supplemental Dataset S1). Hypergeometric analysis demonstrates this is an extremely strong enrichment ($p < 0.01$), and further suggests a role for SlMIXTA-like in L1 layer-specific gene control. By comparison, of the 153 up-regulated genes in the *SlMIXTA*-RNAi lines only three are reportedly L1 layer-specific, showing no enrichment ($p = 0.57$).

The previous observation that *SlMIXTA-like* possessed a fruit skin associated expression profile (Mintz-Oron et al., 2008; Shi et al., 2013), was further confirmed by the data extracted from recently generated large scale transcriptomic analysis of multiple tomato tissues (Itkin et al., 2013), (Fig. 1C). The hypothesis that putative downstream targets of SlMIXTA-like will likely exhibit a similar L1 layer-specific expression pattern was tested by extracting the expression patterns of the *SlMIXTA*-RNAi down-regulated genes in skin and flesh tissues from the dataset, and performing hierarchical clustering (Fig. 6). Data for 91 genes was collected and four major clusters were identified, the largest cluster (Cluster IV) contained *SlMIXTA-like* and 40 other genes (Fig. 6; Table 2; Supplemental Dataset S1). Cluster IV had a high homogeneity (*r*-

value = 0.81), and displayed skin enriched (or L1 layer-specific) expression pattern particularly in the early stages of fruit development (Fig. 6). All of the 16 genes described as potential *SlMIXTA-like* targets involved in cuticle biosynthesis were found to be part of Cluster IV. The expanded expression profiles (including seed, leaf, flower and root expression data) of genes described in this report can be seen in Supplemental Fig. S5.

Finally, of the 143 genes found to be up-regulated in the microarray analysis, one gene was of particular interest and displayed a dramatic up-regulation in *SlMIXTA*-RNAi lines. An HD-ZIP IV transcription factor, *SlANL2b* (*Solyc06g035940*), was up-regulated 43-fold (Supplemental Dataset S1). *SlANL2b* is a close ortholog in tomato to the cuticle regulating *SlCD2* gene (Isaacson et al., 2009; Nadakuduti et al., 2012), and significantly also an ortholog to the epidermis and L1 layer related transcription factors, PROTODERMAL FACTOR 2 (AtPDF2) and ARABIDOPSIS THALIANA MERISTEM LAYER 1 (ATML1) (Supplemental Fig. S6).

3.2.6 Putative *SlMIXTA-like* Downstream Target Genes Encode Members of the Cytochrome P450 CYP77A and CYP86A Subfamilies Catalyzing the Formation of Major Cutin Monomers in Tomato

Members of the cytochrome P450 CYP77A and CYP86A subfamilies have been reported previously to be involved in cutin monomers biosynthesis (largely in *Arabidopsis*), performing mid-chain and terminal oxidation of fatty acids, respectively (Li-Beisson et al., 2009). As three members of these subfamilies were identified here as putative *SlMIXTA-like* downstream targets (Fig. 5; Table 2; Supplemental Fig. S7) we explored the activity of the corresponding recombinant enzymes through expression in yeast cells. Initial incubation of a variety of fatty acids with microsomes of yeast expressing the three CYPs (SlCYP77A1, SlCYP77A2 and SlCYP86A68) confirmed that they were all active enzymes able to catalyze hydroxylation of fatty acids (Fig. 7; Supplemental Fig. S8). More extensive analysis of SlCYP77A1 demonstrated the enzyme was able to hydroxylate C16:0 fatty acids (Fig. 7). To determine the position of the hydroxylation, we performed mass spectrometry analysis on the recombinant SlCYP77A1 assay products and revealed a mixture of 11,16-; 10,16-; 9,16- and 8,16-dihydroxyhexadecanoic acids (Fig. 7C). This result corresponds strongly with the reduced levels of 9/10,16-dihydroxyhexadecanoic acid in fruit of the *SlMIXTA*-RNAi lines.

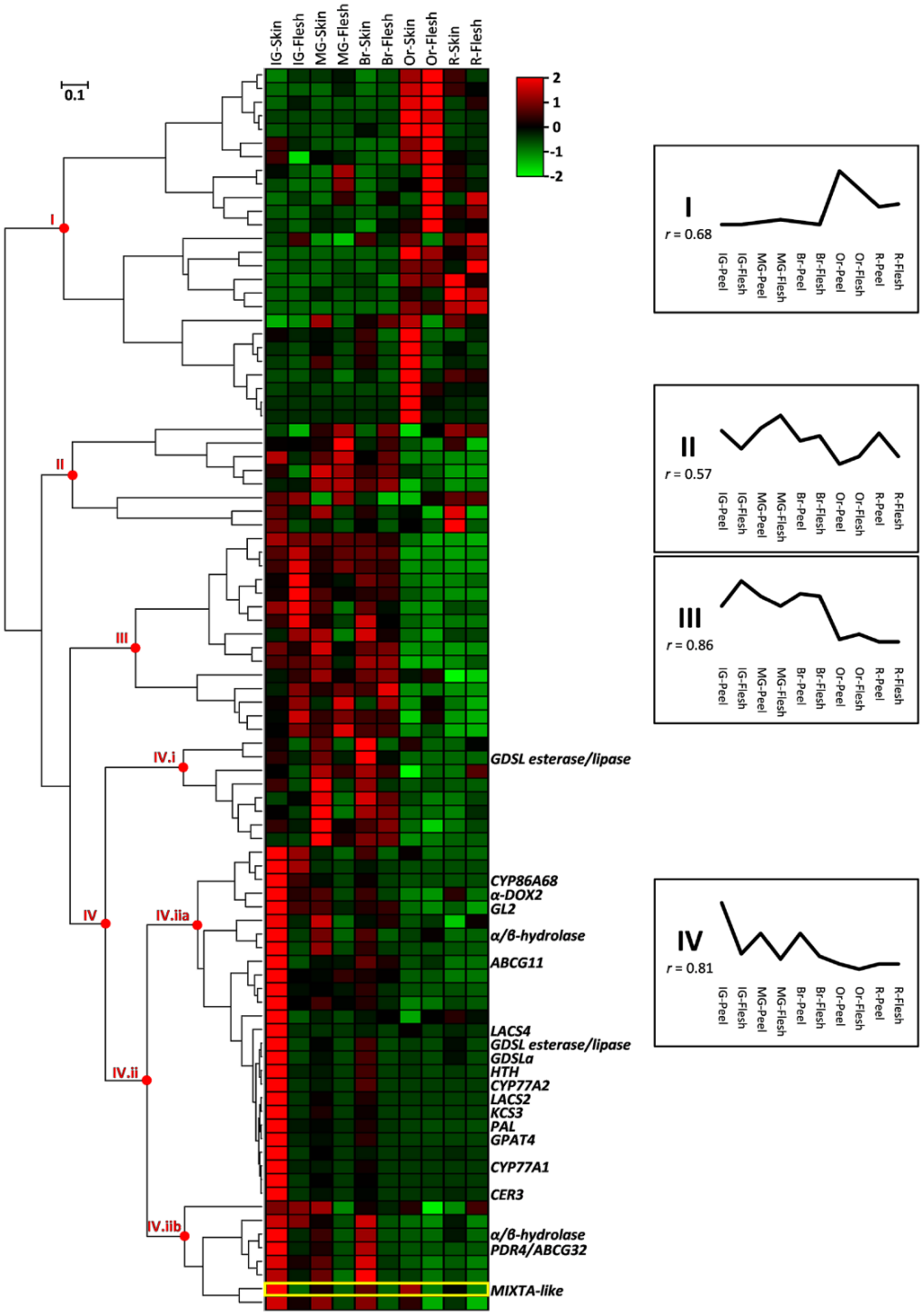

Figure 6. Hierarchical clustering of genes down-regulated in *SlMIXTA*-RNAi lines. The fruit development expression profiles of 91 genes identified as down-regulated in *SlMIXTA*-RNAi lines were extracted from a previously published large scale expression dataset (Itkin et al., 2013), and hierarchical clustering was performed. Four major clusters were identified and their mean representative expression profiles are shown adjacent to the heat map (marked I to IV). Pearson correlation coefficients illustrating the homogeneity of the clusters are displayed below the cluster number. The expression profile of *SlMIXTA-like* located in cluster IV is highlighted by a yellow outline. Additional genes potentially involved in cuticle biosynthesis are labeled and detailed in Table 2. For remaining genes see Supplemental Dataset S1. Red and green colors represent pairwise distances for transcript expression from the mean (black). IG, Immature Green; MG, Mature Green; Br, Breaker; Or, Orange; R, Red.

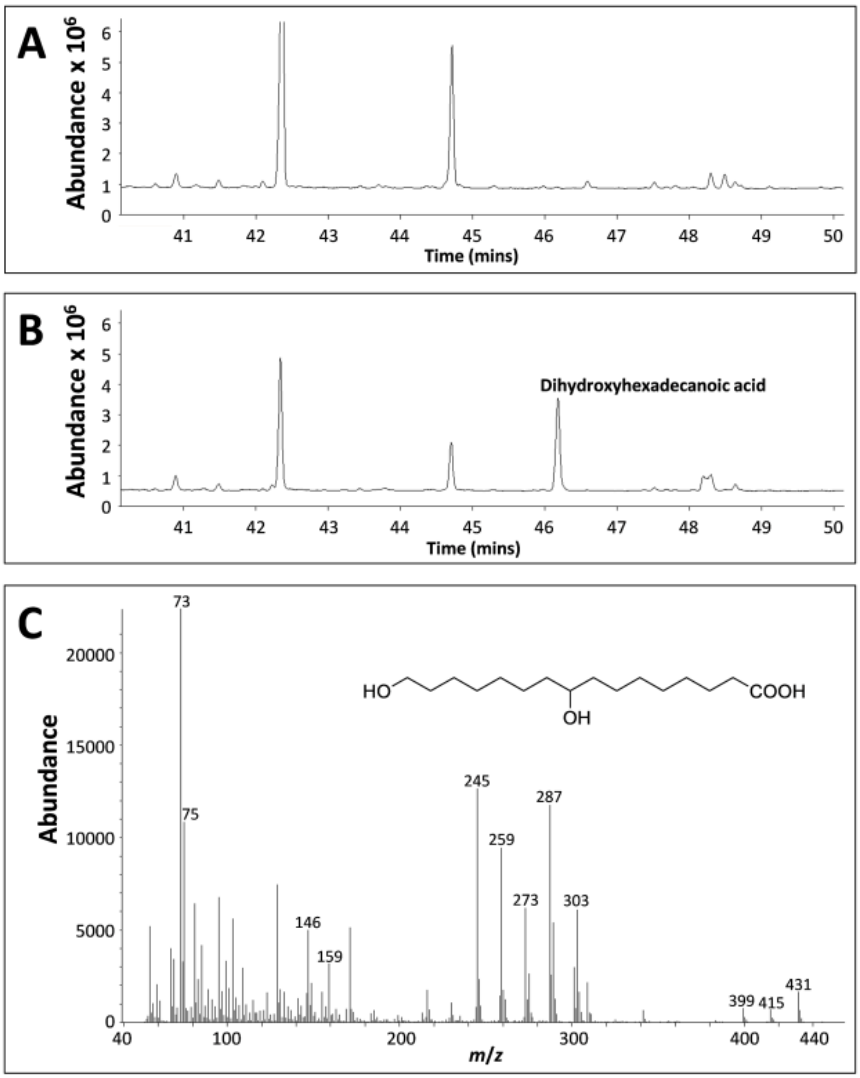

Figure 7. Recombinant SlCYP77A1 catalyzes the formation of dihydroxyhexadecanoic acids. A and B, Microsomes of yeast cells expressing *SlCYP77A1* were incubated with 100 µM of hexadecanoic acid in the absence (A) or in the presence (B) of NADPH. Reactions products were extracted with diethyl ether, derivatized and subjected to GC/MS analysis. C, Fragmentation pattern of the dihydroxyhexadecanoic acid peak is presented and identified to be a mixture of 8,16-; 9,16-; 10,16- and 11,16-dihydroxyhexadecanoic acids. The molecular structure of the most abundant tomato cuticle fatty acid, 9,16-dihydroxyhexadecanoic acid, is displayed.

3.2.7 Silencing of *SlMIXTA-like* Increased Postharvest Fruit Water Loss and Susceptibility to Postharvest Fungal Infection

Post-harvest analysis of *SlMIXTA*-RNAi fruit revealed that reduced expression of *SlMIXTA-like* resulted in an increase in postharvest water loss as well as increased susceptibility to fungal infection (Fig. 8). Fruit of *SlMIXTA*-RNAi lines lost 80% more water than those from WT lines over 30 days after harvest (Fig. 8A). Similarly, the susceptibility to post harvest fungal infection was significantly higher in *SlMIXTA*-RNAi

lines. Fruit at the breaker stage were inoculated with the tomato fruit pathogen *Colletotrichum coccodes*, which causes black dot anthracnose disease (Dillard, 1989). Despite no significant difference in the rate of conidia germination and appressoria formation on the surface of WT and *SlMIXTA*-RNAi fruit (Supplemental Fig. S9), a 5-fold increase in the decay diameter after 1 week of inoculation was observed on *SlMIXTA*-RNAi fruit (Fig. 8B).

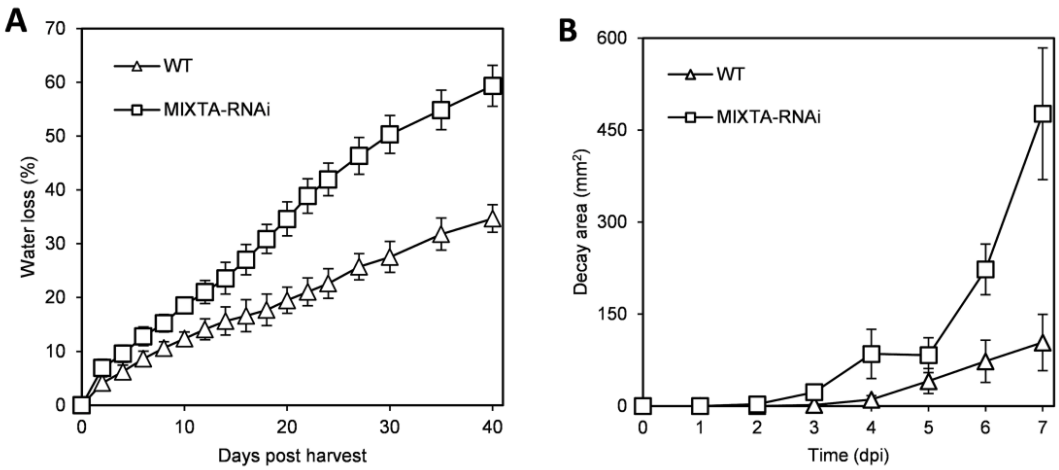

Figure 8. Reduced *SlMIXTA-like* expression impacts post-harvest water loss and susceptibility to fungal infection. A, Water loss progression in fruit of wild-type and *SlMIXTA*-RNAi lines was measured over 40 days of postharvest incubation at room temperature. B, Decay area rates of *Colletotrichum coccodes* colonization were measured after inoculation of breaker stage tomato fruit cuticle during 7 days. Error bars represent standard error (n=30).

3.3 Discussion

3.3.1 *SlMIXTA-like* Forms Part of a Transcriptional Network Regulating the Development of Conical Epidermal Cells in Tomato Fruit

To date, MIXTA orthologs across a variety of plant species have been reported to be involved in the regulation of epidermal cell differentiation (Brockington et al., 2013). The earliest characterized MIXTA ortholog (AmMIXTA) was shown to promote conical epidermal cell development in the petals of *Antirrhinum majus* (Noda et al., 1994; Brockington et al., 2013). Subsequently, members of the MIXTA transcription factor clade from *Arabidopsis*, *Thalictrum thalictroides* and *Petunia hybrida* were also reported to regulate conical epidermal cell development (Baumann et al., 2007; Di Stilio et al., 2009), while orthologs from *Arabidopsis*, *Populus trichopoda*, *Mimulus guttatus*, *A. majus*, *Medicago trunculata* and *Dendrobium crumenatum* have been shown to be

positive regulators of trichome development (Perez-Rodriguez et al., 2005; Gilding and Marks, 2010; Plett et al., 2010; Scoville et al., 2011). Phylogenetic analysis showed that the SlMIXTA-like protein characterized here is most closely related to the *Petunia* PhMYB1 ortholog which has been reported to regulate conical epidermal cell differentiation in petals (Baumann et al., 2007) (Fig. 1A). Four additional tomato proteins were identified through genome analysis and appeared related to the MIXTA/MIXTA-like clade, however phylogenetic analysis found these proteins to be distinct from MIXTA/MIXTA-like orthologs (Supplemental Fig. S1). This relationship was not investigated in more detail as no expression was detected for these genes in previously published large-scale expression studies (Itkin et al., 2013). It is possible that these genes are non-expressed pseudogenes that are no longer under selective pressure to maintain activity.

The prevalence of conical epidermal cells in flower petals suggests an important role for this particular morphology, likely the attraction of pollinators; however, the mode of action for this attraction is not obvious. Research into this question has shown that the reflection of light by the epidermal cells of petals is significantly altered by cell morphology (Gorton and Vogelmann, 1996), and this likely plays a role in pollinator attraction, however more recent research has shown that pollinators are able to discriminate between petal surfaces via tactile sensation (Whitney et al., 2009). The conical epidermal cells of petals likely facilitate the physical interaction between pollinators and flowers (Whitney et al., 2009). In contrast to petals, the abundance of this morphology in fleshy fruit surface has received less attention. As in the case of petals, the conical cells in fruit likely play a role in the reflection of light, and therefore may be involved in the attraction of seed dispersal agents. Recent studies confirm earlier reports that change in epidermal cell morphology can dramatically alter the human perceived glossiness of tomato fruit (Isaacson et al., 2009; Mahjoub et al., 2009; Nadakuduti et al., 2012; Shi et al., 2013; Petit et al., 2014), although how these fruit are viewed by seed dispersers is still not known. While no epidermal specific petal phenotype was observed, leaves of *SlMIXTA*-RNAi lines were small and folded, while fruit were glossier than corresponding wild-type fruit, despite the reduction in cuticle deposition seen in these lines. Morphological examination of tomato fruit silenced for *SlMIXTA-like* expression revealed a flattening of the epidermal cells which likely leads to the glossier surface as light reflects from the surface with less scattering.

The observed enrichment of the L1-box promoter motif (Abe et al., 2001) in the promoters of the genes down-regulated in the *SlMIXTA*-RNAi lines together with the enrichment of L1 layer-specific genes implicate SlMIXTA-like as a possible central regulator of L1 layer cell identity. This might occur through co-regulation with the HD-ZIP IV transcription factor SlGl2, which is significantly down-regulated in lines silenced for *SlMIXTA-like* expression and therefore may occur downstream of SlMIXTA-like in this regulatory pathway. The ortholog of SlGL2 in *Arabidopsis*, AtGL2, is a well characterized regulator of epidermal cell differentiation (Tominaga-Wada et al., 2009). The L1-box motif has been found to be an important binding site for HD-ZIP IV transcription factors regulating epidermal cell differentiation in both *Arabidopsis* and cotton (*Gossypium barbadense*), (Abe et al., 2003; Ohashi et al., 2003; Zhang et al., 2010). Significantly, an HD-ZIP IV ortholog from cotton GbML1, was shown to not only bind the L1-box motif but also a cotton MIXTA family protein, GbMYB25 (Zhang et al., 2010). In *SlMIXTA*-RNAi lines, the HD-ZIP IV transcription factor *SlANL2b* (Supplemental Fig. S6) was massively up-regulated (40-fold; Supplemental Dataset S1). If a similar mechanism found in cotton exists in tomato and SlANL2b can be regarded as having the orthologous function to GbML1 (i.e. binding both the L1-box motif and SlMIXTA-like), then the massive increase in *SlANL2b* expression in *SlMIXTA*-RNAi lines may represent a compensating mechanism for the loss of *SlMIXTA-like* expression.

These results suggest that the influence of *SlMIXTA-like* (and possibly MIXTA orthologs in general) on epidermal cell differentiation may be mediated through a regulatory network with L1-box motif binding HD-ZIP IV transcription factors (such as SlGL2 and SlANL2b). This view of such a network between MIXTA and HD-ZIP IV transcription factors in relation to epidermal cell differentiation identity can be expanded when a recent work on the AP2 domain SlSHN3 transcription factor is considered (Shi et al., 2013). The results of this earlier study suggested that SlSHN3 was able to regulate epidermal cell patterning in tomato via SlGL2 and/or SlMIXTA-like activities. *SlGL2* and *SlMIXTA-like* were both down-regulated in *SlSHN3*-RNAi tomato lines and LUC reporter assays showed that SlSHN3 acted on the promoters of both genes (Shi et al., 2013). This, together with the fact that *SlSHN3* displayed no change in expression in *SlMIXTA*-RNAi lines suggests that in tomato fruit, SlSHN3 appears to act above SlMIXTA-like in the regulatory pathway controlling epidermal cell patterning (Fig. 9).

Finally, it should be noted that while strong evidence is presented for the involvement of L1 layer-specific genes as the mediators of SlMIXTA-like activity in relation to epidermal cell shape it may be that this morphological alteration is in fact a secondary effect caused by the observed reduction in cuticle deposition. Specifically, tomato fruit epidermal cells are either totally, or partially, enveloped by the cuticle, which likely contributes to the cell structure. Recent results have indeed found that the fruit surface structure is influenced by cutin deposition; however in this work a change in cutin deposition was not necessarily shown to result in a change in epidermal cell shape (Petit et al., 2014). Further, silencing of *CHALCONE SYNTHASE* expression (a gene responsible for the inclusion of naringenin chalcone in the tomato cuticle), results in a stiffer, less elastic cuticle, surrounding flatter epidermal cells (Schijlen et al., 2007; España et al., 2014). These results hint at a potential dependence on the surrounding cuticle with regard to epidermal cell structure. Further investigations into the relationship between cuticular lipid composition and epidermal cell development will prove invaluable to our understanding of plant surface formation.

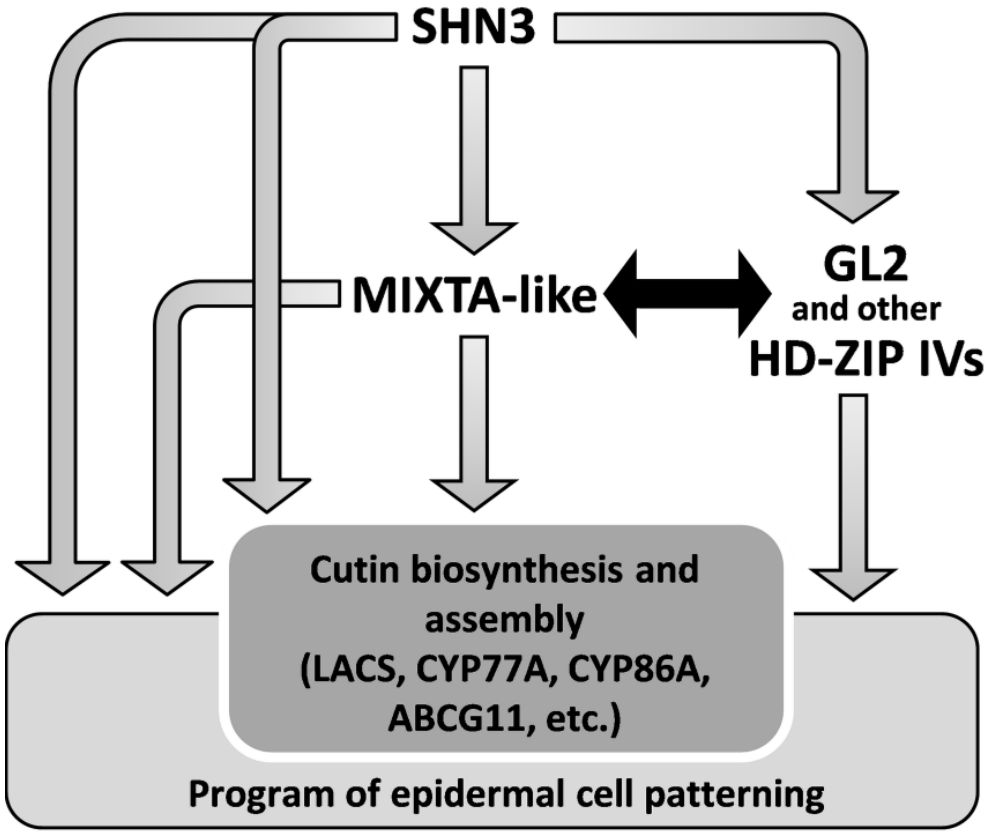

Figure 9. The SlMIXTA-like regulatory network controls cuticle assembly and cell patterning. The SlSHN and SlMIXTA-like proteins directly or indirectly regulate cuticle deposition in tomato fruit skin as part of a larger program of epidermal cell patterning. This network likely involves interaction with additional regulators such as members of the HD-ZIP IV family of transcription factors.

3.3.2 *SlMIXTA-like* is a Positive Regulator of Tomato Fruit Cutin Biosynthesis and Assembly

Expression analysis of *SlMIXTA-like* in developing tomato fruit revealed a skin enriched expression profile (predominantly at the early green stages of fruit development), while transcriptome analysis across multiple tissues and developmental stages revealed that *SlMIXTA-like* was also significantly expressed in the petals and pollen. This expression profile is typical of genes involved in cuticle biosynthesis (Mintz-Oron et al., 2008). Moreover, laser-micro dissection coupled to transcriptomic analysis of tomato fruit cell types showed that *SlMIXTA-like* is expressed in the inner, as well as outer, epidermal layers but not collenchyma, parenchyma or vascular tissues (Matas et al., 2011; Hen-Avivi et al., 2014) (Fig. 1B). The inner epidermal layer of tomato fruit produces a waxy cuticle separating the fleshy endocarp from the locular region of the fruit (Mintz-Oron et al., 2008; Matas et al., 2011) and thus, it seems likely that SlMIXTA-like plays a role in the regulation of this inner cuticle as well as the outer fruit cuticle. It is interesting to note that the previously characterized tomato cuticle regulators, *SlSHN3* and *SlCD2*, are also expressed in both the inner and outer epidermis (Hen-Avivi et al., 2014).

Analysis of the tomato lines altered in *SlMIXTA-like* expression demonstrated a significant correlation between cuticle deposition and *SlMIXTA-like* expression. This was evident in the microscopic analysis which displayed a significantly thinner cuticle in the *SlMIXTA-like* RNAi lines and the chemical analysis, which highlighted that this change can be predominantly attributed to a modification in cutin monomer biosynthesis. In fact, the change in cutin levels in the transgenics correlated strongly with the change in the overall weight of the isolated cuticle. Significant differences in the cutin composition were particularly evident in the highly abundant modified C16 fatty acid, more specifically C16 9/10,16 DiHFA, the dominant cutin monomer of tomato fruit, as well as DFAs and *ω*-HFAs. The saturated fatty acids, however, showed few significant changes in plants exhibiting modified *SlMIXTA-like* expression, suggesting that *SlMIXTA-like* exerts its activity at the downstream modification steps of the cutin biosynthetic pathway. This hypothesis was confirmed through the transcriptional analysis of the transgenic plants. Numerous genes that are directly responsible for the biosynthesis of specific modified fatty acids were down regulated in plants with reduced *SlMIXTA-like* expression. In addition, genes involved in the extracellular transport and the polymerization of the cutin matrix were also found to display similar, *SlMIXTA-like*-dependent, expression patterns. In most cases the enzymatic activity of the proteins

coded by these various genes was inferred through the homology with characterized orthologs, but for a number of the candidate enzymes, assays were performed to confirm these activities. Thus, for a few of the steps in the cutin metabolic pathway, namely the terminal hydroxylation of activated fatty acids by *SlCYP86A68* and the mid-chain hydroxylation of fatty acids by both *SlCYP77A1* and *SlCYP77A2*, we are able to present cohesive data for *SlMIXTA-like* regulated gene expression, enzyme activity and the resultant metabolite change in the fruit skin (Fig. 5; Fig. 7; Table 1). Previously, *SlCYP86A69* was shown to be directly regulated by *SlSHN3*, and the resultant activity responsible for cutin biosynthesis (Shi et al., 2013). While *SlCYP86A69* does not appear to be regulated in an *SlMIXTA-like* dependent manner, we show that *SlCYP77A1* action is responsible for the formation of the major cutin monomer found in tomato skin, namely C16-9/10, 16-DiHFA, and that *SlCYP77A1* is regulated in an *SlMIXTA-like* dependent manner.

The broad spectrum of influence exerted through *SlMIXTA-like* activity strongly suggests a central role for *SlMIXTA-like* in the positive regulation of cuticle deposition (particularly cutin). Significantly, recent work has shown that the *Arabidopsis* orthologs of *SlMIXTA-like*, *AtMYB16* and *AtMYB106*, also play a role in the regulatory network of cuticle assembly (Oshima et al., 2013), although their effect is less specific as they regulate both the wax and cutin biosynthetic pathways. Interestingly, one of the orthologs, *AtMYB106*, is able to regulate the expression of *AtSHN1*, which appears to be an inversion of the relationship seen between these two orthologs in tomato (Fig. 9), pointing to a complex evolutionary relationship between these proteins.

3.3.3 *SlMIXTA-like* Regulates Postharvest Water Loss Prevention and Resistance to Fungal Infection

Previous studies demonstrated the important role of the cuticle in protecting plants from biotic and abiotic stresses, and that abnormal cuticle formation can lead to plants with altered susceptibility to dehydration stress and fungal infection (Bargel et al., 2006; Riederer and Muller, 2006; Isaacson et al., 2009). In the case of *SlMIXTA*-RNAi lines an increase in susceptibility to both fungal infection and postharvest water loss was observed. It seems likely that the significantly thinner cuticle allows easier penetration of the epidermal cells by *C. coccodes* and thus faster proliferation of the fungus. This conclusion was supported by the fact that *C. coccodes* fungus had similar rate of germination and appressoria formation but the decay area was significantly larger.

However, the increased postharvest water loss is more difficult to explain. Previous research has suggested that cuticular waxes rather than the cutin matrix are responsible for the water-proofing of the plant (Vogg et al., 2004; Isaacson et al., 2009). However, in the case of tomato lines reduced in *SlMIXTA-like* expression there appears to be limited changes to the total (epi and intra-) cuticular wax composition. It may be that severity of reduction in the cutin polymer provided a reduced matrix to which the intra-cuticular waxes may be attached and embedded. Therefore it is possible that altered cuticular structure and arrangement is the main factor responsible for the increase in water loss.

Recent work showed that the cuticle is involved in the transmission of osmotic stress signals via ABA biosynthesis (Wang et al., 2011). The fact that *SlMIXTA*-RNAi lines displayed down-regulation of the ABA biosynthesis gene *NINE-CIS-epoxycarotenoid dioxygenase1* (*SlNCED1*) (Sun et al., 2012; Ji et al., 2014) suggests that the reason for the increased susceptibility to dehydration may be due to the impairment of a signal originating from the cuticle (Supplemental Fig. S4; Supplemental Dataset S1). Further, increased cuticle permeability in ABA deficient mutants has been reported (Curvers et al., 2010), suggesting a feedback loop connecting ABA biosynthesis and cuticle formation that might be regulated via the action of SlMIXTA-like. Furthermore, ABA biosynthesis was recently shown to be up-regulated in tomato fruit's resistance response to *Colletotricum* (Alkan et al., 2015). This, therefore, may further contribute to the enhanced fungal colonization of *SlMIXTA*-RNAi fruit surface.

3.3.4 Conclusions

The evolution of land plants resulted in a number of important changes to the epidermal layer of aerial organs including of fleshy fruit. Over time, epidermal cells began to differentiate to form a variety of cell types while concurrently developing the specialized cuticular membrane necessary for overcoming the challenges of life on land. It is thus anticipated that the co-evolution of the epidermis cell layer and the cuticle coating it should intersect, particularly at the regulatory level. Here we provide evidence that SlMIXTA-like transcriptionally modulates epidermal cell patterning as well as cuticle assembly and forms part of a transcriptional regulatory network that mediates the patterning of fruit surface. Hence, this work highlights the strong evolutionary and regulatory relationship between plant epidermal cell development and cuticle deposition and points to *SlMIXTA-like* as a major player in this relationship.

3.4 Methods

3.4.1 Plant Materials and Transformation

Silencing of *SlMIXTA-like* (*Solyc02g088190*) was performed in *S. lycopersicum* L. *cv.* MicroTom (MT). The construct for the post transcriptional silencing (*SlMIXTA*-RNAi) was generated by PCR, isolating a 273 bp fragment of *SlMIXTA* from *cv.* MT cDNA and cloning into pENTR/D-TOPO (Invitrogen). LR Clonase (Invitrogen) was used to recombine this fragment into the pH7GWIWG2(II) binary vector (Karimi et al., 2002). The primers used in the creation of the constructs in this study are listed in Supplemental Table S2. Cotyledon transformation of MT tomato was performed as previously described (Dan et al., 2006). Subsequent gene expression analysis, chemical characterization and fungal infection and water loss assays were performed using at least three independently transformed lines.

3.4.2 *In Silico* Analysis

Nucleotide and protein sequence retrieval from the SOL Genomics Network database was performed via BLAST (Fernandez-Pozo et al., 2015). Protein alignments were performed with ClustalW (Larkin et al., 2007) and the resultant molecular phylogenetic trees visualized using MEGA6 (Tamura et al., 2013). Neighbor-joining trees were constructed with bootstrapping calculated from 1000 instances. Promoter regions consisting of 1 Kb of upstream sequence from the start codons were analyzed for binding motifs using the PLACE database (Higo et al., 1999). Determination of enrichment of promoter motifs and of L1 layer-specific genes was performed using the hypergeometric distribution analysis provided by GeneProf (Halbritter et al., 2014). Promoter motif presence was compared to 6000 kb of randomly extracted genomic DNA spanning all 12 tomato chromosomes (Fernandez-Pozo et al., 2015). Hierarchical clustering of genes based on available large scale expression data (Itkin et al., 2013), was performed using EXPANDER (Ulitsky et al., 2010) with the default parameters.

3.4.3 Gene expression Analysis

Total RNA extractions were performed with Trizol Reagent (Invitrogen) from manually dissected skin and flesh tissues pooled from five to six tomato fruits. Skin tissue can be thought of enriched for epidermal cells. RNA was extracted from mature green peel tissue from three independently transformed tomato lines and wild type lines. The cDNA was synthesized using Invitrogen's SuperScript II reverse transcriptase kit.

Quantitative real-time PCR (qRT-PCR) analysis was performed using gene-specific oligonucleotides on an ABI 7300 instrument (Applied Biosystems, Norwalk, CT, USA) with the Platinum SYBR SuperMix (Invitrogen) under default parameters. Mean expression values were calculated for three independent transformation events. Applied Biosystems software was used to generate expression data. Sequences of gene-specific oligonucleotides are provided in Supplemental Table S2. Microarray analysis was performed using the 34,000 gene EUTOM3 exon array (http://www.eu-sol.net/science/bioinformatics/data-and-databases/all-databases) as described previously (Powell et al., 2012).

3.4.4 Light-, Electron- and Atomic Force- Microscopy

Samples for electron microscopy were prepared and analyzed as described previously (Panikashvili et al., 2009). Samples prepared for TEM analysis were also used for FIB-SEM analysis. The FIB-SEM tomography of the region of interest, containing a number of epidermal cells, was performed with the FEI Slice and View software™. Milling was done at an acceleration voltage of 30 kV and current of 2.7 nA. SEM images of the milled surface were acquired with the through-the-lens detector (TLD, SE mode) in immersion mode and an electron beam of 2 kV, 340 pA and 30 µs of dwell time. Subsequent 3D reconstruction was performed by AVIZO software application. For light microscopy, skin tissue samples were fixed and embedded in wax as described previously (Mintz-Oron et al., 2008). Sections were cut to 5–10 µm on a Leica 2000 microtome, and placed on glass slides. The slides were stained with Sudan IV (Buda et al., 2009) or toluidine blue (Tanaka et al., 2004) and then observed with a Olympus CLSM500 microscope. Freshly harvested skin samples were used for AFM imaging. Samples were mounted on a stub, and transferred to the AFM for imaging. All imaging was performed on a NT-MDT NTEGRA instrument, employing the SMENA scanning head. Imaging was performed either in contact mode using Bruker DNP-S probes or Olympus ORC-PS-W probes with nominal spring constant of 0.1 $N.m^{-1}$, or in semi-contact mode using Olympus AC240TS probes with nominal frequency of 70 kHz and spring constant of 2 $N.m^{-1}$. There was no difference in images obtained by the two modes with exception of one sample with some contamination that was swept aside in contact mode. The raw data were processed only by 2D leveling.

3.4.5 Cuticular Lipid Analyses

Fruit skin discs were prepared for cuticular lipid extraction as previously described (Shi et al., 2013). Cuticular waxes were then extracted and analyzed as previously described (Kurdyukov et al., 2006; Kurdyukov et al., 2006), followed by cutin extraction and analysis as described previously (Franke et al., 2005).

3.4.6 Enzyme Activity Assays

Enzyme activity assays were performed using heterologously expressed SlCYP77A1, SlCYP77A2 and SlCYP68A68 according to methods previously described (Grausem et al., 2014). Briefly, the genes under investigation were cloned and expressed in a yeast expression system specifically developed for the expression of P450 enzymes (Pompon et al., 1996) (Supplemental Table S2). Expression of the tomato P450s was induced, microsomes were extracted, microsomal proteins were incubated with radiolabeled substrate and the enzyme assay initiated by the addition of NADPH. Only three cytochromes P450 are encoded by the yeast genome, and are not expressed or expressed at a negligible level during the applied growth conditions. Further, none of them are able to metabolize fatty acids (Kandel et al., 2005; Sauveplane et al., 2009), ensuring that the metabolism described results from enzymatic reactions catalyzed by the heterologously expressed cytochrome P450s. Completed assays were directly spotted on TLC plates for the separation of possible products formed. Plates were scanned with a radioactivity detector and the areas corresponding to the metabolites were identified for subsequent GC-MS analysis. GC-MS analysis was carried out and analyzed as described previously (Eglinton et al.; Grausem et al., 2014). Metabolites generated from 16-hydroxypalmitic acid were identified as described previously (Li-Beisson et al., 2009). As no standards are available, position of hydroxyl group is given by fragmentation on both sides of the derivatized hydroxyl. This results in ions that allow one to distinguish between products.

3.4.7 Fungal Infection and Dehydration Assays

Colletotrichum coccodes isolate 138 (Alkan et al., 2008) was used to inoculate fruit of freshly harvested breaker stage tomato fruits. The fruits were surface-sterilized in 0.3% (v/v) hypochlorite for 3 min, rinsed thoroughly with sterile water and dried. Drop inoculation was performed directly on the fruit cuticle by applying a 7 µl of a conidia suspension (10^6 conidia.ml^{-1}). Each line had 30 biological inoculation repeats. Following inoculation, fruits were incubated at humid chambers, 22°C and approximately 95%

relative humidity. At 19 hours post inoculation percentage of *C. coccodes* conidia germination and appressorium formation was evaluated under a light-microscope. Disease evaluation of inoculated tomato fruits was performed by measuring the decay diameter, over 7 days post inoculation. The experiment was repeated three times. For water loss measurement assays red stage fruit was harvested and stored at room temperature for forty days. Fruit mass was periodically recorded and water loss percentage calculated.

3.5 Acknowledgements

This work was supported by the Israel Science Foundation (ISF) personal grant to A.A. (ISF Grant No. 646/11). We thank the Adelis Foundation, Leona M. and Harry B. Helmsley Charitable Trust, Jeanne and Joseph Nissim Foundation for Life Sciences, Tom and Sondra Rykoff Family Foundation Research and the Raymond Burton Plant Genome Research Fund for supporting the AA lab activity. AA is the incumbent of the Peter J. Cohn Professorial Chair. We thank Sidney Cohen for assistance in performing the AFM analysis. We thank Gilgi Friedlander for the assistance in the analysis of the microarray data.

3.6 Author Contributions

J.L. designed and performed research, analyzed data, and was the primary writer of the article. A.A., O.L., N.A., T.T., K.R., J-P. F., B.G., F.P. and A.G. performed experiments. F.C. analyzed data, and co-wrote the article. A.A. designed research, analyzed data and co-wrote the article. All authors read, made relevant suggestions and approved the final manuscript.

3.7 Supplemental Data

See ***Appendix A*** (page 173) for supplementary materials

Supplemental Fig. S1. Identification of potential tomato MIXTA/MIXTA-like orthologues. (A) A molecular phylogenetic tree is constructed for potential tomato MIXTA and MIXTA-like orthologues together with described *Arabidopsis* MYB-factors and the well charcaterized MIXTA and MIXTA-like orthologues from *Antirrhinum majus* and *Petunia hybrida* (AmMIXTA and PhMYB1 respectively). The previously described Subgroup 9 containing MIXTA/MIXTA-like and MYB17 orthologues is highlighted as well as the MIXTA/MIXTA-like clade. ClustalW and the MEGA6 software were used to align the proteins and compute the neighbor-joining tree with significance percentages

(bootstrap values out of 1000). The scale bar represents the relative amino acid difference. Alignments can be viewed in Supplemental Fig. S2. (B) The previously described motif characteristic of Subgroup 9 is shown (SB-9). Amino acids previously identified to differentiate between Subgroup 9A and Subgroup 9B are indicated with an asterisk (*).

Supplemental Fig. S2. Protein alignments used to construct molecular phylogenetic trees. (A) Alignment of MYB factors used in Supplemental Fig. S1 (B) Alignment of MIXTA/MIXTA-like proteins used in Fig. 1A. (C) Alignment of HD-ZIP IV factors used in Supplemental Fig. S6. (D) CYP used in Supplemental Fig. S7. ClustalW and the MEGA6 software were used to align the proteins in all cases.

Supplemental Fig. S3. Atomic Force Microscopy (AFM) images of immature green tomato surface of wild-type and *SlMIXTA-like* silenced plants. (A) and (B) Topographic images generated from AFM analysis show the surface of the *SlMIXTA*-RNAi tomato fruit (B) is markedly flatter than the wild-type (A). (C) and (D) Three-dimensional topographic images from AFM analysis confirm the flatter surface observed for *SlMIXTA*-RNAi (D) tomato fruit when compared with wild-type (C). Further, the surface of the fruit from *SlMIXTA-like* silenced plants appear more irregular, exhibiting a small-scale roughness which could be due to the relatively collapsed state of the conical structures.

Supplemental Fig. S4. Validation of microarray-based differential gene expression results by means of quantitative RT-PCR (qRT-PCR) analysis. The analysis with qRT-PCR confirmed the expression profile of eight genes identified in microarray analysis, while also identifying a number of genes not detected in the microarray analysis. *SlSHN3*, *Solyc06g065820*; *Slα-DOX2*, *Solyc03g119060*; *SlLACS4*, *Solyc01g095750*; *SlLACS2*, *Solyc01g109180*; *SlCYP77A2*, *Solyc05g055400*; *SlTMH27*, *Solyc10g055410*; *SlNCED1*, *Solyc07g056570*. *SlCER3*, *Solyc03g117800*; *SlCYP77A1*, *Solyc1g007540*; *SlCYP77A2*, *Solyc05g055400*; *SlCYP86A68*, *Solyc01g094750*; *SlGDSLa*, *Solyc07g049440;* *SlGL2*, *Solyc03g120620*; *SlGPAT4*, *Solyc01g094700*; *SlCD2*, *Solyc01g091630*; *SlDCR,* *Solyc03g025320*; *SlGPAT4*, *Solyc01g094700*; *SlPDF2d*, *Solyc06g050160*; *SlCD1*, *Solyc11g006250*. Values represent mean ± standard error (n=3; *=p<0.05; **= P<0.01).

Supplemental Fig. S5. Normalized expression across 20 tomato tissues of selected genes described in this study to be down regulated in the *SlMIXTA*-RNAi tomato lines. Expression patterns were extracted from the dataset generated by Itkin *et al*. (2013) and are shown in RPKM. IG, immature green; MG, mature green; Br, breaker; Or, orange; Re, red; Y, young. *ABCG32*, *Solyc06g065670*; *ABCG11, Solyc03g019760*; *α-DOX2*, *Solyc03g119060*; *α/β-hydrolase-1*, *Solyc05g054330*; *α/β-hydrolase-2*, *Solyc09g075140*; *CER3*, *Solyc03g117800*; *CYP77A1*, *Solyc1g007540*; *CYP77A2*, *Solyc05g055400*; *CYP86A68*, *Solyc01g094750*; *GDSLa*, *Solyc07g049440*; *GDSL esterase/lipase-1*, *Solyc04g081770*; *GDSL esterase/lipase-2*, *Solyc03g121180*; *GL2*, *Solyc03g120620*; *GPAT4*, *Solyc01g094700*; *HTH*, *Solyc08g080190*; *KCS3*, *Solyc11g072990*; *LACS2*, *Solyc01g109180*; *LACS4*, *Solyc01g095750*; *MIXTA-like*, *Solyc02g088190*; *PAL*, *Solyc05g056170*.

Supplemental Fig. S6. Molecular phylogeny of the HD-ZIP IV family proteins associated with epidermal cell patterning and ones identified in this study. Molecular phylogenetic analysis of the *Arabidopsis* HD-ZIP IV protein clade is shown together with HD-ZIP IV members discussed in this paper. ClustalW and the MEGA6 software were used to align the proteins and compute the neighbor-joining tree with significance percentages (bootstrap values out of 1000). The scale bar represents the relative amino

acid difference. Alignments can be seen in Supplemental Fig. S2. Relevant information regarding functional annotation of some characterized proteins is also displayed.

Supplemental Fig. S7. Molecular phylogeny of the CYP77A and CYP86A family proteins discussed in this study. Molecular phylogenetic analysis of the CYP77A and CYP86A protein clades discussed in this paper is shown. ClustalW and the MEGA6 software were used to align the proteins and compute the neighbor-joining tree with significance percentages (bootstrap values out of 1000). The scale bar represents the relative amino acid difference. Alignments can be seen in Supplemental Fig. S2. Relevant information regarding regulation by SlMIXTA-like and SlSHN3 is displayed.

Supplemental Fig. S8. Radiochromatographic resolution by Thin Layer Chromatography (TLC) of metabolites generated in incubations of dodecanoic acid with microsomes from yeast expressing *SlCYP86A68* or *SlCYP77A2.* (A) and (B) Radiochromatographic resolution by TLC of metabolites detected in samples of microsomes from yeast expressing *SlCYP86A68* incubated with 100 µM dodecanoic acid in the absence (A) or in the presence (B) of NADPH. Incubations were performed for 20 min with 600 mg of microsomal proteins at 27°C and the incubation media was directly spotted on TLC. The reaction product formed is 12-hydroxy-dodecanoic acid acid; Peak S, dodecanoic acid. (C) and (D) Radiochromatographic resolution by TLC of metabolites detected in samples of microsomes from yeast expressing *SlCYP77A2* incubated with 100 µM dodecanoic acid in the absence (C) or in the presence (D) of NADPH. Incubations were performed for 20 min with 600 mg of microsomal proteins at 27°C and the incubation media was directly spotted on TLC. The reaction product formed is 12-hydroxy- dodecanoic acid; Peak S, dodecanoic acid.

Supplemental Fig. S9. Germination rate and appressoria formation of *Colletotrichum coccodes* is unchanged on *SlMIXTA-like* silenced fruit surface. Fungal germination rates were measured in breaker stage tomato fruit inoculated with 7 µl of 10^6 *Colletotrichum coccodes* conidia/ml and incubated at 22°C and 95% relative humidity for 7 days post inoculation. Error bars represent standard error (n=30).

Supplemental Table S1. Quantification of cuticular waxes in fruit of *SlMIXTA-like* silenced lines.

Supplemental Table S2. Oligonucleotides used in this study.

Supplemental Dataset S1. Significantly down-regulated and up-regulated genes in skin tissue of *SlMIXTA*-RNAi lines identified via microarray analysis. Down-regulated genes are listed in Table 1, and up-regulated genes in Table 2.

Supplemental Dataset S2. Generation and analysis of tomato lines over expressing *SlMIXTA-like*.

Supplemental Dataset S3. Microarray gene expression data of SlMIXTA-RNAi lines and Wildtype lines.

Supplemental Movie S1. Three-dimensional reconstruction from FIB-SEM acquisition of an epidermal cell from wild type tomato fruit.

Supplemental Movie S2. Three-dimensional reconstruction from FIB-SEM acquisition of an epidermal cell from tomato fruit silenced for *SlMIXTA-like* expression.

3.8 References

Abe M, Katsumata H, Komeda Y, Takahashi T (2003) Regulation of shoot epidermal cell differentiation by a pair of homeodomain proteins in Arabidopsis. Development **130:** 635-643

Abe M, Takahashi T, Komeda Y (2001) Identification of a cis-regulatory element for L1 layer-specific gene expression, which is targeted by an L1-specific homeodomain protein. Plant J **26:** 487-494

Aharoni A, Dixit S, Jetter R, Thoenes E, van Arkel G, Pereira A (2004) The SHINE clade of AP2 domain transcription factors activates wax biosynthesis, alters cuticle properties, and confers drought tolerance when overexpressed in Arabidopsis. Plant Cell **16:** 2463-2480

Alkan N, Fluhr R, Sherman A, Prusky D (2008) Role of ammonia secretion and pH modulation on pathogenicity of Colletotrichum coccodes on tomato fruit. Mol Plant Microbe Interact **21:** 1058-1066

Alkan N, Friedlander G, Ment D, Prusky D, Fluhr R (2015) Simultaneous transcriptome analysis of Colletotrichum gloeosporioides and tomato fruit pathosystem reveals novel fungal pathogenicity and fruit defense strategies. New Phytol **205:** 801-815

Bargel H, Koch K, Cerman Z, Neinhuis C (2006) Structure–function relationships of the plant cuticle and cuticular waxes – a smart material? . Functional Plant Biology **33:** 893-910

Baumann K, Perez-Rodriguez M, Bradley D, Venail J, Bailey P, Jin H, Koes R, Roberts K, Martin C (2007) Control of cell and petal morphogenesis by R2R3 MYB transcription factors. Development **134:** 1691-1701

Bernard A, Domergue F, Pascal S, Jetter R, Renne C, Faure JD, Haslam RP, Napier JA, Lessire R, Joubès J (2012) Reconstitution of plant alkane biosynthesis in yeast demonstrates that Arabidopsis ECERIFERUM1 and ECERIFERUM3 are core components of a very-long-chain alkane synthesis complex. Plant Cell **24:** 3106-3118

Bessire M, Borel S, Fabre G, Carraça L, Efremova N, Yephremov A, Cao Y, Jetter R, Jacquat AC, Métraux JP, Nawrath C (2011) A member of the PLEIOTROPIC DRUG RESISTANCE family of ATP binding cassette transporters is required for the formation of a functional cuticle in Arabidopsis. Plant Cell **23:** 1958-1970

Bird D, Beisson F, Brigham A, Shin J, Greer S, Jetter R, Kunst L, Wu X, Yephremov A, Samuels L (2007) Characterization of Arabidopsis ABCG11/WBC11, an ATP binding cassette (ABC) transporter that is required for cuticular lipid secretion. Plant J **52:** 485-498

Brockington SF, Alvarez-Fernandez R, Landis JB, Alcorn K, Walker RH, Thomas MM, Hileman LC, Glover BJ (2013) Evolutionary analysis of the MIXTA gene family highlights potential targets for the study of cellular differentiation. Mol Biol Evol **30:** 526-540

Broun P, Poindexter P, Osborne E, Jiang CZ, Riechmann JL (2004) WIN1, a transcriptional activator of epidermal wax accumulation in Arabidopsis. Proc Natl Acad Sci U S A **101:** 4706-4711

Buda GJ, Isaacson T, Matas AJ, Paolillo DJ, Rose JK (2009) Three-dimensional imaging of plant cuticle architecture using confocal scanning laser microscopy. Plant J **60:** 378-385

Chen X, Truksa M, Snyder CL, El-Mezawy A, Shah S, Weselake RJ (2011) Three homologous genes encoding sn-glycerol-3-phosphate acyltransferase 4 exhibit different expression patterns and functional divergence in Brassica napus. Plant Physiol **155:** 851-865

Cominelli E, Sala T, Calvi D, Gusmaroli G, Tonelli C (2008) Over-expression of the Arabidopsis AtMYB41 gene alters cell expansion and leaf surface permeability. Plant J **53:** 53-64

Curvers K, Seifi H, Mouille G, de Rycke R, Asselbergh B, Van Hecke A, Vanderschaeghe D, Höfte H, Callewaert N, Van Breusegem F, Höfte M (2010) Abscisic acid deficiency causes changes in cuticle permeability and pectin composition that influence tomato resistance to Botrytis cinerea. Plant Physiol **154:** 847-860

Dan Y, Yan H, Munyikwa T, Dong J, Zhang Y, Armstrong CL (2006) MicroTom--a high-throughput model transformation system for functional genomics. Plant Cell Rep **25:** 432-441

Depège-Fargeix N, Javelle M, Chambrier P, Frangne N, Gerentes D, Perez P, Rogowsky PM, Vernoud V (2011) Functional characterization of the HD-ZIP IV transcription factor OCL1 from maize. J Exp Bot **62:** 293-305

Di Stilio VS, Martin C, Schulfer AF, Connelly CF (2009) An ortholog of MIXTA-like2 controls epidermal cell shape in flowers of Thalictrum. New Phytol **183:** 718-728

Dillard HR (1989) Effect of temperature, wetness duration, and inoculum density on infection and lesion development of Colletotrichum coccodes on tomato fruit. Phytopathology**:** 1063-1066

Eglinton G, Hunneman DH, McCormick A Gas chromatographic—mass spectrometric studies of long chain hydroxy acids.—III.1 The mass spectra of the methyl esters trimethylsilyl ethers of aliphatic hydroxy acids. A facile method of double bond location.

Fernandez-Pozo N, Menda N, Edwards JD, Saha S, Tecle IY, Strickler SR, Bombarely A, Fisher-York T, Pujar A, Foerster H, Yan A, Mueller LA (2015) The Sol Genomics Network (SGN)-from genotype to phenotype to breeding. Nucleic Acids Res **43:** D1036-1041

Filippis I, Lopez-Cobollo R, Abbott J, Butcher S, Bishop GJ (2013) Using a periclinal chimera to unravel layer-specific gene expression in plants. Plant J **75:** 1039-1049

Franke R, Briesen I, Wojciechowski T, Faust A, Yephremov A, Nawrath C, Schreiber L (2005) Apoplastic polyesters in Arabidopsis surface tissues--a typical suberin and a particular cutin. Phytochemistry **66:** 2643-2658

Gilding EK, Marks MD (2010) Analysis of purified glabra3-shapeshifter trichomes reveals a role for NOECK in regulating early trichome morphogenic events. Plant J **64:** 304-317

Girard AL, Mounet F, Lemaire-Chamley M, Gaillard C, Elmorjani K, Vivancos J, Runavot JL, Quemener B, Petit J, Germain V, Rothan C, Marion D, Bakan B (2012) Tomato GDSL1 is required for cutin deposition in the fruit cuticle. Plant Cell **24:** 3119-3134

Glover BJ (2000) Differentiation in plant epidermal cells. J Exp Bot **51:** 497-505

Gorton HL, Vogelmann TC (1996) Effects of Epidermal Cell Shape and Pigmentation on Optical Properties of Antirrhinum Petals at Visible and Ultraviolet Wavelengths. Plant Physiol **112:** 879-888

Grausem B, Widemann E, Verdier G, Nosbüsch D, Aubert Y, Beisson F, Schreiber L, Franke R, Pinot F (2014) CYP77A19 and CYP77A20 characterized from Solanum tuberosum oxidize fatty acids in vitro and partially restore the wild phenotype in an Arabidopsis thaliana cutin mutant. Plant Cell Environ **37:** 2102-2115

Halbritter F, Kousa AI, Tomlinson SR (2014) GeneProf data: a resource of curated, integrated and reusable high-throughput genomics experiments. Nucleic Acids Res **42:** D851-858

Han J, Clement JM, Li J, King A, Ng S, Jaworski JG (2010) The cytochrome P450 CYP86A22 is a fatty acyl-CoA omega-hydroxylase essential for Estolide synthesis in the stigma of Petunia hybrida. J Biol Chem **285:** 3986-3996

Hen-Avivi S, Lashbrooke J, Costa F, Aharoni A (2014) Scratching the surface: genetic regulation of cuticle assembly in fleshy fruit. J Exp Bot **65:** 4653-4664

Higo K, Ugawa Y, Iwamoto M, Korenaga T (1999) Plant cis-acting regulatory DNA elements (PLACE) database: 1999. Nucleic Acids Res **27:** 297-300

Isaacson T, Kosma DK, Matas AJ, Buda GJ, He Y, Yu B, Pravitasari A, Batteas JD, Stark RE, Jenks MA, Rose JK (2009) Cutin deficiency in the tomato fruit cuticle consistently affects resistance to microbial infection and biomechanical properties, but not transpirational water loss. Plant J **60:** 363-377

Ishida T, Hattori S, Sano R, Inoue K, Shirano Y, Hayashi H, Shibata D, Sato S, Kato T, Tabata S, Okada K, Wada T (2007) Arabidopsis TRANSPARENT TESTA GLABRA2 is directly regulated by R2R3 MYB transcription factors and is involved in regulation of GLABRA2 transcription in epidermal differentiation. Plant Cell **19:** 2531-2543

Itkin M, Heinig U, Tzfadia O, Bhide AJ, Shinde B, Cardenas PD, Bocobza SE, Unger T, Malitsky S, Finkers R, Tikunov Y, Bovy A, Chikate Y, Singh P, Rogachev I, Beekwilder J, Giri AP, Aharoni A (2013) Biosynthesis of antinutritional alkaloids in solanaceous crops is mediated by clustered genes. Science **341:** 175-179

Javelle M, Vernoud V, Depège-Fargeix N, Arnould C, Oursel D, Domergue F, Sarda X, Rogowsky PM (2010) Overexpression of the epidermis-specific homeodomain-leucine zipper IV transcription factor Outer Cell Layer1 in maize identifies target genes involved in lipid metabolism and cuticle biosynthesis. Plant Physiol **154:** 273-286

Jessen D, Olbrich A, Knüfer J, Krüger A, Hoppert M, Polle A, Fulda M (2011) Combined activity of LACS1 and LACS4 is required for proper pollen coat formation in Arabidopsis. Plant J **68:** 715-726

Ji K, Kai W, Zhao B, Sun Y, Yuan B, Dai S, Li Q, Chen P, Wang Y, Pei Y, Wang H, Guo Y, Leng P (2014) SlNCED1 and SlCYP707A2: key genes involved in ABA metabolism during tomato fruit ripening. J Exp Bot **65:** 5243-5255

Kandel S, Morant M, Benveniste I, Blée E, Werck-Reichhart D, Pinot F (2005) Cloning, functional expression, and characterization of CYP709C1, the first sub-terminal hydroxylase of long chain fatty acid in plants. Induction by chemicals and methyl jasmonate. J Biol Chem **280:** 35881-35889

Karimi M, Inzé D, Depicker A (2002) GATEWAY vectors for Agrobacterium-mediated plant transformation. Trends Plant Sci **7:** 193-195

Kolattukudy PE (2001) Polyesters in higher plants. Adv Biochem Eng Biotechnol **71:** 1-49

Kosma DK, Murmu J, Razeq FM, Santos P, Bourgault R, Molina I, Rowland O (2014) AtMYB41 activates ectopic suberin synthesis and assembly in multiple plant species and cell types. Plant J **80:** 216-229

Kurdyukov S, Faust A, Nawrath C, Bär S, Voisin D, Efremova N, Franke R, Schreiber L, Saedler H, Métraux JP, Yephremov A (2006) The epidermis-specific extracellular BODYGUARD controls cuticle development and morphogenesis in Arabidopsis. Plant Cell **18:** 321-339

Kurdyukov S, Faust A, Trenkamp S, Bär S, Franke R, Efremova N, Tietjen K, Schreiber L, Saedler H, Yephremov A (2006) Genetic and biochemical evidence for involvement of HOTHEAD in the biosynthesis of long-chain alpha-,omega-dicarboxylic fatty acids and formation of extracellular matrix. Planta **224:** 315-329

Larkin MA, Blackshields G, Brown NP, Chenna R, McGettigan PA, McWilliam H, Valentin F, Wallace IM, Wilm A, Lopez R, Thompson JD, Gibson TJ, Higgins DG (2007) Clustal W and Clustal X version 2.0. Bioinformatics **23:** 2947-2948

Li Y, Beisson F, Koo AJ, Molina I, Pollard M, Ohlrogge J (2007) Identification of acyltransferases required for cutin biosynthesis and production of cutin with suberin-like monomers. Proc Natl Acad Sci U S A **104:** 18339-18344

Li-Beisson Y, Pollard M, Sauveplane V, Pinot F, Ohlrogge J, Beisson F (2009) Nanoridges that characterize the surface morphology of flowers require the synthesis of cutin polyester. Proc Natl Acad Sci U S A **106:** 22008-22013

Machado A, Wu Y, Yang Y, Llewellyn DJ, Dennis ES (2009) The MYB transcription factor GhMYB25 regulates early fibre and trichome development. Plant J **59:** 52-62

Mahjoub A, Hernould M, Joubès J, Decendit A, Mars M, Barrieu F, Hamdi S, Delrot S (2009) Overexpression of a grapevine R2R3-MYB factor in tomato affects vegetative development, flower morphology and flavonoid and terpenoid metabolism. Plant Physiol Biochem **47:** 551-561

Martin C, Glover BJ (2007) Functional aspects of cell patterning in aerial epidermis. Curr Opin Plant Biol **10:** 70-82

Martin LB, Rose JK (2014) There's more than one way to skin a fruit: formation and functions of fruit cuticles. J Exp Bot **65:** 4639-4651

Matas AJ, Yeats TH, Buda GJ, Zheng Y, Chatterjee S, Tohge T, Ponnala L, Adato A, Aharoni A, Stark R, Fernie AR, Fei Z, Giovannoni JJ, Rose JK (2011) Tissue- and cell-type specific transcriptome profiling of expanding tomato fruit provides insights into metabolic and regulatory specialization and cuticle formation. Plant Cell **23:** 3893-3910

Millar AA, Clemens S, Zachgo S, Giblin EM, Taylor DC, Kunst L (1999) CUT1, an Arabidopsis gene required for cuticular wax biosynthesis and pollen fertility, encodes a very-long-chain fatty acid condensing enzyme. Plant Cell **11:** 825-838

Mintz-Oron S, Mandel T, Rogachev I, Feldberg L, Lotan O, Yativ M, Wang Z, Jetter R, Venger I, Adato A, Aharoni A (2008) Gene expression and metabolism in tomato fruit surface tissues. Plant Physiol **147:** 823-851

Nadakuduti SS, Pollard M, Kosma DK, Allen C, Ohlrogge JB, Barry CS (2012) Pleiotropic phenotypes of the sticky peel mutant provide new insight into the role of CUTIN DEFICIENT2 in epidermal cell function in tomato. Plant Physiol **159:** 945-960

Nakamura M, Katsumata H, Abe M, Yabe N, Komeda Y, Yamamoto KT, Takahashi T (2006) Characterization of the class IV homeodomain-Leucine Zipper gene family in Arabidopsis. Plant Physiol **141:** 1363-1375

Neinhuis C, Barthlott W (1997) Characterization and distribution of waterrepellent, self-cleaning plant surfaces. Annals of Botany **79:** 667-677

Noda K, Glover BJ, Linstead P, Martin C (1994) Flower colour intensity depends on specialized cell shape controlled by a Myb-related transcription factor. Nature **369:** 661-664

Ohashi Y, Oka A, Rodrigues-Pousada R, Possenti M, Ruberti I, Morelli G, Aoyama T (2003) Modulation of phospholipid signaling by GLABRA2 in root-hair pattern formation. Science **300:** 1427-1430

Oshima Y, Shikata M, Koyama T, Ohtsubo N, Mitsuda N, Ohme-Takagi M (2013) MIXTA-like transcription factors and WAX INDUCER1/SHINE1 coordinately regulate cuticle development in Arabidopsis and Torenia fournieri. Plant Cell **25:** 1609-1624

Panikashvili D, Savaldi-Goldstein S, Mandel T, Yifhar T, Franke RB, Höfer R, Schreiber L, Chory J, Aharoni A (2007) The Arabidopsis DESPERADO/AtWBC11 transporter is required for cutin and wax secretion. Plant Physiol **145:** 1345-1360

Panikashvili D, Shi JX, Schreiber L, Aharoni A (2009) The Arabidopsis DCR encoding a soluble BAHD acyltransferase is required for cutin polyester formation and seed hydration properties. Plant Physiol **151:** 1773-1789

Panikashvili D, Shi JX, Schreiber L, Aharoni A (2011) The Arabidopsis ABCG13 transporter is required for flower cuticle secretion and patterning of the petal epidermis. New Phytol **190**: 113–124

Perez-Rodriguez M, Jaffe FW, Butelli E, Glover BJ, Martin C (2005) Development of three different cell types is associated with the activity of a specific MYB transcription factor in the ventral petal of Antirrhinum majus flowers. Development **132:** 359-370

Pinot F, Beisson F (2011) Cytochrome P450 metabolizing fatty acids in plants: characterization and physiological roles. FEBS J **278:** 195-205

Plett JM, Wilkins O, Campbell MM, Ralph SG, Regan S (2010) Endogenous overexpression of Populus MYB186 increases trichome density, improves insect pest resistance, and impacts plant growth. Plant J **64:** 419-432

Pollard M, Beisson F, Li Y, Ohlrogge JB (2008) Building lipid barriers: biosynthesis of cutin and suberin. Trends Plant Sci **13:** 236-246

Pompon D, Louerat B, Bronine A, Urban P (1996) Yeast expression of animal and plant P450s in optimized redox environments. Methods Enzymol **272:** 51-64

Powell AL, Nguyen CV, Hill T, Cheng KL, Figueroa-Balderas R, Aktas H, Ashrafi H, Pons C, Fernández-Muñoz R, Vicente A, Lopez-Baltazar J, Barry CS, Liu Y, Chetelat R, Granell A, Van Deynze A, Giovannoni JJ, Bennett AB (2012) Uniform ripening encodes a Golden 2-like transcription factor regulating tomato fruit chloroplast development. Science **336:** 1711-1715

Rani SH, Krishna TH, Saha S, Negi AS, Rajasekharan R (2010) Defective in cuticular ridges (DCR) of Arabidopsis thaliana, a gene associated with surface cutin formation, encodes a soluble diacylglycerol acyltransferase. J Biol Chem **285:** 38337-38347

Rerie WG, Feldmann KA, Marks MD (1994) The GLABRA2 gene encodes a homeo domain protein required for normal trichome development in Arabidopsis. Genes Dev **8:** 1388-1399

Riederer M, Muller C (*eds*) (2006) Biology of the Plant Cuticle. Annual Plant Reviews Vol 23. Blackwell, Oxford, UK

Sauveplane V, Kandel S, Kastner PE, Ehlting J, Compagnon V, Werck-Reichhart D, Pinot F (2009) Arabidopsis thaliana CYP77A4 is the first cytochrome P450 able to catalyze the epoxidation of free fatty acids in plants. FEBS J **276:** 719-735

Schnurr J, Shockey J, Browse J (2004) The acyl-CoA synthetase encoded by LACS2 is essential for normal cuticle development in Arabidopsis. Plant Cell **16:** 629-642

Scoville AG, Barnett LL, Bodbyl-Roels S, Kelly JK, Hileman LC (2011) Differential regulation of a MYB transcription factor is correlated with transgenerational epigenetic inheritance of trichome density in Mimulus guttatus. New Phytol **191:** 251-263

Seo PJ, Lee SB, Suh MC, Park MJ, Go YS, Park CM (2011) The MYB96 transcription factor regulates cuticular wax biosynthesis under drought conditions in Arabidopsis. Plant Cell **23:** 1138-1152

Shi JX, Adato A, Alkan N, He Y, Lashbrooke J, Matas AJ, Meir S, Malitsky S, Isaacson T, Prusky D, Leshkowitz D, Schreiber L, Granell AR, Widemann E, Grausem B, Pinot F, Rose JK, Rogachev I, Rothan C, Aharoni A (2013) The tomato SlSHINE3 transcription

factor regulates fruit cuticle formation and epidermal patterning. New Phytol **197:** 468-480

Shi JX, Malitsky S, De Oliveira S, Branigan C, Franke RB, Schreiber L, Aharoni A (2011) SHINE transcription factors act redundantly to pattern the archetypal surface of Arabidopsis flower organs. PLoS Genet **7:** e1001388

Stracke R, Werber M, Weisshaar B (2001) The R2R3-MYB gene family in Arabidopsis thaliana. Curr Opin Plant Biol **4:** 447-456

Sun L, Sun Y, Zhang M, Wang L, Ren J, Cui M, Wang Y, Ji K, Li P, Li Q, Chen P, Dai S, Duan C, Wu Y, Leng P (2012) Suppression of 9-cis-epoxycarotenoid dioxygenase, which encodes a key enzyme in abscisic acid biosynthesis, alters fruit texture in transgenic tomato. Plant Physiol **158:** 283-298

Takada S, Takada N, Yoshida A (2013) ATML1 promotes epidermal cell differentiation in Arabidopsis shoots. Development **140:** 1919-1923

Tamura K, Stecher G, Peterson D, Filipski A, Kumar S (2013) MEGA6: Molecular Evolutionary Genetics Analysis version 6.0. Mol Biol Evol **30:** 2725-2729

Tanaka T, Tanaka H, Machida C, Watanabe M, Machida Y (2004) A new method for rapid visualization of defects in leaf cuticle reveals five intrinsic patterns of surface defects in Arabidopsis. Plant J **37:** 139-146

Tominaga-Wada R, Iwata M, Sugiyama J, Kotake T, Ishida T, Yokoyama R, Nishitani K, Okada K, Wada T (2009) The GLABRA2 homeodomain protein directly regulates CESA5 and XTH17 gene expression in Arabidopsis roots. Plant J **60:** 564-574

Tominaga-Wada R, Nukumizu Y, Sato S, Wada T (2013) Control of plant trichome and root-hair development by a tomato (Solanum lycopersicum) R3 MYB transcription factor. PLoS One **8:** e54019

Ulitsky I, Maron-Katz A, Shavit S, Sagir D, Linhart C, Elkon R, Tanay A, Sharan R, Shiloh Y, Shamir R (2010) Expander: from expression microarrays to networks and functions. Nat Protoc **5:** 303-322

Vogg G, Fischer S, Leide J, Emmanuel E, Jetter R, Levy AA, Riederer M (2004) Tomato fruit cuticular waxes and their effects on transpiration barrier properties: functional characterization of a mutant deficient in a very-long-chain fatty acid beta-ketoacyl-CoA synthase. J Exp Bot **55:** 1401-1410

Walford SA, Wu Y, Llewellyn DJ, Dennis ES (2011) GhMYB25-like: a key factor in early cotton fibre development. Plant J **65:** 785-797

Walford SA, Wu Y, Llewellyn DJ, Dennis ES (2012) Epidermal cell differentiation in cotton mediated by the homeodomain leucine zipper gene, GhHD-1. Plant J **71:** 464-478

Wang ZY, Xiong L, Li W, Zhu JK, Zhu J (2011) The plant cuticle is required for osmotic stress regulation of abscisic acid biosynthesis and osmotic stress tolerance in Arabidopsis. Plant Cell **23:** 1971-1984

Whitney HM, Bennett KM, Dorling M, Sandbach L, Prince D, Chittka L, Glover BJ (2011) Why do so many petals have conical epidermal cells? Ann Bot **108:** 609-616

Whitney HM, Chittka L, Bruce TJ, Glover BJ (2009) Conical epidermal cells allow bees to grip flowers and increase foraging efficiency. Curr Biol **19:** 948-953

Yang W, Pollard M, Li-Beisson Y, Beisson F, Feig M, Ohlrogge J (2010) A distinct type of glycerol-3-phosphate acyltransferase with sn-2 preference and phosphatase activity producing 2-monoacylglycerol. Proc Natl Acad Sci U S A **107:** 12040-12045

Yang W, Simpson JP, Li-Beisson Y, Beisson F, Pollard M, Ohlrogge JB (2012) A land-plant-specific glycerol-3-phosphate acyltransferase family in Arabidopsis: substrate specificity, sn-2 preference, and evolution. Plant Physiol **160:** 638-652

Yeats T, Martin L, Viart H, Isaacson T, He Y, Zhao L, Matas A, Buda G, Domozych D, Clausen M, Rose J (2012) The identification of cutin synthase: formation of the plant polyester cutin. Nature Chemical Biology **8:** 609-611

Yeats TH, Huang W, Chatterjee S, Viart HM, Clausen MH, Stark RE, Rose JK (2014) Tomato Cutin Deficient 1 (CD1) and putative orthologs comprise an ancient family of cutin synthase-like (CUS) proteins that are conserved among land plants. Plant J **77:** 667-675

Zhang F, Zuo K, Zhang J, Liu X, Zhang L, Sun X, Tang K (2010) An L1 box binding protein, GbML1, interacts with GbMYB25 to control cotton fibre development. J Exp Bot **61:** 3599-3613

Chapter 4

Research Results

Genome Investigation Suggests *MdSHN3*, an APETALA2-domain Transcription Factor Gene, to be a Positive Regulator of Apple Fruit Cuticle Formation and an Inhibitor of Russet Development

This chapter has been compiled from a manuscript published in *Journal of Experimental Botany*, as referenced below:

Lashbrooke J, Aharoni A, Costa F (2015) Genome investigation suggests *MdSHN3*, an *APETALA2*-domain transcription factor gene, to be a positive regulator of apple fruit cuticle formation and an inhibitor of russet development. *Journal of Experimental Botany*. doi:10.1093/jxb/erv366

4.1 Introduction

The plant cuticle is a continuous lipophilic layer covering the above ground epidermal layer of the plant. While the cuticle contributes to the structural support of the cell, its principal role is likely the interaction point between the plant and its environment where it contributes to the protection against both biotic and abiotic stresses (Bargel *et al.*, 2006; Yeats and Rose, 2013). In particular, the cuticle structure is highly adapted to efficiently overcome dehydration stress (McCourt *et al*., 2004). Consisting of an ester bonded matrix of medium chain length fatty acids embedded with very long chain fatty acids the cuticle is extremely hydrophobic, and provides a robust barrier for movement of water and other ions (Kunst and Samuels, 2003; Pollard *et al.*, 2008; Samuels *et al.*, 2008).

The regulation of water loss is vitally important not only for the plant, but also in terms of agriculture management, since excessive water loss results in significant decreases to postharvest fruit quality (Albert *et al*. 2013; Lara *et al.*, 2014). This is particularly true for apple (*Malus x domestica* Borkh.), a species for which its storage capacity is largely responsible for its economic success. An ability to maintain acceptable levels of water loss over an extended postharvest can ensure fruit delivery to world-wide markets and the availability of apples year round. While mild cuticle failure may lead to excess water loss or an increase in fungal infection rates (Shi *et al.*, 2013), severe cuticle failure in fruit results in a disorder known as russeting (Lara *et al.*, 2014). This disorder results from the development of a series of microscopic cracks in the cuticle and the subsequent formation of a waterproofing periderm layer consisting largely of suberin (Khanal *et al.*, 2013). Suberin is an aliphatic polymer possessing less elasticity and less water retention qualities than cutin (Beisson *et al*., 2012; Kolattukudy, 2001; Schreiber, 2010). A russeted surface is typically rough and corky and is generally considered an undesirable trait for commercialization (Andre *et al.*, 2013), although there a number of russeted apple cultivars exist for a niche market. Apples are particularly susceptible to russet, with many naturally occurring cultivars consistently displaying this physiology, while usually non-russeted cultivars may develop russet due to environmental stresses (Curry, 2012; Knoche *et al.*, 2011). An impaired cuticular structure may also affect the mechanical strength of the apple peel, impacting handling and postharvest processing (Saladié *et al.*, 2007). Moreover, the development of cuticular cracks also accelerate the development of flesh browning due to an enhanced

oxidative process (Lara *et al.*, 2014), and may result in softer internal tissue due to the loss of an external mechanical support (Saladié *et al.*, 2005; Saladié *et al.*, 2007).

In light of the importance of proper cuticle formation in fruit crop production, particularly in apple, an understanding of the biosynthesis and regulation of this layer is vital. The majority of the previous research concerning these topics has been performed in tomato and has recently been reviewed by Martin and Rose (2014) and Hen-Avivi *et al*. (2014). Investigation of the transcriptional regulation of cuticle formation in fruit suggests a complex network of transcription factors playing a role in both epidermal cell identity and cuticle formation. The WAX INDUCER1/SHINE1 (WIN1/SHN1) clade of APETELA2 (AP2)-domain transciption factors have been reported to be major factors in this network (Hen-Avivi *et al.*, 2014; Shi *et al.*, 2013; Shi *et al.*, 2011). Three members of this family from *Arabidopsis* have been characterized, and demonstrated to act redundantly during cuticle deposition and epidermal cell patterning (Aharoni *et al.*, 2004; Broun *et al.*, 2004; Kannangara *et al.*, 2007; Shi *et al.*, 2011). Further, in tomato *SlSHN3* has been identified as a positive regulator of cuticle deposition. These genes have been demonstrated to exert their influence through the downstream regulation of other transcription factors as well as cuticle biosynthesis genes (Hen-Avivi *et al.*, 2014; Shi *et al.*, 2013).

While the fruit cuticle has been largely investigated in tomato, very little is known regarding the regulatory process occurring in apple. Work presented by Albert *et al.*, (2013), identified the expression profile of a number of apple genes orthologous to characterized cuticle formation genes from other species, but provided no functional information concerning the apple genes themselves. In this work a QTL mapping was performed to identify genes involved in apple fruit cuticle assembly. For this purpose, a full-sib population generated by crossing 'Golden Delicious' and 'Braeburn' ('GxB') apple cultivars was employed, since it showed a consistent and year-stable russet segregation among seedlings, although both parental cultivars have a normal shiny skin. The subsequent *in silico* anchoring of these genomic regions on the assembled version of the apple genome (Velasco *et al.*, 2010) led to the identification of a series of genes potentially involved in the cuticle formation. Candidate genes were tested via expression analysis to provide further evidence regarding their involvement in cuticle deposition. Individuals identified as having improperly formed cuticles were analyzed via light microscopy and tensile testing. The results display a tight link between improper cuticle deposition and russet formation and identified an apple ortholog to

the SHN clade of transcription factors that is likely responsible for regulating fruit cuticle assembly in apple.

4.2 Results

4.2.1 Cuticle Phenotyping Detects Differences in Tensile Properties

The development of russeting on fruit collected from each seedling of the 'GxB' progeny was evaluated over two years. For both seasons, 16 out of 88 individuals showed visual development of russeting, which occurred with different phenotypic penetrance. The surface area of fruit displaying russet formation spanned from an estimated 5 to 100%. The development of russeting, within the seedlings of 'GxB' population, exhibited a 3:1 segregation ratio, supported by the statistical test of χ^2 = 2.17. However, as russet formation is a result of extreme cuticle failure, this visual analysis fails to identify cuticles that are improperly formed, but not compromised severely enough to result in russeting. Consequently, in order to obtain a more precise characterization of fruit cuticle performance, a mechanical test was carried out. The tensile analysis performed making use of a Texture Analyzer generated mechanical profiles that highlighted the mechanical strength and tensile progression until to the breaking point (Fig. 1; Supp. Fig. 2).

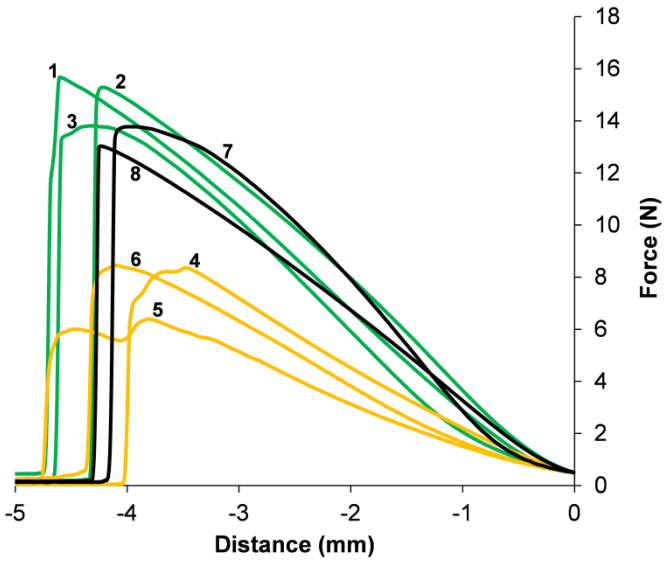

Figure 1. Mechanical tensile profile of apple fruit skin tissue. Mechanical tensile profiles of skin tissues from a selected subset of the population are shown. Black lines indicate parental cultivars, Green lines indicate progeny deemed to have regular cuticles, and yellow lines show cultivars considered to have compromised cuticles. Specifically, 1: GxB 3, 2: GxB 6, 3: GxB 11, 4: GxB 30, 5: GxB 59, GxB 90, 7: 'Braeburn', 8: 'Golden Delicious'.

The digital analysis of each tensile mechanical pattern led to the identification of five main parameters, considered in this study as novel descriptors for the characterization of fruit skin behavior. The projection of these five parameters in a two-dimensional (2D)-PCA hyperspace (Fig. 2) defined by the first two principal components (explaining in total 97.09% of the phenotypic variance, PC1: 74.80% and PC2: 22.29%) revealed their effect in the determination of the cuticle mechanical properties. The loading plot of parameters indicated that Area, Maximum Force and Linear Distance were commonly projected towards the PC1, therefore playing a similar role in the explanation of the total phenotypic variance. While the other two variables (Gradient and Maximum Force Distance) were oppositely oriented in the other two quadrants of the 2D-PCA plot (along the PC2), explaining a different portion of the total variance. The employment of these variables generated a wide data distribution, which, in general, followed a normal distribution, exception made for Maximum Force and Area, characterized by a more skewed type of trait segregation. The general distribution of data, with respect to the position of the two parental cultivars suggested a transgressive type of segregation, with the seedlings exceeding the value of the two parents (Supp. Fig. 3). Generally, the mechanical data indicated that 'Golden Delicious' displays a slightly higher cuticular performance in terms of strength than 'Braeburn'. Among the indexes, the Gradient resulted to be the mechanical parameter most statistically correlated with the russeting phenotype visually inspected (r=0.35, *P*-value ≤0.05).

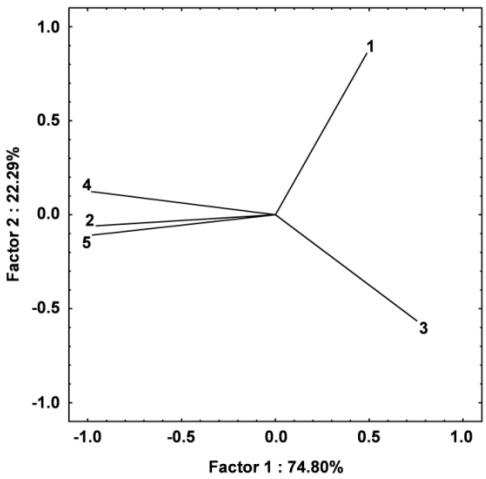

Figure 2. Principle Component Analysis loadings of mechanical traits. The projection of five parameters identified during tensile testing of the skin tissues over the hyper-space defined by PC1 and PC2 is illustrated. The variables are indicated with a numerical code: 1, Gradient; 2, Maximum Force; 3, Maximum Force Distance; 4, Area; 5, Linear Distance. See Supp. Fig. 2 for more detail on how each parameter is determined.

4.2.2 QTL Mapping Identifies Two Regions Linked to Cuticle Formation

The molecular map of the 'GxB' progeny was represented by 605 markers, uniformly distributed over 17 chromosomes (haploid number for apple), covering a total length of 1195.69 cM, with an averaged distance between adjacent markers of approximately 2 cM. This map was finally employed in a QTL mapping survey to identify putative genomic regions involved in the genetic control of fruit cuticle performance and the potential for russeting development. As phenotypic data, the five mechanical parameters, as well as the visual scoring of russeting (thought as absence/presence of russeting and its coverage on the skin surface) were considered. By the joint analysis of these datasets, seven major QTL-intervals were identified within the 'GxB' genome, three located on chromosome 2 and four on chromosome 15 (Fig. 3, Supp. Fig. 4 and Table 1).

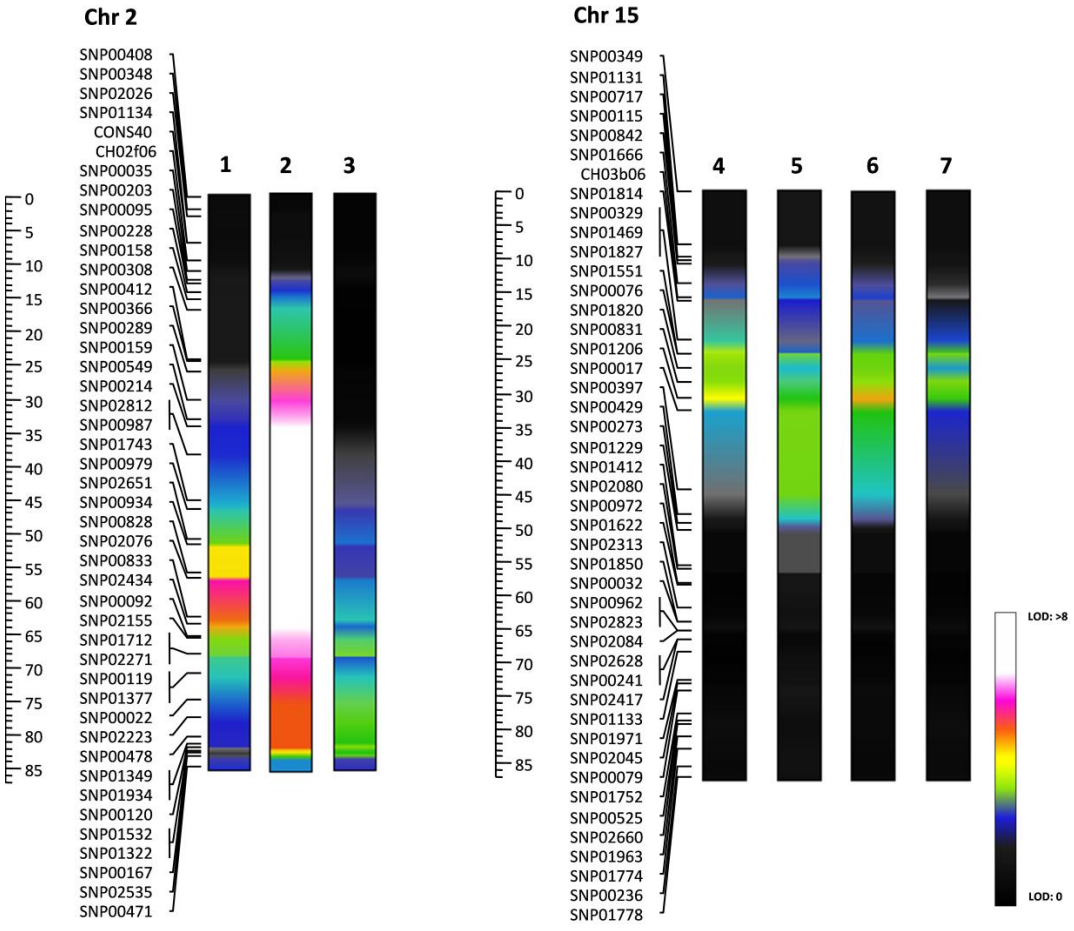

Figure 3. Heat-Map pattern of LODs for the QTL intervals detected for cuticle performance and russeting on chromosome 2 and 15. The traits are indicated according to a numerical code as follows: 1, Russeting; 2, % of Russeting; 3, Gradient; 4, Maximum Force, 5, Maximum Force Distance; 6, Area, 7, Linear Distance.

Table 1. Details of the QTLs associated with visual inspection of russeting as well as cuticle mechanical parameters.

LG	Trait	Marker	cM	LOD	%exp
2	Russet	SNP02076	56.60	6.91	30.3
	% Russeting	SNP02076	56.60	13.02	49.4
	Gradient	SNP01349	81.20	4.8	30.4
15	Maximum Force	SNP01551	24	6.26	37.7
	Max Force Distance	SNP01206	30.7	4.41	28.3
	Area	SNP01551	24	6.41	38.4
	Linear Distance	SNP01551	24	5.16	32.3

For each trait, the linkage group, the marker coincident with the highest LOD score and the expressed variance are reported.

The first QTL identified on chromosome 2 was related to the Gradient, showing a maximum LOD (logarithm of odds) value of 4.8 (30% of expressed variance) and located towards the end of the linkage group (81.2 cM). The second cluster of QTLs, positioned on the same linkage group, was instead related to the Russeting phenotype. QTLs related to both Russeting and percentage Russeting, were characterized by a similar LOD shape (Supp. Fig. 4), but with a different magnitude. The percentage of Russeting, which showed the greatest variance, was associated to a QTL with a LOD value of 13.02 (49.4% of expressed variance), higher with respect to the qualitative evaluation (presence/absence) of russeting (LOD value of 6.91, 30.3 % of phenotypic variance explained). These two QTLs were located on linkage group 2, at 56.6 cM from the top of the chromosome (Fig. 3).

The second cluster of QTLs, more related to mechanical behavior parameters, was instead located on chromosome 15. These genomic regions were associated to the four mechanical parameters, digitally obtained from the tensile profile generated by the texture analyzer during the assessment of the skin tissue of the fruit collected from the 'GxB' population. These QTLs, related to Maximum Force, Maximum Force Distance, Area and Linear Distance, spanned from a LOD value of 4.41 to 6.41 (Fig. 3, Supp. Fig. 4), with a corresponding range of phenotypic variance from 28.3 to 38.4% (Table 1). The estimated mean of the distribution associated with each of the four genotypic classes was calculated for the QTL clusters located on chromosome 2 and 15. In both chromosomes the targeted QTLs seemed to be determined by a specific allelic combination. In chromosome 2, the QTL for both Russeting and Gradient was associated with the "bd" allelic configuration (Supp. Fig. 5A), while in chromosome 15 the QTL was determined by "ad" (Supp. Fig. 5B). It is worth noting that in both chromosomes the allele "d" of 'Braeburn' is associated with the presence of the QTL,

and this is the apple cultivar known to transmit the russeting trait when used as parental genotype in controlled crossing (Wood, 2001).

4.2.3 Expression Profiling of Candidate Genes in Selected Progeny Links the AP2-Type MdSHN3 Transcription Factor with Proper Cuticle Formation

To better investigate the genetic mechanisms underlying the control of fruit cuticle properties in apple, an *in silico* gene mining was performed by anchoring the QTL genomic intervals targeted on chromosomes 2 and 15 on the assembled version of the 'Golden Delicious' apple genome (Velasco et al., 2010), and identifying a total of 3841 and 1675 predicted genes, respectively (Supp. Table 2 and 3). Through manual inspection, within these two gene lists, a set of candidates was identified based on similarity to previously characterized cuticle related genes from other plant species. The full list of candidate cuticle genes together with their similarity to characterized orthologs is provided in Table 2.

Three seedlings showing compromised cuticle structure were selected based on prior tensile testing as well as the appearance of russeting (GxB 30, GxB 59 and GxB 90), and three seedlings with regular skin (GxB 3, GxB 6 and GxB 11). These lines were used together with both parental cultivars for more detailed investigation. Light microscopy on cross sections of skin tissues confirmed a correlation between the tensile tests (particularly the Maximum Force parameter) and cuticle formation (Fig. 4 and Supp Fig. 6). Lines with fruit skin requiring less force to break during the tensile testing showed dramatically thinner and sometimes cracked cuticles when compared to the parents as well as to the progeny identified as displaying regular cuticle performance during the mechanical testing (Fig. 4). While russet was not necessarily observed to cover the entire fruit (as seen in the fruit image in Fig. 4F), microscopy showed that in compromised cuticle lines even areas where the production of russet was absent the cuticle was dramatically thinner (Fig. 4F).

Table 2. Genes identified in the QTL regions putatively linked to cuticle biosynthesis or regulation

Gene ID	Chr.	Name	Description/role	Ortholog ID	Homology (Idendities/Positives)	Reference
MDP0000287191	2	WSD11	Wax ester synthase/diacylglycerol acyltransferase	AT5G53390	31% / 50%	(Takeda et al., 2013)
MDP0000250127	2	KAS1	Crucial for fatty acid synthesis	AT5G46290	74% / 84%	(Wu and Xue, 2010)
MDP0000069348	2	CER1	Likely aldehyde decarbonylase involved in wax synthesis	AT1G02205	57% / 72%	(Bourdenx *et al.*, 2011)
MDP0000297929	2	DGAT1	Lipid biosynthesis	AT2G19450	74% / 83%	(Zhang *et al.*, 2009)
MDP0000938736	15	KCS11	Biosynthesis of very long chain fatty acids	AT2G26640	79% / 88%	(Blacklock and Jaworski, 2006; Li-Beisson et al., 2013)
MDP0000178263	15	SHN3	Transcriptional regulator of cuticle biosynthesis	AT5G25390	58% / 68%	(Aharoni et al., 2004)
MDP0000729533	2	BAHD ACYL-TRANSFERASE	Transferring acyl groups other than amino-acyl groups	AT3G26040	40% / 58%	(Kosma *et al.*, 2012; Li-Beisson *et al.*, 2013)
MDP0000391122	2	BAHD ACYL-TRANSFERASE	Transferring acyl groups other than amino-acyl groups	AT3G26040	38% / 54%	(Kosma *et al.*, 2012; Li-Beisson *et al.*, 2013)

CER1, ECERIFERUM1; DGAT1, DIACYLGLYCEROL O-ACYLTRANSFERASE1; KAS1, *KETOACYL-ACP SYNTHASE1*; KCS11, 3-KETOACYL-COA SYNTHASE11; WSD11, WAX ESTER SYNTHASE/DIACYLGLYCEROL ACYLTRANSFERASE11.

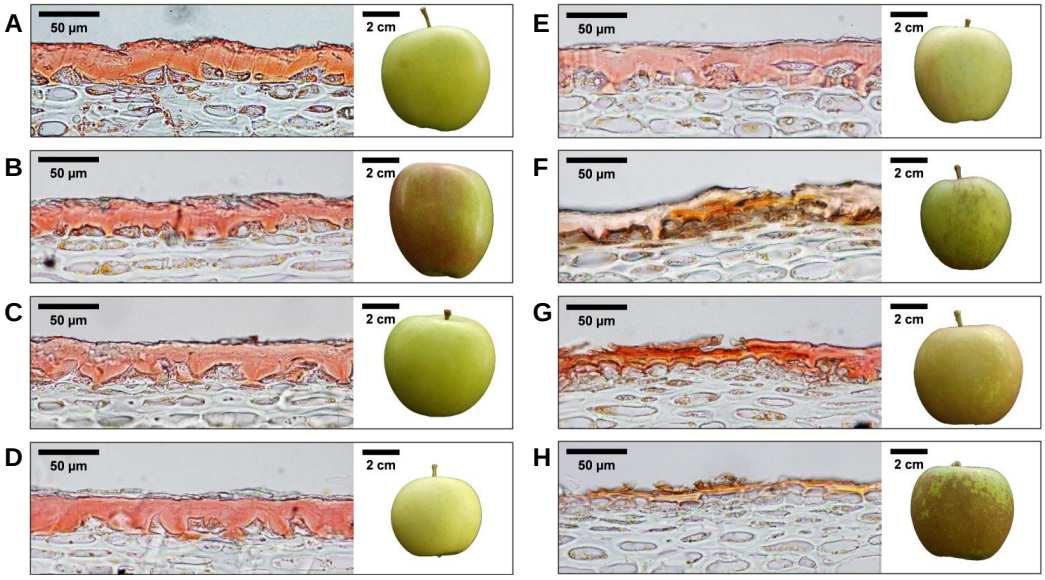

Figure 4. Histological analysis of apple skin tissues in a selected subset of the population. Light microscopy analysis of skin samples stained with Sudan IV are shown, together with photographs of whole apples. Sudan IV stains the cuticular lipids a pink/orange color. (A-B) Parental lines 'Golden Delicious' (A) and 'Braeburn' (B), show regular cuticles. (C-E) Selected progeny with regular skin are shown: (C), GxB 3; (D), GxB 6; (E), GxB 11. (F-H) Selected progeny with compromised cuticles are shown: (F), GxB 30; (G), GxB 59; (H), GxB 90. Thinner, cracked cuticles are clearly visible in these lines. While whole apple photographs show the presence of russet on the surface of the fruit.

Expression analysis was performed on candidate genes in the selected progeny and parents to identify a potential link between the candidates and the observed cuticular phenotypes. The early green stage of fruit development was selected for expression analysis, as already at this stage early signs of russet formation could be seen in selected progeny. Of the eight genes (located within the QTLs mapped on chromosome 2 and 15) identified as potential candidates, expression was detected for six (Fig. 5). No expression was detected in any of the samples for the WAX ESTER SYNTHASE/DIACYLGLYCEROL ACYLTRANSFERASE (*WSD11*, *MDP0000287191*) and *KETOACYL-ACP SYNTHASE1 (KAS1*, *MDP0000250127*) orthologs. Only one candidate gene showed an expression pattern that segregated with the compromised cuticle phenotype, *MDP0000178263* (*MdSHN*3) (Fig. 5F). Sequence analysis and construction of a phylogenetic tree revealed that *MdSHN3* is an ortholog of the cuticle-associated SHN1/WIN1 clade of AP2-domain transcription factors, (Fig. 6). *MdSHN3* was expressed at relatively similar levels across the parental cultivars and the three selected progeny showing regular cuticles, however in the three selected progeny showing compromised cuticles, *MdSHN3* was expressed up to 25-fold less. Expression analysis for *MdSHN3* was extended to include the mature green and harvest stage, showing that expression levels

for *MdSHN3* remain low in the lines with compromised cuticles throughout development (Supp. Fig. 7). A 70-fold decrease in *MdSHN3* expression was observed at the mature green stage for lines with compromised cuticles, while the difference at the harvest stage was lower (25-fold; Supp. Fig. 7).

Finally it is interesting to note the expression pattern of *MDP0000391122* (a *BAHD acyltransferase*), which shows similar expression levels in the parental cultivar 'Braeburn', as well as in the progeny lines with compromised cuticles, while expression in the parental cultivar 'Golden', and the seedlings with regular cuticles show a 15-fold decrease in expression (Fig. 5B).

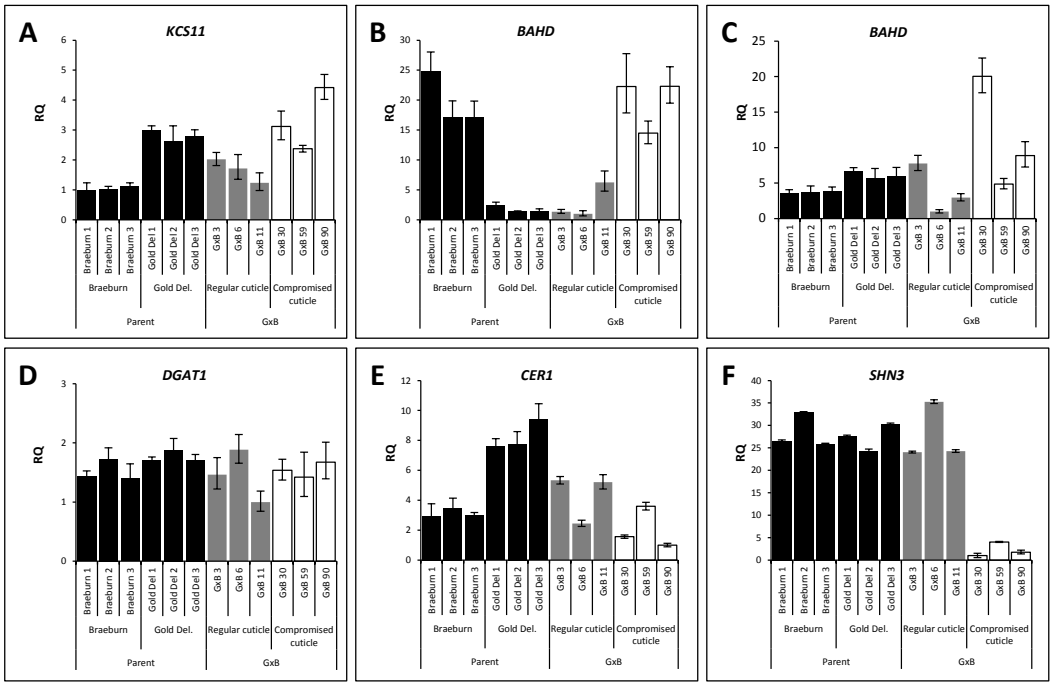

Figure 5. Expression analysis of candidate genes in early green stage peel tissue. Expression of candidate genes was performed via quantitative Real Time-PCR. (A) *KCS11*, *3-KETOACYL-COA SYNTHASE11*; (B) *BAHD ACYL-TRANSFERASE* (*MDP0000391122*); (C) *BAHD ACYL-TRANSFERASE* (*MDP0000729533*); (D) *DGAT1*, *DIACYLGLYCEROL O-ACYLTRANSFERASE1*; (E) *CER1*, *ECERIFERUM1*; (F) *SHN3*. Parent lines are colored black, progeny determined to possess regular cuticle are grey, and progeny displaying compromised cuticles are white. Error bars show standard error (n=3).

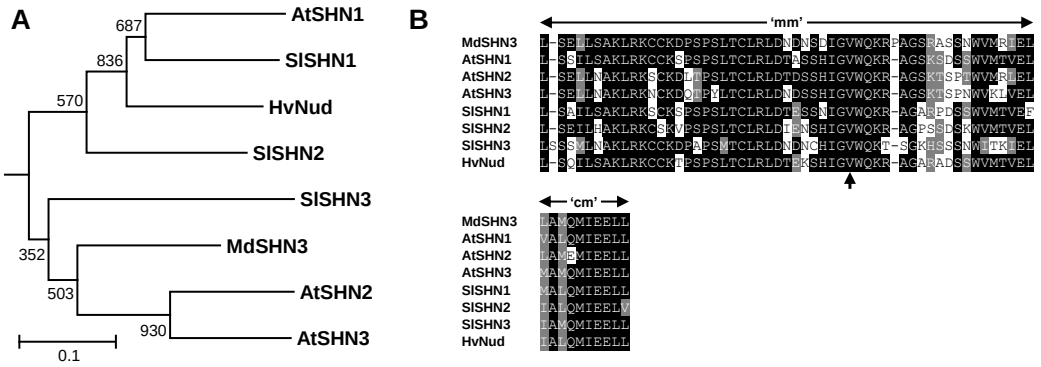

Figure 6. Molecular phylogeny and sequence analysis of *MdSHN3*. (A) Molecular phylogeny of characterized members of the SHN1/WIN1 clade transcription factors shows *MdSHN3* to be a member of this clade. (B) Alignments of two domains shown to be functionally relevant to this clade are displayed, with the functionally critical valine residue indicated with an arrow. Alignments were performed using Clustal Omega, and neighbor-joining phylogenetic trees constructed with MEGA 5.0. Values at branch points are bootstrap values calculated from 1000 replicates. AtMYB9 was used as an outlier to create a root for tree and is not shown. 'mm', middle motif; 'cm', C-terminal motif.

4.3 Discussion

4.3.1 Use of Five Novel Mechanical Parameters Allows for a High Throughput Analytical Characterization of Apple Cuticle Performance

The plant cuticle plays a vital role in the protection of whole organs and especially fruit, preserving the integrity and quality during development and also during postharvest storage (Albert *et al.* 2013). In apple, the formation of russet is caused directly by cuticle failure. In our efforts to identify QTL regions linked to this disorder we characterized the visible russet formation in the 'GxB' progeny as well as the mechanical properties of the fruit skin tissue in this population. Russet can be considered a secondary effect due to cuticle failure, and is not necessarily present in fruit displaying mildly compromised cuticles. This was confirmed by microscopic observations showing dramatically thinner cuticles in lines with compromised cuticle formation yet lacking extensive russet formation (Fig. 4). Analyzing the mechanical properties of the cuticles therefore allowed us to target the potential cause of the russet seen in the population. This was accomplished using an instrument previously employed for the dissection of the apple fruit texture complexity (Longhi *et al.*, 2012). By the controlled tension applied on the skin portion isolated from the apple of the 'GxB' progeny, five parameters were derived, which were eventually implemented as quantitative traits for a specific and detailed QTL mapping assay. In fact, these parameters, allow the characterization of a

continuous trait distribution, which is a fundamental requirement for QTL computation. Among the five parameters, Area, Maximum Force and Linear Distance were commonly oriented over the 2D-PCA plot, and can be considered as describing cuticle strength, a trait specifically associated with the cutin matrix (Pollard *et al*., 2008; Schreiber, 2010). The other two variables, Maximum Force Distance and Gradient, displayed different projections. The Maximum Force Distance which showed an almost opposite orientation with regards to the first set of parameters is likely also associated with the mechanical strength of the skin. An interesting observation is the orthogonal projection of the Gradient parameter, explaining novel phenotypic variance when compared to the other variables measured. This parameter is related to the skin elasticity properties, rather than to the strength of the skin and correlates most strongly with the visually observed russeting phenotype (Fig. 2). Russeted skin tissue is known to have an altered elasticity when compared with regular peels (Khanal *et al.*, 2013). These parameters can therefore be used for a more specific and analytic characterization of the fruit cuticle performance and subsequent russeting in a reliable and high-throughput fashion. The development of these novel parameters allowed, in fact, a more precise, comprehensive and reliable characterization of the peel behavior in apple, further validated by the QTL mapping survey. The detection of two QTL regions specifically associated to these parameters (one in common with the russeting visually scored) confirms their efficiency in describing this particular phenotype.

4.3.2 QTLs on Chromosome 2 and 15 are Associated with Cuticle Formation and Subsequent Russeting

The implementation of the mechanical parameters and the russeting evaluation together with the genotypic data, allowed the identification of a set of QTLs on two specific chromosomes, 2 and 15. The QTLs identified on chromosome 2 were associated with the visual inspection for russeting and the Gradient parameter (describing elasticity) of the tensile profile. This supports the link between russet formation and a modulation in the elasticity of the cuticle. Regarding the estimation of russeting, the highest LOD value was detected for the evaluation of the percentage of corky tissue over the fruit surface, validating the fact that a quantitative type of trait provide a more reliable and precise data than a qualitative scoring for QTL investigation. This may also be the reason for the different resolution and position (although overlaying) for the QTL detected for the Gradient parameter (Fig. 3 and Supp Fig. 4).

The other measured tensile parameters (Maximum Force, Area Linear Distance and Maximum Force Distance) were associated with a QTL region on chromosome 15 (Fig. 3). These parameters can all be thought to describe the strength of the cuticle and all predicted highly similar QTL-LOD profiles. These parameters are able to identify weaker cuticles that may not have been compromised to the extent to which they develop russet. This is vitally important when investigating the primary cause of russet formation.

It is interesting to note that chromosomes 2 and 15 arose from a single ancestral chromosome during the recent genome duplication event in apple which resulted in several chromosome pairings (Velasco *et al.*, 2010). The involvement of more than one chromosome in the control of the cuticle biosynthesis in fleshy fruits is neither novel nor surprising, as demonstrated by the widespread localization of genes described in tomato fruit cuticle biosynthesis (Hen-Avivi *et al.*, 2014; Martin and Rose, 2014). Whole genome duplication events however can allow species to generate diversification and novelties within its metabolism (Mühlhausen and Kallmar, 2013). For example, the sequencing of the tomato genome (The Tomato Genome Consortium, 2012) revealed that genome duplication events likely determined the sub-functionalization of new gene family members, crucial for the establishment of fruit specific functions, including ripening. In the case of this study, it appears that the QTL identified on chromosome 15 can be thought of as primary cause of cuticle failure, while the QTL on chromosome 2 is possibly related to enhancing the subsequent production of russeted tissue.

The analysis of the effect of each QTL detected over the 'GxB' genome highlighted in this particular genetic background that cuticular performance, as well as the russeting trait, was under a recessive genetic control. By plotting the estimated mean of the distribution associated to each of the four genotypic classes it can be seen that the trait was associated to the combination of two specific alleles. Between the two varieties, moreover, the allele "d" of 'Braeburn' was the one required for the expression of the phenotype in both cases: the occurrence of russeting on chromosome 2 and the cuticle mechanical performance on chromosome 15. This finding validates the hypothesis of a recessive genetic control, as initially suggested by the segregation ratio of 3:1, following the observation that approximately 20% of the progeny showed a russeting phenotype. The slightly lower incidence of observed russeting than would be

expected in a 3:1 segregation can be explained by the fact that the russet is a secondary consequence of cuticle failure, which does not always result in russet formation.

The markers identified in correspondence of the highest LOD value for both QTL regions may be exploited in the future as important tools in marker assisted programs for the achievement of two important goals. First of all, the marker associated to the QTL on chromosome 2 can be useful for the advanced selection of those seedlings which have inherited the alleles associated with russeting. While this trait is considered valuable in some heirloom and traditional varieties (such as 'Renetta Canada', 'Renetta Grigia' or 'Tyroler Spitzlederer'), it is typically an undesirable trait, due to both consumer preference and long term storage ability. In our study we have demonstrated the fact that russeting can occur in progenies made from crossing of two regular skin varieties (i.e. 'Golden Delicious' and 'Braeburn') at a relatively high rate. It would therefore be advantageous to screen for this phenotype at an early stage.

The identification of the QTL on chromosome 15 associated with cuticle performance can be employed to select novel accessions characterized by better performing cuticles. Taking into consideration that the horticultural management and production system for apple postharvest storage is an essential step to guarantee its marketability, a high performing cuticle is a fundamental requirement to guarantee and maintain favorable fruit quality. Furthermore, as russeting is a secondary effect of cuticle failure one would also be selecting against potential russet formation.

4.3.3 MdSHN3 Promotes Cuticle Biosynthesis and Prevents Russet in Apple

Analysis of the two chromosomal regions identified via QTL analysis revealed eight potential genes involved in cuticle biosynthesis and regulation. These genes included an ortholog to *AtWSD11* on chromosome 2, shown previously to be involved in wax ester synthesis in *Arabidopsis*, where it is required to prevent organ fusions caused by a malformed cuticle (Takeda *et al.*, 2013). An ortholog to the fatty acids synthesis gene *AtKAS1* (Wu and Xue, 2010) was also identified in the QTL on chromosome 2, as well as an ortholog to *AtCER1*, an aldehyde decarbonylase (Bourdenx *et al.*, 2011). This latter gene has been shown to be involved in cuticle wax synthesis in *Arabidopsis* and cucumber (Bernard *et al.*, 2012; Bourdenx *et al.*, 2011; Wang *et al.*, 2015). Finally, also on chromosome 2, an ortholog to the lipid biosynthesis *AtDGAT1* gene (Zhang *et al.*, 2009) was identified, as well as two BAHD acyl-transferase genes. This class of BAHD acyl-transferases have been shown to be involved in cutin and suberin polymer

biosynthesis (Kosma *et al.*, 2012; Molina and Kosma, 2015; Panikashvili *et al.*, 2009). Two further genes were identified in the QTL region on chromosome 15, including an ortholog of the *Arabidopsis 3-KETOACYL-COA SYNTHASE11* (*AtKCS11*), a gene involved in the biosynthesis of very long chain fatty acids (Blacklock and Jaworski, 2006), and *MdSHN3*, an AP2-domain transcription factor belonging to the *SHN1*/*WIN1* clade (Aharoni *et al.*, 2004; Broun *et al.*, 2004; Shi *et al.*, 2013).

In order to determine the expression profile of these genes in progeny with a range of cuticle phenotypes a subset was selected. This subset was represented by three progeny with regular peels, and three with compromised cuticles (as determined by tensile testing) as well as the two parental lines (Fig. 4). Deficient cuticle formation was confirmed via histological analysis, showing a dramatic reduction in the normally thick apple cuticles in the progeny of lines with compromised cuticles. This confirmation via histological analysis validated the mechanical testing performed on the whole population and illustrated the damage caused by cuticle reduction and russet formation. Expression analysis of the eight genes in this selected subset of lines revealed only the expression of *MdSHN3* to segregate exclusively with the various phenotypes associated with an improperly formed cuticle (Fig. 5F). Specifically, *MdSHN3* showed a decrease in expression between 25- and 70-fold in the progeny with compromised cuticles depending on developmental stage.

Another gene showing an interesting expression profile is the BAHD acyl-transferase gene (*MDP0000391122*). The expression profile of this gene is significantly higher in the three seedlings with compromised cuticles, as well as the parental line ‘Braeburn’ (Fig. 5B). Although this expression pattern does not segregate with the cuticle phenotype it may indicate a role for this gene in the secondary formation of russet. BAHD acyl-transferases have in fact been implicated in suberin biosynthesis (Kosma *et al.*, 2012; Molina and Kosma, 2015) and as ‘Braeburn’ is the parental line thought to be responsible for genetically transmitting this phenomenon it is conceivable that *MDP0000391122* plays a role in suberin biosynthesis in lines with compromised cuticles.

The *SHN1*/*WIN1* transcription factor displaying an expression pattern segregating with the compromised cuticle phenotype is a strong candidate to be the underlying factor of the russeting phenotype. *SHN* transcription factors have previously been identified and characterized in *Arabidopsis*, tomato and barley (Aharoni *et al.*, 2004; Shi *et al.*, 2013; Taketa *et al.*, 2008). In both *Arabidopsis* and tomato characterized

orthologs control cuticle deposition as part of a transcriptional network of epidermal cell differentiation (Aharoni *et al.*, 2004; Shi *et al.*, 2013; Shi *et al.*, 2011). Transgenic lines in tomato with reduced expression of *SlSHN3* showed a severe disruption of normal fruit cuticle deposition, which resulted in an increase to both susceptibility to fungal infection and postharvest water loss (Buxdorf *et al.*, 2014; Shi *et al.*, 2013). While *Arabidopsis* overexpressing *AtSHN1* resulted in increased drought tolerance and recovery (Aharoni *et al.*, 2004). In barley a SHN ortholog, HvNud, regulates the biosynthesis of lipids which coat the caryopses (dry fruit of barley) (Taketa *et al.*, 2008). This lipid coverage of barley grains can be seen as analogous to the cuticle of fleshy fruit.

Sequence analysis of the *MdSHN3* protein confirmed the presence of the AP2 domain, characteristic of the larger family, and also the two conserved motifs characteristic of the SHN1/WIN1 sub-clade (Fig. 6B). The so called 'middle motif' ('mm') and the 'C-terminal motif' ('cm') have been recognized as important regulatory domains for this clade of transcription factors (Aharoni *et al.*, 2004). Furthermore, the conserved valine residue in the 'mm' identified by Taketa *et al*. (2008) and demonstrated to be critical for SHN enzyme function is also present in the MdSHN3 protein (Fig. 6B).

Taken together, the expression pattern, the identification of conserved functional protein domains, and the genomic location within the high confidence interval of a QTL linked strongly to skin strength, it is likely that in apple fruit *MdSHN3* positively regulates cuticle deposition and subsequent thickness. This might occur via the transcriptional control of downstream cuticle biosynthesis target genes as was previously demonstrated in tomato (Shi *et al.*, 2013). Expression of *MdSHN3* throughout apple fruit development (as shown to be the case in fruit with regular skin; Supp. Fig. 7) is therefore crucial to promote proper cuticle formation. The histological analysis of the fruit skin of the progeny with decreased *MdSHN3* expression illustrates the major reduction in cuticle formation in these lines, which subsequently resulted in diminished peel strength, and an increased potential for russet development.

4.3.4 Conclusions

The simultaneous investigation of the tensile performance of apple cuticles and the occurrence of russeting demonstrated the relationship between these two properties, i.e. cuticle failure is a prerequisite for apple russet formation. These parameters, together with the markers identified within the QTLs detected over two chromosomes

can be considered as a valuable tools in assisted breeding programs, in order to predict the development of this undesirable trait in seedlings. The recent advances in the understanding of cuticle biology in model species such as *Arabidopsis* and tomato can now be applied to agriculturally important crops. In this case we expanded on prior knowledge and provide evidence that an apple ortholog of *SHN3* positively regulates cuticle biosynthesis, thus preventing apple russet. This knowledge in terms of apple production is invaluable when one considers the economic importance of a long postharvest storage for apple fruit. The identification of a functional ortholog of the SHN1/WIN1 clade of transcription factors in apple further highlights the importance of this clade of transcription factors as primary regulators of epidermal processes, particularly cuticle biosynthesis.

4.4 Methods

4.4.1 Plant Material and Fruit Russeting Evaluation

To perform QTL mapping analysis oriented in the determination of the genomic regions involved in proper cuticle formation, eighty-eight (88) individuals from the 'Golden Delicious' x 'Braeburn' ('GxB') population were selected. Within the breeding program, this population was chosen for showing a stable and consistent development of the russeting phenotype through consecutive years. The progeny was planted originally in 2003, at the experimental orchard of the Fondazione Edmund Mach (Northern Italy), and maintained following standard technical agricultural management for pruning, crop load and pest-disease control.

Fruit for mechanical tensile testing and microscopy analysis were collected at commercial harvest, established according to standard indexes, such as skin and seed color as well as starch accumulation (defined on a starch value of 7, based on a 1 to 10 scale, corresponding to the full presence of starch and absence by its complete degradation, respectively) and assessed after two weeks of shelf-life at room temperature. For each individual, five apples were collected and fruit russeting was initially visually inspected. The development of the suberized layer was assessed for two years consecutively. Fruit russeting was scored visually for its presence/absence and the estimated percentage of the fruit surface covered by russeting.

4.4.2 Tensile Mechanical Phenotyping

The structure of the apple fruit cuticle was assessed with a novel analytical approach, making use of a TA-XT*plus* texture analyzer. Data for each individual line represents repeats from five apples, from which two peel stripes each were isolated. Peel strips were all cut with a width of 1 cm and a length of 5.5 cm. The strips were then transferred to the texture analyzer (TAXT instrument, Stable MicroSystem, Godalming UK; Supp. Fig. 1) where they were clamped at the ends and pulled apart. The force required to stretch (and snap) the strips was recorded in relation to the distance the strips were pulled. The texture analyzer instrument settings were as follows: pre-test and test speed of 1 $mm.sec^{-1}$, post-test speed of 5 $mm.sec^{-1}$, target mode distance and trigger force of 50 g. The tension strength was applied until reaching the distance of 5 mm. From the mechanical profiling resulting from the tensile test, five main parameters were identified through the use of an ad hoc macro compiled with the Exponent v4.0 software (provided with the instrument), and represented by Gradient, Maximum Force, Maximum Force Distance, Area and the Linear Distance of the mechanical profile (Supp. Fig. 2 and Table 3). The digital data of these parameters were then further used as phenotypic data in the final QTL mapping computation.

4.4.3 QTL Mapping

The molecular map of this population was made within the international effort of the 'Golden Delicious' apple genome sequencing, in order to assembe the several contigs into scaffolds. A subset of this progeny was selected for the specific purpose of this study, considering only those individuals bearing a sufficient number of fruit. In the end, a total of 88 individuals were tested with 605 molecular markers, including SSR and SNP type (for more detail see Di Guardo *et al.*, 2013; Costa *et al.*, 2014). Markers were grouped and ordered along linkage groups using the Haldane's mapping function implemented in JoinMap 4 (Van Ooijen, 2006). Mapping parameters were set at a LOD value of 5 and at a recombination frequency of 0.5. Marker data were integrated with phenotypic data to perform a QTL mapping analysis, computed with MapQTL 6.0 (Van Ooijen, 2009). QTL interval were identified through the Interval Mapping algorithm, and a LOD value of 3.0 was considered as the threshold to consider a QTL as true (established after running 1000 permutation). Linkage groups and QTLs were visualized with MapChart (Voorrips, 2002) and Herry Plotter softwares (Longhi *et al.*, 2012). Each

interval was further anchored and aligned on the assembled version of the apple genome.

Table 3. Parameters measured during the tensile testing of apple peels

Parameter	Description	Unit
Gradient	Elasticity module (also known as Young's module) calculated at the fixed distance established at 1 mm of tension	N/mm
Maximum Force	Highest force value detected over the entire mechanical profile	N
Maximum Force Distance	Point over the x-axis corresponding to the Maximum Force value	mm
Area	Area calculated below the line of the mechanical profile	N*mm
Linear Distance	Derived length of the mechanical profile	N*mm

See Supp. Fig. 2 for more detail on how each parameter is determined.

4.4.4 Light Microscopy

For light microscopy, peel tissue samples were fixed and embedded in wax as described previously (Mintz-Oron *et al.*, 2008). Sections were cut to a thickness of 9 µm on an Leica 2000 microtome, and placed on glass slides. The slides were stained with Sudan IV (Buda *et al.*, 2009) and then observed with an Olympus CLSM500 microscope.

4.4.5 *In Silico* Analysis

Nucleotide and protein sequence retrieval from the Genome Database for Rosaceae (Jung *et al.*, 2014) was performed via BLAST. Protein alignments were performed using Clustal Omega (Sievers *et al.*, 2011) and the resultant molecular phylogenetic trees visualised using MEGA5 (Tamura *et al.*, 2011) under default parameters.

4.4.5 Nucleic Acid Extraction and Expression Analysis

Apple fruits at three stages of development (early green, mature green and harvest stage) were harvested and the skin tissue collected and immediately frozen in liquid nitrogen and ground into a fine powder. Total RNA extractions were performed using the RNeasy kit (QIAGEN, Netherlands) according to the standard protocol. DNase-treated total RNA was then used to synthesise cDNA using the SuperScript VILO cDNA synthesis kit (Invitrogen, MA, USA). Quantitative real-time PCR (qRT-PCR) analysis was performed using gene-specific oligonucleotides on an ABI ViiA 7 instrument (Applied Biosystems, CT, USA) with the Fast SYBR Green Master Mix (Applied Biosystems, CT, USA) under default parameters. Expression was normalised using oligos amplifying a fragment of the housekeeping gene, *Md8283* (5'-CTCGTCGTCTTGTTCCCTGA-3' and 5'-GCCTAAGGACAGGTGGTCTATG-3'). The StepOne software (Applied Biosystems, CT, USA)

was used to generate expression data. Sequences of the gene-specific oligonucleotides are provided in Supp. Table 1.

4.5 Acknowledgements

The authors thank Marco Fontanari for his support in phenotyping, and Pierluigi Magnago for the maintenance of the 'G×B' progeny. JL performed this work as part of his PhD studies funded by the Fondazione Edmund Mach. This work was supported by the Israel Science Foundation (ISF) personal grant to AA (ISF grant no. 646/11). AA is the incumbent of the Peter J. Cohn Professorial Chair.

4.6 Supplemental Data

See ***Appendix B*** (page 197) for supplementary materials

Supplementary Figure 1. Texture Analyzer device employed in this investigation. Clamps used to hold the peel for the tensile analysis are shown.

Supplementary Figure 2. Mechanical tensile profile with the five parameters identified by the macro highlighted. A dashed vertical black line indicates the point at -1 mm where the anchor was placed. The red circle indicates the intercept between the anchor and the mechanical profile, used to compute the Gradient (or elasticity module). The black arrow points the Maximum Force value, which represents the Force requires to break the peel. On the y-axis and x-axis force in Newtons (N) and the distance (mm) values are displayed respectively.

Supplementary Figure 3. Trait distribution over the 'GxB' progeny. For each measured parameter, the trait distribution is depicted. The position of the two parental cultivars is indicated with a black arrow (GD: 'Golden Delicious', B: 'Braeburn'). A fitting line for the normal distribution is shown. The x-axis of each panel shows the trait assessed, while the number of observations for each trait is reported on the y-axis.

Supplementary Figure 4. LOD profile for the QTL associated to the two indexes. Used to estimate the russeting development (Russet and % Russet), as well as the five tensile parameters employed to characterize the mechanical performance of the apple fruit cuticle. Panel a and b pointed out the QTL profiles detected in chromosome 2, while panel c refers to chromosome 15. For each panel the dashed line indicates the threshold value established at LOD 3. Chromosomal position of genes identified as potential candidates are shown.

Supplementary Figure 5. Estimated Mean of the total distribution associated to each genotype class. Panel A reports the estimated mean calculated for the percentage of Russeting mapped on chromosome 2. Panel B is reports the estimated mean of the Maximum Force, mapped on chromosome 15. In both panel, the x-axis reports the cM of each respective linkage group. LOD value and estimated mean are reported on the y-axis and depicted by colored lines as indicated in the legend.

Supplementary Figure 6. Force required to break peels. Mechanical test of selected subset of progeny and parental lines indicates the dramatic reduction in require force to

break peels of lines with compromised cuticles. Parent lines are colored black, progeny determined to possess regular cuticle are grey, and progeny displaying compromised cuticles are white. Error bars show standard error, (n=5).

Supplementary Figure 7. Developmental gene expression analysis of *MdSHN3* in three specific stages of the fruit development. Early green (EG), mature green (MG) and harvest (Har). Parent lines are colored black, progeny determined to possess regular cuticle are grey, and progeny displaying compromised cuticles are white. Error bars show standard error (n=3). RQ, Relative quantification.

Supplementary Table 1. Oligonucleotides used in this study.

Supplementary Table 2. List of genes annotated within the QTL interval identified on chromosome 2.

Supplementary Table 3. List of genes annotated within the QTL interval identified on chromosome 15.

4.7 References

Aharoni A, Dixit S, Jetter R, Thoenes E, van Arkel G, Pereira A. 2004. The SHINE clade of AP2 domain transcription factors activates wax biosynthesis, alters cuticle properties, and confers drought tolerance when overexpressed in Arabidopsis. *Plant Cell* **16**, 2463-2480.

Albert Z, Ivanics B, Molnár A, Miskó A, Tóth M, Papp I. 2013. Candidate genes of cuticle formation show characteristic expression in the fruit skin of apple. *Plant. Growth Regul*. **70**, 71-78.

Andre CM, Larsen L, Burgess EJ, Jensen DJ, Cooney JM, Evers D, Zhang J, Perry NB, Laing WA. 2013. Unusual immuno-modulatory triterpene-caffeates in the skins of russeted varieties of apples and pears. *J Agric Food Chem* **61**, 2773-2779.

Bargel H, Koch K, Cerman Z, Neinhuis C. 2006. Structure–function relationships of the plant cuticle and cuticular waxes – a smart material? . *Functional Plant Biology* **33**, 893-910.

Beisson F, Li-Beisson Y, Pollard M. 2012. Solving the puzzles of cutin and suberin polymer biosynthesis. *Curr Opin Plant Biol* **15**, 329-337.

Bernard A, Domergue F, Pascal S, Jetter R, Renne C, Faure JD, Haslam RP, Napier JA, Lessire R, Joubès J. 2012. Reconstitution of plant alkane biosynthesis in yeast demonstrates that Arabidopsis ECERIFERUM1 and ECERIFERUM3 are core components of a very-long-chain alkane synthesis complex. *Plant Cell* **24**, 3106-3118.

Blacklock BJ, Jaworski JG. 2006. Substrate specificity of Arabidopsis 3-ketoacyl-CoA synthases. *Biochem Biophys Res Commun* **346**, 583-590.

Bourdenx B, Bernard A, Domergue F, Pascal S, Léger A, Roby D, Pervent M, Vile D, Haslam RP, Napier JA, Lessire R, Joubès J. 2011. Overexpression of Arabidopsis

ECERIFERUM1 promotes wax very-long-chain alkane biosynthesis and influences plant response to biotic and abiotic stresses. *Plant Physiol* **156**, 29-45.

Broun P, Poindexter P, Osborne E, Jiang CZ, Riechmann JL. 2004. WIN1, a transcriptional activator of epidermal wax accumulation in Arabidopsis. *Proc Natl Acad Sci U S A* **101**, 4706-4711.

Buda GJ, Isaacson T, Matas AJ, Paolillo DJ, Rose JK. 2009. Three-dimensional imaging of plant cuticle architecture using confocal scanning laser microscopy. *Plant J* **60**, 378-385.

Buxdorf K, Rubinsky G, Barda O, Burdman S, Aharoni A, Levy M. 2014. The transcription factor SlSHINE3 modulates defense responses in tomato plants. *Plant Mol Biol* **84**, 37-47.

Costa F, Cappellin L, Farneti B, Tadiello A, Romano A, Soukoulis C, Sansavini S, Velasco R, Biasioli F. 2014. Advances in QTL mapping for ethylene production in apple (Malus × domestica Borkh.). *Postharvest Technol. Biol*. **87**, 126-132.

Curry E. 2012. Increase in Epidermal Planar Cell Density Accompanies Decreased Russeting of 'Golden Delicious' Apples Treated with Giberellin A_{4+7} A. *HortScience* **47**, 232-237.

Di Guardo M, Tadiello A, Farneti B, Lorenz G, Masuero D. 2013. A Multidisciplinary Approach Providing New Insight into Fruit Flesh Browning Physiology in Apple (Malus x domestica Borkh.). *PLoS ONE* **8**, e78004.

Hen-Avivi S, Lashbrooke J, Costa F, Aharoni A. 2014. Scratching the surface: genetic regulation of cuticle assembly in fleshy fruit. *J Exp Bot* **65**, 4653-4664.

Jung S, Ficklin SP, Lee T, Cheng CH, Blenda A, Zheng P, Yu J, Bombarely A, Cho I, Ru S, Evans K, Peace C, Abbott AG, Mueller LA, Olmstead MA, Main D. 2014. The Genome Database for Rosaceae (GDR): year 10 update. *Nucleic Acids Res* 42, D1237-1244.

Kannangara R, Branigan C, Liu Y, Penfield T, Rao V, Mouille G, Höfte H, Pauly M, Riechmann JL, Broun P. 2007. The transcription factor WIN1/SHN1 regulates Cutin biosynthesis in Arabidopsis thaliana. *Plant Cell* **19**, 1278-1294.

Khanal BP, Grimm E, Knoche M. 2013. Russeting in apple and pear: a plastic periderm replaces a stiff cuticle. *AoB Plants* **5**, pls048.

Kolattukudy PE. 2001. Polyesters in higher plants. *Adv Biochem Eng Biotechnol* **71**, 1-49.

Kosma DK, Molina I, Ohlrogge JB, Pollard M. 2012. Identification of an Arabidopsis fatty alcohol:caffeoyl-Coenzyme A acyltransferase required for the synthesis of alkyl hydroxycinnamates in root waxes. *Plant Physiol* **160**, 237-248.

Kunst L, Samuels AL. 2003. Biosynthesis and secretion of plant cuticular wax. *Prog Lipid Res* **42**, 51-80.

Knoche M, Khanal BP. 2011. Russeting and Microcracking of 'Golden Delicious' Apple Fruit Concomitantly Decline Due to Gibberellin A_{4+7} Application. *J Amer Soc Hort Sci* **136**, 159-164.

Lara I, Belge B, Goulao LF. 2014. The fruit cuticle as a modulator of postharvest quality. *Postharvest Biol. Technol*. **87**, 103-112.

Li-Beisson Y, Shorrosh B, Beisson F, Andersson MX, Arondel V, Bates PD, Baud S, Bird D, Debono A, Durrett TP, Franke RB, Graham IA, Katayama K, Kelly AA, Larson T, Markham JE, Miquel M, Molina I, Nishida I, Rowland O, Samuels L, Schmid KM, Wada H, Welti R, Xu C, Zallot R, Ohlrogge J. 2013. Acyl-lipid metabolism. *Arabidopsis Book* 11, e0161.

Longhi S, Moretto M, Viola R, Velasco R, Costa F. 2012. Comprehensive QTL mapping survey dissects the complex fruit texture physiology in apple (Malus x domestica Borkh.). *J Exp Bot* **63**, 1107-1121.

Martin LB, Rose JK. 2014. There's more than one way to skin a fruit: formation and functions of fruit cuticles. *J Exp Bot* **65**, 4639-4651.

McCourt RM, Delwiche CF, Karol KG. 2004. Charophyte algae and land plant origins. *Trends Ecol Evol* **19**, 661-666.

Mintz-Oron S, Mandel T, Rogachev I, Feldberg L, Lotan O, Yativ M, Wang Z, Jetter R, Venger I, Adato A, Aharoni A. 2008. Gene expression and metabolism in tomato fruit surface tissues. *Plant Physiol* 147, 823-851.

Molina I, Kosma D. 2015. Role of HXXXD-motif/BAHD acyltransferases in the biosynthesis of extracellular lipids. *Plant Cell Rep* **34**, 587-601.

Mühlhausen S, Kollmar M. 2013. Whole genome duplication events in plant evolution reconstructed and predicted using myosin motor proteins. BMC Evol Biol 13, 202.

Panikashvili D, Shi JX, Schreiber L, Aharoni A. 2009. The Arabidopsis DCR encoding a soluble BAHD acyltransferase is required for cutin polyester formation and seed hydration properties. *Plant Physiol* **151**, 1773-1789.

Pollard M, Beisson F, Li Y, Ohlrogge JB. 2008. Building lipid barriers: biosynthesis of cutin and suberin. *Trends Plant Sci* **13**, 236-246.

Saladié M, Rose JKC, Watkins CB. 2005. Characterization of DFD (Delayed Fruit Deterioration): a new tomato mutant. *Acta horticulturae*, 79-84.

Saladié M, Matas AJ, Isaacson T, Jenks MA, Goodwin SM, Niklas KJ, Xiaolin R, Labavitch JM, Shackel KA, Fernie AR, Lytovchenko A, O'Neill MA, Watkins CB, Rose JK. 2007. A reevaluation of the key factors that influence tomato fruit softening and integrity. *Plant Physiol* 144, 1012-1028.

Samuels L, Kunst L, Jetter R. 2008. Sealing plant surfaces: cuticular wax formation by epidermal cells. *Annu Rev Plant Biol* **59**, 683-707.

Schreiber L. 2010. Transport barriers made of cutin, suberin and associated waxes. *Trends Plant Sci* **15**, 546-553.

Shi JX, Adato A, Alkan N, He Y, Lashbrooke J, Matas AJ, Meir S, Malitsky S, Isaacson T, Prusky D, Leshkowitz D, Schreiber L, Granell AR, Widemann E, Grausem B, Pinot F, Rose JK, Rogachev I, Rothan C, Aharoni A. 2013. The tomato SlSHINE3 transcription

factor regulates fruit cuticle formation and epidermal patterning. *New Phytol* 197, 468-480.

Shi JX, Malitsky S, De Oliveira S, Branigan C, Franke RB, Schreiber L, Aharoni A. 2011. SHINE transcription factors act redundantly to pattern the archetypal surface of Arabidopsis flower organs. *PLoS Genet* **7**, e1001388.

Sievers F, Wilm A, Dineen D, Gibson TJ, Karplus K, Li W, Lopez R, McWilliam H, Remmert M, Söding J, Thompson JD, Higgins DG. 2011. Fast, scalable generation of high-quality protein multiple sequence alignments using Clustal Omega. *Mol Syst Biol* **7**, 539.

Takeda S, Iwasaki A, Matsumoto N, Uemura T, Tatematsu K, Okada K. 2013. Physical interaction of floral organs controls petal morphogenesis in Arabidopsis. *Plant Physiol* **161**, 1242-1250.

Taketa S, Amano S, Tsujino Y, Sato T, Saisho D, Kakeda K, Nomura M, Suzuki T, Matsumoto T, Sato K, Kanamori H, Kawasaki S, Takeda K. 2008. Barley grain with adhering hulls is controlled by an ERF family transcription factor gene regulating a lipid biosynthesis pathway. *Proc Natl Acad Sci U S A* 105, 4062-4067.

Tamura K, Peterson D, Peterson N, Stecher G, Nei M, Kumar S. 2011. MEGA5: molecular evolutionary genetics analysis using maximum likelihood, evolutionary distance, and maximum parsimony methods. *Mol Biol Evol* **28**, 2731-2739.

Tomato Genome Consortium. 2012. The tomato genome sequence provides insights into fleshy fruit evolution. *Nature* **485**, 635-641.

Velasco R, Zharkikh A, Affourtit J, Dhingra A, Cestaro A, Kalyanaraman A, Fontana P, Bhatnagar SK, Troggio M, Pruss D, Salvi S, Pindo M, Baldi P, Castelletti S, Cavaiuolo M, Coppola G, Costa F, Cova V, Dal Ri A, Goremykin V, Komjanc M, Longhi S, Magnago P, Malacarne G, Malnoy M, Micheletti D, Moretto M, Perazzolli M, Si-Ammour A, Vezzulli S, Zini E, Eldredge G, Fitzgerald LM, Gutin N, Lanchbury J, Macalma T, Mitchell JT, Reid J, Wardell B, Kodira C, Chen Z, Desany B, Niazi F, Palmer M, Koepke T, Jiwan D, Schaeffer S, Krishnan V, Wu C, Chu VT, King ST, Vick J, Tao Q, Mraz A, Stormo A, Stormo K, Bogden R, Ederle D, Stella A, Vecchietti A, Kater MM, Masiero S, Lasserre P, Lespinasse Y, Allan AC, Bus V, Chagné D, Crowhurst RN, Gleave AP, Lavezzo E, Fawcett JA, Proost S, Rouzé P, Sterck L, Toppo S, Lazzari B, Hellens RP, Durel CE, Gutin A, Bumgarner RE, Gardiner SE, Skolnick M, Egholm M, Van de Peer Y, Salamini F, Viola R. 2010. The genome of the domesticated apple (Malus × domestica Borkh.). *Nat Genet* 42, 833-839.

Van Ooijen JW. 2006. JoinMap 4. Software for the calculation of genetic linkage maps in experimental populations. Wageningen, The Netherlands: Kyazma BV.

Van Ooijen JW. 2009. MapQTL 6.0. Software for the mapping of quantitative trait loci in experimental populations of diploid species. Wageningen, The Netherlands: Kyazma BV.

Voorrips RE. 2002. MapChart: software for the graphical presentation of linkage maps and QTLs. *J Hered* **93**, 77-78.

Wang W, Zhang Y, Xu C, Ren J, Liu X, Black K, Gai X, Wang Q, Ren H. 2015. Cucumber ECERIFERUM1 (CsCER1), which influences the cuticle properties and drought tolerance of cucumber, plays a key role in VLC alkanes biosynthesis. *Plant Mol Biol* **87**, 219-233.

Wood GA. 2001. Sensitivity of apple (Malus domestica) indicator cultivars to russet ring disease, and the results of graft transmission trials of other fruit affecting disorders of apple, *New Zealand Journal of Crop and Horticultural Science*, **29**, 255-265.

Wu GZ, Xue HW. 2010. Arabidopsis β-ketoacyl-[acyl carrier protein] synthase i is crucial for fatty acid synthesis and plays a role in chloroplast division and embryo development. *Plant Cell* **22**, 3726-3744.

Yeats TH, Rose JK. 2013. The formation and function of plant cuticles. *Plant Physiol* **163**, 5-20.

Zhang M, Fan J, Taylor DC, Ohlrogge JB. 2009. DGAT1 and PDAT1 acyltransferases have overlapping functions in Arabidopsis triacylglycerol biosynthesis and are essential for normal pollen and seed development. *Plant Cell* **21**, 3885-3901.

Chapter 5

Research Results

MYB107 and MYB9 are Members of a Multi-species Clade of Transcription Factors Regulating Suberin Formation

This chapter has been compiled from a manuscript submitted to *Nature Communications* as referenced below, and is written in the format of that journal.

Lashbrooke J, Levy-Samocha D, Tzfadia O, Zeisler V, Trainotti L, Schreiber L, Costa F, Aharoni A (2015). MYB107 and MYB9 are Members of a Cross-species Clade of Transcription Factors Regulating Suberin Formation. *Nature Communications*. *In submission.*

5.1 Introduction

The plant cuticle is an apoplastic lipophilic layer enveloping and covering the plant. It is comprised typically of a cutin polymer consisting of medium length fatty acids, embedded with very long chain fatty acid waxes[1,2]. During normal growth this layer covers all above ground organs including leaves, flowers and fruit. The cutin polymer and embedded waxes are typically translucent, allowing for photosynthesis, while also providing a strong water proofing barrier, and are thus crucial to the plant's terrestrial survival[2-4]. While control of water movement can be considered the principal role of the cuticle, additional roles include structural support and protection against pathogen infection and herivory[3,4]. In the event of wounding or damage to the surface the plant is able to produce suberin[5]. This polymer is analogous to cutin, but consists of slightly longer chain length fatty acids as well as a polyphenol domain[6-8]. Embedded waxes in suberin may consist alkyl ferulates that are not typically found in cutin[9]. This wound response suberin is typically brown and rough in appearance and can be seen on the surface of fruit, leaves and stems, where it fulfils a similar role as regular cuticle, although it is less elastic, and typically a less efficient water barrier[7,10].

Suberin is not exclusively produced as a wounding polymer; in fact, the majority of deposition of this polymer occurs during normal growth in roots, bark, seeds and specialised organs such as *Solanum tuberosum* (potato) tubers[7,8]. Here its primary roles are that of osmotic regulation, and protection from biotic stress. It is within these tissues that the suberin research has been focussed, yet in comparison to our understanding of cutin biosynthesis relatively little is known regarding many of the mechanisms involved in suberin formation. Considering the impact a greater understanding of suberin biosynthesis and its regulation may have with regards to the development of crops with superior drought tolerance investigation of these processes is likely to receive increased attention in the future.

Thus far, several genes coding for enzymes involved in suberin biosynthesis have been described, primarily those responsible for aliphatic monomer formation, such as *β-KETOACYL-CoA SYNTHASEs* (*KCS2*/*DAISY*[11,12] and *KCS20*[12]), fatty acid cytochrome P450 oxidases (*CYP86A1*[13] and *CYP86B1*[14,15]), *FATTY ACYL-COA REDUCTASEs*[16,17], and *GLYCEROL-3-PHOSPHATE ACYLTRANSFERASE5* (*GPAT5*[18,19]); and those responsible for aromatic monomer inclusion, such as *ALIPHATIC SUBERIN FERULOYL TRANSFERASE* (*ASFT*)[15,20]. Recently ATP-BINDING CASSETTE G transporters

(ABCG2, ABCG6 and ABCG20) have been identified as key transporters of suberin monomers[21]. Typically these genes have been characterized in *Arabidopsis* where they are expressed in suberin forming tissues, such as the root and integument layer of the seed coat. While currently no genes responsible for the extracellular polymerisation of the suberin polymer have been described. Currently several transcription factors influencing plant cutin and wax formation have been identified, while only one regulatory gene for suberin synthesis has been characterized. The recently described MYB factor, AtMYB41, was demonstrated to be a positive regulator of suberin biosynthesis in *Arabidopsis*, able to activate ectopic suberin synthesis in multiple plant tissues[22]. *AtMYB41* expression is induced under drought, ABA and salt treatments and in normal growth conditions likely plays a role in the plant's response to abiotic stresses[23].

This study aimed to identify genes active during suberin formation, particularly those involved in regulating the biosynthesis of suberin monomers and its deposition in the course of plant development. While our leading findings were through examination of suberization in fruit skin surface (in transgenic tomato and natively, russeted apple), we subsequently focused on suberin deposition in the *Arabidopsis* seed coat. It appeared that the gene expression program as a consequence of russeting, a naturally occurring suberization phenomenon of apple surface[10,24], and suberization due to genetically altered cutin and cuticular deficiency in tomato skin, is vastly analogous. Interrogating multiple other transcriptomics datasets associated with suberin formation uncovered a conserved gene expression signature associated with suberin monomer biosynthesis and polymer assembly. Central elements in this gene expression signature were *AtMYB107* and its close homolog *AtMYB9*, a pair of *Arabidopsis* transcription factors that likely represent a clade of proteins playing a significant role in developmental suberin deposition in suberized layers of numerous plant species. Arabidopsis *atmyb107* and *atmyb9* mutants displayed a significant reduction in particular seed coat aliphatics and aromatic components that are considered characteristics of the suberin polymer. The apparent regulation by AtMYB107 and AtMYB9 of both the aliphatic and aromatic monomers biosynthesis pathways serves as an excellent base for studying the crosstalk between these pathways which results in suberin polymer formation. Moreover it could also teach us how the coordination between biosynthesis, transport and assembly in the developing suberized organs takes place in a way facilitating the establishment of an optimal barrier function in boundary

tissue layers as for instance in root peridermis and endodermis, seed coat, and tuber and fruit skin.

5.2 Results

5.2.1 Silencing the Tomato *DEFECTIVE IN CUTICULAR RIDGES* Results in Intensive Suberization of the Tomato Fruit Surface

Earlier work showed that *DEFECTIVE IN CUTICULAR RIDGES (DCR)*, a member of the BAHD family of acyltransferases, is required for incorporation of the most abundant cutin monomer into the polymeric structure of the *Arabidopsis* flower cuticle[25]. Notably, the same component, namely 9(10),16-dihydroxyhexadecanoic acid (C16-9/10,16-DHFA), is the most abundant cutin monomer of tomato, cherry and other fleshy fruit species[26-28]. This similarity in cutin monomer composition of *Arabidopsis* petals and fleshy fruit, particularly tomato, suggested that DCR might play an important role in forming the tomato fruit surface. In order to test this hypothesis, the tomato *DCR* ortholog (Solyc03g025320; Supplementary Fig. 1) was identified and silenced. Expression analysis shows the tomato *DCR* is preferentially expressed in the skin tissue when compared to the flesh (i.e. pericarp) (Fig. 1a). Furthermore, it is highly expressed at the early stages of fruit development and decreased sharply during maturation and ripening. This can be considered a typical expression profile of genes involved in fruit cuticle biosynthesis[28].

Tomato plants silenced for *SlDCR* expression (Fig. 1b) displayed several surface phenotypes including organ fusions of leaves and flowers (Supplementary Fig. 2). However, the most striking phenotype was the fruit surface of the *SlDCR*-RNAi lines, which showed major cracking and browning, resembling the surface of potato tubers and increasing in intensity during fruit development, potentially indicative of suberin formation (Fig. 1c). Light microscopy analysis suggested a reduction in cuticle deposition in the *SlDCR*-RNAi fruit when compared to wild type (Supplementary Fig. 3). Further analysis via Scanning Electron Microscopy (SEM) revealed microscopic cracks between cells, as well as larger fissures across the fruit surface (Fig. 1c,d). Finally, Transmission Electron Microscopy (TEM) analysis showed what appear to be lipid inclusion bodies in the cytosol of the *SlDCR*-RNAi fruit epidermal cells (Fig. 1e).

Chemical characterization of the brown, rough surface coating the *SlDCR*-RNAi fruit was subsequently performed. The results showed a significant reduction in the

majority of the quantified cutin monomers (Fig. 1g), notably, a massive reduction in levels of C16-9/10,16-DHFA, the major tomato fruit cutin monomer. This monomer typically accounts for an excess of 90% of the tomato fruit cutin polymer. Constituents that displayed a significant increase in deposition included the terminally hydroxylated and dicarboxylic fatty acids (C16-ω HFA and C16:0 DFA, respectively) as well as the phenolic, ferulic acid. Significantly, these metabolic changes conform to the described differences between cutin and suberin[7,8], suggesting suberization of *SlDCR*-RNAi fruit surface.

To examine if suberin-associated genes were activated in the epidermal cells of *SlDCR*-RNAi fruit, examination of the expression of two tomato orthologs of well characterized suberin biosynthesis genes (ASFT[15] and GPAT5[18]) was performed. The skin tissue of mature green tomato fruit was examined as fruit at this stage showed definitive signs of assumed suberin formation. The results revealed that expression of the single *ASFT* ortholog in tomato (*Solyc03g097500*; Supplementary Fig. 4) was dramatically increased in the skin of *SlDCR*-RNAi fruit (in excess of 350-fold, Fig. 1f). Phylogenetic analysis of the tomato GPAT family revealed two potential GPAT5 orthologs (Solyc04g011600 and Solyc05g053030) (Supplementary Fig. 5). Expression analysis of the GPAT family members in the *SlDCR*-RNAi fruit revealed that only *Solyc04g011600* (*SlGPAT5*) displayed a significantly altered expression, showing a greater than 350-fold increase in expression compared to wild type fruit skin (Fig. 1f; Supplementary Fig. 5). Importantly, SlGPAT4 and SlGPAT6, both considered to be involved in cutin polymer formation[29,30], showed no change in expression (Supplementary Fig. 5).

The secondary nature of the suberin-like layer that coated the *SlDCR*-RNAi fruit (i.e. a response to wounding rather than a direct response to *SlDCR* silencing) was demonstrated through the partial covering of developing fruit with petroleum jelly. The jelly acted to simulate a properly functioning water-proofing cuticle. Regions of *SlDCR*-RNAi fruit covered with the jelly did not develop any visible suberization as compared to non-covered ones, thus, decoupling the surface phenotype directly with *SlDCR* expression (Supplementary Fig. 6).

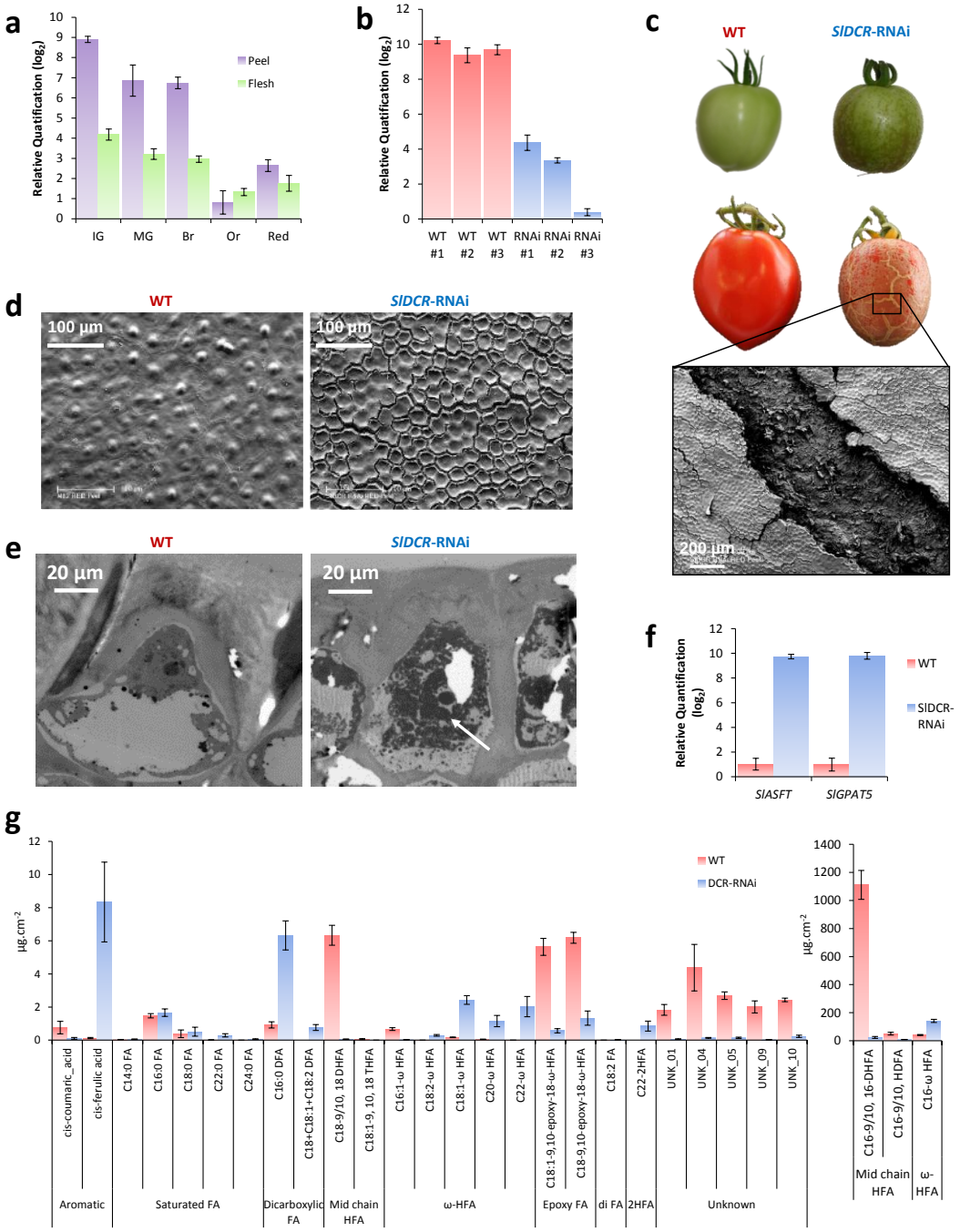

Figure 1. Silencing of *SlDCR* in tomato leads to suberization of the fruit surface. (a) Quantification of *SlDCR* expression in developing tomato fruit via quantitative Real Time-PCR (qRT-PCR) shows a skin enriched expression profile. IG, immature green; MG, mature green; Br, breaker; Or, orange. **(b)** Confirmation of silencing in mature green stage skin tissue via qRT-PCR of *SlDCR* in transgenic lines (*SlDCR*-RNAi). **(c)** Fruit surface phenotype of *SlDCR*-RNAi fruit at the mature green and red developmental stage. Loss of epidermal layer in the marked cracked fruit region is revealed by Scanning Electron Microscopy (SEM). **(d)** SEM analysis of red stage fruit surface shows cracking between cells. **(e)** TEM analysis of fruit epidermal cell at the red development stage shows reduced cuticle and an increase in lipid inclusion bodies in the cytosol of *SlDCR*-RNAi cells (white arrow). **(f)** Expression analysis via qRT-PCR shows a massive increase in expression of *SlASFT* and *SlGPAT5* (over 350-fold) in *SlDCR*-RNAi mature green fruit skin. **(g)** Chemical analysis via Gas Chromatography-MS (GC-MS) of the fruit surface polymer in *SlDCR*-RNAi lines shows a massive decrease in C16-9/10,16-DHFA, and an increase in monomers typically found in suberin polymer. Error bars show standard error, n = 4.

5.2.2 The Russeting of Apple Fruit Surface Resembles the Phenotype of *SlDCR* Silenced Tomato Fruit

Following the results obtained from silencing *SlDCR* in tomato fruit, similar, but naturally occurring, phenomena were sought in other fruit species. Apple russet is the suberization of the surface of apple fruit reported to occur in response to cuticle damage as a developmental process in some cultivars[10,24]. In order to assess the suberization observed in the *SlDCR*-RNAi fruit it was compared with that found in russeted apples. A regular skinned clone of the apple cultivar Golden Delicious ('Reinders') was analysed in conjunction with a clone deriving from a somatic mutation for this cultivar that shows highly russeted fruits ('Rugiada') (Fig. 2a). As in the case of *SlDCR*-RNAi tomato fruit, the surface of the 'Rugiada' fruit appeared brown, rough and cracked. Light microscopy and SEM analysis highlighted the dramatically reduced cuticle of these russeted apples leading to this phenotype (Fig. 2b; Supplementary Fig. 7).

Chemical analysis of the depolymerised cuticle polymer was subsequently performed, and revealed a number of striking changes between the two apple clones (Fig. 2c). The russet apple skin tissue showed a radical reduction in the mid chain hydroxylated fatty acid, C16-9/10,16-DHFA, as well as the terminal hydroxylated fatty acid, C16-ω-HFA, and the epoxy FA, C18:1-9,10-epoxy-19-ω-HFA. This was coupled with massive increases in C20- and C22-ω-HFAs, as well as the saturated C22:0 FA. Significantly, an increase in the phenolics, benzoic acid, ferulic acid and cinnamic acid was also observed. These metabolic changes are indicative of suberin formation[7,9], and confirm the presence of this polymer in the surface of russeted apples.

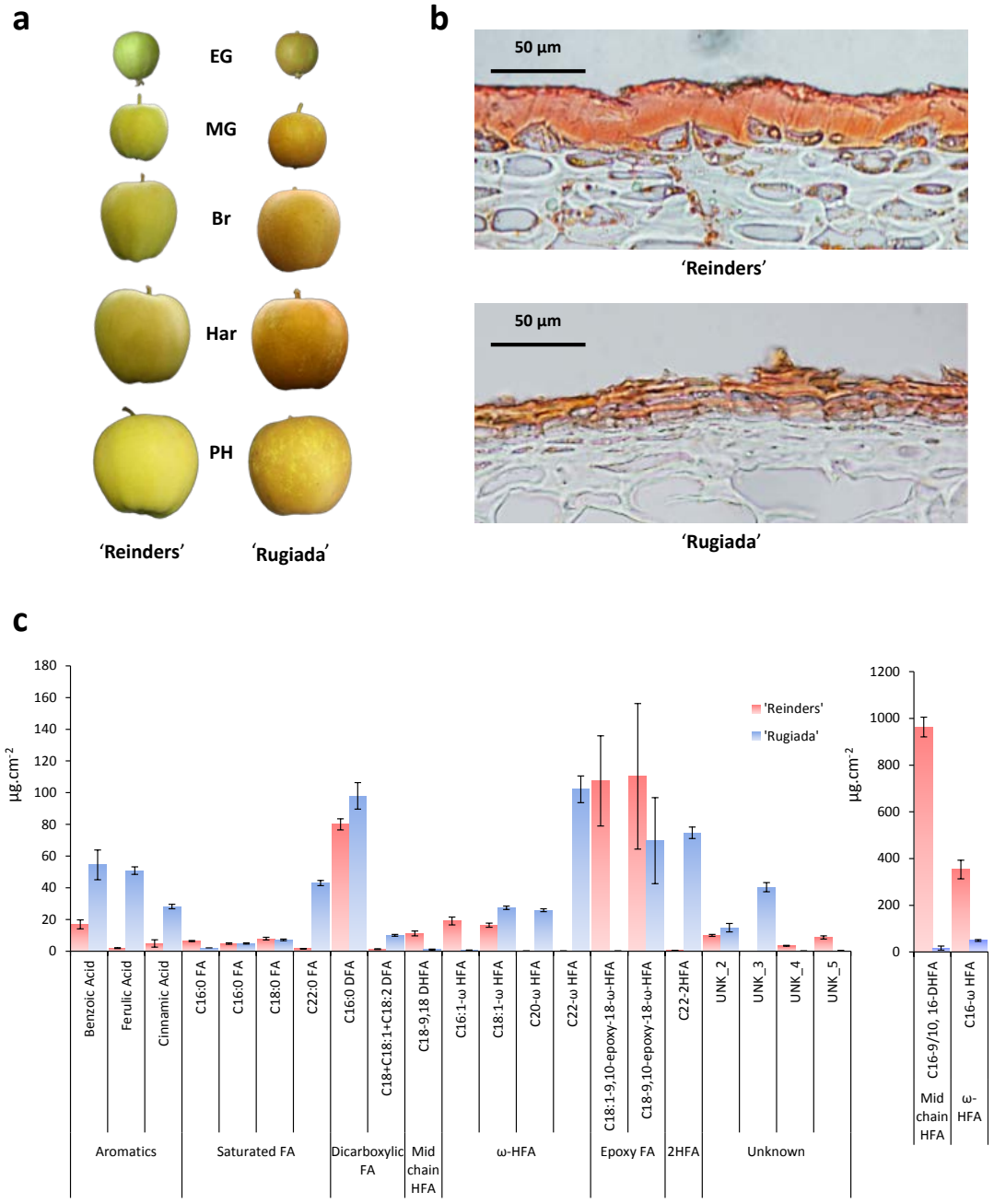

Figure 2. Surface phenotype and chemical composition of apple russet. (a) Two Golden Delicious apple clones were analysed in this work, the normal skinned 'Renders' clone, and the russeted 'Rugiada' clone. 'Rugiada' displays a rough, brown and cracked fruit surface. EG, early green; MG, mature green; Br, breaker; Har, harvest; PH, post-harvest. **(b)** Light microscopy of the epidermal layer of harvest stage fruit from 'Renders' and 'Rugiada' shows a dramatic reduction in cuticle deposition. The lipid staining Sudan IV stains the cuticle components red. **(c)** Chemical analysis via GC-MS of the surface polymer of these two clones highlights the dramatic reduction in C16-9/10,16-DHFA and C16-ω-HFA monomers, while an increase in longer chain length C20- and C22-ω-HFA is observed, together with an increase in aromatics. Error bars show standard error, n = 4.

5.2.3 Significant Correspondence between the Transcriptional Profile of Surface Tissue in Russeted Apple and the Suberized Skin of *SlDCR* Silenced Tomato Fruit

Investigation into the similarity between the transcriptional changes occurring during russet development in apple and the suberization phenotype of *SlDCR*-RNAi fruit skin was performed. Transcriptome analysis of russeted apple consisted of analysing both skin and flesh tissues at five developmental stages in the regular skinned 'Reinders' clone and the russeted 'Rugiada' clone. Global transcript profiling in tomato fruit skin tissue from *SlDCR*-RNAi lines was compared with wild type tissue at the mature green stage. A set of 504 genes significantly up regulated in *SlDCR*-RNAi skin tissue were detected (*p*-value < 0.05) (Supplementary Dataset 1). Cross comparison of the apple and tomato datasets identified a set of 70 orthologous gene groups that were up regulated in both the *SlDCR*-RNAi tomato fruit skin and russeted apple skins (Supplementary Table 1). GO-enrichment analysis of the orthologous gene list found a significant enrichment (p-value < 0.001) for biosynthetic processes involved in aromatic compounds, phenylpropanoids, suberin, fatty acids, and lignin (Supplementary Fig. 8).

Closer examination of common orthologous genes in the apple and tomato datasets revealed that the characterised suberin biosynthesis genes (*ASFT*, *GPAT5* and *CYP86B1*) display almost exclusive expression in the suberized skin tissues (Fig. 3; Supplementary Dataset 1 and 2). Further genes up regulated in the suberized skins of tomato and apple with a potential role in suberin biosynthesis, included genes involved in phenylpropanoid biosynthesis, *4-COUMARATE:COA LIGASE 5* (*4CL5*), *FERULIC ACID 5-HYDROXYLASE 1* (*FAH1*) and *CAFFEOYL COENZYME A DEPENDENT O-METHYLTRANSFERASE 1*; fatty acid biosynthesis, *FATTY ACYL-ACP THIOESTERASES B* (*FATB*); suberin monomer transport and polymerisation, *ATP-BINDING CASSETTE G20* (*ABCG20*), *GLYCOSYLPHOSPHATIDYLINOSITOL-ANCHORED LIPID PROTEIN TRANSFER 5* (*LTPG5*), and a number of GDSL-motif esterase/acyltransferase/lipase genes; and transcriptional regulators, *NAC DOMAIN CONTAINING PROTEIN 39* (*NAC39*), *MYB DOMAIN PROTEINS* (*MYB67* and *MYB107*), and *WRKY DNA-BINDING PROTEIN 28* (*WRKY28*) (Fig. 3; Supplementary Table 1).

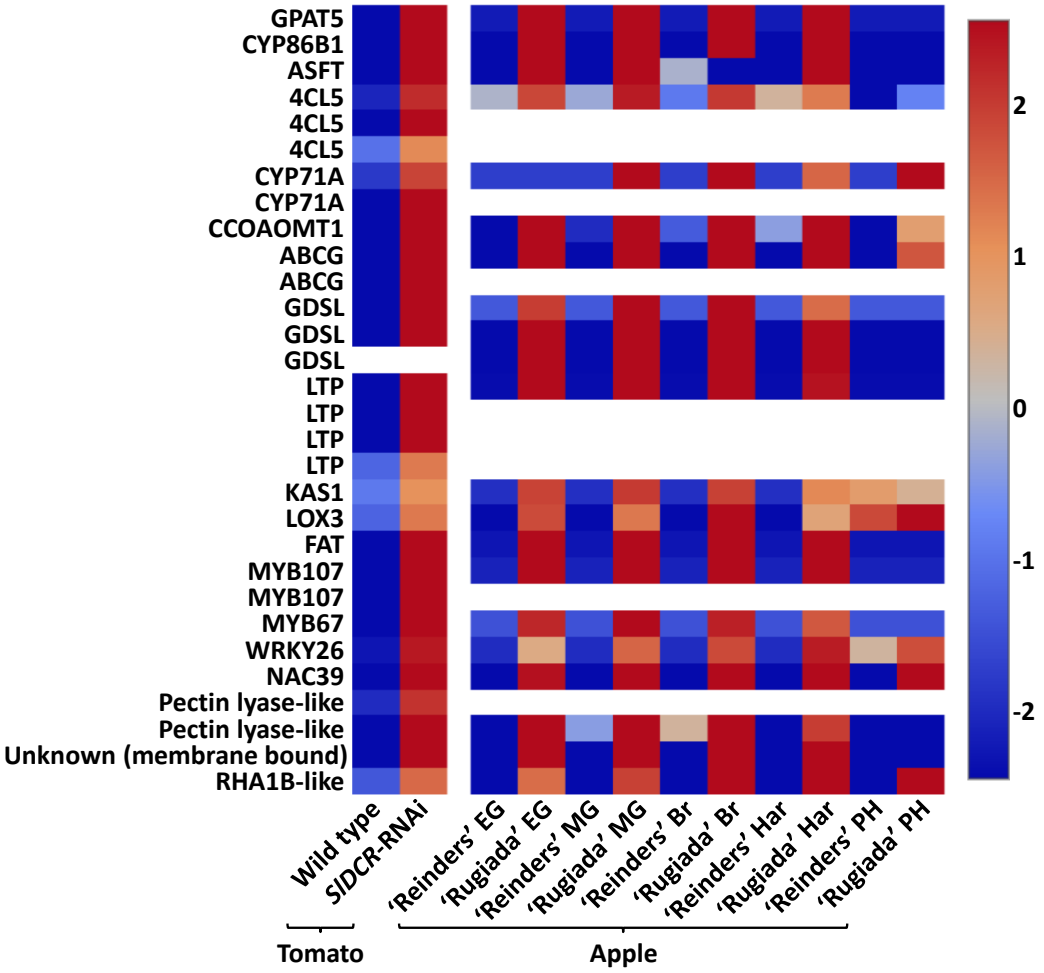

Figure 3. Orthologous genes upregulated in both the suberized fruit skin tissues of *SlDCR*-RNAi and russeted apple. Genes upregulated in *SlDCR*-RNAi compared to wild-type and in the russeted 'Rugiada' clone compared to the regular skinned 'Reinders' were depicted in a heat map. For a full list of identified genes and the corresponding expression patterns see Supplementary Dataset 1 and 2 and Supplementary Table 1. Scale bar indicates $\log_2$(fold-change) of expression when compared to the mean of expression for each gene. EG, early green; MG, mature green; Br, breaker; Har, harvest; PH, post-harvest.

5.2.4 Comparative Transcriptome Analysis Reveals a Multi-species Gene Expression Signature for Suberin Biosynthesis

Since the initial transcriptomic comparison between suberized tomato and russeted apple tissues identified a significant correspondence between the upregulated transcripts it was attempted to extend the comparative analysis to multiple other species and thus create a species-wide transcriptional signature of suberin formation. To this end, a collection of multi-tissue transcriptome datasets was identified from several species, each possessing an association with suberin deposition. Apart from the

above apple and *SlDCR*-RNAi fruit transcriptome data, this collection included profiled seed tissues during development in *Arabidopsis*[31], all major organs of *Vitis vinifera* (Grapevine)[32], Tomato[33] and Potato[34], and the roots of *Oryza sativa* (Rice) during waterlogging[35]. Each of the seven transcriptome datasets was subsequently used for co-expression analysis in which orthologs of three known Arabidopsis genes involved in suberin biosynthesis (i.e. *GPAT5*[18], *ASFT*[15], and/or *CYP86B1*[14]) were used as 'baits' (i.e. combined). These genes were selected based on their orthology to the characterised genes, and their expression patterns in the respective datasets (Supplementary Fig. 9). Orthology between genes in the generated co-expression lists (Supplementary Dataset 3) was then determined, identifying 1454 gene ortholog groups. The co-expressed orthologs were ranked based on their frequency of occurrence in the seven datasets; two sets of orthologs were found in all seven lists, three in six, 11 in five, and 10 in four experiments (26 in total). We considered the list of 26 genes as a suberin gene expression signature, spanning multiple tissues and species. The suberin signature included several genes previously shown to be involved in multiple steps of suberin formation as well as those associated with fatty acid synthesis, lignin/phenylpropanoid metabolism, transport, extracellular polymerization and transcriptional regulation (Fig. 4; Supplementary Table 2).

5.2.5 Identification of a MYB Transcription Factor Clade Linked to Suberin Biosynthesis across Multiple Plant Species

In order to examine the possible association of the candidates identified through the multi-species co-expression analysis to suberin deposition, *Arabidopsis* T-DNA knockout lines were acquired for the corresponding genes (Supplementary Table 2 and 3). After screening for homozygous insertions, lines representing 21 genes of the total 26 (including 10 of the 15 genes co-expressed in five or more experiments, Fig. 4) were analyzed for seed permeability. Seed staining via tetrazolium chloride is commonly used in *Arabidopsis* to identify an increase in seed permeability which may indicate altered suberin deposition in the seed coat. T-DNA lines representing known suberin biosynthesis genes (*ASFT*, *GPAT5* and *CYP86B1*) were included in the analysis as positive controls. Tetrazolium staining of these controls showed similar results to the ones described previously as both *asft* and *gpat5* knockouts showed strong staining, while *cyp86b1* was not stained significantly [14,15,18]. Permeability assays performed on seeds derived from the confirmed homozygous insertions for the candidate genes identified a highly significant increase in staining when compared to wild type for *myb107*

(*at3g02940*), *myb9* (*at5g16770*; closely related in sequence to *MYB107*), *abcg20* (*at5g13580*) and *nac38* (*at2g24430*) mutants ($p < 0.005$; Fig. 5; Supplementary Fig. 10 and 11). These genes can be considered strong candidates to act in the process of suberin deposition in the Arabidopsis seed coat.

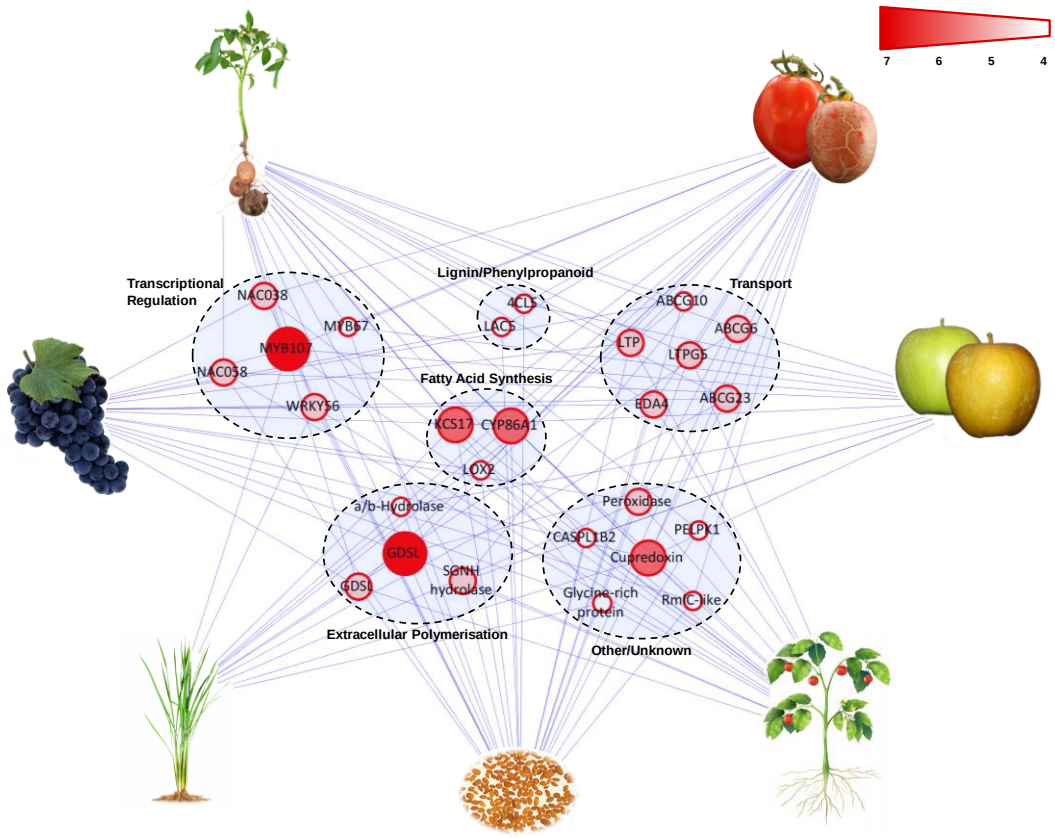

Figure 4. Multi-species gene expression signature for suberin biosynthesis. Orthologues genes identified through the multi-species multi-gene co-expression analysis are represented graphically. Genes identified to be co-expressed with three 'baits' representing known suberin synthesis genes were identified in seven data sets and compared for orthology. Clockwise from top right the images represent transcriptomics datasets that examined expression in: *SlDCR*-RNAi vs. wild-type fruit skin tissues, russeted vs. regular skinned apples surface tissues, multiple tissue types from whole tomato plant, *Arabidopsis* seeds tissues, waterlogged rice roots vs, wild-type roots, whole grapevine plant tissues and whole potato plant tissues. Edges represent presence of the corresponding ortholog to the expression dataset, while nodes represent orthologous gene groups. Scale bar indicates the number of experiments in which orthologous gene group have been identified (from 4 out of 7 to 7 out of 7 transcriptome datasets; 7/7 is presented by the largest and most intensely red colored circle). Genes are also grouped based on their proposed function. For respective gene IDs see Supplementary Table 2 and for details of the co-expression parameters see Supplementary Table 5.

Of these significant candidates, we chose to characterize thoroughly the MYB9 and MYB107 protein pair. Molecular polygenetic examination of this clade of transcription factors from Arabidopsis, tomato, apple, potato, grape and rice revealed that all could be positioned in one of two previously defined MYB family subgroups (Subgroup 10 or 24; Fig. 6). These subgroups have been previously shown to be phylogenetically adjacent, and part of a phylogenetic branch containing further subgroups 9 and 11[36]. Analysis of the members of these four subgroups identified protein motifs not previously described (Fig. 6), and suggested that defining subgroup 10 or 24 as one single clade may be more appropriate. Specifically, analysing for the conserved motifs located in these proteins carboxy terminus identified two neighbouring motifs (termed here SUB-I and SUB-II; located C-terminal to the R3-MYB repeat) which were present in the MYB proteins from all six plant species examined. A third motif, found adjacent to the C-terminal (termed SUB-III), was found to be present in all members, barring the monocotyledonous rice ortholog (OsMYB93) (Fig. 6). Screening of the MYB factors from the adjacent subgroups (i.e. 9 and 11), which contain the previously reported suberin (MYB41) and cutin regulators (MYB16 and MYB106) for these newly identified motifs returned no hits.

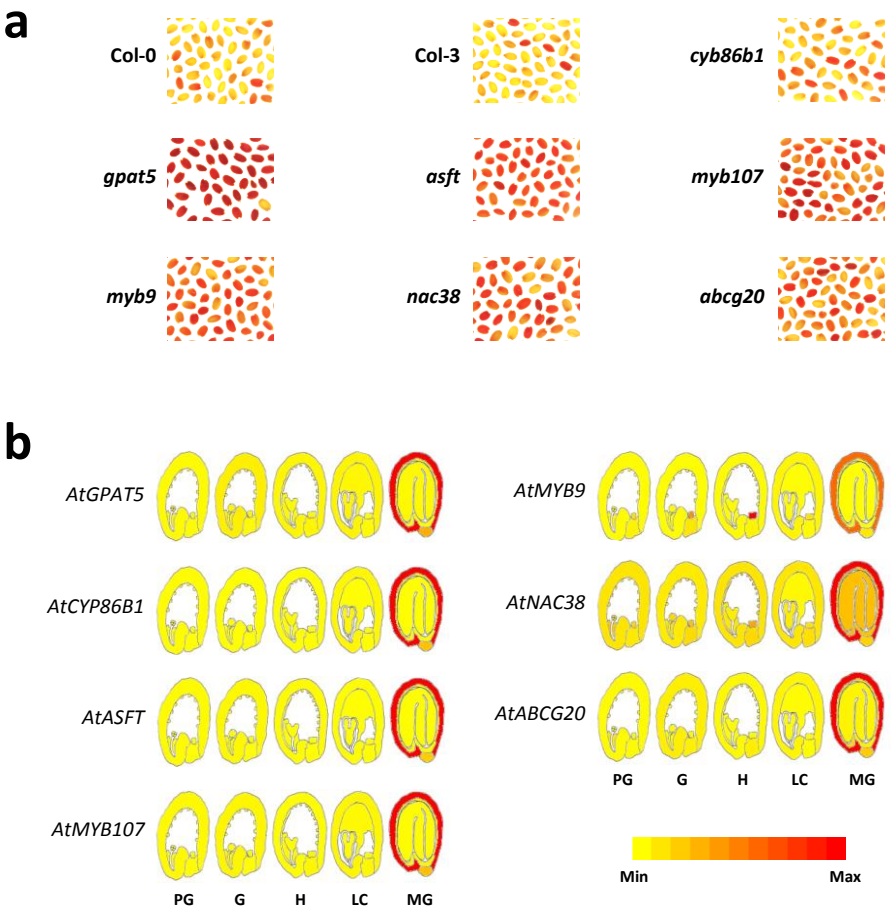

Figure 5. Identification of candidate genes involved in suberin deposition in *Arabidopsis* seeds. (**a**) Tetrazolium salt penetration assays for seeds of *Arabidopsis* T-DNA insertion lines identified an increase in seed permeability (resulting in red staining of seeds) for *myb107*, *myb9*, *nac38*, and *abcg20* mutant lines. Controls for staining (*asft* and *gpat5*) and negative ones (*cyp86b1* and Col-0 and Col-3 wild-types), were included. As reported previously, *asft* and *gpat5* seeds show strong staining while *cyp86b1* seeds do not stain significantly more than the controls[18,37]. (**b**) 'Electronic Fluorescent Pictographs' representing expression profile in seed tissues of the genes described above (obtained from The Arabidopsis eFP Browser; http://bbc.botany.utoronto.ca/efp/[38]). Intense, developmentally late seed coat expression profile can be seen for all genes. PG, pre-globular; G, globular; H, heart; LC, linear cotyledon; MG, mature green.

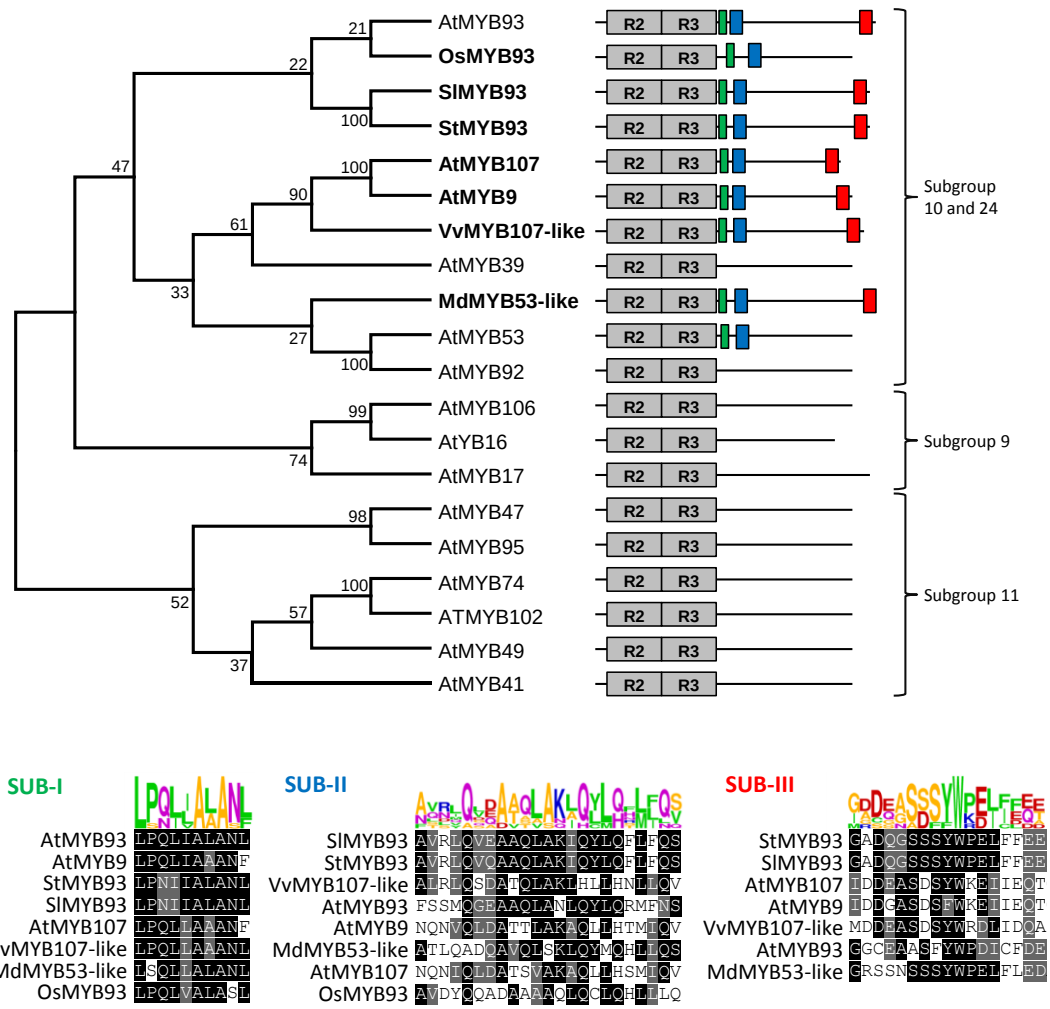

Figure 6. Identification of a clade of MYB-factors likely involved in suberin formation across multiple species. Molecular phylogenetic analysis of *Arabidopsis* MYB factors from subgroups 9, 10, 11 and 24 was performed together with the MYB factors identified in this study to be expressed in suberin forming tissues. While subgroup 9 and 11 form separate clades, division of subgroups 10 and 24 was not previously resolved. Protein domain analysis identified three carboxyl terminal motifs specific to this combined clade which may be involved in regulation of suberin formation (SUB-I, SUB-II and SUB-III). The motifs are marked on the gene structure and shown in full below. ClustalW and the MEGA6 software were used to align the proteins and compute the neighbor-joining tree with significance percentages (bootstrap values out of 1000).

5.2.6 MYB107 and MYB9 Regulate the Aliphatic and Aromatic Pathways of Suberin Formation

Further characterisation of the *Arabidopsis* *myb107* and *myb9* T-DNA lines was performed. The T-DNA insert of the *myb107* line (SAIL_242_B04.V1) is in the 5'UTR of *AtMYB107* and causes a significant down regulation of *AtMYB107* expression in seeds at the mature green stage (up to 40-fold) (Fig. 7). With regards the *myb9* line (GK-661C10-

023861) the T-DNA insertion is 5' of the 5'UTR, and results in an 8-fold down regulation of *AtMYB9* (Fig. 7). Interestingly, expression analysis shows that *MYB107* is up regulated in *myb9* lines, while no significant change in expression for *MYB9* in *myb107* lines was observed (Fig. 7e). Further expression analysis for genes potentially regulated by MYB107 and MYB9 was performed using mature green embryo stage seeds from the T-DNA lines. Results show very little downstream expression effect in *myb9* knockouts, while *MYB107* appears be a major regulator of expression of suberin formation in *Arabidopsis* seeds (Fig. 7e). Significantly down regulated genes in *myb107* lines included *ASFT* and *CYP86B1* (suberin biosynthesis), *4CL5* and *LAC5* (phenylpropanoid/lignin metabolism), *CASPL1B2* (a casparian strip membrane protein) and *At2g23540* (a GDSL-motif esterase). A molecular phylogenetic construction of the identified GDSL-motif esterase and its related proteins identified the gene as a close relative to the cutin synthase clade[39] of GDSL-motif esterases (Supplementary Fig. 12), and is proposed here, together with the proteins identified in tomato, potato, apple, rice and grape (Supplementary Table 2), as a suberin synthase (SUS) protein (Supplementary Fig. 12).

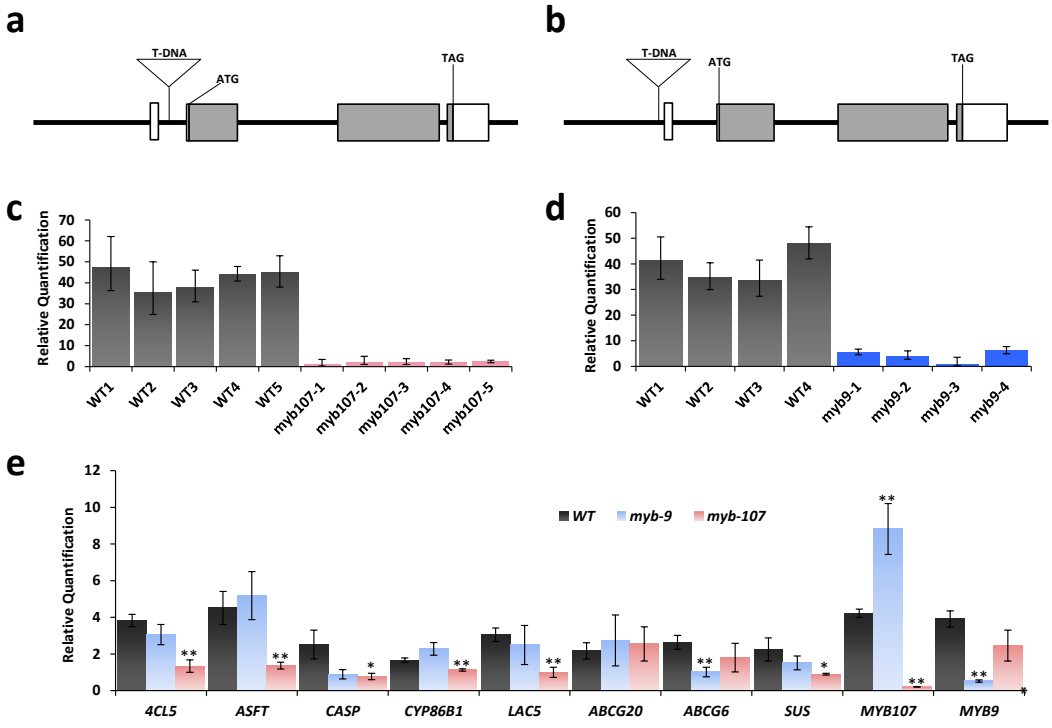

Figure 7. Characterization of *myb107* and *myb9* T-DNA insertion lines. (**a**) Schematic of T-DNA insertion location for *Arabidopsis myb107* and (**b**) *myb9* lines. (**c**) Quantification of expression of *AtMYB107* in *Arabidopsis* seeds at the mature green embryo stage via quantitative Real Time-PCR (qRT-PCR) analysis is shown. Expression is down regulated up to 40-fold in *myb107* lines. (**d**) Quantification of expression of *AtMYB9* in *Arabidopsis* seeds at the mature green embryo stage via qRT-PCR analysis is shown. Expression is down regulated up to 20-fold in *myb9* lines. (**e**) qRT-PCR expression of potential downstream target genes indicates *AtMYB107* to be a primary regulator of suberin synthesis gene expression.

Additionally mature dry seeds of the *myb107* and *myb9* mutant lines were analysed for the chemical composition of the seed coat polyester layer (Fig. 8). Both lines showed a significant reduction for a number of constituents of the seed coat polymer, specifically aliphatics including C20, C22 and C24 terminal hydroxyl fatty acids, C24 dicarboxylic fatty acids and C20 fatty alcohol; and the aromatic, ferulic acid. These compounds are seen as characteristic of the suberin polymer[7].

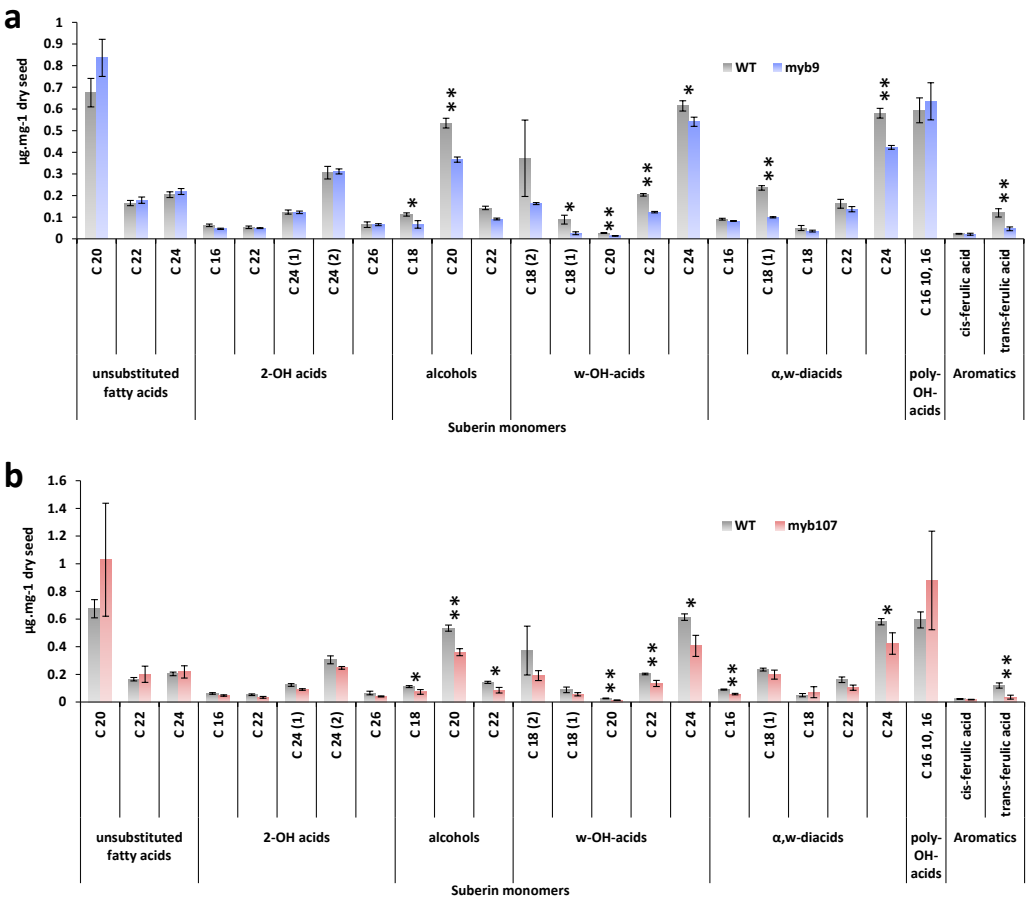

Figure 8. Chemical analysis of seed coat polymer from *myb9* and *myb107* lines. Chemical analysis via GC-MS of the depolymerised seed coat polymer was performed for mature dry seeds from (**a**) *myb9* and (**b**) *myb107* T-DNA insertion lines. A decrease in aliphatic and aromatic constituents can be observed. Error bars represent standard error, n = 3.

5.3 Discussion

The creation of transgenically manipulated tomato plants that display a strongly suberized fruit surface has allowed for a comprehensive analysis of genes involved in suberin biosynthesis. This phenotype was achieved through the silencing of the BAHD acyltransferase *SlDCR*, and highlights the importance of the relatively poorly understood role that this gene plays in cuticle (and specifically cutin) biosynthesis. Apparently DCR is

primarily involved in the inclusion of mid chain hydroxylated C16 fatty acids in the cutin matrix. Highlighted in the chemical analysis performed here (Fig. 1) and in the characterization of *Arabidopsis dcr* mutants, which showed strong flower phenotypes linked to the reduction of C16 mid chain hydroxylated fatty acids[25]. As the cutin covering the non-floral organs of *Arabidopsis* is particular in that it contains low levels of these C16 mid chain hydroxylated fatty acids, and instead high concentrations of dicarboxylic fatty acids[7,9,40], there was a less dramatic effect to the rest of the plant[25]. It is possible that due to this flower specific phenotype (in *Arabidopsis*), DCR has been relatively overlooked as a crucial component of cutin biosynthesis. However, considering that C16 mid chain hydroxylated fatty acids typically occur in fruit cutin at levels exceeding 90% of the total matrix[7,26-28] this oversight is unfortunate. Our results demonstrate the vital role played by DCR in tomato fruit cutin formation, and this can be assumed to be the case in other cutin matrices with a high content of C16 mid chain hydroxylated fatty acids. As proposed by earlier research it seems that DCR may in fact be involved in an alternate pathway for cutin polymerisation[25,41,42] whereby some form of cytosolic oligomerization occurs via the esterification of a mid-chain hydroxylated fatty acid to the mid-chain hydroxyl group of a second molecule. This form of polymerisation would result in the typical branching observed in the secondary structure of the cutin matrix[1,6,43,44].

In parallel to the suberized tomato lines, russeted apples were also assessed, and it was found that the suberization of these fruits' surface was chemically similar. Signature metabolites for suberin formation previously described and observed in these lines included the increase of ferulates[45], an increase in DFAs[14,26,46] and the increase in chain length of the modified FAs[14,26]. Production of suberin on the surface of tomato and apple fruit allowed for a transcriptomic investigation into the underlying mechanisms controlling this process, and through the comparative approach employed here a list of candidates for suberin biosynthesis was generated. Some notable genes included tomato and apple orthologs to *Arabidopsis* genes previously characterised for suberin biosynthesis, *ASFT*[15], *GPAT5*[18], *CYP86B1*[14] and *KCS2*/*DAISY*[11] (Fig. 3; Supplementary Table 1). The presence of these genes in the analysis indicates the effectiveness of the approach, and lends credibility to further findings. The remaining genes fell in to a variety of functional categories, including phenylpropanoid, lignin and lipid metabolism (Supplementary Fig. 8 and Supplementary Table 1). The enrichment for genes involved in these processes is expected, but also highlights the specific

metabolism underlying suberin formation and can be linked to the metabolic changes observed.

By widening the analysis to include additional species (potato, *Arabidopsis*, rice and grapevine) and additional suberin accumulating organs (seeds, tubers and roots) it was possible to generate a more robust description of gene expression during suberin formation. This multi-species gene expression signature highlighted a number of genes which may be considered fundamental to suberin formation across plant species (Fig. 4). The majority of the genes identified have not been associated with suberin formation in the past; however a few of the genes have recently been identified as playing a role in this process validating the approach. These include *ABCG6* and *ABCG20*, a pair of homologous transporters shown to contribute to suberin formation in *Arabidopsis* seed coots[21]; as well *CYP86A1*, a cytochrome P450 involved in the synthesis of terminal hydroxy fatty acids with chain lengths less than 20 carbons[13].

Classification of the identified genes into functional categories highlights the processes involved in suberin deposition, and includes fatty acid synthesis, lignin/phenylpropanoid metabolism, transporters, transcriptional regulators, extracellular polymerisation (Fig. 4). Genes involved in lignin/phenylpropanoid metabolism included *At4CL5*, a gene coding for a rare 4CL isoenzyme that is somewhat disparate from the other members of this family[47,48]. Previous analysis of the lignin content of *4cl5* mutants found no change when compared to wild type, despite the enzyme showing the relevant *in vitro* activity[47]. Taken together with the results found here suggests that this class of *4CLs* may be specific to suberin formation, contributing the aromatic fraction. In addition to the ABCG transporters described previously, the lipid transporter LTPG5 was implicated as central to suberin formation. Previously LTPG1 was shown to be active in the transport of cuticular lipids[49], while LTPGs in general have recently been shown to be functional in the development of both seed coat and pollen apoplastic barriers[50]. It is therefore likely that LTPG5 is in fact specific to suberin deposition. Regarding the genes identified as potentially involved in extracellular polymerisation, one candidate is particularly interesting. Orthologs to this *GDSL esterase* (*At2g23540*), were identified in all seven co-expression experiments, and are therefore very likely involved in the extracellular polymerisation of suberin monomers. Phylogenetic analysis found this clade of GDSLs to be closely related to the recently described cutin synthase (CUS)[51] clade of GDSL esterases (Supplementary Fig. 12) and are therefore named here as suberin synthases (SUS).

Finally, one of the most interesting of the functional groups identified is the transcriptional regulators. MYB, WRKY and NAC factors were all demonstrated to be involved, with MYBs orthologous to AtMYB107 appearing in all seven co-expression analyses. Indeed, further molecular phylogenetic and protein motif analysis of the identified MYB factors propose they form part of a clade of factors containing MYB107, MYB9, MYB93 and MYB53. Previously this clade has been described as two separate groups (subgroup 10 and 24), but results presented here suggest that this division may not be so straight forward. Members from both previously defined subgroups 10 and 24 possess newly identified protein motifs (SUB-I, SUB-II and SUB-III), while these motifs are absent from members of neighbouring subgroups. Importantly these motifs were identified in the factors from all six species discussed here, namely SlMYB93, MdMYB53-like, AtMYB107, AtMYB9, StMYB93, VvMYB107-like and OsMYB93, and may be used in the future to define this clade. In order to confirm the hypothesis that the clade was indeed involved in the regulation of suberin formation *Arabidopsis myb107* and *myb9* mutant lines were analysed. Results indicated that seeds from these lines possess an increased permeability, likely due to the characterised reduction in suberin content of the seed coat polyester of these plants. Metabolic changes to the seed coat polyester of these lines is in agreement with previously described changes for observed in seeds from characterised suberin mutant lines[14,18].

Expression analysis of these lines, however, revealed a complex interaction between these two MYB factors. While in *myb107* lines, a number of suberin formation genes were down regulated, this was not the case in *myb9* lines. Additionally *AtMYB107* showed a 2-fold up regulation in *myb9* lines, possibly a result of compensation for the down regulation of *AtMYB9*. Promoter binding assays may be required to fully understand the relationship between these two proteins, but it appears they are part of a signal feedback loop.

It is significant to note that members of the neighbouring clade of MYB transcription factors include AtMYB16 and AtMYB106, both of which have been demonstrated to regulate cutin formation[52]; AtMYB74 and AtMYB102, which have been found to be involved in the plant's response to wounding, salt and osmotic stresses[53,54]; and AtMYB41, a previously identified suberin regulator[22]. Together with the classification of AtMYB107 and AtMYB9 as regulators of suberin one is presented with a clade of closely related plant surface regulators, with a particular association to osmotic

stress. The evolutionary origin of this clade is therefore very likely linked to the colonisation of dry terrestrial environments by the first land plants.

5.4 Methods

5.4.1 Plant Material and Transformation

Silencing of *SlDCR* (*Solyc03g025320*) was performed in *S. lycopersicum* L. *cv.* M82. The construct for the post transcriptional silencing (SlDCR-RNAi) was generated by PCR, isolating a 378 bp fragment of *SlDCR* from *cv.* M82 cDNA and cloning into pENTR/D-TOPO (Invitrogen). LR Clonase (Invitrogen) was used to recombine this fragment into the pK7GWIWG2(II) binary vector[55]. The primers used in the creation of this construct are listed in Supplementary Table 3. Cotyledon transformation of tomato (*cv.* M82) was performed as previously described[56]. Two clones of apple (*cv.* Golden Delicious) were analysed in this work: the normal skinned 'Reinders' clone and the russeted 'Rugiada' clone. Three trees for each clone were grown in the experimental orchard of the Fondazione Edmund Mach (Northern Italy) and maintained following standard technical agricultural management for pruning, crop load and pest-disease control. *Arabidopsis thaliana* plants were grown in a controlled climate room at 20°C, 70% relative humidity, with a 16-h/8-h light/dark cycle. Lines (including Col-0 ecotype and T-DNA insertion lines) were obtained from the Arabidopsis Biological Resource Centre, and are listed in Supplementary Table 4. The T-DNA insertion lines were identified using the SIGnAL T-DNA Express Arabidopsis Gene Mapping Tool (http://signal.salk.edu/cgi-bin/tdnaexpress) and screening primers (Supplementary Table 4) designed using the T-DNA Primer Design tool (http://signal.salk.edu/tdnaprimers.2.html), both provided by the Salk Institute Genomic Analysis Laboratory[57]. Homozygous lines were identified before continuing with downstream analysis.

5.4.2 Sequence Retrieval and Analysis

Nucleotide and protein sequence retrieval was performed via BLAST analysis. Data were acquired for the various the species from the following databases, making use of the gene IDs curated by these databases: SOL Genomics Network database[58], Grape Genome Database[59], Spud DB[60], The Arabidopsis Information Resource[61], Rice Genome Annotation Project[62], and Genome Database for Rosaceae[63]. Orthology between species was determined via alignment of relevant protein sequences with the ortholog database from PLAZA Comparative Genomics Platform[64]. Gene Orthology enrichment

was performed using this tool from PLAZA Comparative Genomics Platform[64]. Protein alignments were performed using ClustalW[65] and the resultant molecular phylogenetic trees visualized using MEGA6[66]. Neighbour-joining trees were constructed with bootstrapping calculated from 1000 instances. Motif discovery was performed for the identified clade of MYB factors using The MEME Suite[67]. Identified motifs were screened for presence in neighbouring proteins to confirm conservation and then visualised using Weblogo[68].

5.4.3 Light and Electron Microscopy

Samples for electron microscopy were fixed and prepared as described previously[25]. For SEM, samples were analysed using an XL30 ESEM FEG microscope (FEI) at 5 to 10 kV. For TEM sections (70 nm) were observed with a Technai T12 Transmission Electron Microscope. For light microscopy, skin tissue samples were fixed and embedded in wax as described previously[28]. Sections were cut to 5–10 µm on a Leica 2000 microtome, and mounted on glass slides. The slides were stained with Sudan IV[69] and then observed with an Olympus CLSM500 microscope.

5.4.4 Chemical Analysis of Cutin and Suberin Polymers from Fruit Surface and Seed Coat

Fruit skin discs of apple and tomato were prepared for cutin analysis from five fruit per biological sample as previously described[70]. Isolated cuticles were then washed twice in chloroform for 60 seconds so as to remove all non-polymerised extra and intracuticular waxes, before cutin extraction and gas chromatographic (GC) analysis was performed as described previously[9]. Extraction and subsequent chemical analysis of the seed coat polyester was performed as described previously[9,11,13,14].

5.4.5 Gene Expression Analysis

Nucleic acids were extracted using the 'CTAB method' as described previously[71]. qRT-PCR analysis was performed for RNA extracted from the mature green stage skin of tomatoes, and the mature green stage of seeds from *Arabidopsis*. The SuperScript VILO cDNA synthesis kit (Invitrogen, MA, USA) was used to synthesise cDNA from DNase treated total RNA extractions. Analysis was performed using gene-specific oligonucleotides on an ABI 7300 instrument (Applied Biosystems, Norwalk, CT, USA) with the Fast SYBR Green Master Mix (Applied Biosystems, CT, USA) under default parameters. The StepOne software (Applied Biosystems, CT, USA) was used to generate

expression data. Sequences of gene specific oligonucleotides are provided in Supplementary Table 3. High-throughput Illumina strand-specific RNASeq was performed from RNA extracted from the skin and flesh tissue of five developmental stages of apple for both the 'Reinders' and 'Rugiada' clones (20 samples in total), and from mature green stage tomato skin from wild type and *SlDCR*-RNAi lines in duplicate (4 samples in total). Library preparation was performed according to previously described methods[72], and samples run on the Illumina HiSeq 2000 under default parameters generating 50bp single end reads. Reads were mapped to either the apple[63] or tomato[58] predicted transcriptome according to methods described previously[73] generating normalised RPKM values for each gene.

5.4.6 Multi-species and Multi-gene Co-expression Analysis

Genes that are co-expressed with the orthologs to ASFT, GPAT5 and/or CYP86B1 in tomato, apple, grape, potato and *Arabidopsis* were determined making use of methodologies previously described[73]. First large scale expression datasets for these species was obtained from literature, with the proviso that at least one of the samples analysed in the dataset was a suberin accumulating tissue. To this end datasets were acquired covering multiple organs and developmental stages for tomato[33], potato[34], and grape[32], while a dataset analysing tissue types of developing seeds was acquired for *Arabidopsis*[31]. The apple dataset utilised was generated as part of this work, and included skin and flesh tissue of developing apple fruit. Then orthologs of ASFT, GPAT5 and/or CYP86B1 were identified in each species and used as 'baits' in the co-expression analysis, which made use of a previously described R script[73]. A list of genes was created for each 'bait' with each gene assigned an *r*-value as an indicator of the level of similarity of expression pattern between the gene and respective bait. Next, a list of co-expressed genes for each species was determined by selecting genes that were co-expressed with multiple 'baits' (ie, possessing an *r*-value above a cut-off dependant on the complexity of the specific dataset). A summary of baits used and *r*-value cut-offs employed can be seen in Supplementary Table 5. Before comparison of these lists two further gene lists were retrieved, one from rice genes identified in a large scale expression analysis to be co-expressed with suberin formation[35], and the second from the genes identified in this study to be up regulated in the fruit skins of *SlDCR*-RNAi tomato lines. Finally these seven gene lists were compared through the orthology of the respective members of the lists and a co-expression network between the various experiments was visualized using the Cytoscape software[74].

5.4.7 Insulation of Fruit with Petroleum Jelly

In an effort to show the secondary nature of suberin formation on the fruit of *SlDCR*-RNAi lines fruit at the early green stage were half-covered with petroleum jelly. This acted as a water proof layer during development as was reapplied if necessary due to growth of the fruit. Fruit at mature green and red ripe stage were harvested, the jelly removed, and photographed to compare surface formation of suberin.

5.4.8 Seed Coat Permeability Assay

In order to test the permeability of *Arabidopsis* seed coats, tetrazolium salt penetration assays were performed[75]. Seed samples (50 mg each) were incubated in 700 µl 1% aqueous solution of 2,3,5-triphenyltetrazolium chloride (TTC) at 30°C for 48 hours. After incubation, the seed were washed twice with water and observed under a dissection microscope. Images were acquired and qualitatively observed by eye for the degree of 'redness', indicating movement of the tetrazolium salt into the seed, and staining of the embryonic tissue. Further, an in house MATLAB (The MathWorks, Massachusetts, United States) script was also used to quantitatively asses the redness of the individual seeds in each image by quantifying the RGB spectra.

5.5 Acknowledgements

This work was supported by the Israel Science Foundation (ISF) personal grant to A.A. (ISF Grant No. 646/11). We thank the Adelis Foundation, Leona M. and Harry B. Helmsley Charitable Trust, Jeanne and Joseph Nissim Foundation for Life Sciences, Tom and Sondra Rykoff Family Foundation Research and the Raymond Burton Plant Genome Research Fund for supporting the AA lab activity. AA is the incumbent of the Peter J. Cohn Professorial Chair. JL performed this research as part of a PhD funded by Fondazione Edmund Mach.

5.6 Author Contributions

J.L. designed and performed research, analyzed data, and was the primary writer of the manuscript. D.L-S., O.T., and V.Z. performed experiments. L.T. and L.S. analyzed data. F.C. analyzed data, and co-wrote the article. A.A. designed research, analyzed data and co-wrote the article. All authors read, made relevant suggestions and approved the final manuscript.

5.7 Supplementary Data

See ***Appendix C*** (page 204) for supplementary materials

Supplementary Table 1. Orthologous genes from tomato and apple enriched in both *SlDCR*-RNAi fruit skin and russeted apple skin

Supplementary Table 2. Multi-species gene expression signature for suberin biosynthesis

Supplementary Table 3. Oligonucleotides used in this study for cloning and qRT-PCR analysis.

Supplementary Table 4. Oligonucleotides used in this study for the screening of *Arabidopsis* T-DNA insertion lines.

Supplementary Table 5. Parameters used for co-expression analysis.

Supplementary Figure 1. Protein alignment of tomato and *Arabidopsis* DCR. ClustalW and the MEGA6 software were used to align the proteins in all cases. The HXXXDG domain is indicated.

Supplementary Figure 2. Organ fusion phenotypes resulting from silencing of *SlDCR* in tomato. (**a**) Leaves of *SlDCR*-RNAi lines were crinkled. (**b**) Fusion of anthers of *SlDCR*-RNAi lines. (**c**) Fusion of sepals of *SlDCR*-RNAi lines.

Supplementary Figure 3. Light microscopy of fruit cuticle of *SlDCR*-RNAi lines. (**a**) Wild type and (**b**) *SlDCR*-RNAi cuticles are stained red with Sudan IV. A dramatic reduction in cuticle is observed in *SlDCR*-RNAi lines.

Supplementary Figure 4. Protein alignment of tomato and *Arabidopsis* ASFT. ClustalW and the MEGA6 software were used to align the proteins. The HXXXDG domain is indicated.

Supplementary Figure 5. Expression analysis of the *GPAT* gene family in tomato silenced for *SlDCR*. (**a**) Molecular phylogenetic analysis of the *Arabidopsis* GPAT protein clade is shown together with GPAT members from tomato analysed in this work. ClustalW and the MEGA6 software were used to align the proteins and compute the neighbour-joining tree. The scale bar represents the relative amino acid difference. Relevant information regarding functional annotation of some characterized proteins is also displayed. (**b**) qRT expression data for the *GPATs* in mature green stage tomato peel.

Supplementary Figure 6. Application of petroleum jelly to developing tomato fruit silenced for *SlDCR* expression. (**a**) Jelly was applied at the immature green stage of tomato development to half the tomato. (**b**) Tomatoes on the plant, still with jelly covering and (**c**) removed from the plant and jelly removed, showing absence of suberin formation in areas previously covered with jelly.

Supplementary Figure 7. SEM analysis of Apple surface. The normal skinned 'Reinders' clone shows a thick cuticle layer, and a relatively smooth surface, while the cuticle layer of the russeted 'Rugiada' clone is not observable and the fruit surface is extremely rough. s, fruit surface; c, cuticle layer; ec, epidermal cell.

Supplementary Figure 8. GO enrichment analysis of orthologous genes found up regulated in suberized tomato and apple fruit surfaces.

Supplementary Figure 9. Expression patterns of the co-expression 'baits' and the described MYB factors. Data was extracted from the relevant large scale expression

experiments used in this work to perform the multi gene co-expression analysis. Data is shown for (**a**) tomato[33], (**b**) apple (See Supplementary Dataset 2), (**c**) *Arabidopsis*[31], (**d**) potato[34], (**e**) grape[32], (**f**) rice[35] and (**g**) *SlDCR*-RNAi tomato (See Supplementary Dataset 1). For full descriptions of samples see the referenced works.

Supplementary Figure 10. Tetrazolium chloride staining assay. Tetrazolium chloride staining of *Arabidopsis* seeds from T-DNA insertion lines. Increase in red staining results from seed permeability. See Supplementary Table 4 for accessions.

Supplementary Figure 11. Quantification of stain intensity in tetrazolium chloride staining assay. Data from images collected in Supplementary Figure 10 was quantified as a measure of red spectrum intensity. Significant increase in staining intensity is marked with ** (p-value < 0.005).

Supplementary Figure 12. Molecular phylogenetic analysis of cutin synthase (CUS) and suberin synthase (SUS) proteins. GDSL-motif esterases from *Arabidopsis* with the CUS clade highlighted. The proposed SUS clade is also shown. ClustalW and the MEGA6 software were used to align the proteins and compute the neighbour-joining tree with significance percentages (bootstrap values out of 1000). The scale bar represents the relative amino acid difference.

Supplementary Dataset 1. RNAseq analysis of mature green stage skin tissues of SlDCR-RNAi and Wild type tomato fruit.

Supplementary Dataset 2. Large scale RNAseq expression analysis of skin and flesh tissue of developing apple.

Supplementary Dataset 3. Genes identified in the multi-gene co-expression analysis from tomato, apple, *Arabidopsis*, potato and grape.

5.8 References

1 Heredia, A. Biophysical and biochemical characteristics of cutin, a plant barrier biopolymer. *Biochim Biophys Acta* **1620**, 1-7 (2003).

2 Bargel, H., Koch, K., Cerman, Z. & Neinhuis, C. Structure–function relationships of the plant cuticle and cuticular waxes – a smart material? . *Functional Plant Biology* **33**, 893-910 (2006).

3 Chen, G. *et al.* A functional cutin matrix is required for plant protection against water loss. *Plant Signal Behav* **6**, 1297-1299, doi:10.4161/psb.6.9.17507 (2011).

4 Isaacson, T. *et al.* Cutin deficiency in the tomato fruit cuticle consistently affects resistance to microbial infection and biomechanical properties, but not transpirational water loss. *Plant J* **60**, 363-377, doi:10.1111/j.1365-313X.2009.03969.x (2009).

5 Dean, B. B. & Kolattukudy, P. E. Synthesis of Suberin during Wound-healing in Jade Leaves, Tomato Fruit, and Bean Pods. *Plant Physiol* **58**, 411-416 (1976).

6 Beisson, F., Li-Beisson, Y. & Pollard, M. Solving the puzzles of cutin and suberin polymer biosynthesis. *Curr Opin Plant Biol* **15**, 329-337, doi:10.1016/j.pbi.2012.03.003 (2012).

7 Pollard, M., Beisson, F., Li, Y. & Ohlrogge, J. B. Building lipid barriers: biosynthesis of cutin and suberin. *Trends Plant Sci* **13**, 236-246, doi:10.1016/j.tplants.2008.03.003 (2008).

8 Schreiber, L. Transport barriers made of cutin, suberin and associated waxes. *Trends Plant Sci* **15**, 546-553, doi:10.1016/j.tplants.2010.06.004 (2010).

9 Franke, R. *et al.* Apoplastic polyesters in Arabidopsis surface tissues--a typical suberin and a particular cutin. *Phytochemistry* **66**, 2643-2658, doi:10.1016/j.phytochem.2005.09.027 (2005).

10 Lashbrooke, J., Aharoni, A. & Costa, F. Genome investigation suggests MdSHN3, an APETALA2-domain transcription factor gene, to be a positive regulator of apple fruit cuticle formation and an inhibitor of russet development. *J Exp Bot*, doi:10.1093/jxb/erv366 (2015).

11 Franke, R. *et al.* The DAISY gene from Arabidopsis encodes a fatty acid elongase condensing enzyme involved in the biosynthesis of aliphatic suberin in roots and the chalaza-micropyle region of seeds. *Plant J* **57**, 80-95, doi:10.1111/j.1365-313X.2008.03674.x (2009).

12 Lee, S. B. *et al.* Two Arabidopsis 3-ketoacyl CoA synthase genes, KCS20 and KCS2/DAISY, are functionally redundant in cuticular wax and root suberin biosynthesis, but differentially controlled by osmotic stress. *Plant J* **60**, 462-475, doi:10.1111/j.1365-313X.2009.03973.x (2009).

13 Höfer, R. *et al.* The Arabidopsis cytochrome P450 CYP86A1 encodes a fatty acid omega-hydroxylase involved in suberin monomer biosynthesis. *J Exp Bot* **59**, 2347-2360, doi:10.1093/jxb/ern101 (2008).

14 Compagnon, V. *et al.* CYP86B1 is required for very long chain omega-hydroxyacid and alpha, omega -dicarboxylic acid synthesis in root and seed suberin polyester. *Plant Physiol* **150**, 1831-1843, doi:10.1104/pp.109.141408 (2009).

15 Molina, I., Li-Beisson, Y., Beisson, F., Ohlrogge, J. B. & Pollard, M. Identification of an Arabidopsis feruloyl-coenzyme A transferase required for suberin synthesis. *Plant Physiol* **151**, 1317-1328, doi:10.1104/pp.109.144907 (2009).

16 Vishwanath, S. J. *et al.* Suberin-associated fatty alcohols in Arabidopsis: distributions in roots and contributions to seed coat barrier properties. *Plant Physiol* **163**, 1118-1132, doi:10.1104/pp.113.224410 (2013).

17 Domergue, F. *et al.* Three Arabidopsis fatty acyl-coenzyme A reductases, FAR1, FAR4, and FAR5, generate primary fatty alcohols associated with suberin deposition. *Plant Physiol* **153**, 1539-1554, doi:10.1104/pp.110.158238 (2010).

18 Beisson, F., Li, Y., Bonaventure, G., Pollard, M. & Ohlrogge, J. B. The acyltransferase GPAT5 is required for the synthesis of suberin in seed coat and root of Arabidopsis. *Plant Cell* **19**, 351-368, doi:10.1105/tpc.106.048033 (2007).

19 Li, Y. *et al.* Identification of acyltransferases required for cutin biosynthesis and production of cutin with suberin-like monomers. *Proc Natl Acad Sci U S A* **104**, 18339-18344, doi:10.1073/pnas.0706984104 (2007).

20 Gou, J. Y., Yu, X. H. & Liu, C. J. A hydroxycinnamoyltransferase responsible for synthesizing suberin aromatics in Arabidopsis. *Proc Natl Acad Sci U S A* **106**, 18855-18860, doi:10.1073/pnas.0905555106 (2009).

21 Yadav, V. *et al.* ABCG transporters are required for suberin and pollen wall extracellular barriers in Arabidopsis. *Plant Cell* **26**, 3569-3588, doi:10.1105/tpc.114.129049 (2014).

22 Kosma, D. K. *et al.* AtMYB41 activates ectopic suberin synthesis and assembly in multiple plant species and cell types. *Plant J* **80**, 216-229, doi:10.1111/tpj.12624 (2014).

23 Cominelli, E., Sala, T., Calvi, D., Gusmaroli, G. & Tonelli, C. Over-expression of the Arabidopsis AtMYB41 gene alters cell expansion and leaf surface permeability. *Plant J* **53**, 53-64, doi:10.1111/j.1365-313X.2007.03310.x (2008).

24 Khanal, B. P., Grimm, E. & Knoche, M. Russeting in apple and pear: a plastic periderm replaces a stiff cuticle. *AoB Plants* **5**, pls048, doi:10.1093/aobpla/pls048 (2013).

25 Panikashvili, D., Shi, J. X., Schreiber, L. & Aharoni, A. The Arabidopsis DCR encoding a soluble BAHD acyltransferase is required for cutin polyester formation and seed hydration properties. *Plant Physiol* **151**, 1773-1789, doi:10.1104/pp.109.143388 (2009).

26 Kolattukudy, P. E. Polyesters in higher plants. *Adv Biochem Eng Biotechnol* **71**, 1-49 (2001).

27 Peschel, S., Franke, R., Schreiber, L. & Knoche, M. Composition of the cuticle of developing sweet cherry fruit. *Phytochemistry* **68**, 1017-1025, doi:10.1016/j.phytochem.2007.01.008 (2007).

28 Mintz-Oron, S. *et al.* Gene expression and metabolism in tomato fruit surface tissues. *Plant Physiol* **147**, 823-851, doi:10.1104/pp.108.116004 (2008).

29 Yang, W. *et al.* A distinct type of glycerol-3-phosphate acyltransferase with sn-2 preference and phosphatase activity producing 2-monoacylglycerol. *Proc Natl Acad Sci U S A* **107**, 12040-12045, doi:10.1073/pnas.0914149107 (2010).

30 Chen, X. *et al.* Three homologous genes encoding sn-glycerol-3-phosphate acyltransferase 4 exhibit different expression patterns and functional divergence in Brassica napus. *Plant Physiol* **155**, 851-865, doi:10.1104/pp.110.169482 (2011).

31 Le, B. H. *et al.* Global analysis of gene activity during Arabidopsis seed development and identification of seed-specific transcription factors. *Proc Natl Acad Sci U S A* **107**, 8063-8070, doi:10.1073/pnas.1003530107 (2010).

32 Fasoli, M. *et al.* The grapevine expression atlas reveals a deep transcriptome shift driving the entire plant into a maturation program. *Plant Cell* **24**, 3489-3505, doi:10.1105/tpc.112.100230 (2012).

33 Consortium, T. G. The tomato genome sequence provides insights into fleshy fruit evolution. *Nature* **485**, 635-641, doi:10.1038/nature11119 (2012).

34 Xu, X. *et al.* Genome sequence and analysis of the tuber crop potato. *Nature* **475**, 189-195, doi:10.1038/nature10158 (2011).

35 Shiono, K. *et al.* Microarray analysis of laser-microdissected tissues indicates the biosynthesis of suberin in the outer part of roots during formation of a barrier to radial oxygen loss in rice (Oryza sativa). *J Exp Bot* **65**, 4795-4806, doi:10.1093/jxb/eru235 (2014).

36 Dubos, C. *et al.* MYB transcription factors in Arabidopsis. *Trends Plant Sci* **15**, 573-581, doi:10.1016/j.tplants.2010.06.005 (2010).

37 Kosma, D. K., Molina, I., Ohlrogge, J. B. & Pollard, M. Identification of an Arabidopsis fatty alcohol:caffeoyl-Coenzyme A acyltransferase required for the synthesis of alkyl hydroxycinnamates in root waxes. *Plant Physiol* **160**, 237-248, doi:10.1104/pp.112.201822 (2012).

38 Winter, D. *et al.* An "Electronic Fluorescent Pictograph" browser for exploring and analyzing large-scale biological data sets. *PLoS One* **2**, e718, doi:10.1371/journal.pone.0000718 (2007).

39 Yeats, T. *et al.* The identification of cutin synthase: formation of the plant polyester cutin. *Nature Chemical Biology* **8**, 609-611, doi:10.1038/NCHEMBIO.960 (2012).

40 Bonaventure, G., Beisson, F., Ohlrogge, J. & Pollard, M. Analysis of the aliphatic monomer composition of polyesters associated with Arabidopsis epidermis: occurrence of octadeca-cis-6, cis-9-diene-1,18-dioate as the major component. *Plant J* **40**, 920-930, doi:10.1111/j.1365-313X.2004.02258.x (2004).

41 Domínguez, E., Heredia-Guerrero, J. A. & Heredia, A. Plant cutin genesis: unanswered questions. *Trends Plant Sci*, doi:10.1016/j.tplants.2015.05.009 (2015).

42 Rani, S. H., Krishna, T. H., Saha, S., Negi, A. S. & Rajasekharan, R. Defective in cuticular ridges (DCR) of Arabidopsis thaliana, a gene associated with surface cutin formation, encodes a soluble diacylglycerol acyltransferase. *J Biol Chem* **285**, 38337-38347, doi:10.1074/jbc.M110.133116 (2010).

43 Domínguez, E., Cuartero, J. & Heredia, A. An overview on plant cuticle biomechanics. *Plant Sci* **181**, 77-84, doi:10.1016/j.plantsci.2011.04.016 (2011).

44 Kolattukudy, P. E. Biopolyester membranes of plants: cutin and suberin. *Science* **208**, 990-1000, doi:10.1126/science.208.4447.990 (1980).

45 Serra, O., Figueras, M., Franke, R., Prat, S. & Molinas, M. Unraveling ferulate role in suberin and periderm biology by reverse genetics. *Plant Signal Behav* **5**, 953-958 (2010).

46 Yang, W. *et al.* A land-plant-specific glycerol-3-phosphate acyltransferase family in Arabidopsis: substrate specificity, sn-2 preference, and evolution. *Plant Physiol* **160**, 638-652, doi:10.1104/pp.112.201996 (2012).

47 Costa, M. A. *et al.* Characterization in vitro and in vivo of the putative multigene 4-coumarate:CoA ligase network in Arabidopsis: syringyl lignin and sinapate/sinapyl alcohol derivative formation. *Phytochemistry* **66**, 2072-2091, doi:10.1016/j.phytochem.2005.06.022 (2005).

48 Hamberger, B. & Hahlbrock, K. The 4-coumarate:CoA ligase gene family in Arabidopsis thaliana comprises one rare, sinapate-activating and three commonly occurring isoenzymes. *Proc Natl Acad Sci U S A* **101**, 2209-2214, doi:10.1073/pnas.0307307101 (2004).

49 DeBono, A. *et al.* Arabidopsis LTPG is a glycosylphosphatidylinositol-anchored lipid transfer protein required for export of lipids to the plant surface. *Plant Cell* **21**, 1230-1238, doi:10.1105/tpc.108.064451 (2009).

50 Edstam, M. M. & Edqvist, J. Involvement of GPI-anchored lipid transfer proteins in the development of seed coats and pollen in Arabidopsis thaliana. *Physiol Plant* **152**, 32-42, doi:10.1111/ppl.12156 (2014).

51 Yeats, T. H. *et al.* Tomato Cutin Deficient 1 (CD1) and putative orthologs comprise an ancient family of cutin synthase-like (CUS) proteins that are conserved among land plants. *Plant J* **77**, 667-675, doi:10.1111/tpj.12422 (2014).

52 Oshima, Y. *et al.* MIXTA-like transcription factors and WAX INDUCER1/SHINE1 coordinately regulate cuticle development in Arabidopsis and Torenia fournieri. *Plant Cell* **25**, 1609-1624, doi:10.1105/tpc.113.110783 (2013).

53 Xu, R. *et al.* Salt-induced transcription factor MYB74 is regulated by the RNA-directed DNA methylation pathway in Arabidopsis. *J Exp Bot*, doi:10.1093/jxb/erv312 (2015).

54 Denekamp, M. & Smeekens, S. C. Integration of wounding and osmotic stress signals determines the expression of the AtMYB102 transcription factor gene. *Plant Physiol* **132**, 1415-1423 (2003).

55 Karimi, M., Inzé, D. & Depicker, A. GATEWAY vectors for Agrobacterium-mediated plant transformation. *Trends Plant Sci* **7**, 193-195 (2002).

56 Dan, Y. *et al.* MicroTom--a high-throughput model transformation system for functional genomics. *Plant Cell Rep* **25**, 432-441, doi:10.1007/s00299-005-0084-3 (2006).

57 Alonso, J. M. *et al.* Genome-wide Insertional mutagenesis of Arabidopsis thaliana. *Science* **301**, 653-657, doi:10.1126/science.1086391 (2003).

58 Fernandez-Pozo, N. *et al.* The Sol Genomics Network (SGN)-from genotype to phenotype to breeding. *Nucleic Acids Res* **43**, D1036-1041, doi:10.1093/nar/gku1195 (2015).

59 Vitulo, N. *et al.* A deep survey of alternative splicing in grape reveals changes in the splicing machinery related to tissue, stress condition and genotype. *BMC Plant Biol* **14**, 99, doi:10.1186/1471-2229-14-99 (2014).

60 Hirsch, C. D. *et al.* Spud DB: A Resource for Mining Sequences, Genotypes, and Phenotypes to Accelerate Potato Breeding. *Plant Genome* **7**, doi:10.3835/plantgenome2013.12.0042 (2014).

61 Lamesch, P. *et al.* The Arabidopsis Information Resource (TAIR): improved gene annotation and new tools. *Nucleic Acids Res* **40**, D1202-1210, doi:10.1093/nar/gkr1090 (2012).

62 Kawahara, Y. *et al.* Improvement of the Oryza sativa Nipponbare reference genome using next generation sequence and optical map data. *Rice* **6**, doi:10.1186/1939-8433-6-4 (2013).

63 Jung, S. *et al.* The Genome Database for Rosaceae (GDR): year 10 update. *Nucleic Acids Res* **42**, D1237-1244, doi:10.1093/nar/gkt1012 (2014).

64 Proost, S. *et al.* PLAZA 3.0: an access point for plant comparative genomics. *Nucleic Acids Research* **43**, D974-D981, doi:10.1093/nar/gku986 (2015).

65 Larkin, M. A. *et al.* Clustal W and Clustal X version 2.0. *Bioinformatics* **23**, 2947-2948, doi:10.1093/bioinformatics/btm404 (2007).

66 Tamura, K., Stecher, G., Peterson, D., Filipski, A. & Kumar, S. MEGA6: Molecular Evolutionary Genetics Analysis version 6.0. *Mol Biol Evol* **30**, 2725-2729, doi:10.1093/molbev/mst197 (2013).

67 Bailey, T. L. *et al.* MEME SUITE: tools for motif discovery and searching. *Nucleic Acids Research* **37**, W202-W208, doi:10.1093/nar/gkp335 (2009).

68 Crooks, G. E., Hon, G., Chandonia, J. M. & Brenner, S. E. WebLogo: A sequence logo generator. *Genome Research* **14**, 1188-1190, doi:10.1101/gr.849004 (2004).

69 Buda, G. J., Isaacson, T., Matas, A. J., Paolillo, D. J. & Rose, J. K. Three-dimensional imaging of plant cuticle architecture using confocal scanning laser microscopy. *Plant J* **60**, 378-385, doi:10.1111/j.1365-313X.2009.03960.x (2009).

70 Shi, J. X. *et al.* The tomato SlSHINE3 transcription factor regulates fruit cuticle formation and epidermal patterning. *New Phytol* **197**, 468-480, doi:10.1111/nph.12032 (2013).

71 Reid, K. E., Olsson, N., Schlosser, J., Peng, F. & Lund, S. T. An optimized grapevine RNA isolation procedure and statistical determination of reference genes for real-time RT-PCR during berry development. *Bmc Plant Biology* **6**, doi:10.1186/1471-2229-6-27 (2006).

72 Zhong, S. *et al.* High-throughput illumina strand-specific RNA sequencing library preparation. *Cold Spring Harb Protoc* **2011**, 940-949, doi:10.1101/pdb.prot5652 (2011).

73 Itkin, M. *et al.* Biosynthesis of antinutritional alkaloids in solanaceous crops is mediated by clustered genes. *Science* **341**, 175-179, doi:10.1126/science.1240230 (2013).

74 Shannon, P. *et al.* Cytoscape: A software environment for integrated models of biomolecular interaction networks. *Genome Research* **13**, 2498-2504, doi:10.1101/gr.1239303 (2003).

75 Molina, I., Ohlrogge, J. B. & Pollard, M. Deposition and localization of lipid polyester in developing seeds of Brassica napus and Arabidopsis thaliana. *Plant Journal* **53**, 437-449, doi:10.1111/j.1365-313X.2007.03348.x (2008).

Chapter 6

General Discussion and Concluding Remarks

This chapter serves to conclude the ideas and results presented in this thesis. In an effort to maintain consistency, the chapter is written in the style of *Journal of Experimental Botany*.

6.1 General Discussion

6.1.1 Research Approach and Overview

In order to fulfil the general aim of this work, to identify and/or characterise genetic factors that contribute to the formation of the fleshy fruit surface, a variety of techniques were employed. These included: (i) detailed functional characterisation of genes selected due to their homology with genes known to contribute to surface aspects of non-fruit species; (ii) QTL mapping of an apple population segregating for cuticle performance; (iii) large-scale transcriptomic analysis of fruit with altered surface properties and cuticle formation; and (iv) comparative genomic analysis of plants producing the apolastic polymer, suberin. The range of methods applied throughout this work has allowed for a detailed understanding of the mode of action of a number of specific genes, while also revealing general global patterns of gene action with regard to fruit surface formation. Due to the relative ease of research when using tomato as a model, and the economic importance of apple, these species were selected as primary focus points. Interestingly, a number of significant parallels between the mechanisms underlying surface formation in the two species were identified. This is specifically evidenced in Chapter 4 by the identification of a SHN1/WIN1 transcription factor with a potential role in cuticle formation in apple. Members of this gene family have been characterised as regulators of cuticle biosynthesis in both *Arabidopsis* (Aharoni *et al.*, 2004) and significantly also in tomato (Shi *et al.*, 2013). This recent work by Shi *et al.* (2013) formed the basis of the investigation into the tomato *MIXTA-like* gene characterised in Chapter 3. Further, the work of Chapter 4 highlighted the potential for wounding induced suberisation of fruit surface, which prompted the extensive investigation in Chapter 5 of the genes involved in this process in both tomato and apple, again confirming the parallel mechanisms between these two species.

6.1.2 A Network of Surface Regulators

One of the significant themes to emerge from this work is the concept of a network of transcriptional regulators controlling epidermal cell identity together with cuticle biosynthesis. This is specifically investigated and discussed with relation to tomato fruit surface in Chapter 3. A MYB transcription factor, SlMIXTA-like, which was earlier identified as a downstream target of the tomato SHN3 transcription factor (Shi *et al.*, 2013), was extensively characterised. Orthologs to SHN3 in *Arabidopsis* have been previously found to be regulators of both cuticle deposition and surface patterns

(Aharoni *et al.*, 2004; Shi *et al.*, 2011), while recently the regulation of cuticle deposition in *Arabidopsis* was shown to be mediated by MIXTA-like transcription factors (Oshima *et al.*, 2013). In the case of tomato fruit surface as evidenced in Chapter 3, it appears that SlSHN3 acts upstream of SlMIXTA-like, which in turn regulates cuticle deposition together with the formation of conical epidermal cells. The regulation of cuticle deposition was primarily due to modification of cutin biosynthesis, while it seems likely that the regulation of conical epidermal cell formation may be mediated though the interaction with HD-ZIP IV transcription factors. The recent work by Oshima *et al.* (2013) found that in *Arabidopsis* the MIXTA-like protein (AtMYB106) acted upstream of AtSHN3, while in this work the inverse relationship is observed in tomato. This hints at a complicated evolutionary relationship between these regulatory elements. Significantly, in the genomic investigation of apple presented in Chapter 4, a member of the SHN1/WIN1 transcription factor family was identified as a potential primary regulator of cuticle biosynthesis in apple fruit. Expression of this gene, *MdSHN3*, was strongly linked with proper cuticle formation in the apple population analysed, while the absence of expression resulted in thin cuticles prone to suberisation. Additionally, a SHN1/WIN1 transcription factor, HvNud, has previously been found to regulate the biosynthesis of the lipids coating barley grains (Taketa et al., 2008). SHN1/WIN1 transcription factors therefore appear to regulate lipid barriers across diverse species. Further work to investigate the role played by MIXTA-like proteins in the MdSHN3 and HvNud mediated regulation of lipid barriers may prove interesting.

Another sub-group of MYB factors identified in this research to be regulators of surface properties was a clade containing MYB107 and MYB9. The comparative genomics approach employed in Chapter 5 identified orthologs of these factors to be positive regulators of suberin formation in a number of species and tissues. This role was subsequently confirmed via transcriptomic and chemical analysis of *myb107* and *myb9 Arabidopsis* mutants. Phylogenetic analysis of *Arabidopsis* MYB factors shows that AtMYB107 and AtMYB9 are part of a group of 6 MYB factors phylogenetically distinct from the rest of MYB family. Additionally, the group of MYB factors most closely related to the AtMYB107 clade (based on sequence similarity) contains the MIXTA-like factors, AtMYB16 and AtMYB106; a known suberin regulator, AtMYB41 (Kosma *et al.*, 2014); and factors that respond to wounding, salt and osmotic stresses and are expressed in stomatal guard cells, AtMYB102 and AtMYB74 (Denekamp and Smeekens, 2003; Xu *et al.*, 2015). This interesting observation hints at an evolutionary relationship between

these MYB factors involved in surface functions, particularly in regard to water stress responses and the formation of apoplastic diffusion barriers. Due to the impact these aspects have on the agricultural industry further research into this interesting clade may prove worthwhile.

6.1.3 Important Steps Identified for Surface Polymer Biosynthesis

A number of genes coding for key biosynthetic steps in the formation of cutin and suberin were identified and/or characterised in this work. The most extensively characterised gene in this regard is the tomato *DCR* gene, discussed in Chapter 5. Previously the *Arabidopsis* ortholog, *AtDCR*, was found to be required for the incorporation of mid-chain dihydroxy fatty acids into the cutin matrix. As *Arabidopsis* cutin (with the exception of that found on the flower surface) contains low levels of these particular fatty acids, the effect of *dcr* mutants was mostly limited to flower surface features. However, in many fruit species, including tomato and apple, the major monomer found in fruit cutin (levels above 90%) is the C16 mid-chain dihydroxy fatty acid. Silencing of *SlDCR* expression in tomato resulted in dramatic fruit phenotypes, including the production of a suberized layer replacing the damaged cutin. Further analysis suggested that an accumulation of lipids was occuring in the epidermal cells of the silenced DCR lines, possibly representing a blockage in the cutin pathway prior to extracellular transport. The precise mechanism of DCR action is still unclear, but it appears to be somehow involved in the acyl transfer of these mid chain dihydroxy fatty acids. It is possible that a cutin oligomer is being formed that incorporates the mid chain dihydroxy fatty acid before extracellular transport occurs.

The tomato lines generated were subsequently analysed, in conjunction with russeted apples, to characterise the mechanisms underlying suberin formation in fruit surface. In the case of apple russet formation, the previously discussed MdSHN3 is proposed as an important factor in the prevention of this phenotype (Chapter 4). However it should be noted that, as in the case of the suberisation of *SlDCR* silenced tomato fruit, russet is a secondary phenotype associated with cuticle failure. As such, the failure in any number of steps in cuticle biosynthesis may lead to russet formation. This fact is highlighted by recent work similar to that presented in Chapter 4 involving the QTL mapping for an apple population segregating for russet formation (Falginella *et al.*, 2015). In that work the authors identified a different linkage group, housing a different gene from the one presented in Chapter 4. Specifically, an ATP-BINDING

CASSETTE G transporter potentially involved in the extracellular transport of cutin monomers was identified. Again, it is important to realise that this gene is involved in proper cuticle formation, and as in the case of *MdSHN3*, a mutation in this gene leads indirectly to russet formation. In order to identify genes involved directly in suberin biosynthesis (russet formation in apple) large scale transcriptomic analysis of tomato silenced for *SlDCR* and a russeted apple mutant was performed (Chapter 5). This work resulted in the generation of an interesting list of potential genes involved in the biosynthesis of fruit suberin. Important mentions include: *FERULIC ACID 5-HYDROXYLASE 1*, *4-COUMARATE:COA LIGASE 5*, *GLYCOSYLPHOSPHATIDYLINOSITOL-ANCHORED LIPID PROTEIN TRANSFER 5* (*LTPG5*) and a number of GDSL-motif esterase/acyltransferase/lipase genes. Enriching this candidate list through comparison with published data from a number of other species (rice, potato, grape and *Arabidopsis*) resulted in the generation of a multi-species gene signature for suberin biosynthesis and highlighted the importance of two genes potentially involved in the extracellular transport and polymerisation of suberin monomers. The first, *LTPG5*, is part of a family of genes shown to be responsible for the active transport of monomers of apoplastic barriers in seeds, pollen and stems (DeBono *et al.*, 2009; Edstam and Edqvist, 2014). The second is a GDSL-motif esterase, named in Chapter 5 as a suberin synthase (SUS), and is likely analogous in function to the recently described extracellular cutin synthases (Yeats *et al.*, 2012; Yeats *et al.*, 2014).

6.2 Conclusions and Future Prospects

In its entirety, this work highlights the complexity of cuticle formation in general and specifically in fleshy fruit. While most steps of the core metabolic pathways for cutin and wax monomer biosynthesis have been elucidated there still remains much to discover regarding suberin monomer biosynthesis, and the regulation of these pathways as well as the precise mechanisms of the extracellular transport and polymerisation.

While recent work has highlighted the importance of the extracellular cutin synthase enzymes (Yeats *et al.*, 2012; Yeats *et al.*, 2014), the work performed to characterise the role of *SlDCR* in tomato fruit cuticle formation (Chapter 5), adds further evidence to the idea that multiple modes of polymerisation occur (Domínguez *et al.*, 2015). DCR type enzymes may in fact be a crucial step in an alternate form of cutin polymerisation. Further, as highlighted above, a number of novel steps were also

suggested for suberin biosynthesis in Chapter 5. These results, taken together with the current knowledge of apoplastic polymer biosynthesis (Domínguez *et al.*, 2015; Martin and Rose, 2014), begin to portray a detailed understanding of the metabolic processes involved. Future work will likely address the complexities of monomer transport from the endoplasmic reticulum to the cell membrane, as this still remains a poorly understood aspect.

Finally, work throughout all three research chapters highlighted, identified, and characterised aspects of transcriptional regulation during cuticle formation. The interaction between these various factors, as well as the global link to epidermal cell development, is a fascinating avenue of research, and one that is receiving increasing attention. What is clear from the results presented here is that the proteins involved in surface regulation across both organs and species are highly conserved. Many of these mechanisms likely arose during colonisation of terrestrial environments by early land plants, and while over evolutionary time, surfaces have become increasingly diverse and specialized, the underlying regulators have remained closely related. These results will be built on in the future, allowing for an increasingly detailed understanding of the regulatory mechanisms at play, and importantly also providing potential targets for global manipulation of fruit cuticle formation.

Furthering these lines of research is both fundamentally interesting and also of particular applied interest with regards to the fleshy fruit due to the impact the cuticle has on quality traits. These traits include pathogen resistance, appearance, texture and shelf life. Improving fruit cuticle traits therefore has the potential to bolster fruit crop production, securing farmer welfare while providing higher quality products to the consumer. Increasing our understanding of the relationship between cuticle structure and fruit surface characteristics will allow us to control these important traits, finally leading to the improvements in fruit production and quality.

6.3 References

Aharoni A, Dixit S, Jetter R, Thoenes E, van Arkel G, Pereira A. 2004. The SHINE clade of AP2 domain transcription factors activates wax biosynthesis, alters cuticle properties, and confers drought tolerance when overexpressed in Arabidopsis. Plant Cell **16**, 2463-2480.

DeBono A, Yeats TH, Rose JK, Bird D, Jetter R, Kunst L, Samuels L. 2009. Arabidopsis LTPG is a glycosylphosphatidylinositol-anchored lipid transfer protein required for export of lipids to the plant surface. Plant Cell **21**, 1230-1238.

Denekamp M, Smeekens SC. 2003. Integration of wounding and osmotic stress signals determines the expression of the AtMYB102 transcription factor gene. Plant Physiol **132**, 1415-1423.

Domínguez E, Heredia-Guerrero JA, Heredia A. 2015. Plant cutin genesis: unanswered questions. Trends Plant Sci. 10.1016/j.tplants.2015.05.009.

Edstam MM, Edqvist J. 2014. Involvement of GPI-anchored lipid transfer proteins in the development of seed coats and pollen in Arabidopsis thaliana. Physiol Plant **152**, 32-42.

Falginella L, Cipriani G, Monte C, Gregori R, Testolin R, Velasco R, Troggio M, Tartarini S. 2015. A major QTL controlling apple skin russeting maps on the linkage group 12 of 'Renetta Grigia di Torriana'. BMC Plant Biol **15**, 150.

Kosma DK, Murmu J, Razeq FM, Santos P, Bourgault R, Molina I, Rowland O. 2014. AtMYB41 activates ectopic suberin synthesis and assembly in multiple plant species and cell types. Plant J **80**, 216-229.

Martin LB, Rose JK. 2014. There's more than one way to skin a fruit: formation and functions of fruit cuticles. J Exp Bot **65**, 4639-4651.

Oshima Y, Shikata M, Koyama T, Ohtsubo N, Mitsuda N, Ohme-Takagi M. 2013. MIXTA-like transcription factors and WAX INDUCER1/SHINE1 coordinately regulate cuticle development in Arabidopsis and Torenia fournieri. Plant Cell **25**, 1609-1624.

Shi JX, Adato A, Alkan N, He Y, Lashbrooke J, Matas AJ, Meir S, Malitsky S, Isaacson T, Prusky D, Leshkowitz D, Schreiber L, Granell AR, Widemann E, Grausem B, Pinot F, Rose JK, Rogachev I, Rothan C, Aharoni A. 2013. The tomato SlSHINE3 transcription factor regulates fruit cuticle formation and epidermal patterning. New Phytol **197**, 468-480.

Shi JX, Malitsky S, De Oliveira S, Branigan C, Franke RB, Schreiber L, Aharoni A. 2011. SHINE transcription factors act redundantly to pattern the archetypal surface of Arabidopsis flower organs. PLoS Genet **7**, e1001388.

Taketa S, Amano S, Tsujino Y, Sato T, Saisho D, Kakeda K, Nomura M, Suzuki T, Matsumoto T, Sato K, Kanamori H, Kawasaki S, Takeda K. 2008. Barley grain with adhering hulls is controlled by an ERF family transcription factor gene regulating a lipid biosynthesis pathway. *Proc Natl Acad Sci U S A* 105, 4062-4067.

Xu R, Wang Y, Zheng H, Lu W, Wu C, Huang J, Yan K, Yang G, Zheng C. 2015. Salt-induced transcription factor MYB74 is regulated by the RNA-directed DNA methylation pathway in Arabidopsis. J Exp Bot.

Yeats T, Martin L, Viart H, Isaacson T, He Y, Zhao L, Matas A, Buda G, Domozych D, Clausen M, Rose J. 2012. The identification of cutin synthase: formation of the plant polyester cutin. Nature Chemical Biology **8**, 609-611.

Yeats TH, Huang W, Chatterjee S, Viart HM, Clausen MH, Stark RE, Rose JK. 2014. Tomato Cutin Deficient 1 (CD1) and putative orthologs comprise an ancient family of cutin synthase-like (CUS) proteins that are conserved among land plants. Plant J **77**, 667-675.

Appendices

Supplemental Materials

These appendices contain supplemental data relating to Chapters 3, 4 and 5.

Appendix A

Supplemental data for Chapter 3.

Supplemental Table S1. Quantification of cuticular waxes in fruit of *SlMIXTA-like* silenced lines.

	Wild type		*SlMIXTA*-RNAi	
Waxes	**Average**	**SE**	**Average**	**SE**
Free fatty acids				
C12 FA (dodecanoic acid (12:0))	0.02	0	0.03	0
C14 FA (tetradecanoic acid (14:0))	0.09	0	0.08	0
C15 FA (pentadecanoic acid (15:0))	0.03	0	0.03	0
C16 FA (hexadecanoic acid (16:0))	8.32	0.35	7.54	0.42
C17 FA (heptadecanoic acid (17:0))	0.12	0	0.11	0.01
C18:1 FA (octadecenoate (18:1))	0.41	0.04	0.45	0.04
C18:2 FA (octadecadienoate (18:2))	0.43	0.02	0.44	0.03
C18 FA (octadecanoic acid (18:0))	6.2	0.13	8.14	0.92
C22 FA (docosanoic acid (22:0))	0.25	0.02	0.19	0.02
C23 FA (tricosanoic acid (23:0))	0.47	0.05	0.26	0.04
C24 FA (tetracosanoic acid (24:0))	1.89	0.3	1.8	0.19
C25 FA (pentacosanoic acid (25:0))	0.29	0.03	0.2	0.03
C26 FA (hexacosanoic acid (26:0))	0.52	0.09	0.45	0.04
C30 FA (triacontanoic acid (30:0))	0.33	0.16	0.11	0.01
C31 FA (hentriacontanoic acid (31:0))	0.52	0.09	0.44	0.06
Subtotal	19.9	0.65	20.27	1.1
Alcohols				
C23-1-ol (1-tricosanol (23:0))	0.13	0.02	0.14	0.02
C29-1-ol (1-nonacosanol (29:0))	0.14	0.01	0.16	0.01
C32-1-ol (1-dotriacontanol (32:0))	0.28	0.01	0.25	0.01
C34-1-ol (1-tetratricontanol (34:0))	0.13	0.01	0.09	0.01
Subtotal	0.68	0.05	0.63	0.03
Alkanes				
C23 Alk (n-tricosane (23:0))	0.3	0.04	0.28	0.07
C27 Alk (n-heptacosane (27:0))	0.29	0.01	0.46	0.15
C29 Alk (n-nonacosane (29:0))	8.96	0.5	7.9	0.45
C30 Alk (n-triacontane (30:0))	2.26	0.21	2.5	0.14
C31 Alk (n-hentriacontane (31:0))	38.53	6.1	52.27	3.57
C32 Alk (n-dotriacontane (32:0))	4.59	0.57	4.76	0.28
C33 Alk (n-tritriacontane (33:0))	12.98	2.7	12.25	0.62
Subtotal	67.91	10.03	80.41	4.87
Sterols				
Taraxerol	1.13	0.19	0.92	0.07
α-amyrin	1.74	0.29	1.46	0.11
β-amyrin	5.15	1.08	7.05	0.73
δ-amyrin	2.58	0.49	2.15	0.19
Subtotal	10.6	2.05	11.58	0.89
Other				
C33-1-al (1-tritriacontanal (33:0))	1.72	0.22	2.24	0.21
para-Hydroxy Benzoic Acid	0.22	0.03	0.11	0.01
Naringenin	5.23	1.67	5.22	0.72
Naringenin dimer	1.12	0.31	2.13	0.1
Subtotal	8.28	2.22	9.7	0.71
Unknowns	2.35	1.07	0.37	0.18
Total Wax	109.72	13.01	122.95	5.57

Cuticular waxes quantified from enzymatically isolated tomato fruit cuticles (red stage fruit). Concentrations (µg/cm-2) shown for lines lines silenced for *SlMIXTA-like* (SlMIXTA-RNAi) and the corresponding wild type (WT). Monomers that show significant changes (Student's t-test) from the wild type are indicated with an outline ($p<0.1$, n=3), or shaded ($p<0.05$, n=3); Red = increase, Green = decrease; FA, Fatty acid; Alk, Alkane.

Supplemental Table S2. Oligonucleotides used in this study.

Gene	SGN ID	Primers	Sequence
SlMIXTA-like	Solyc02g088190	ATG_F	TTCAGTCGACATGGGTCGATCTCCGTGT
		stop_R	TGGTCTAGAGGTCAGGCTTTCAGCACG
		RNAi-F	TTCAGTCGACATGGGTCGATCTCCGTGT
		RNAi-R	ATATCTCGAGGCCGACCACCTATTCCC
		RT_F	GCGAGCGCTAGTGCTGGTAT
		RT_R	TAATATGTTGCGCATTTTCGAAA
SlCYP77A1	Solyc11g007540	ATG_F	GGTACCAACAACAATGGAGCCTTTC
		stop_R	GAATTCCGACTTATAATCTTAATTATGAGCAT
		YeDP60-F	CGGGATCCTTAATAATGGAGCCTTTCATTTTCAC
		YeDP60-R	CGGAATTCTTTATGAGCATTACTTAATTATG
		RT_F	TTTCATTTTCACAATTTCCGCC
		RT_R	CTGGAGGTCCGGGAGGTAG
SlCYP77A2	Solyc05g055400	ATG_F	ATGGATTCTTTCTCTACTTCTTCACTTT
		stop_R	TTACATTCTTGGTTTAATTTTAGCTCTT
		YeDP60-F	CGGGATCCTTAATAATGGATTCTTTCTCTACTTC
		YeDP60-R	CCGGTACCTTTACATTCTTGGTTTAATTTTA
		RT_F	CATCCACCTACGTACATGTCATTGA
		RT_R	ATCCGAAATCCCGGGTAAGA
SlCYP86A68	Solyc01g094750	ATG_F	ATGGATATTGCTATAGCTTTGTTGCT
		stop_R	CTATATTTGGATTAATTGCACCTCTTT
		YeDP60-F	CGGGATCCTTAATAATGGATATTGCTATAGCTTTG
		YeDP60-R	CCGGTACCTTTATATTTGGATTAATTGCACC
		RT_F	TTAAAGGGTCCACGTGTTTGG
		RT_R	CACGCGCGGAGATTATCTACT
SlSHN3	Solyc06g065820	RT_F	ATGCAAAGCTGAGGAAATGTTG
		RT_R	GATGTTTTTTGCCACACTCCAA
SlLACS2	Solyc01g109180	RT_F	TTGACAAAAAGGCAGGTCCCT
		RT_R	CGGATTAACACCACGATTTCG
SlLACS4	Solyc01g095750	RT_F	GTGCACCTTGACCCTGTACCA
		RT_R	GGTAGTATTTGAGAAACTGGGCTCTCT
Slα-DOX2	Solyc03g119060	RT_F	GCAGGAATGAGAATCAACTGGTATG
		RT_R	CTAAGCCACTCAATACTGGTCCAAA
SlGPAT4	Solyc01g094700	RT_F	CGCGATTGCGTACGTATTTG
		RT_R	GCGAAGCCAGCTCAATGTC
SlSlGDSLb (CD1)	Solyc11g006250	RT_F	TGTTTACGCGTTTTGGGACC
		RT_R	TCATTGGATTCATAAGCTCCGTT
SlGDSLa	Solyc07g049440	RT_F	AGCAAACGCGAAAATTCCAG
		RT_R	GGCATAAAATTGCTCCGAGC
SlGL2	Solyc03g120620	RT_F	CCCCTCTCCAGCACTCTCTTT
		RT_R	CCTCAACTTCCTCCGTCGTTT
SlDCR	Solyc03g025320	RT_F	TGATTCAGCAAGCCATAGCG
		RT_R	CCGGCATCTTTGTACGCAA
SlCER3	Solyc03g117800	RT_F	CGGGTGGGCTAGTTCATCTTC
		RT_R	CAGCCTCCCACACAACATCA
SlTMH27	Solyc10g055410	RT_F	AGATTGCAGTTGTGGAAGTGA
		RT_R	CAAGCCCAAAAAGTCATAACC
SlNCED3	Solyc07g056570	RT_F	GCCAGCTAAAATCCACCATGATAG
		RT_R	GCTTCTGAATCACATCGTAGCTAAGAG
SlCD2	Solyc01g091630	RT_F	TGAGACTTGCATAGACGCGG
		RT_R	TTGTCATGCGTTGTGCTAGCT
SlPDF2d	Solyc06g050160	RT_F	GAGTGCCAGCAGGACCCTC
		RT_R	CCTGGGACAACACATCCCAT
SlASR1 (endogenous control)	Solyc04g071610	RT_F	CCTGTTCCACCACAAGGACAA
		RT_R	GTGCCAAGTTTACCGATTTGC

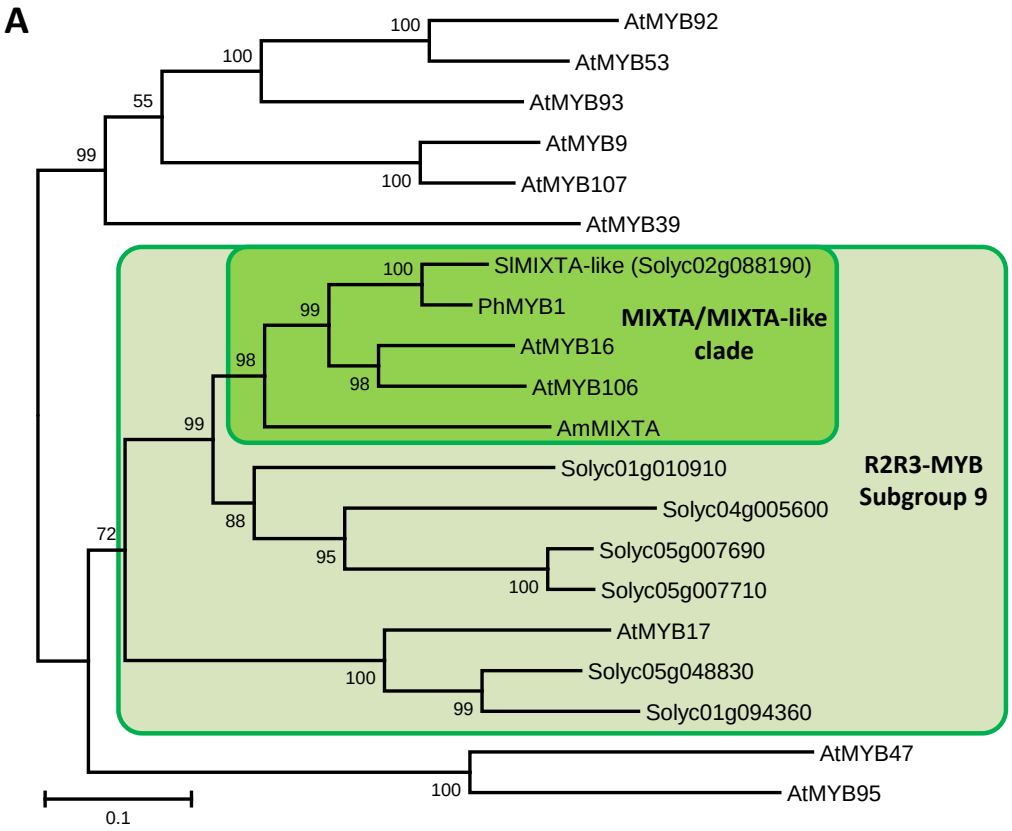

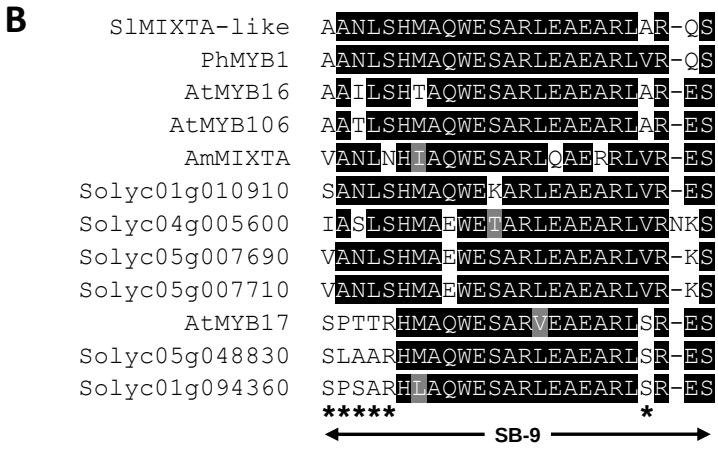

Supplemental Fig. S1. Identification of potential tomato MIXTA/MIXTA-like orthologues. (A) A molecular phylogenetic tree is constructed for potential tomato MIXTA and MIXTA-like orthologues together with described *Arabidopsis* MYB-factors and the well charcaterized MIXTA and MIXTA-like orthologues from *Antirrhinum majus* and *Petunia hybrida* (AmMIXTA and PhMYB1 respectively). The previously described Subgroup 9 containing MIXTA/MIXTA-like and MYB17 orthologues is highlighted as well as the MIXTA/MIXTA-like clade. ClustalW and the MEGA6 software were used to align the proteins and compute the neighbor-joining tree with significance percentages (bootstrap values out of 1000). The scale bar represents the relative amino acid difference. Alignments can be viewed in Supplemental Fig. S2. (B) The previously described motif characteristic of Subgroup 9 is shown (SB-9). Amino acids previously identified to differentiate between Subgroup 9A and Subgroup 9B are indicated with an asterisk (*).

A

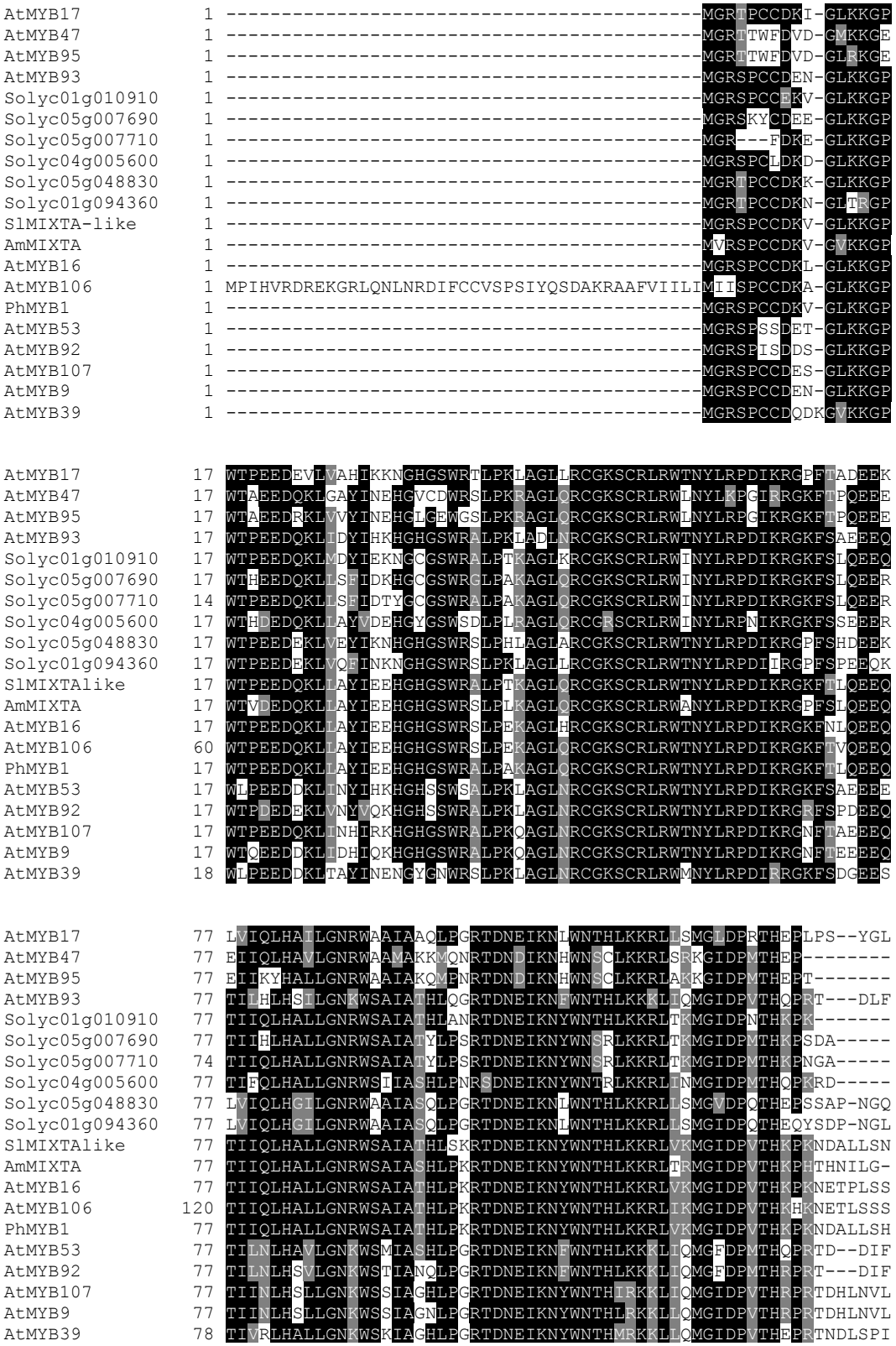

```
AtMYB17          230 ---------------------------------------------SWGGKE---------
AtMYB47          210 ------------------------------------------------------------
AtMYB95          213 ------------------------------------------------------------
AtMYB93          271 LDHVPFSLQ---------------------------------TPLNSEDHFIDNLVKHPT
Solyc01g010910   243 LSLIMVPNN-----------------------------NSITGAGLIDNSCLIGTEN---
Solyc05g007690   243 IFAKDAPTTTKFDVDDDQNL-----------------HNLSTINSCFEDDQLLQTELP--
Solyc05g007710   239 IFANNAPTTTKVDDDDHQNL-----------------QNLSTINSCFEDDQLLQTELP--
Solyc04g005600   243 NIEENVEVG----------------------------EDLCIFEDTITKDNDIQTEF---
Solyc05g048830   230 DVSFA-------------------------------AYQNEETEWKNSQPY-------
Solyc01g094360   229 ELGVAGSPVT---------------------------GSNQHEYKEWKIGQPY-------
SlMIXTAlike      288 ESEEDWKEFGNSSTGHLPQYSKDVINENSISFTSGLQDLTLPMDTTWTTESSRSNTEQIS
AmMIXTA          230 DYEVNNIMG----------------------------MIEFNNNSNYFADSLRLPG----
AtMYB16          243 EPEHDWINS----------------------------TMHEFETTQMGEG---------
AtMYB106         310 EHEHDWIR-----------------------------------QINCGSGG---------
PhMYB1           296 ESEEDWKGFGNSSTGHLPEY-KDGINENSMSLTSTLQDLTMPMDTTWTAESLRSNAEDIS
AtMYB53          234 ---------------------------------------------DDNHFSQNT-----
AtMYB92          242 SNMEPSSVF-----------------------------------PQNLDDNHFKFSTQRENL
AtMYB107         247 PPLISTS------------------------------------PDESKETQMMVK------
AtMYB9           259 PLLVPAS------------------------------------PEESKETQRMIK------
AtMYB39          266 NTAKPGT------------------------------------STTTKVNDHIRTGMMPCY


AtMYB17          236 ----VTVAIHGSDYSPYS-NDLEDDSTDSALQLLLDFPISDDDMSFLEENIDSYSQAPPI
AtMYB47          210 ----ERDSMMGQKIDGSEGEDIQIWGEEE--VRRLMEIDAMDMYEMTSYDAVMYESSHIL
AtMYB95          213 ----LISCYM--EIDETMSIDELPCDDSISGFVAFDDYSLIDPYRDGVYVSDFYDETEHL
AtMYB93          298 DHEHEHDDNPSSWVLPSLIDNNPKTVTSSLPHNNPADASSSSSYGGCEAASFYWPD-ICF
Solyc01g010910   271 ---FVENNINGISYSNYPNLNTIQGFTHLDHVLGSREEEDDNDNND----NTYWNTILKS
Solyc05g007690   284 ---SFVQEFSGV-FPEYT-QNSTNG-LQVDNIMGSFYGDFE-DNK-----LINWNNFPNY
Solyc05g007710   280 ---SFVQEFSGV-FPEYA-QNSTNG-LQVDNFMGSYSEDFE-DNKL----LINWNNFPNY
Solyc04g005600   272 ---SIIEGLDEL-FPEYG-YSQNPGNYSSEVQMDGCFGNFE-DNK-----STNWNNIAHL
Solyc05g048830   250 ----TEDVLQGYDDTSSS-SGLED-SSESALQLLLDFP-SNNDMSFLGH-SDTYSLYPEF
Solyc01g094360   255 ----TEDFLQG-SDTSSS-NAMED-SSESALQLLLDFP-SNNDMSFLGH-SDSYSLYP-F
SlMIXTAlike      348 PAN-FVETFTDLLLS-NSGDGDLSEGGGIESDNGGEGSGSGNPNENSEDNKNYWNSIFNL
AmMIXTA          258 ----FVEGITDISSSNIVLGAGVL--PSNSDNVVGYFEENWSSVLNNVASSSSMDSPDVL
AtMYB16          265 ----IEEGFTGLLLGGDSIDRSFS--GDKNE-TAGESSGG--DCNYYEDNKNYLDSIFNF
AtMYB106         326 ----IGEGFTSLLIG-DSVGRGLP--TGKNEATAGVGNES--EYNYYEDNKNYWNSILNL
PhMYB1           355 HGNNFVETFTDLLLS-TSGDGGLS-GNGIDSDNGG-GSGN-DPSETCGDNKNYWNSIFNL
AtMYB53          243 --SPIWLHEPPS-LNQTMLPTHDPCAQS-VDGFGSNQASSSHDQEVAVTDSVDWPDHHLF
AtMYB92          269 PVSPIWLSDPSS-TTPAHVNDDLIFNQYGIEDVNSN-ITSSSGQESGASASAAWPD-HLL
AtMYB107         266 -NKEIMKYNDHTS-----------NPSSI-STFTQD-HQPWCDIIDDEASDSYWKEIIEQ
AtMYB9           278 -NKDIVDYHHHDAS----------NPSSSNSTFTQDHHHPWCDTIDDGASDSFWKEIIEQ
AtMYB39          291 YGDQLLETPSTGSVSVSPETTSLNHPSTAQHSSGSDFLEDWEKFLDDETSDSCWKSFLDL


AtMYB17          291 GLVSMVSKF----------
AtMYB47          264 DHLF--------------
AtMYB95          267 DLFLL-------------
AtMYB93          357 DESLMNVIS---------
Solyc01g010910   324 CTS-FVDGSSVF*------
Solyc05g007690   332 LVN-SPIGSPVF*------
Solyc05g007710   329 LVN-SPIDCIN*-------
Solyc04g005600   321 VMT-SPIGSPLL*------
Solyc05g048830   302 LSESSFKGSSAQHEVGFL*
Solyc01g094360   305 LSESS*------------
SlMIXTAlike      406 VNNPSPSDSS-MF*-----
AmMIXTA          312 VNA---SSSYKMY------
AtMYB16          316 VDP-SPSDSP-MF------
AtMYB106         377 VDS-SPSDSATMF------
PhMYB1           411 VNS-SPSDSA-MF------
AtMYB53          299 DDSMFPDISYQS-------
AtMYB92          326 DDSIFSDIP----------
AtMYB107         312 TCSEPWPFRE---------
AtMYB9           327 TCSEPWPFPE---------
AtMYB39          351 TSPTSSPVPW---------
```

B

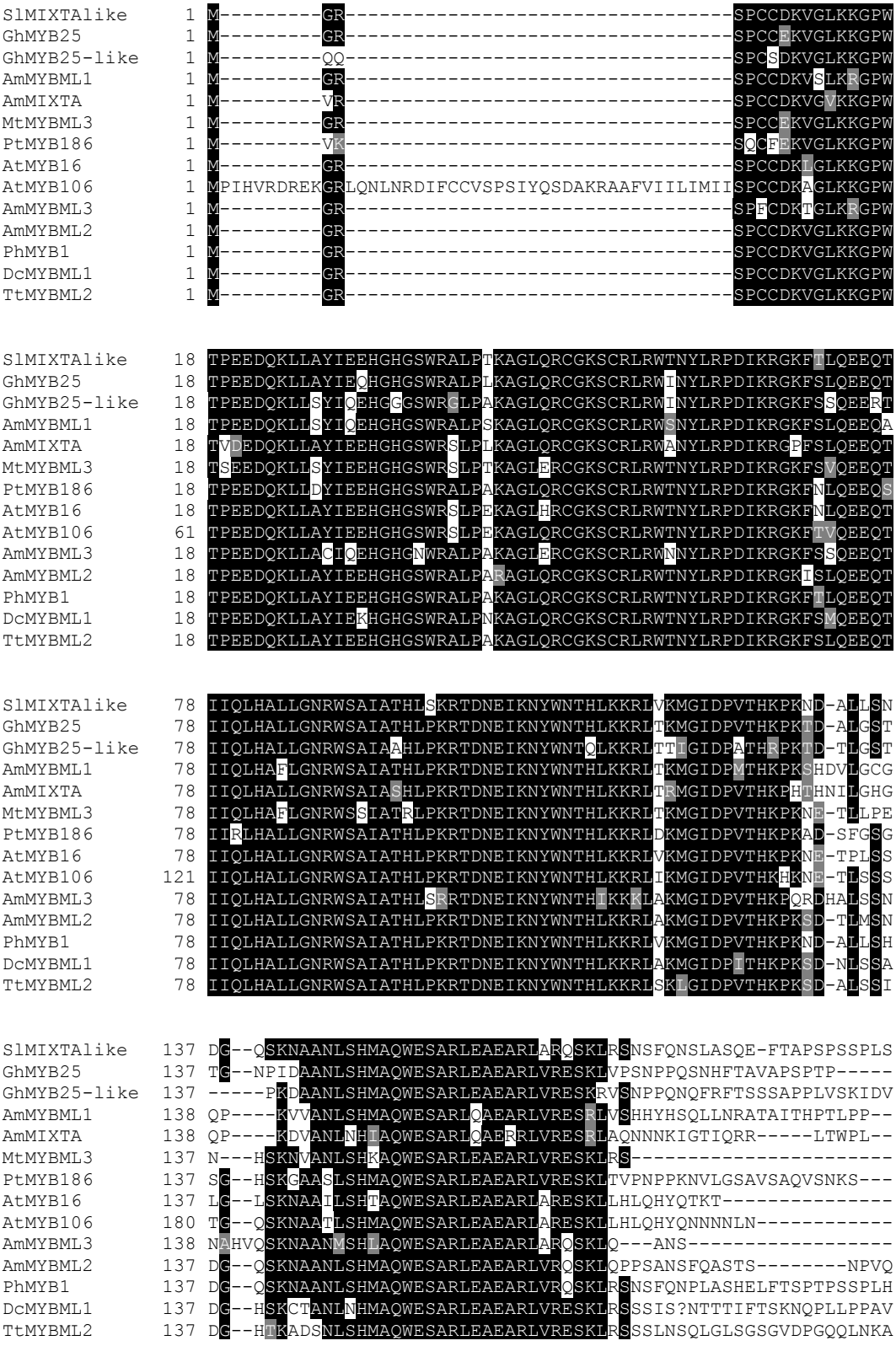

```
SlMIXTAlike   194 KPVVAP------ARCLNVLKAWNGVWTKPMN----EGSVASASAGISVAGALARDLESPT
GhMYB25       190 ----ATRPQ-----CLDVLKAWQGVVCGLFT----------------FNMDNNNLQSPT
GhMYB25-like  192 GLAHATKPQ-----CLDVLKAWQRVVTGLFT----------------FNTDN--LQSPT
AmMYBML1      192 -------------CLDVLKVWHGAWTTRPGKD-----IITSAMFNGFFASNNGNLESPT
AmMIXTA       187 -------------CLDNEQSNH-------------------------YHS---------
MtMYBML3      171 ------------------------------------------------QLQHQFGSNT
PtMYB186      192 SATPTERPR-----CLDVLKAWQGVVFSMFS----------------VGSSDS-LESPT
AtMYB16       180 ---------------SSQPHHHHGFTHKSLLP----------NWTTKPHED-QQQLESPT
AtMYB106      226 ---------------KSAAPQQHCFTQKTST----------NWTKPNQGNGDQQLESPT
AmMYBML3      177 ------------------------------------------------------------
AmMYBML2      187 KSMGQA-------RCLDVLKAWNGVVWGKND--------EAAGVSVTVTTGIVGELGSPT
PhMYB1        195 KPIVTPTKAPGSPRCLDVLKAWNGVWTKPMNDVLHADGSTSASATVSVN-ALGLDLESPT
DcMYBML1      194 PMTPAAS------PCLDVLSAWQGAWTKPAAN----------NSQGRGYT---IDLESPT
TtMYBML2      195 TSTSTQP------QCLNVMKAWQGIWSKPTKCG---------LVTGEGSSTGGLDLESPT

SlMIXTAlike   244 STLGYFENAQHITSSGIGGSSNTVLYEFVGNSSGSSEGGIMNN----------DESEEDW
GhMYB25       224 S-----------------------------TLNFMENTTTLPMSSSSSVNGMFNENFGW
GhMYB25-like  228 S-----------------------------TSSFTEN--TLPISSVG-----FIDSFVG
AmMYBML1      233 SIL----------------------KSSDNMLNASTSVGLLHE---------NPFITDM
AmMIXTA       199 ----------------------------ALLNSISAVGLNQD---------NSFTN--
MtMYBML3      181 S------------------------VFPSQSSSSSSNQVLNIK---------EEGEKEW
PtMYB186      229 S-----------------------------TLNFSENALAIPLIGVQK---NPTTTLAF
AtMYB16       214 S-----------------------------TVSFSE---MKES---------IP-----
AtMYB106      260 S-----------------------------TVTFSENLLMPLG---------IPTDSSR
AmMYBML3      177 ------------------------------------------------------------
AmMYBML2      232 S---------------------------TLSSAAGTNGIMK----------EESEEEW
PhMYB1        254 STLSYFENAQHISTGMIQENS-TSLFEFVGNSSGSSEGGIMN----------EESEEDW
DcMYBML1      235 S-----------------------------TLSFSDNMM-------------APTISGM
TtMYBML2      240 S-----------------------------TLCFSDNSMPVLTVGFSD----NPTMSSL

SlMIXTAlike   294 KEFGNSSTG------------HLPQYSKDVINENSISFTSGLQDLTLPMDTTWTTESSR
GhMYB25       254 NSSINPCE----------SGDILKVEYGSDQIPELKERLDHPMELHEM-DCSSEG-----
GhMYB25-like  251 NS-NNSCC----------GNNWECVEK-SSQVAELQEILDNSMGLHDILDLSSED-----
AmMYBML1      261 SYVGKPSNV---------------YEDWVKGIMDNSNELNKIIEPIDSTHYV--------
AmMIXTA       218 -YSARPDN--------------------NNIYDD-YEVNNIMGMIEFNNNS---------
MtMYBML3      207 KGYEDST---------------HLLEF-KDLVENSSMAFSSTLQ----------------
PtMYB186      256 ATNNAICNRGTTVSEFDRGNQLECFEK-LKDPAQVRRNLDSSMAIHGISPYAGDHN----
AtMYB16       227 ----------------------AKIEFVGSS---TGVTLMKEPEHDWINSTM--------
AtMYB106      281 NRNNNNNESS------------AMIFLAVSSSTSSDVSLVKEHEHDWIR-----------
AmMYBML3      177 ------------------------------ECG-----------------------------
AmMYBML2      253 K---------------------QMPEN-RDEIGN-ATPFTSNWES---------------
PhMYB1        302 KGFGNSSTG------------HLPEY-KDGINENSMSLTSTLQDLTMPMDTTWTAESLR
DcMYBML1      252 GLAEDSTR---------------EDQEWKCLRKTGFSMHIAAP---FVSTEAS------
TtMYBML2      266 DLIPNSSSGTFEGAPVKEECDEEYMGGEYKRMVNSAVPINTGLQDMGFSTTVDS------

SlMIXTAlike   341 SNTEQISPAN--------FVETFTDLLLSNSGDGDLSEGGGTESD-NGGEGSGSGNPNEN
GhMYB25       298 TWFQELFG-------FNGL-----------------------------------------
GhMYB25-like  294 VWFQGSYR-------AENMMEGYSDTLMVCDSGDH------PKSLSMEPRQNFNVGTSNA
AmMYBML1      298 AHDDDSIGFP-------GFMEGSTNLVT-------------STVRTNG----PDDDNVVG
AmMIXTA       247 NYFADSLRLP-------GFVEGITDISS-------------SNIVLGAGVLPSNSDNVVG
MtMYBML3      235 ---HEMTMIN-------VAEEGFTNLLLDNSNSGDLSLSPESGGECNTCDGSGSGGGSDF
PtMYB186      311 AWFVDSSANENA--PMGNIIDGFS-EILVCNSLDP------NPTCSGE-----NINDNYA
AtMYB16       254 HEFETTQMGE-------GIEEGFTGLLLGGDSIDR----SFSGDKNE-TAGESSGGDCNY
AtMYB106      318 ---QINCGSG-------GIGEGFTSLLIG-DSVGR----GLPTGKNEATAGVGNESEYNY
AmMYBML3      180 ------------------------------------------GGSDTGG---GGSDC
AmMYBML2      275 EQVALNSSEA-------CSSREFRGKLYGLVTECFLCRWRGMRIVGYTNSGGNDVGVSDY
PhMYB1        348 SNAEDISHGN-------NFVETFTDLLLSTSGDGGLS-GNGTDSD-NGG-GSGN-DPSET
DcMYBML1      287 SWLSESSG--G------GDFAAGFTGMLS-DKANEQNSEDGCNDSDNAECGSCVDVEESEG
TtMYBML2      320 PWSSESSKVGNEHIPVTNFIEGFTNLLLGNSINDRNSVD--NTSGDGDSSDNGDADAMDC
```

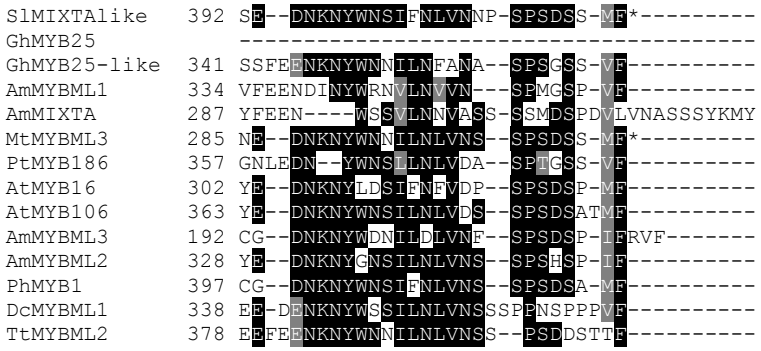

C

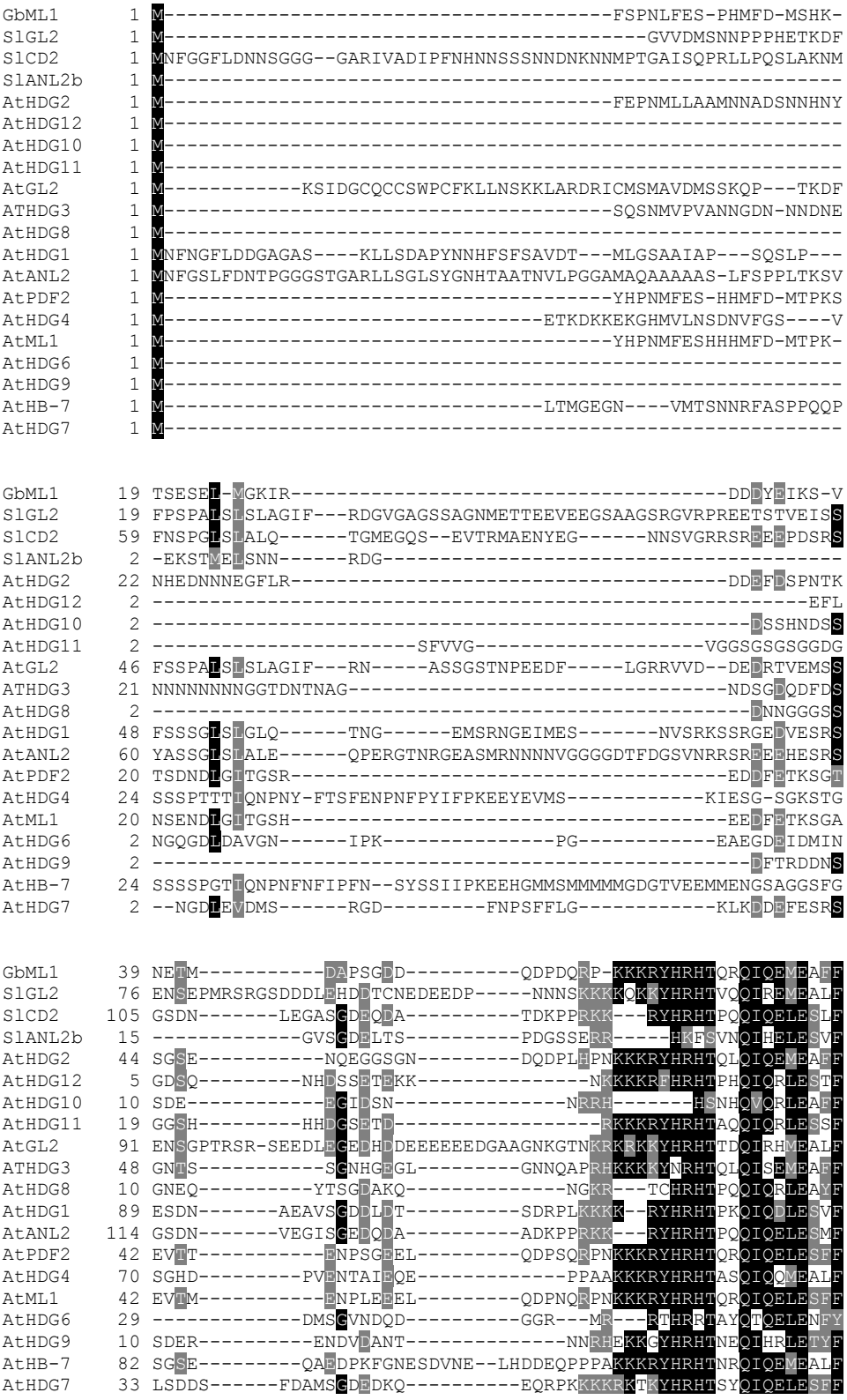

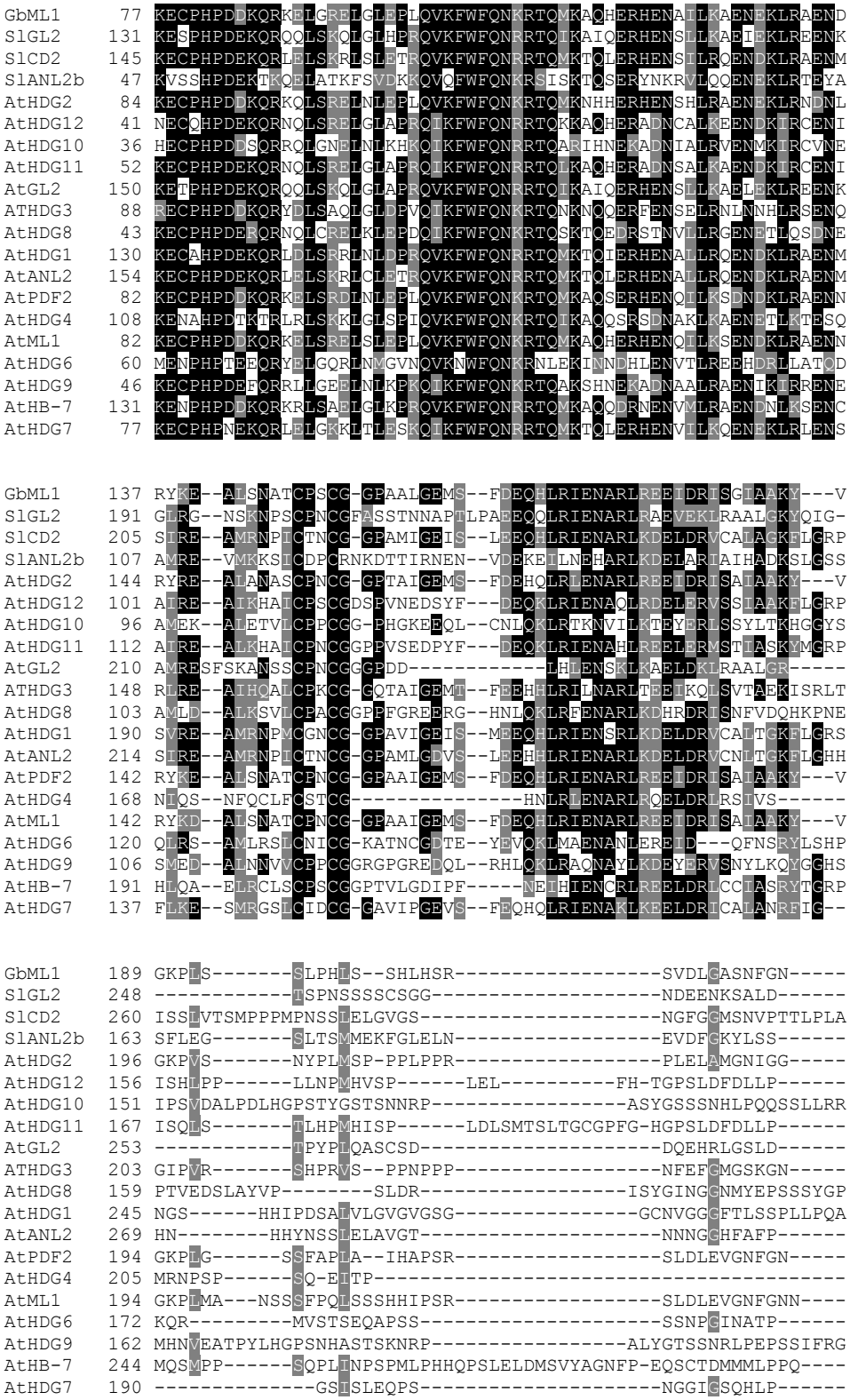

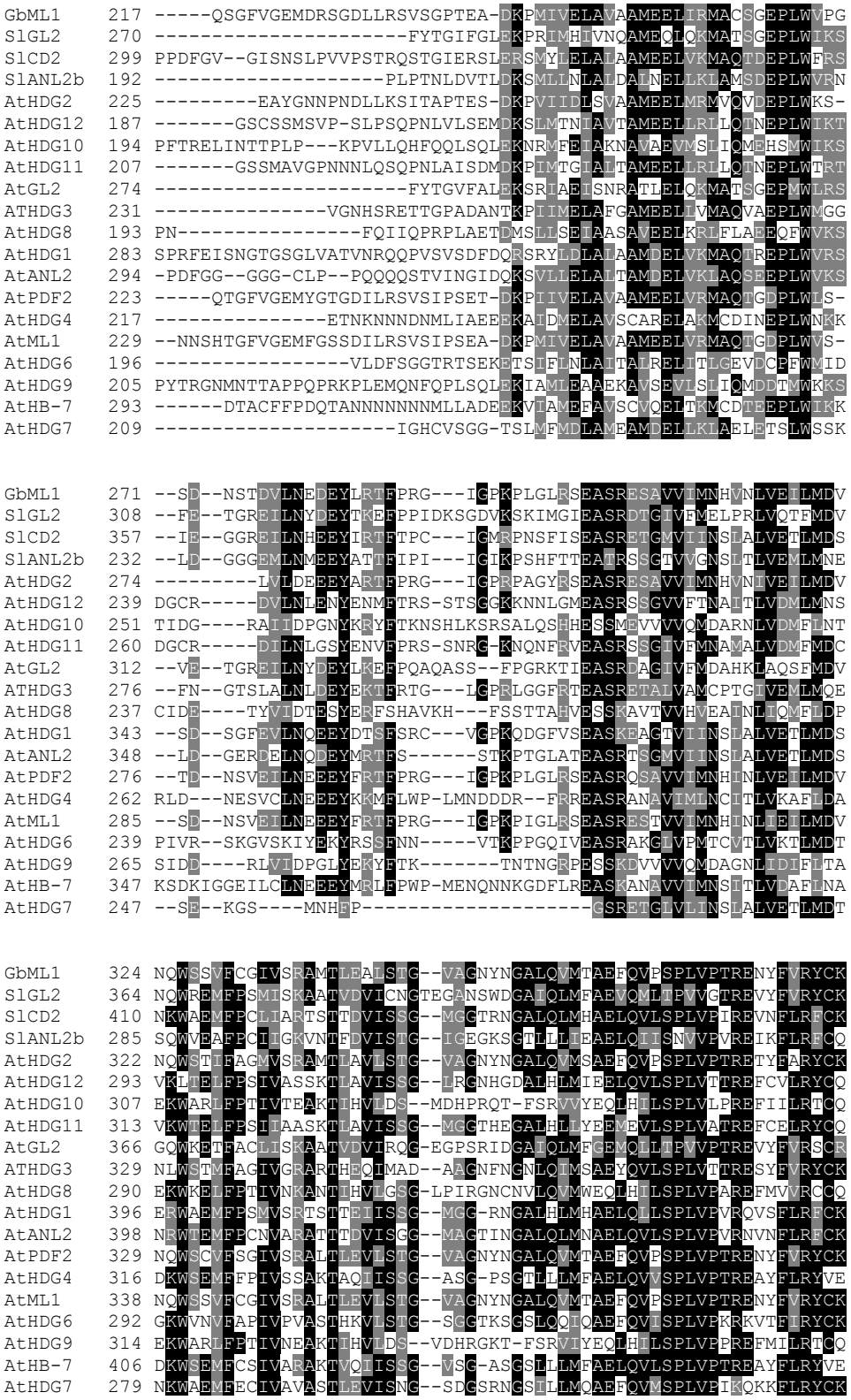

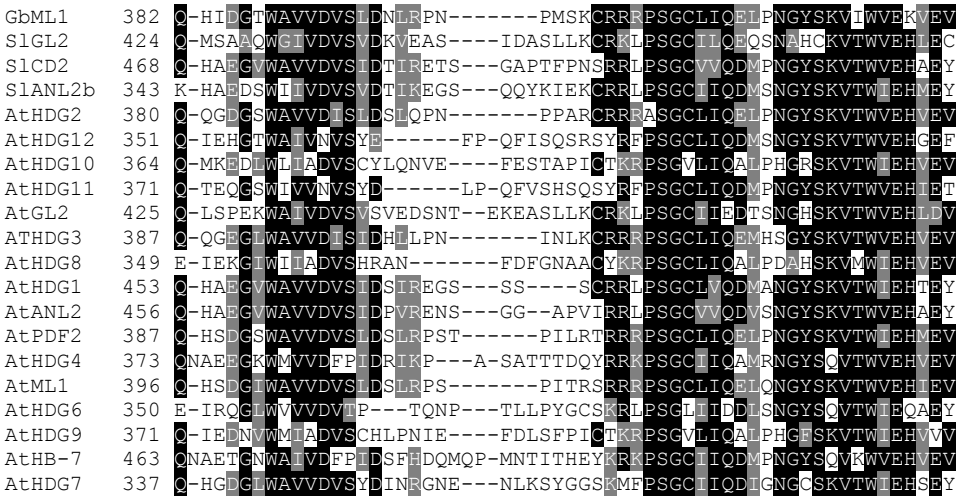

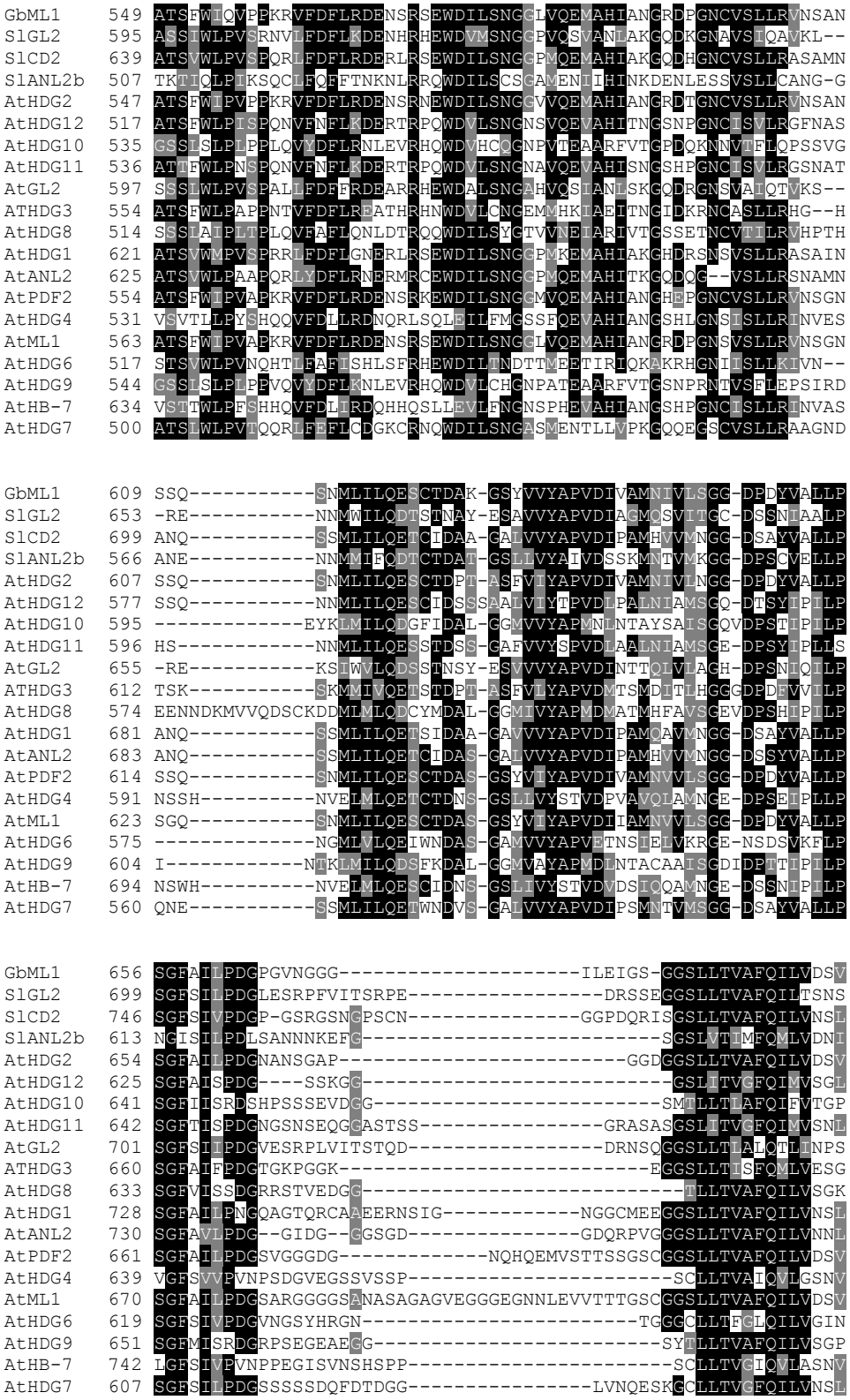

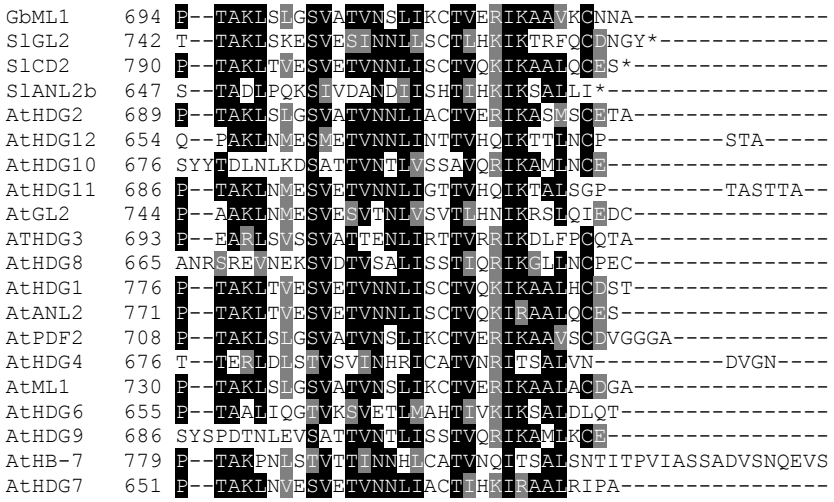

D

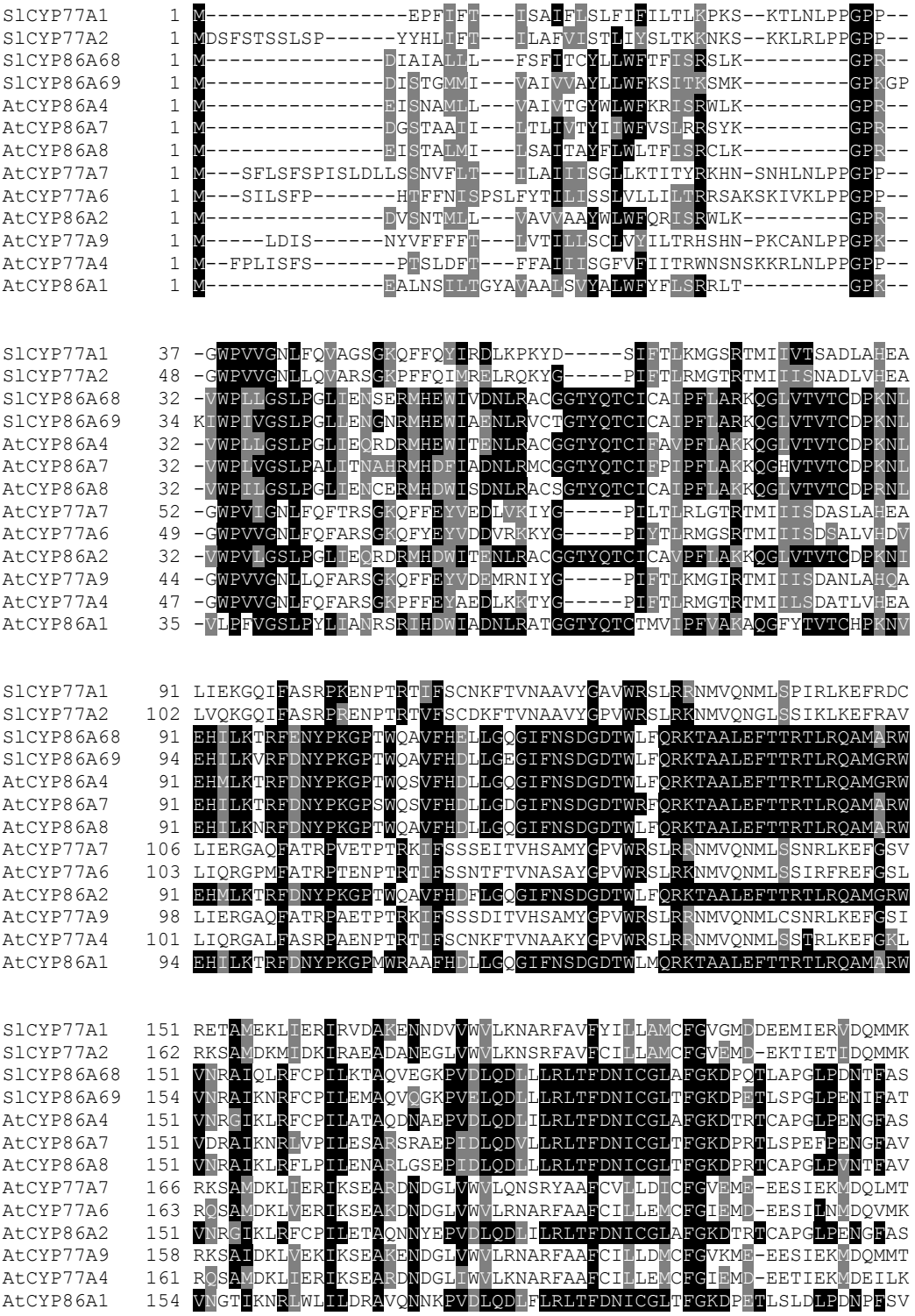

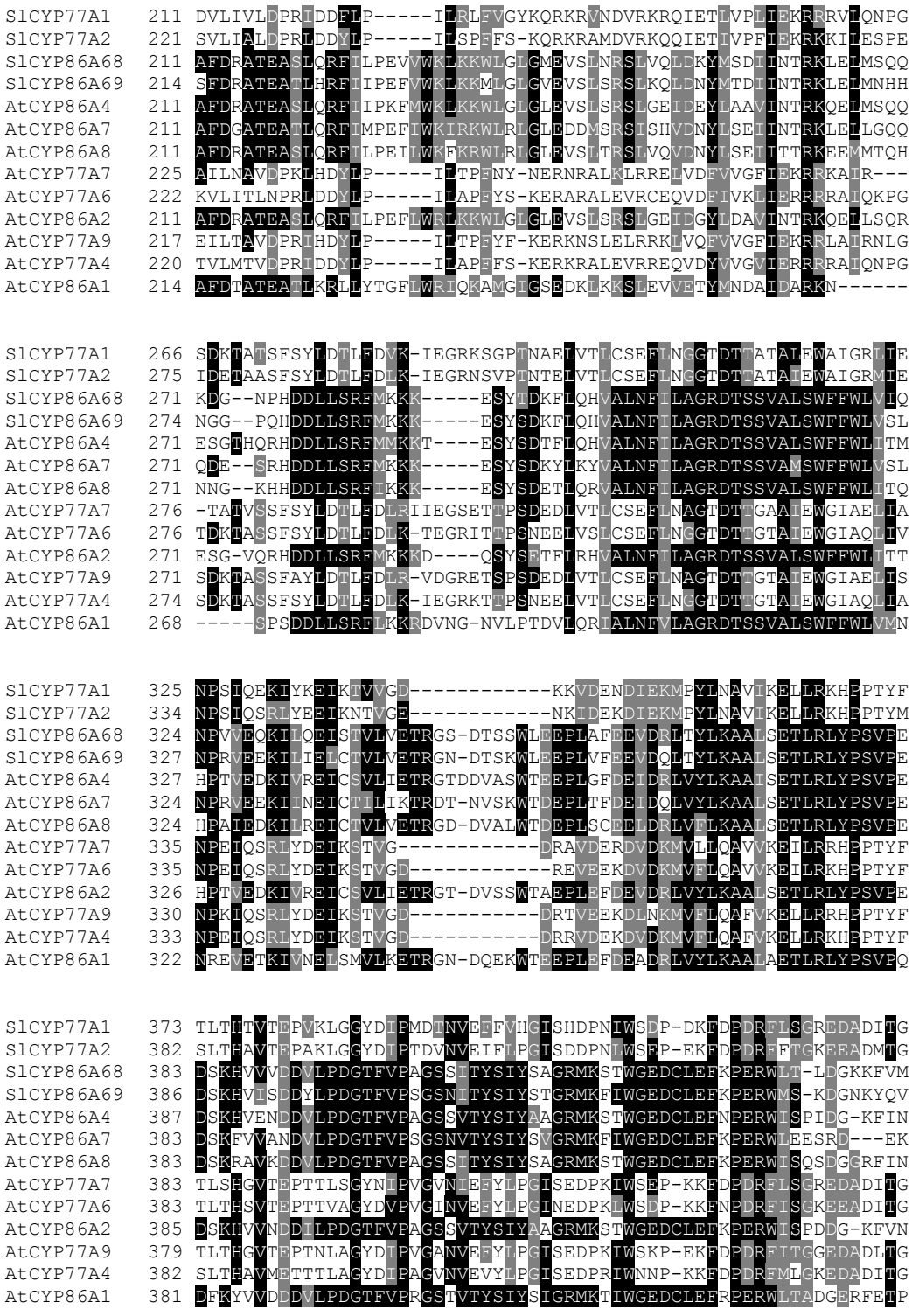

```
SlCYP77A1    432 VKAVKMMPFGVGRRICPGLGMATVHLNLMLARMVQEFEWLAYPGNSEVDFSEKLEFTVVM
SlCYP77A2    441 VSGVKMMPFGMGRRICPGLNMATVHVSLMLARLIQEFEWSD-EENTRVDFTEKLEFTVVM
SlCYP86A68   442 HEQYKFVAFNAGPRICLGKDLAYLQMKSVAAAVLLRHRLTVAPGHK---VEQKMSLTLFM
SlCYP86A69   445 QDAFRFVAFNAGPRICLGKDLAYLQMKSIAAAVLLRHRLAVAPGHK---VEQKMSLTLFM
AtCYP86A4    446 HDQYRFVAFNAGPRICLGKDLAYLQMKTIAAAVLLRHRLTVVPGHK---VEQKMSLTLFM
AtCYP86A7    440 CNQYKFVAFNAGPRICLGKDLAYLQMKSITASILLRHRLTVAPGHR---VEQKMSLTLFM
AtCYP86A8    443 HDPFKFVAFNAGPRICLGKDLAYLQMKSIASAVLLRHRLTVVTGHK---VEQKMSLTLFM
AtCYP77A7    442 VAGVKMMPFGVGRRICPGMGMATVHVHLMIARMVQEFEWLAYPPQSEMDFAGKLVFAVVM
AtCYP77A6    442 VTGVKMMPFGIGRRICPGLAMATVHVHLMLAKMVQEFEWSAYPPESEIDFAGKLEFTVVM
AtCYP86A2    444 HDQYRFVAFNAGPRICLGKDLAYLQMKTIAAAVLLRHRLTVAPGHK---VEQKMSLTLFM
AtCYP77A9    438 VAGVKMMPFGIGRRICPGLGMAVVHVELMLSRMVQEFEWSSYPPESQVDFTGKLVFAVVM
AtCYP77A4    441 ISGVKMMPFGVGRRICPGLAMATIHVHLMLARMVQEFEWCAHPPGSEIDFAGKLEFTVVM
AtCYP86A1    441 KDGYKFVAFNAGPRTCLGKDLAYNQMKSVASAVLLRYRVFPVPGHR---VEQKMSLTLFM

SlCYP77A1    492 KNPLRAKVKPRT*-----------------------------------------
SlCYP77A2    500 KNTLRAKIKPRM*-----------------------------------------
SlCYP86A68   499 KDGLKVNLRPRELTPFVNSVKE-VQLI-----------QI*--------------
SlCYP86A69   502 KYGLVVNVNPRDLTPILAKIENFCKIDHSCGGEHMINNGINQPGATAVNGIAA*-
AtCYP86A4    503 KNGLLVNLYKRDLQGIIKSLVV-KKSD--GVSNGQCNGVIGEGVAVYLNTGVAVV
AtCYP86A7    497 KFGLKMDVFKRDLTLPVEKVVNEMRKK-------------------------
AtCYP86A8    500 KYGLLVNVHERDLTAIAADLRE-CKSN-------VVNDGVGNGVSS---------
AtCYP77A7    502 KKPLRAMVRPRVQ-----------------------------------------
AtCYP77A6    502 KKPLRAMVKPRV------------------------------------------
AtCYP86A2    501 KNGLLVNVHKRDLEVMMKSLVP-KERNDVVVLNGKCNGGIGEGVAVNAAVAVAV-
AtCYP77A9    498 KNPLRARVKARV------------------------------------------
AtCYP77A4    501 KNPLRAMVKPRI-----------------------------------------
AtCYP86A1    498 KNGLRVYLQPRGEVLA-------------------------------------
```

Supplemental Fig. S2. Protein alignments used to construct molecular phylogenetic trees. (A) Alignment of MYB factors used in Supplemental Fig. S1 (B) Alignment of MIXTA/MIXTA-like proteins used in Fig. 1A. (C) Alignment of HD-ZIP IV factors used in Supplemental Fig. S6. (D) CYP used in Supplemental Fig. S7. ClustalW and the MEGA6 software were used to align the proteins in all cases.

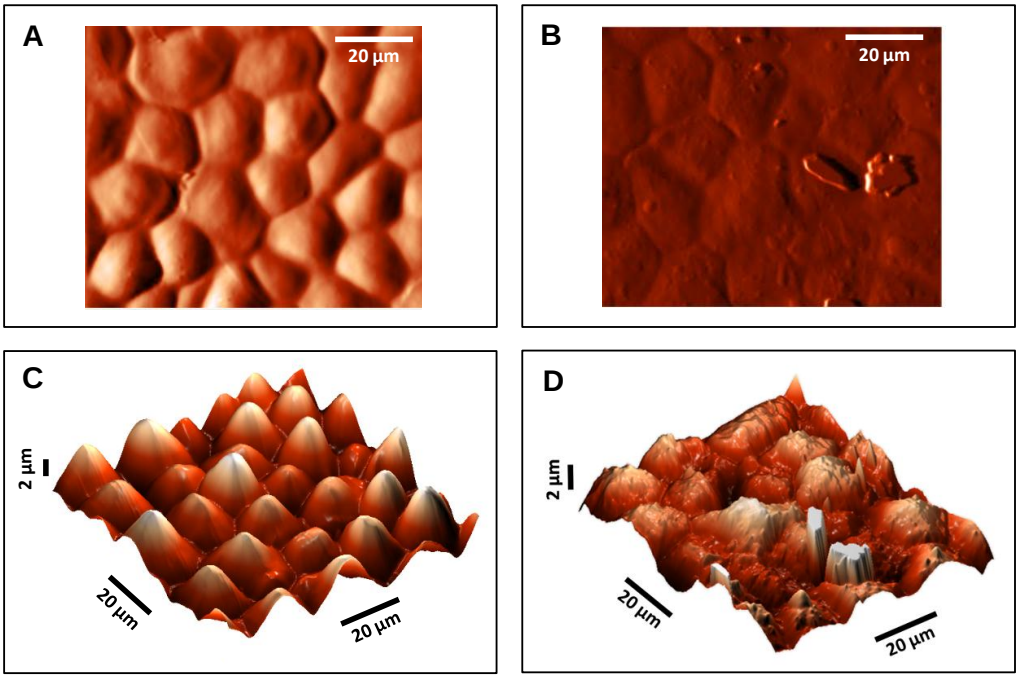

Supplemental Fig. S3. Atomic Force Microscopy (AFM) images of immature green tomato surface of wild-type and *SlMIXTA-like* silenced plants. (A) and (B) Topographic images generated from AFM analysis show the surface of the *SlMIXTA*-RNAi tomato fruit (B) is markedly flatter than the wild-type (A). (C) and (D) Three-dimensional topographic images from AFM analysis confirm the flatter surface observed for *SlMIXTA*-RNAi (D) tomato fruit when compared with wild-type (C). Further, the surface of the fruit from *SlMIXTA-like* silenced plants appear more irregular, exhibiting a small-scale roughness which could be due to the relatively collapsed state of the conical structures.

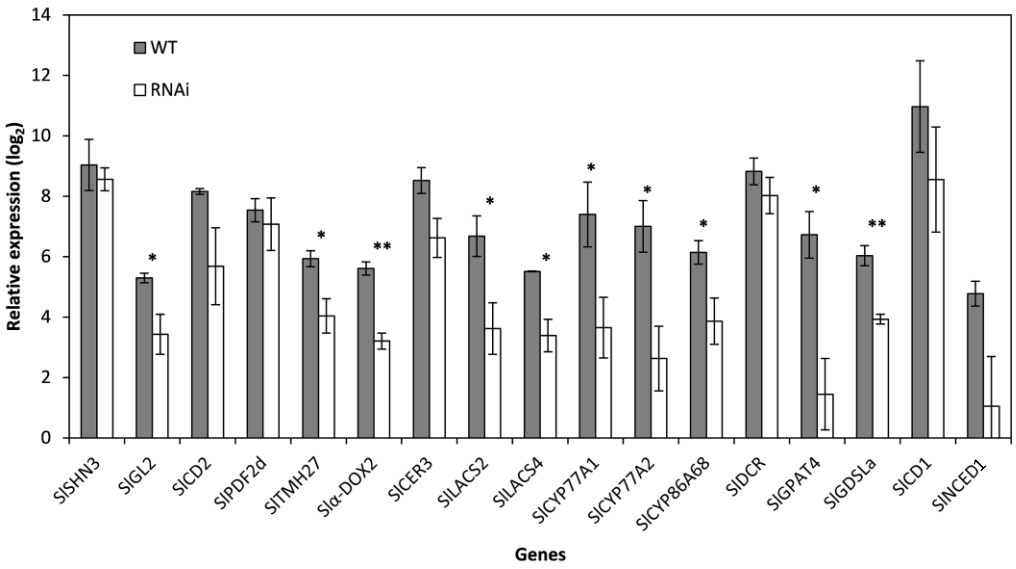

Supplemental Fig. S4. Validation of microarray-based differential gene expression results by means of quantitative RT-PCR (qRT-PCR) analysis. The analysis with qRT-PCR confirmed the expression profile of eight genes identified in microarray analysis, while also identifying a number of genes not detected in the microarray analysis. *SlSHN3*, *Solyc06g065820*; *Slα-DOX2*, *Solyc03g119060*; *SlLACS4*, *Solyc01g095750*; *SlLACS2*, *Solyc01g109180*; *SlCYP77A2*, *Solyc05g055400*; *SlTMH27*, *Solyc10g055410*; *SlNCED1*, *Solyc07g056570*. *SlCER3*, *Solyc03g117800*; *SlCYP77A1*, *Solyc1g007540*; *SlCYP77A2*, *Solyc05g055400*; *SlCYP86A68*, *Solyc01g094750*; *SlGDSLa*, *Solyc07g049440; SlGL2*, *Solyc03g120620*; *SlGPAT4*, *Solyc01g094700*; *SlCD2*, *Solyc01g091630*; *SlDCR, Solyc03g025320*; *SlGPAT4*, *Solyc01g094700*; *SlPDF2d*, *Solyc06g050160*; *SlCD1*, *Solyc11g006250*. Values represent mean ± standard error (n=3; *=p<0.05; **= P<0.01).

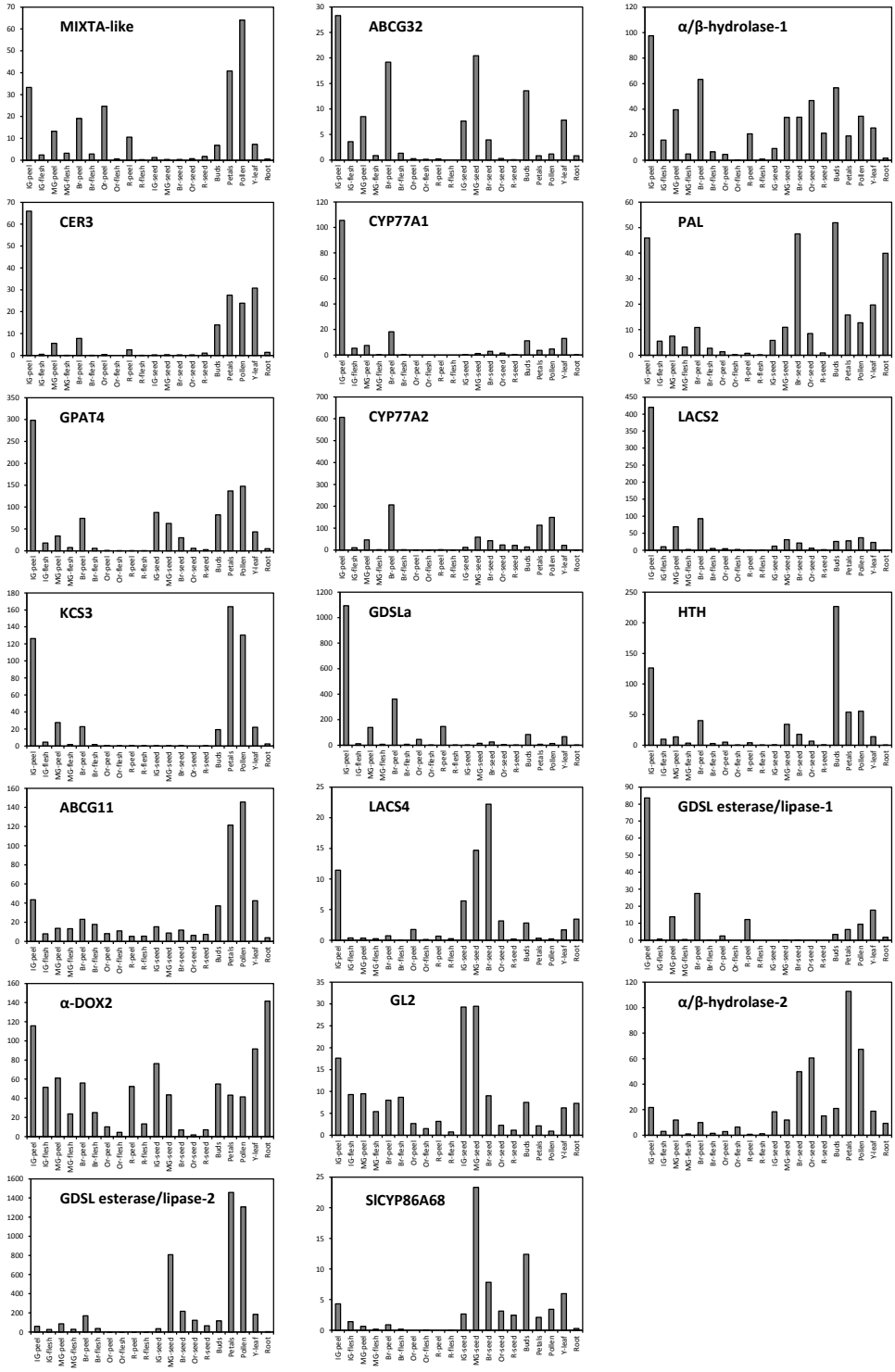

Supplemental Fig. S5. Normalized expression across 20 tomato tissues of selected genes described in this study to be down regulated in the *SlMIXTA*-RNAi tomato lines. Expression patterns were extracted from the dataset generated by Itkin *et al*. (2013) and are shown in RPKM. IG, immature green; MG, mature green; Br, breaker; Or, orange; Re, red; Y, young. *ABCG32*, *Solyc06g065670*; *ABCG11, Solyc03g019760*; *α-DOX2*, *Solyc03g119060*; *α/β-hydrolase-1*, *Solyc05g054330*; *α/β-hydrolase-2*, *Solyc09g075140*; *CER3*, *Solyc03g117800*; *CYP77A1*, *Solyc1g007540*; *CYP77A2*, *Solyc05g055400*; *CYP86A68*, *Solyc01g094750*; *GDSLa*, *Solyc07g049440*; *GDSL esterase/lipase-1*, *Solyc04g081770*; *GDSL esterase/lipase-2*, *Solyc03g121180*; *GL2*, *Solyc03g120620*; *GPAT4*, *Solyc01g094700*; *HTH*, *Solyc08g080190*; *KCS3*, *Solyc11g072990*; *LACS2*, *Solyc01g109180*; *LACS4*, *Solyc01g095750*; *MIXTA-like*, *Solyc02g088190*; *PAL*, *Solyc05g056170*.

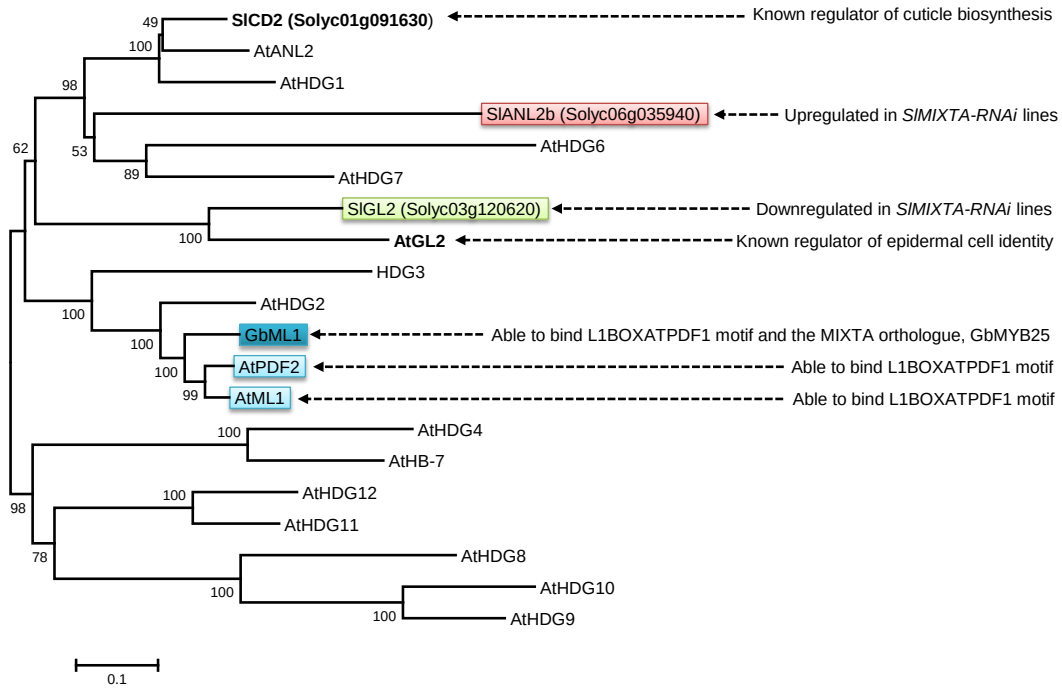

Supplemental Fig. S6. Molecular phylogeny of the HD-ZIP IV family proteins associated with epidermal cell patterning and ones identified in this study. Molecular phylogenetic analysis of the *Arabidopsis* HD-ZIP IV protein clade is shown together with HD-ZIP IV members discussed in this paper. ClustalW and the MEGA6 software were used to align the proteins and compute the neighbor-joining tree with significance percentages (bootstrap values out of 1000). The scale bar represents the relative amino acid difference. Alignments can be seen in Supplemental Fig. S2. Relevant information regarding functional annotation of some characterized proteins is also displayed.

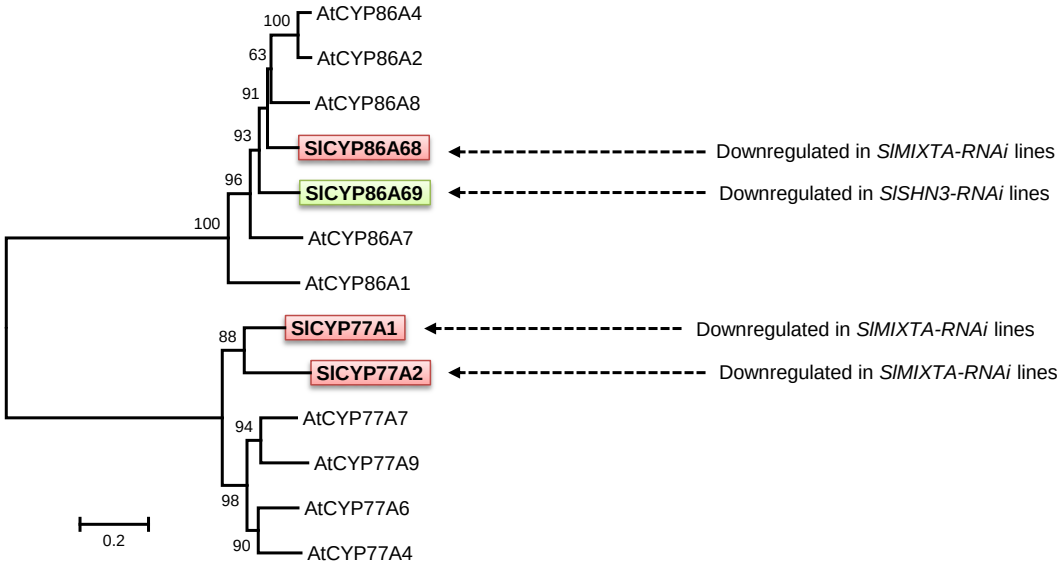

Supplemental Fig. S7. Molecular phylogeny of the CYP77A and CYP86A family proteins discussed in this study. Molecular phylogenetic analysis of the CYP77A and CYP86A protein clades discussed in this paper is shown. ClustalW and the MEGA6 software were used to align the proteins and compute the neighbor-joining tree with significance percentages (bootstrap values out of 1000). The scale bar represents the relative amino acid difference. Alignments can be seen in Supplemental Fig. S2. Relevant information regarding regulation by SlMIXTA-like and SlSHN3 is displayed.

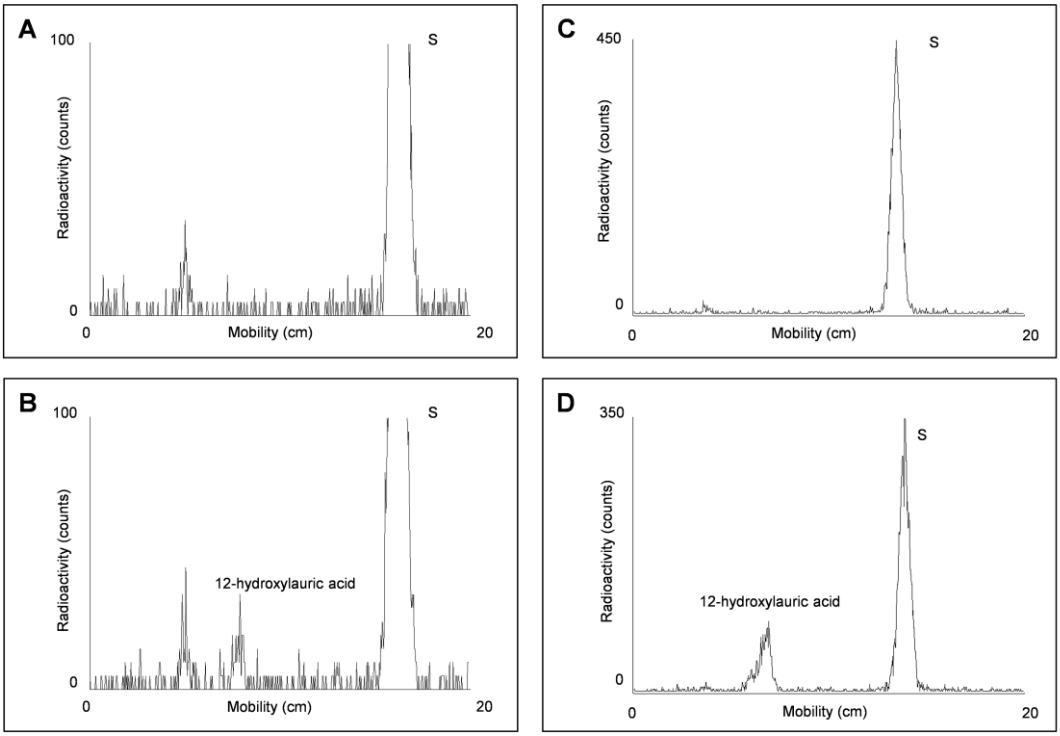

Supplemental Fig. S8. Radiochromatographic resolution by Thin Layer Chromatography (TLC) of metabolites generated in incubations of dodecanoic acid with microsomes from yeast expressing *SlCYP86A68* or *SlCYP77A2.* (A) and (B) Radiochromatographic resolution by TLC of metabolites detected in samples of microsomes from yeast expressing *SlCYP86A68* incubated with 100 µM dodecanoic acid in the absence (A) or in the presence (B) of NADPH. Incubations were performed for 20 min with 600 mg of microsomal proteins at 27°C and the incubation media was directly spotted on TLC. The reaction product formed is 12-hydroxy-dodecanoic acid acid; Peak S, dodecanoic acid. (C) and (D) Radiochromatographic resolution by TLC of metabolites detected in samples of microsomes from yeast expressing *SlCYP77A2* incubated with 100 µM dodecanoic acid in the absence (C) or in the presence (D) of NADPH. Incubations were performed for 20 min with 600 mg of microsomal proteins at 27°C and the incubation media was directly spotted on TLC. The reaction product formed is 12-hydroxy- dodecanoic acid; Peak S, dodecanoic acid.

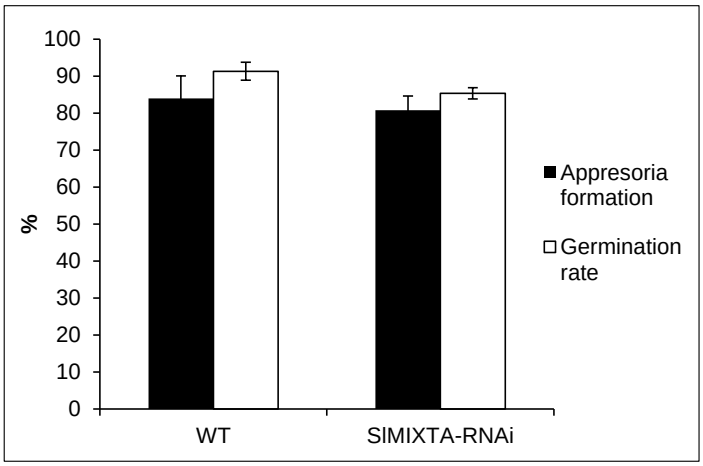

Supplemental Fig. S9. Germination rate and appressoria formation of *Colletotrichum coccodes* is unchanged on *SlMIXTA-like* silenced fruit surface. Fungal germination rates were measured in breaker stage tomato fruit inoculated with 7 µl of 10^6 *Colletotrichum coccodes* conidia/ml and incubated at 22°C and 95% relative humidity for 7 days post inoculation. Error bars represent standard error (n=30).

Supplemental Dataset S1. Significantly down-regulated and up-regulated genes in skin tissue of *SlMIXTA*-RNAi lines identified via microarray analysis. Down-regulated genes are listed in Table 1, and up-regulated genes in Table 2. (Online resource: http://jmp.sh/vJrIUdx).

Supplemental Dataset S2. Generation and analysis of tomato lines over expressing *SlMIXTA-like*.

Materials and Methods

The construct for over *SlMIXTA*-like expression (*SlMIXTA*-OE) was generated by isolating the full 1254 bp coding sequence from *cv.* MT cDNA and cloning into pART27 via the pART7 (Gleave et al., 1992). Primers used are described in S2 Table. Transformation was performed as described in the main text.

Results

Preliminary analysis of lines over expressing *SlMIXTA-like* displayed a significant increase in fruit cutin deposition (See table below). These results confirm the hypothesis that *SlMIXTA-like* is a regulator of cuticle deposition in tomato fruit.

References

Gleave AP. A versatile binary vector system with a T-DNA organisational structure conducive to efficient integration of cloned DNA into the plant genome. Plant Mol Biol. 1992;20(6):1203-7. PubMed PMID: 1463857.

Table. Quantification of cutin monomer composition in fruit of lines over expressing *SlMIXTA-like*.

	Wild type		*SlMIXTA*-OE	
Cutin Monomers	**Average**	**SE**	**Average**	**SE**
Aromatic				
cis-Coumaric acid	0.92	0.23	1.43	0.61
trans-Coumaric acid	50.52	1.57	112.65	13.85
Subtotal	51.44	1.44	114.09	13.68
Saturated fatty acids (FA)				
C16:0 FA	2.84	0.14	3.02	0.14
C18:0 FA	5.51	0.26	5.11	0.25
Subtotal	8.35	0.4	8.13	0.39
Dicarboxylic fatty acids (DFA)				
C16:0 DFA	24.92	1.34	62.78	5.36
C16-9,10 hydroxy-DFA	67.53	4.73	142.87	15.52
Subtotal	92.46	4.78	205.64	20.88
Mid chain hydroxylated fatty acids (HFA)				
C16-9/10,16 DiHFA	797.66	43.11	1290.24	92.25
C18-9,18 DiHFA	2.97	0.33	6.46	0.53
C18:1-9,10,18-TriHFA	1	0.27	2.49	0.49
C18-9,10 DiHFA	43.69	3.72	87.57	8.09
Subtotal	845.31	47.32	1386.76	101.16
Terminal hydroxylated fatty acids (ω HFA)				
C16:1-ω HFA	7.37	0.6	10.37	2.76
C16-ω HFA	142.55	1.82	228.43	17.98
Subtotal	149.91	2.28	238.8	20.16
Epoxy fatty acids				
C18:1-9,10-epoxy-18- ω -HFA	2.34	0.24	5.93	0.79

C18-9,10-epoxy-18- ω -HFA	3.44	0.31	9.95	1.96
Subtotal	5.78	0.55	15.88	2.75
Other				
Naringenin	22.58	4.89	12.67	4.66
Naringenin dimer	23.88	0.49	28.21	2.79
Subtotal	46.46	4.66	40.88	7.01
Unknown				
Subtotal	187.38	6.46	289.03	16.9
Total	1387.09	53.86	2299.2	174.83

Cutin monomers quantified after BF3 depolymerisation of enzymatically isolated, dewaxed tomato fruit cuticles (red stage fruit). Concentrations (µg/cm^{-2}) shown for lines over expressing *SlMIXTA-like* (*SlMIXTA*-OE) and the corresponding wild type (WT). Extractions were performed on three independently transformed lines. Monomers that show significant changes (Student's *t*-test) from the wild type are indicated with a red outline (p<0.1, n=3), or shaded red (p<0.05, n=3).

Supplemental Dataset S3. Microarray gene expression data of SlMIXTA-RNAi lines and Wildtype lines. (Online resource: http://jmp.sh/vJrIUdx).

Supplemental Movie S1. Three-dimensional reconstruction from FIB-SEM acquisition of an epidermal cell from wild type tomato fruit. (Online resource: http://jmp.sh/vJrIUdx).

Supplemental Movie S2. Three-dimensional reconstruction from FIB-SEM acquisition of an epidermal cell from tomato fruit silenced for *SlMIXTA-like* expression. (Online resource: http://jmp.sh/vJrIUdx).

Appendix B

Supplemental data for Chapter 4.

Supplementary Table 1.

Supplementary Table 1. Oligos used in this study to measure gene expression

Gene ID	Name	Forward primer	Reverse primer
MDP0000287191	WSD11	CTCTGCAATGCATGTTCAGCAT	GGTCATGTGAGATGTTGCTTCTGT
MDP0000250127	KAS1	TGAAGAAGCAACATGAGGTTAACG	GGCTCAGTGCTCCCTTTCCT
MDP0000069348	CER1	TGATTGGCCATGGAAACCA	AATGACCCAAGGAGCCATGAT
MDP0000938736	KCS11	CTGTTATACAGGTGCCTCCCAATC	AGCTGATCAAGGGCACCAAA
MDP0000178263	SHN3	CTGCCACCGACCAAAACACT	TGGGTCTTTGCAGCATTTCC
MDP0000729533	BAHD-type acyl-transferase	GATGTGGTGCCTCTCGTAGCA	TGGCGGTGAGTTTAGGAAATCTAG
MDP0000391122	BAHD-type acyl-transferase	GCCAGTCAAGGATCCTCACAAG	CCCGCCACATTCAAAGAAGTT
MDP0000297929	DGAT1	GACGGCAATTCCTTGAACGA	CCGGCGTCGCAGATTTT

Supplementary Table 2. List of genes annotated within the QTL interval identified on chromosome 2. (Online resource: http://jmp.sh/vJrIUdx).

Supplementary Table 3. List of genes annotated within the QTL interval identified on chromosome 15. (Online resource: http://jmp.sh/vJrIUdx).

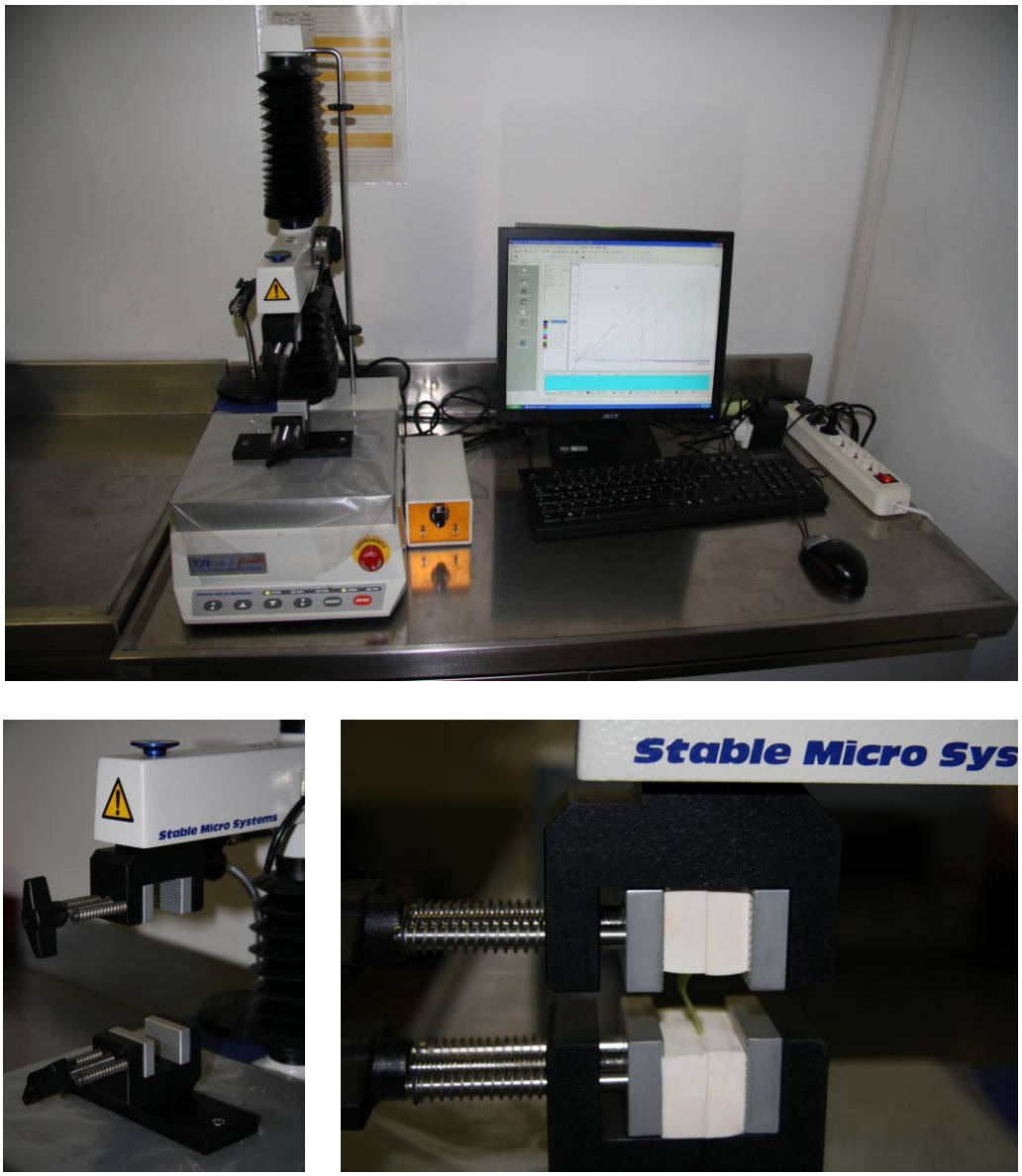

Supplementary Figure 1. Texture Analyzer device employed in this investigation. Clamps used to hold the peel for the tensile analysis are shown.

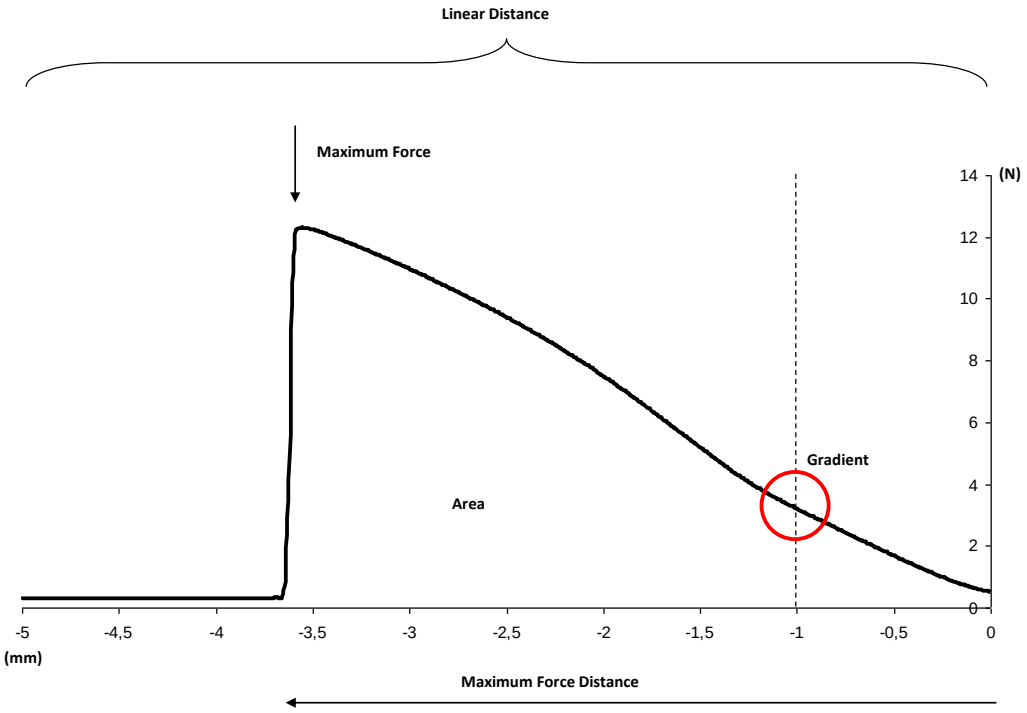

Supplementary Figure 2. Mechanical tensile profile with the five parameters identified by the macro highlighted. A dashed vertical black line indicates the point at -1 mm where the anchor was placed. The red circle indicates the intercept between the anchor and the mechanical profile, used to compute the Gradient (or elasticity module). The black arrow points the Maximum Force value, which represents the Force requires to break the peel. On the y-axis and x-axis force in Newtons (N) and the distance (mm) values are displayed respectively.

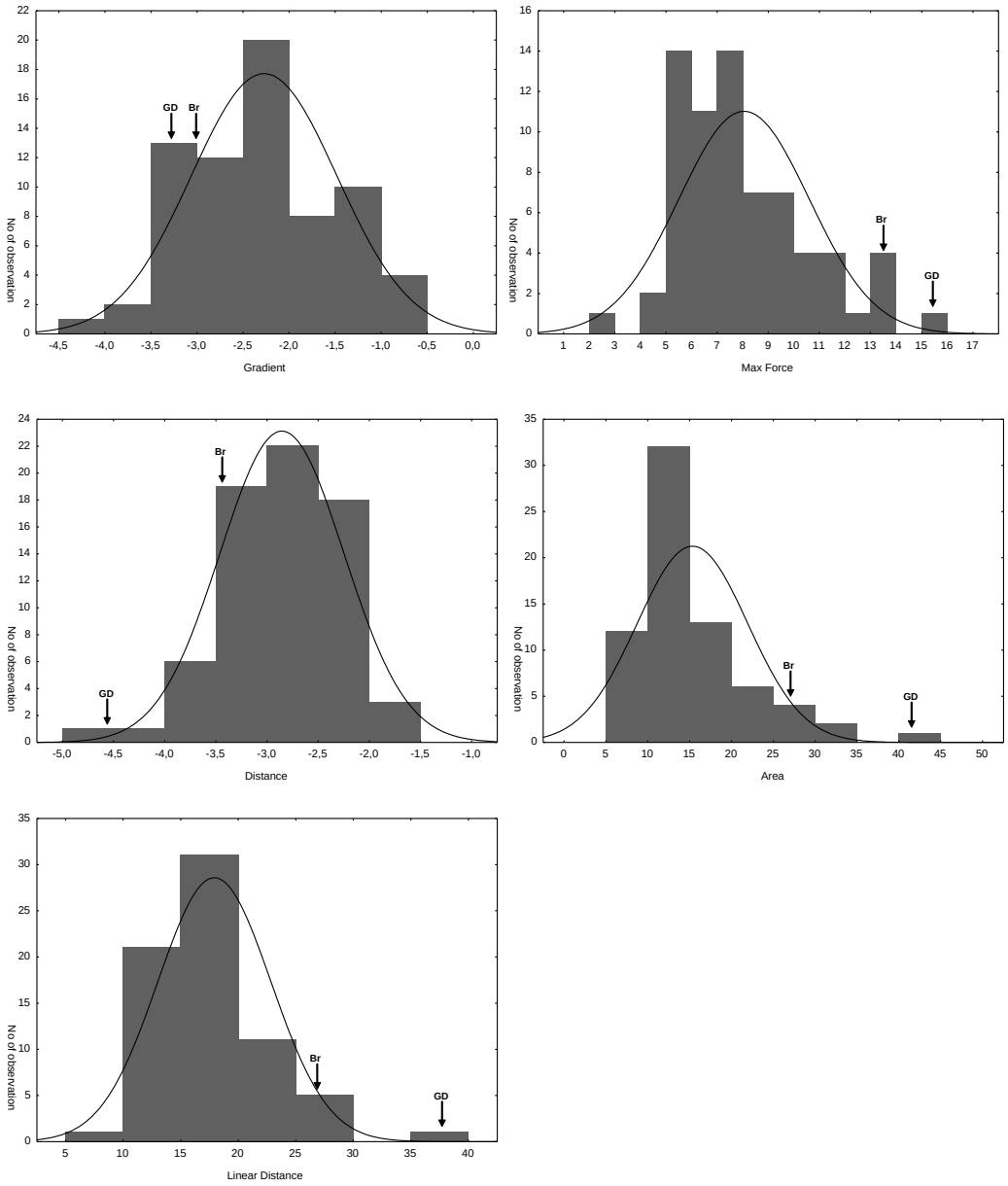

Supplementary Figure 3. Trait distribution over the 'GxB' progeny. For each measured parameter, the trait distribution is depicted. The position of the two parental cultivars is indicated with a black arrow (GD: 'Golden Delicious', B: 'Braeburn'). A fitting line for the normal distribution is shown. The x-axis of each panel shows the trait assessed, while the number of observations for each trait is reported on the y-axis.

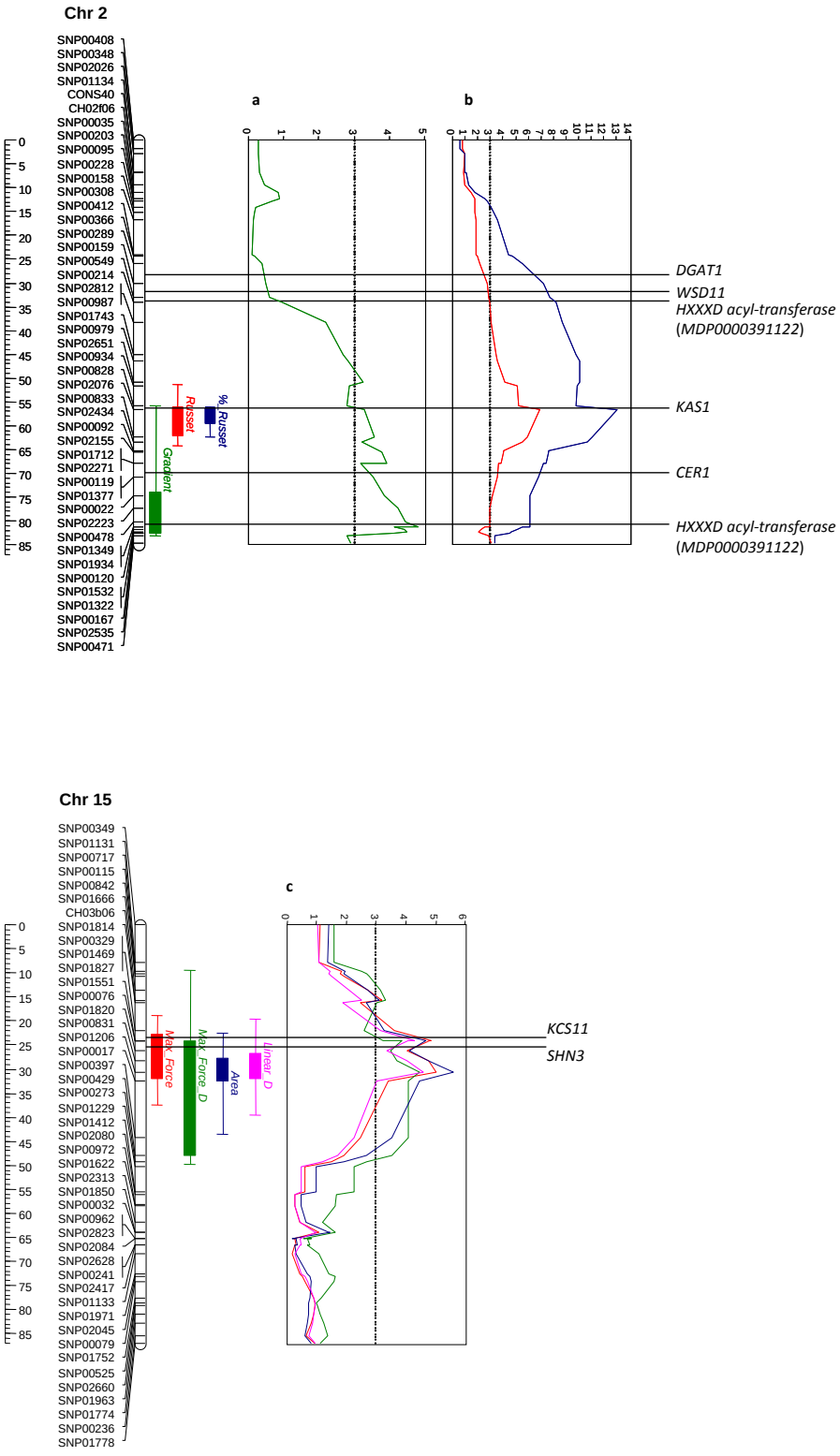

Supplementary Figure 4. LOD profile for the QTL associated to the two indexes. Used to estimate the russeting development (Russet and % Russet), as well as the five tensile parameters employed to characterize the mechanical performance of the apple fruit cuticle. Panel a and b pointed out the QTL profiles detected in chromosome 2, while panel c refers to chromosome 15. For each panel the dashed line indicates the threshold value established at LOD 3. Chromosomal position of genes identified as potential candidates are shown.

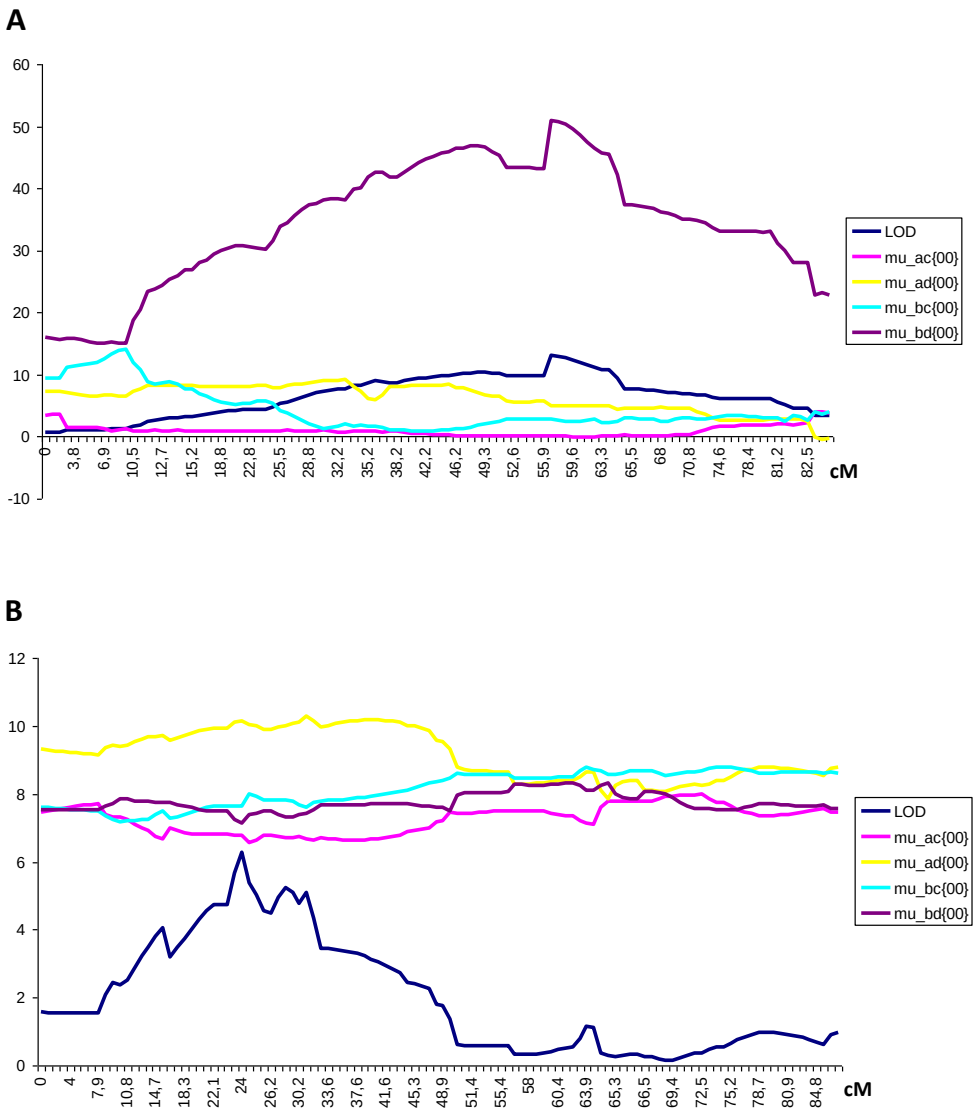

Supplementary Figure 5. Estimated Mean of the total distribution associated to each genotype class. Panel A reports the estimated mean calculated for the percentage of Russeting mapped on chromosome 2. Panel B is reports the estimated mean of the Maximum Force, mapped on chromosome 15. In both panel, the x-axis reports the cM of each respective linkage group. LOD value and estimated mean are reported on the y-axis and depicted by colored lines as indicated in the legend.

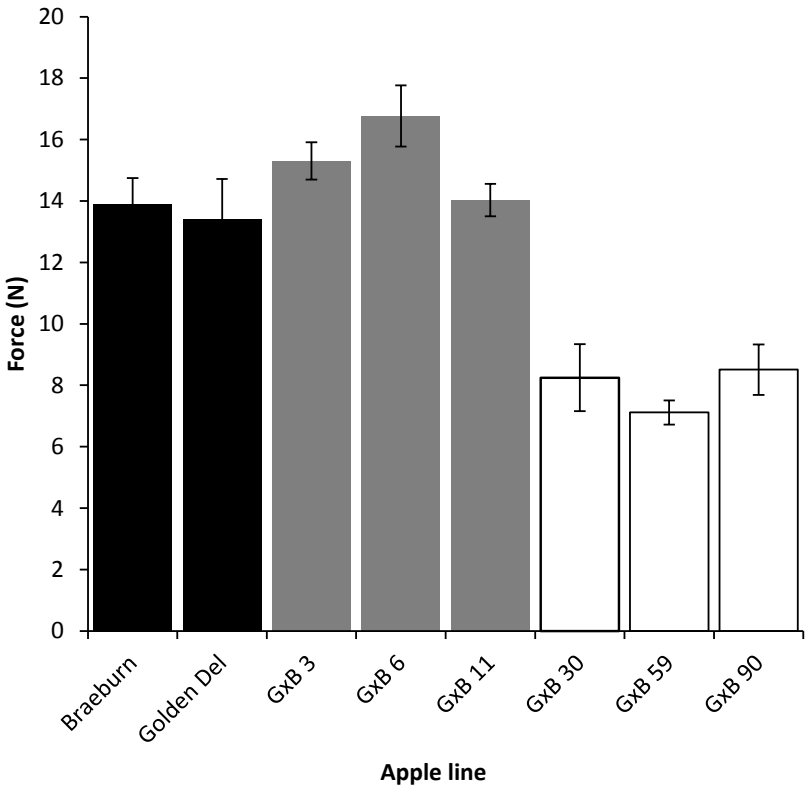

Supplementary Figure 6. Force required to break peels. Mechanical test of selected subset of progeny and parental lines indicates the dramatic reduction in require force to break peels of lines with compromised cuticles. Parent lines are colored black, progeny determined to possess regular cuticle are grey, and progeny displaying compromised cuticles are white. Error bars show standard error, (n=5).

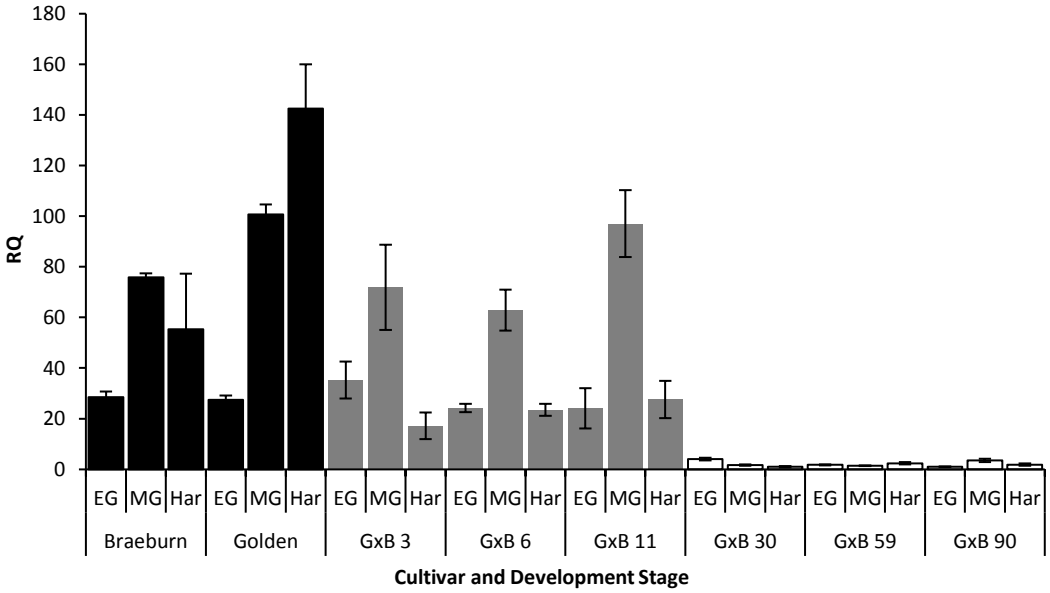

Supplementary Figure 7. Developmental gene expression analysis of *MdSHN3* in three specific stages of the fruit development. Early green (EG), mature green (MG) and harvest (Har). Parent lines are colored black, progeny determined to possess regular cuticle are grey, and progeny displaying compromised cuticles are white. Error bars show standard error (n=3). RQ, Relative quantification.

Appendix C

Supplemental data for Chapter 5.

Supplementary Table 1. Orthologous genes from tomato and apple enriched in both *SlDCR*-RNAi fruit skin and russeted apple skin

Orthologue Annotation	Tomato ID	$Log_2(DE)^a$	Apple ID	Russeted skin enrichment[b]	Functional Category
ASFT	Solyc03g097500	4.7	MDP0000258308	3 of 4	Suberin biosynthesis
CYP86B1	Solyc02g014730	2.0	MDP0000234292	4 of 4	Suberin biosynthesis
GPAT5	Solyc04g011600	2.1	MDP0000150502	4 of 4	Suberin biosynthesis
DAISY/KCS2/KCS1/KCS11	Solyc10g009240 Solyc08g067410	2.8 2.5	MDP0000296089	3 of 3	Suberin/Cutin Biosynthesis
4CL	Solyc03g117870 Solyc06g068650 Solyc12g042460	2.2 3.1 2.3	MDP0000260512	4 of 5	Phenylpropanoid metabolism
CCOAOMT1	Solyc01g107910 Solyc02g093230 Solyc02g093250 Solyc02g093270 Solyc10g050160	3.8 2.8 4.0 3.7 4.1	MDP0000226279	5 of 5	Phenylpropanoid metabolism
Caffeic acid 3-O-methyltransferase	Solyc10g005060	4.0	MDP0000224878	4 of 4	Phenylpropanoid metabolism
HYDROXYCINNAMOYL-COA SHIKIMATE/QUINATE HYDROXYCINNAMOYL TRANSFERASE	Solyc03g117600	2.9	MDP0000264424	3 of 3	Phenylpropanoid metabolism
FERULIC ACID 5-HYDROXYLASE 1	Solyc00g247300 Solyc12g042480	1.5 2.2	MDP0000127182 MDP0000193880	4 of 4 4 of 4	Phenylpropanoid metabolism
UDP-GLUCOSYL TRANSFERASE	Solyc01g095620	2.0	MDP0000146703	4 of 5	Flavanoid metabolism
Pectin lyase-like superfamily	Solyc02g093580 Solyc03g111690	3.7 2.9	MDP0000256522	4 of 4	Lignin metabolism
CYP98A3	Solyc01g096670	2.4	MDP0000428573 MDP0000563553	3 of 4 3 of 3	Lignin metabolism
GLUCURONOXYLAN METHYLTRANSFERASE 1	Solyc11g031950	2.0	MDP0000230688	3 of 4	Lignin metabolism
Pectin lyase-like	Solyc09g091430	2.5	MDP0000181608	3 of 4	Lignin metabolism
UDP Glucose Epimerase	Solyc02g069580	1.7	MDP0000507227	4 of 5	Carbohydrate metabolism
Rhamnogalacturonate lyase family protein	Solyc11g011300	1.7	MDP0000176803 MDP0000253529	5 of 5 4 of 4	Carbohydrate metabolism
BETA-GALACTOSIDASE 4	Solyc12g008840	1.5	MDP0000151981	3 of 4	Carbohydrate metabolism
PGSIP1 - PLANT GLYCOGENIN-LIKE STARCH INITIATION PROTEIN 1	Solyc11g005760	1.1	MDP0000277292	4 of 5	Carbohydrate metabolism
glycosyl hydrolase	Solyc08g082250	2.6	MDP0000131267	4 of 5	Carbohydrate metabolism
GLUCURONIC ACID SUBSTITUTION OF XYLAN 2	Solyc04g078990	2.0	MDP0000188710	4 of 4	Carbohydrate metabolism
O-Glycosyl hydrolase	Solyc12g014420	4.2	MDP0000321326	3 of 4	Carbohydrate metabolism
GLUCURONIDASE 3	Solyc07g007550	1.4	MDP0000199066 MDP0000088659	3 of 4 3 of 4	Carbohydrate metabolism
Pyruvate kinase	Solyc10g083720	1.7	MDP0000141814	4 of 5	Carbohydrate metabolism
ENDO-BETA-MANNASE 2	Solyc07g053920	1.7	MDP0000322330	3 of 4	Carbohydrate metabolism
LOX3, LOX4	Solyc03g122340	1.8	MDP0000264666 MDP0000423544	4 of 5 3 of 4	Lipid metabolism

Supplementary Table 1 (*cont.*).

GDSL-like Lipase/Acylhydrolase	Solyc03g115960	2.9	MDP0000266176	3 of 3	Lipid metabolism
GDSL-like	Solyc02g090210	4.4	MDP0000119418 MDP0000226662	4 of 4 4 of 4	Lipid metabolism
GDSL-like Lipase/Acylhydrolase	Solyc11g007180	2.0	MDP0000136589	4 of 4	Lipid metabolism
FATTY ACYL-ACP THIOESTERASE (FAT)	Solyc03g097390	1.7	MDP0000229149	4 of 4	Lipid metabolism
KAS1	Solyc02g070790	1.5	MDP0000189976	4 of 5	Lipid metabolism
LTP	Solyc06g054070 Solyc09g065420 Solyc09g065430 Solyc09g082270	1.7 2.2 4.8 5.0	MDP0000246150	4 of 4	Transporter/Lipid
Synaptotagmin-1-like	Solyc01g006620	1.5	MDP0000139392	4 of 5	Extracellular transport
ABCG16/ABGC6/ABCG20	Solyc05g054890 Solyc09g005970	2.1 2.6	MDP0000250717 MDP0000265619	5 of 5 4 of 5	Extracellular transport
Yellow Stripe like protein	Solyc03g031920 Solyc03g082620	1.1 1.9	MDP0000217063 MDP0000244211	3 of 3 5 of 5	Other (Transport)
Calcium-transporting ATPase	Solyc02g064680	1.1	MDP0000319861 MDP0000121822	3 of 4 5 of 5	Other (Chloroplast)
PHOTOSYSTEM I SUBUNIT G	Solyc07g066150	1.6	MDP0000481097	5 of 5	Other (Photosynthesis)
Expansin	Solyc06g005560 Solyc06g051800 Solyc06g076220	3.5 1.6 1.5	MDP0000504183	3 of 3	Other (cell growth)
extensin family protein	Solyc02g078040	1.7	MDP0000287357	4 of 4	Other (cell growth)
UBIQUITIN-CONJUGATING ENZYME19	Solyc11g065190	2.2	MDP0000267657	3 of 4	Other (cell growth)
strictosidine synthase	Solyc02g082900	1.1	MDP0000230954	3 of 3	Other (Alkaloid biosynthesis)
Cytochrome b561	Solyc09g019980	1.3	MDP0000267606	4 of 4	Other (brassinosteroid)
CHORISMATE MUTASE 1	Solyc02g088460	2.4	MDP0000191851	3 of 4	Other (Aromatic amino acid biosynthesis)
SERINE CARBOXYPEPTIDASE-LIKE 45	Solyc03g118370	2.0	MDP0000202104 MDP0000201966	3 of 3 3 of 4	Other (proteolysis)
metallopeptidase activity	Solyc08g076970	2.8	MDP0000418633	3 of 4	Other (proteolysis)
WRKY28	Solyc07g056280	7.0	MDP0000257129	5 of 5	Regulation
NAC39	Solyc08g006020 Solyc08g074300	3.4 1.3	MDP0000232008	5 of 5	Regulation
MYB107	Solyc04g056310 Solyc04g074170	1.9 1.9	MDP0000145757	4 of 4	Regulation
MYB67	Solyc10g005240	2.1	MDP0000226667	4 of 4	Regulation
MYB102	Solyc02g079280 Solyc10g005460	2.5 1.2	MDP0000197283 MDP0000492221	5 of 5 3 of 3	Regulation
MYB52	Solyc03g098270	3.0	MDP0000265114	4 of 4	Regulation
RECEPTOR KINASE 1	Solyc02g079590	1.3	MDP0000782875 MDP0000186156	3 of 3 3 of 4	Regulation
E3 ubiquitin-protein ligase RHA1B-like	Solyc08g081370	1.8	MDP0000184029 MDP0000237761	5 of 5 3 of 4	Regulation
CYCLIN D3	Solyc04g078470	2.6	MDP0000286130	4 of 5	Regulation
ABCB1	Solyc09g008240	1.6	MDP0000320690 MDP0000183294	3 of 3 4 of 5	Regulation
PROTEIN PHOSPHATASE	Solyc03g007230 Solyc06g051940	2.0 1.4	MDP0000296566	3 of 3	Regulation
CYP94B	Solyc07g006890	2.1	MDP0000228366	4 of 5	Regulation
O-fucosyltransferase	Solyc01g086640	1.7	MDP0000169312	3 of 3	Unknown
Unknown	Solyc04g078190	1.4	MDP0000420727	5 of 5	Unknown
Unknown	Solyc05g010010	4.1	MDP0000279566	4 of 4	Unknown
SGP1	Solyc07g064290	2.2	MDP0000129000	4 of 5	Unknown
Unknown	Solyc05g008210 Solyc05g008220	2.5 3.3	MDP0000247147	4 of 4	Unknown
BLUE COPPER BINDING PROTEIN	Solyc07g008110 Solyc07g008140	1.6 1.2	MDP0000204569	5 of 5	Unknown

Supplementary Table 1 (*cont.*).

alpha/beta-Hydrolase	**Solyc02g085180**	1.7	**MDP0000271408**	4 of 5	Unknown
PAR1 protein	**Solyc03g025670**	5.6	**MDP0000235103**	4 of 5	Unknown
Unknown (membrane bound)	**Solyc05g054900**	2.7	**MDP0000175065** **MDP0000185485**	3 of 3 4 of 4	Unknown
Unknown	**Solyc06g068620**	2.4	**MDP0000512591**	3 of 4	Unknown
Unknown	**Solyc02g082740**	2.3	**MDP0000242399** **MDP0000242401**	5 of 5 4 of 5	Unknown
Unknown	**Solyc12g009000**	1.5	**MDP0000788707**	3 of 3	Unknown
Unknown	**Solyc04g056580**	1.8	**MDP0000443966**	3 of 4	Unknown
Unknown	**Solyc01g080750**	1.5	**MDP0000213488**	3 of 4	Unknown

[a] Log_2(Differential Expression) *SlDCR*-RNAi vs Wildtype. See Supplementary Dataset 1 for details.
[b] Number of developmental stages in which Russeted skin tissue ('Rugiada' clone) displays a 2 fold increase in expression when compared with normal skin tissue ('Renders' clone) at the same stage. See Supplementary Dataset 2 for details.
See Fig.3 for expression patterns of selected genes.

Supplementary Table 2. Multi-species gene expression signature for suberin biosynthesis

Gene Name	Experiments represented	Genes identified as co-expressed with suberin biosynthesis
MYB107*	7	AT3G02940; VIT_16s0039g01710; Solyc04g074170; MDP0000145757; PGSC0003DMP400011365; LOC_Os03g27090
SUS*	7	MDP0000119418; MDP0000226662; AT2G23540; Solyc02g090210; PGSC0003DMP400017853; VIT_07s0255g00030; LOC_Os07g47210.1
DAISY/KCS2*	6	MDP0000296089; AT4G34510; Solyc05g009280; PGSC0003DMP400025664; ; LOC_Os03g12030.1; Solyc10g009240
CYP86A1*	6	AT5G58860; Solyc06g076800; PGSC0003DMP400052827; VIT_06s0004g06210; LOC_Os02g44654.2
Cupredoxin	6	MDP0000185485; Solyc05g054900; PGSC0003DMP400040688; VIT_16s0013g00590; LOC_Os04g46120.1
ABCG20*	5	MDP0000250717; AT5G13580; PGSC0003DMP400041348; LOC_Os01g61940.1; Solyc05g054890
LTPG5*	5	MDP0000246150; AT3G22600; Solyc06g054060; PGSC0003DMP400033570; Solyc09g082270
NAC038*	5	AT2G24430; Solyc08g006020; PGSC0003DMP400026135; VIT_04s0008g02710; Solyc08g006020
WRKY56*	5	AT1G64000; Solyc08g081630; PGSC0003DMP400021797; VIT_15s0046g02150; LOC_Os01g53260.1
LTP	5	AT3G22620; Solyc09g082290; PGSC0003DMP400028420; VIT_05s0020g03750; Solyc03g005210
NAC058	5	MDP0000130785; AT3G18400; Solyc12g036480; PGSC0003DMP400009522; VIT_17s0000g03660
Peroxidase	5	AT1G68850; Solyc05g010330; VIT_01s0010g01090; LOC_Os06g16350.1
SGNH hydrolase*	5	MDP0000302547; AT5G37690; Solyc11g011110; PGSC0003DMP400027503
GDSL-motif esterase*	5	AT1G74460; Solyc03g115960; PGSC0003DMP400033937; VIT_17s0000g06290
ABCG23	5	AT5G19410; ; PGSC0003DMP400042299; VIT_06s0009g03380; LOC_Os05g31910.2; Solyc03g113690
EDA4	5	AT2G48140; Solyc09g065440; PGSC0003DMP400033636; VIT_07s0151g00700
LOX2	4	AT3G45140; Solyc09g055890; VIT_14s0128g00780; Solyc03g122340
RmlC-like cupins	4	AT5G39110; PGSC0003DMP400027184; VIT_14s0128g00690; Solyc01g102900

Supplementary Table 2 (*cont.*).

4CL5	4	MDP0000260512; AT3G21230; PGSC0003DMP400034532; Solyc06g068650
LAC5	4	AT2G40370; Solyc06g050530; PGSC0003DMP400052877; Solyc06g050530
ABCG10	4	AT1G53270; PGSC0003DMP400021989; VIT_19s0014g01540; LOC_Os01g42900.1
MYB67*	4	MDP0000226667; AT3G12720; PGSC0003DMP400019994; Solyc10g005240
alpha/beta-Hydrolase	4	MDP0000145289; AT4G24140; LOC_Os06g04169.1; Solyc08g008610
CASPL1B2	4	AT4G20390; Solyc02g069730; PGSC0003DMP400036745; Solyc02g069730
Glycine-rich protein	4	Solyc01g060260; PGSC0003DMP400013364; VIT_05s0077g01330; LOC_Os01g14990.1
PELPK1*	4	AT5G09530; Solyc04g007810; PGSC0003DMP400001617; Solyc01g105770
ABCG35	3	Solyc09g091660; VIT_09s0002g05530; Solyc03g120980
Synaptotagmin-1-like*	3	AT5G12970; Solyc01g006620; PGSC0003DMP400037009;
Rhamnogalacturonate lyase	3	MDP0000144890; PGSC0003DMP400025712; Solyc11g011300
LACS2	3	Solyc01g095750; PGSC0003DMP400000465
Xanthine/uracil permease family	3	AT1G49960; PGSC0003DMP400044823; Solyc01g106920
Pectin lyase-like superfamily	3	MDP0000256522; AT5G63180; Solyc02g093580
unknown function	3	MDP0000279566; LOC_Os05g50160.1; Solyc05g010010
CASPL1D2	3	AT3G06390; PGSC0003DMP400039275; Solyc01g067300
ATL1	3	MDP0000192786; AT1G04360; Solyc09g066300
Unknown function	3	PGSC0003DMP400021659; LOC_Os10g37400.1; Solyc08g083090
Unknown function	3	PGSC0003DMP400033569; VIT_07s0151g00740; LOC_Os07g07860.1
Heavy metal transport	3	PGSC0003DMP400011529; VIT_15s0045g01140; Solyc10g039390
Unknown function	3	MDP0000229149; VIT_17s0000g01090; Solyc03g097390
LTP	3	AT5G13900; Solyc01g103060; PGSC0003DMP400036008
Unknown function	3	MDP0000136589; PGSC0003DMP400033851; Solyc11g007180
PDLP4	3	AT3G04370; Solyc05g055930; Solyc05g055930
PELPK2	3	AT5G09520; Solyc04g014320; Solyc04g014330

Genes identified from datasets described in the text from Tomato, Apple, *Arabidopsis*, Potato, Grape and Rice. A graphical representation of the data can be seen in Fig. 4.
*A homozygous *Arabidopsis* T-DNA line was identified for these genes.

Supplementary Table 3. Oligonucleotides used in this study for cloning and qRT-PCR analysis.

Gene	Gene ID	Primers	Sequence
SlDCR	Solyc03g025320	RNAi-F	TCATATTCCACCTTAAATACTCCTTC
		RNAi-R	TTAGATAGGTTGAGTTTGACTCGAGTG
		RT_F	TGATTCAGCAAGCCATAGCG
		RT_R	CCGGCATCTTTGTACGCAA
SlGPAT5	Solyc04g011600	RT_F	CACTAACTCGGGCGTGCTCT
		RT_R	AGTACGTCACGGCCGGTATC
SlGPAT5b	Solyc05g053030	RT_F	TGGCAAAGTCATAGTCAAAGGAAAT
		RT_R	GTGCGGTGAGTGCATACGAA
SlGPAT4	Solyc01g094700	RT_F	CGCGATTGCGTACGTATTTG
		RT_R	GCGAAGCCAGCTCAATGTC
SlGPAT6	Solyc09g014350	RT_F	GGTACACCCCCACCACCC
		RT_R	CCTAGTGCAACAGCAGTAACAACG
SlGPAT6-like-a	Solyc02g087500	RT_F	CCGTGGCACGAGCTGTTC
		RT_R	CACACCTTTTCCCACATGATGA
SlGPAT6-like-b	Solyc04g005840	RT_F	TGGATCCCGATTGGATTCAT
		RT_R	GAACGCCTAACGCCCAAAA
SlGPAT6-like-c	Solyc10g084900	RT_F	GTTTCATCAAAAAGCTAACCCCACTA
		RT_R	CACTGAGACGCACACATGCA
SlGPAT9	Solyc08g082340	RT_F	TCCTGGGTGGGTCGGATTA
		RT_R	ATTTCACGATCCTTGGCTTCTG
SlGPAT1	Solyc07g056320	RT_F	GGAACAACATGTAGGGAGCCATAT
		RT_R	TTGTGTTCATAGCCACTGGTACTATTTC
SlASFT	Solyc03g097500	RT_F	GGGTGAAATTGCGAGAGGTTT
		RT_R	ATACTCAGGCTTTGGTGGATTTCTAG
SlASR1 (endogenous control for tomato)	Solyc04g071610	RT_F	CCTGTTCCACCACAAGGACAA
		RT_R	GTGCCAAGTTTACCGATTTGC
AtMYB107	At3g02940	RT_F	CCTCTCTCACATTGACGATCAGC
		RT_R	TCGAAATCAAGGGCGGAATA
AtMYB9	At5g16770	RT_F	CAGTCTCAAAACTTCTCTCACATTCTTG
		RT_R	TGAAAACCGGGTTGTATGGG
AtASFT	At5g41040	RT_F	TCGAGCCTCAACTGCCAAA
		RT_R	TTTTTCGATAAGCTCCCCAGC
At4CL5	At3g21230	RT_F	TTTCACATTTACGCTCTCGACG
		RT_R	TTCAACTCGAACCTCGGCAC
AtGPAT5	At3g11430	RT_F	CCCGGAGAACTACAACCACG
		RT_R	GCCGCTTCACTAGTCTTCCGT
AtCYP86B1	At5g23190	RT_F	AACGGTGGTCCACGCCTT
		RT_R	TTGTACCGATAAACTATTGCGGC
AtSUS	At2g23540	RT_F	TATTGGCGACATGCTTGAACAT
		RT_R	CAACGTTCCCGATCACAAACTT
AtCASPL1B2	At4g20390	RT_F	ACAAGCACGCCAAGTGGAAC
		RT_R	GGCGAATGCTGCGATGAT
AtLAC5	At2g40370	RT_F	AGCCAAAGCTTCCGGTCACT
		RT_R	TTGAGACCGAGTCCGATGGT
AtABCG6	At5g13580	RT_F	TGTCTTCAGCGGATCGCC
		RT_R	ACTCGGTGCGGTTCTCATGT
AtABCG20	At3g53510	RT_F	AATTCGGTCACCCAATTCCTG
		RT_R	TCCTTCTGGCGAATCTTCCA
AtUBIQUITIN-C (endogenous control for *Arabidopsis*)	At5g25760	RT_F	AGCGCGACTGTTTAAAGAATACA
		RT_R	TTGTGCCATTGAATTGAACCC

Supplementary Table 4. Oligonucleotides used in this study for the screening of *Arabidopsis* T-DNA insertion lines.

Gene ID	Name	Stock ID	Left Primer	Right Primer
AT5G41040	ASFT	SALK_062055C	AAACACATCCATGGCTGTAGC	TTACTATCCTCTCGCTGGACG
AT5G41040	ASFT	SALK_101708	CAAAAATTGGGAGGCCTACTC	AGGATCGGGTTTGGTAATGTC
AT5G23190	CYP86B1	SALK_130265	TACACGAGAACCAAGAGCCAC	CCCTTCTCATCTCTCAGACCC
AT5G23190	CYP86B1	SALK_130268	CTTCTTCCTCCAGTGACCCTC	TTCTGGTCCAAACACAGGTTC
AT3G11430	GPAT5	SALK_018117C	TGGTTGAAAATACAAAGATCCG	TTCGGACAAATGGTGAATTTC
AT3G11430	GPAT5	SALK_142456C	ATTCGGTCGTGTCAGAGTTTG	ATACCACAGGGTCCATTAGGG
AT1G72520	LOX4	SALK_071732C	GTTGGTTCCAAATACACACGG	AGCCAAAGAAGAGTAAAGCGG
AT1G72520	LOX4	SALK_138527	CAAACCGATCTTCAATATCCG	TTGTTTTTGTTCCTCACCGTC
AT1G17420	LOX3	SALK_062064	CGCATTTCAAGAAGAGGACAC	GTAAGGAACCTCTTTGCCACC
AT1G17420	LOX3	SALK_147830C	TAGCGTTCAACATAGGTTCGG	ACGCATGGTTAAGAGATGACG
AT1G74460	GDSL-like-1	SALK_138130C	TCGATCATCTGCCTGAATTTC	TTTCGTTCAAGATTCCACCAC
AT1G74460	GDSL-like-1	SALK_150084C	TCAGTGTCCAACGGCTTAAAC	TTTCGTTCAAGATTCCACCAC
AT2G23540	SUS	CS325715	ATCCAAATCCTGGTTCACTCC	AACACGGTTCACTCAAACTCC
AT2G23540	SUS	SALK_016914	TACCAACGATATCACCGATGG	TTGACTTGAGAGATTTTGGGTG
AT3G22600	LTP	SALK_007462C	TGGGATGCGTACATGTGTATG	ATGTAGTTGAGACACGGCGAC
AT3G22600	LTP	CS873225	TAGACCGTCACAAAGACCACC	ACAACAAAGCAATATCACCCG
AT5G12970	Synaptotagmin-1-like	SALK_079441C	GTAGCTTGTGCCTGAACCTTG	TATTGCGTGGCTAAGTATGGG
AT5G12970	Synaptotagmin-1-like	CS834176	CAGAGGGACTAATTGGAAGCC	CACTGTCGCTGTTACTTGAGC
AT3G55090	ABCG16	SALK_087501	ATCCCATACGTCAATTCTCCC	ACGTGGACACACCGTCTTTAG
AT3G55090	ABCG16	SALK_119868C	TTCTTCCACAATCTCAATGCC	CAGACGCTCAATCCTCAACTC
AT5G13580	ABGC6	SALK_006247	AACAACAATGGAAAGCCACAG	TTAGCCGGAGAAGAAAAGAGG
AT3G53510	ABCG20	SALK_011548C	GTTGGAAATCCAATTAACCCC	TTGAAATCCGATTGGCTAATG
AT3G53510	ABCG20	SALK_086914	GTTGGAAATCCAATTAACCCC	TTGAAATCCGATTGGCTAATG
AT2G24430	NAC38	SALK_103716C	AATATCCTGTATTCGTCGCCC	ATGAACGGAAGTCATGCATTC
AT2G24430	NAC38	SALK_025040C	GTCGCAAGTCATCCTTGTCTC	TCCGTTCGATAAGCTCATGTC
AT3G12720	MYB67	CS473352	GTGCTCATTCGCTTCTACGAC	CTCTTCCCACATCTCTGCAAC
AT1G17950	MYB52	SALK_118938C	TGGTTTGATTGGATCTTTTGG	AACCCTGAGAGGCAGAGTTTC
AT1G17950	MYB52	SALK_138624C	AAAAGGATGTTCATTTGGTGG	TGCAAGTAAATGAGTAATGGTGC
AT4G36990	HSFB1	SALK_012292	ACTCCGATCTTCTCCGTTCTC	CAGACTTTGCTGCTTTTCCAC
AT4G36990	HSFB1	SALK_149259	CGAGGGAAAAATATTCAACGG	GGATCTGTTGACGGACATACG
AT1G65790	Receptor Kinase 1	SALK_024564C	ATTACATGACTTGGTCCGCAG	ACGTATGGGTTGCAAACAGAG
AT1G65790	Receptor Kinase 1	CS818550	TGTACTTTGTTGACCAAAGCC	ATTGGGATGGGATCAGAAAAC
AT2G18360	Alpha/beta hydrolase	SALK_062293C	CGTTTCAAGCCCACTGTTTAG	GGGTTTTGAAGTTTAGACCCG
AT2G18360	Alpha/beta hydrolase	CS441284	GGGTCTAAACTTCAAAACCCG	TGACACTTTTGTAATTGGGCC
AT4G05100	MYB74	SALK_073544C	TTGATTGACTTAATGGCCCAC	CTCCACGTCTTGATCTTCTCG
AT3G02940	MYB107	CS811227	TTGATGTGTTTTCTGATTTTTGC	GCTGAATTGGACTGGTGAGAC
AT5G16770	MYB9	SALK_149765C	TGGAATCGCAGTTTTTCTAGC	CGTGCATAAATATTTGCATGTG
AT5G16770	MYB9	CS463394	TAACGTCTCCACGTGGAAAAC	TCCATGGCCCTTTCTTTAGAC
AT1G04220	DAISY/KCS2	SALK_033206C	CTTCAGACCGTCTAAACGCAG	CTTTTTCGCAACACTAGTGGC
AT1G04220	DAISY/KCS2			
AT3G25640	MIZU like	SALK_026189C	ATCAAAGCGGCAAATAAAATC	ACCCATTGTTATAGGCCCAAC
AT3G25640	MIZU like	SALK_062005C	GACGTGCCATATCCTTACATTC	TAAACGAGTCGGGTCATCTTG
AT4G34510	KCS17	SALK_041520C	TTTATTACGAGAATGCCACCG	TAACTTTTTGACTCGAAGGCG
AT4G34510	KCS17	CS412227	ACTGTCCATGGATGCTAATGG	CTAGCTCATCAATCACGGCTC
AT4G34250	KCS16	SALK_035139C	TGTTATCAAGAGAAGCAGCAGC	AGCCTTACGTGTTGCATGATC
AT4G34250	KCS16	SALK_110690C	TGTTATCAAGAGAAGCAGCAGC	AGCCTTACGTGTTGCATGATC
AT5G47635	PollenOle1	SALK_097824C	ACTGCATCGACCAATCAGATC	AACAAGAAGCAACGGATGATG
AT5G47635	PollenOle1	CS848051	ACGACAAAACCAACACCTCTG	ATCCAAAAGGAGGTCCAAATG
AT5G37690	SGNH hydrolase	SALK_056924C	ACCATGAATGTTGGGGTACTG	GTGTCAACGAATGGGTATTGG
AT5G37690	SGNH hydrolase	SALK_004046C	CCCTACACAATCAGCTTACGG	TAAAGACCCGTAACGCAAATG
AT5G09530	PELPK1	SALK_125547C	TGTTTGAGGCGGTGAGTAATC	CCTAAGGTACCGGAGATCCAG
AT5G09530	PELPK1	SALK_007409C	TGTTTGAGGCGGTGAGTAATC	CCTAAGGTACCGGAGATCCAG
AT1G64000	WRKY56	SALK_130727	CAGTCAAGCGAGCAAGATTTC	GGAGGAAAGACTTAGGCAGTTG
AT5G58860	CYP86A1	SALK_049867	TTCCTCATCTTCCACGTCATC	ACCAGGATTTCAAATACGTCG
AT5G58860	CYP86A1	SALK_050126	TTCCTCATCTTCCACGTCATC	ACCAGGATTTCAAATACGTCG

Supplementary Table 5. Parameters used for co-expression analysis.

Species	Baits	r-value cut-off	No. of identified co-expressed genes
Tomato	*SlASFT* (*Solyc03g097500*); *SlCYP86B1* (*Solyc02g014730*); *GPAT5* (*Solyc04g011600*)	0.75	650
Apple	*MdCYP86B1* (*MDP0000234292*); *MdGPAT5* (*MDP0000150502*)	0.70	305
Arabidopsis	*AtASFT* (*At5g41040*); *AtCYP86B1* (*At5g23190*); *AtGPAT5* (*At3g11430*)	0.75	289
Grapevine	VvGPAT5 (VIT_13s0019g01990); VvASFT (VIT_17s0000g00950); VvCYP86B1 (VIT_01s0011g02060)	0.65	201
Potato	*StCYP86B1* (*PGSC0003DMP400018704*); *StASFT* (*PGSC0003DMP400054926*)	0.65	252

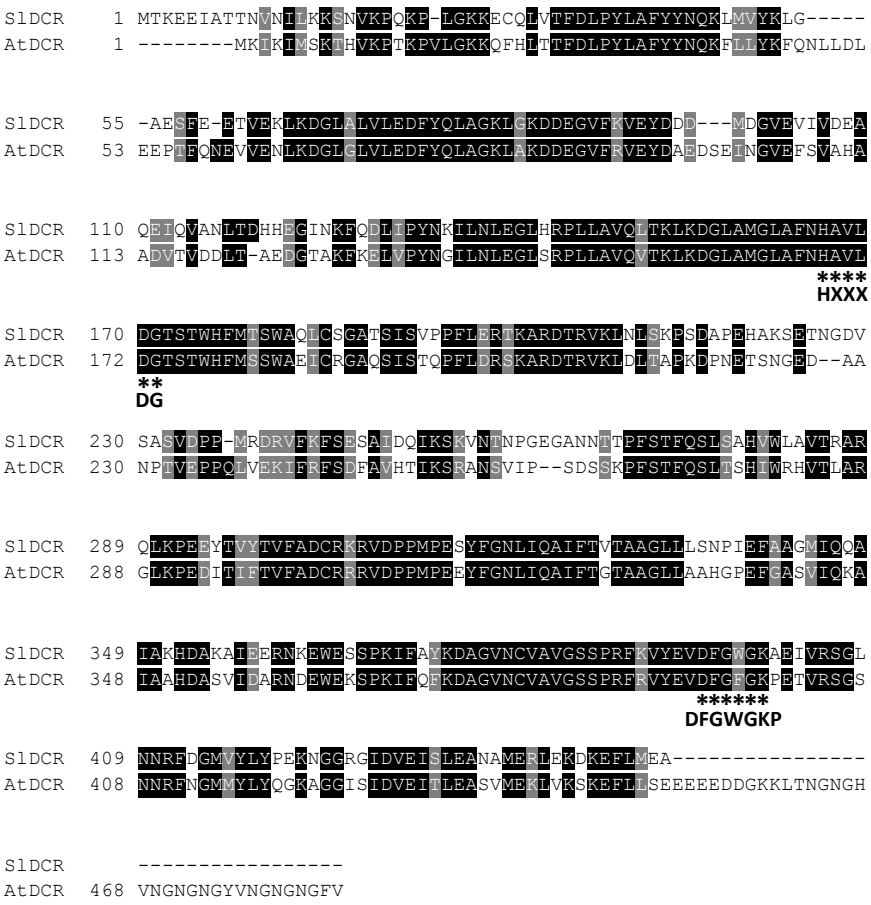

Supplementary Figure 1. Protein alignment of tomato and *Arabidopsis* DCR. ClustalW and the MEGA6 software were used to align the proteins in all cases. HXXXDG domain is indicated.

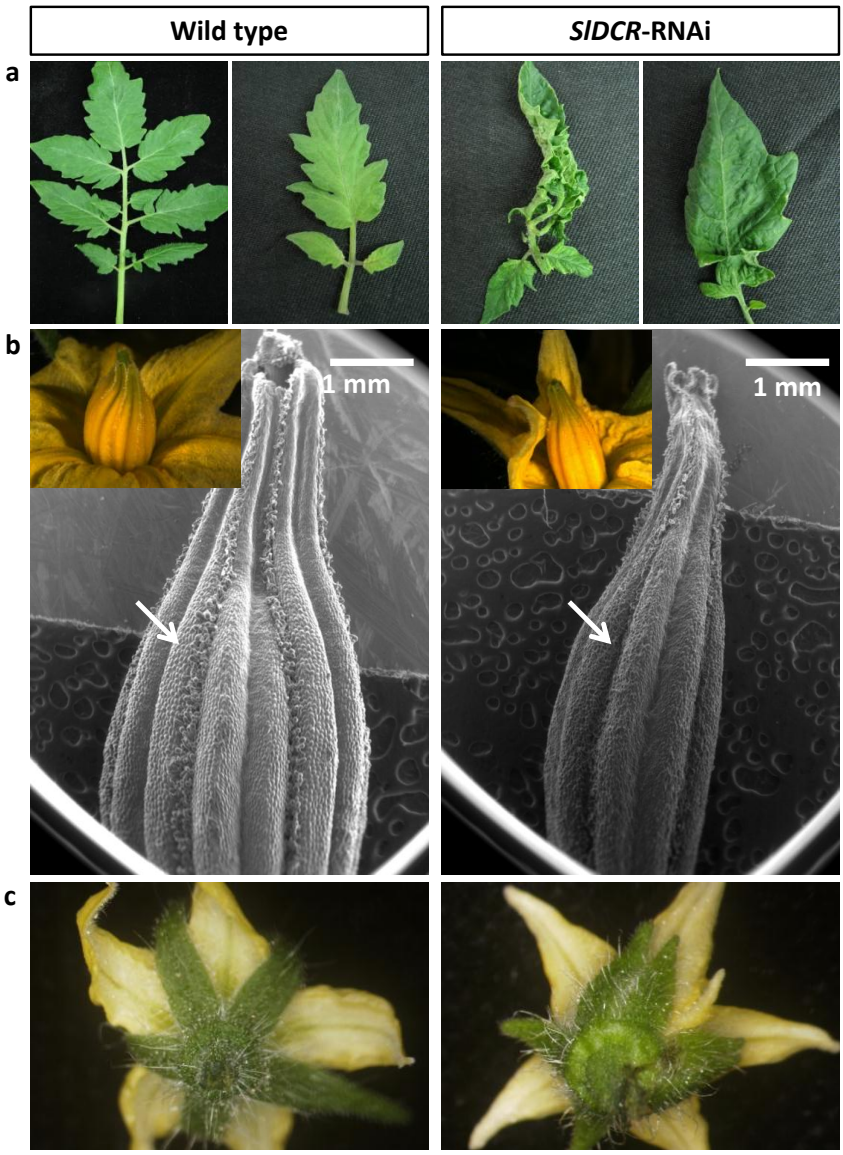

Supplementary Figure 2. Organ fusion phenotypes resulting from silencing of *SlDCR* in tomato. (**a**) Leaves of *SlDCR*-RNAi lines were crinkled. (**b**) Fusion of anthers of *SlDCR*-RNAi lines. (**c**) Fusion of sepals of *SlDCR*-RNAi lines.

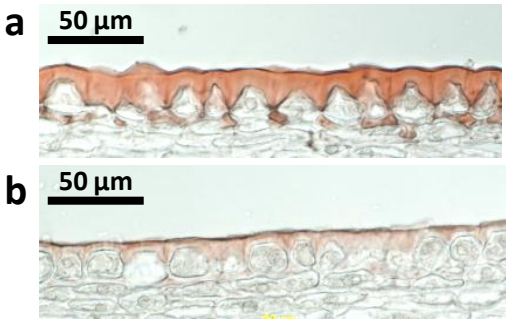

Supplementary Figure 3. Light microscopy of fruit cuticle of *SlDCR*-RNAi lines. (**a**) Wild type and (**b**) *SlDCR*-RNAi cuticles are stained red with Sudan IV. A dramatic reduction in cuticle is observed in *SlDCR*-RNAi lines.

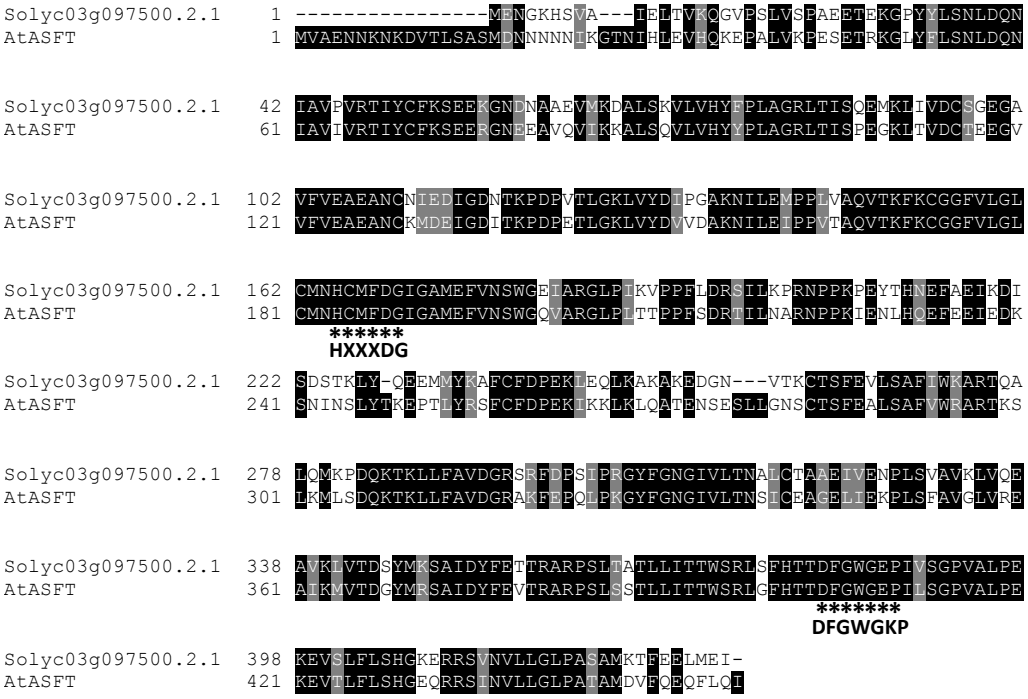

Supplementary Figure 4. Protein alignment of tomato and *Arabidopsis* ASFT. ClustalW and the MEGA6 software were used to align the proteins. The HXXXDG domain is indicated.

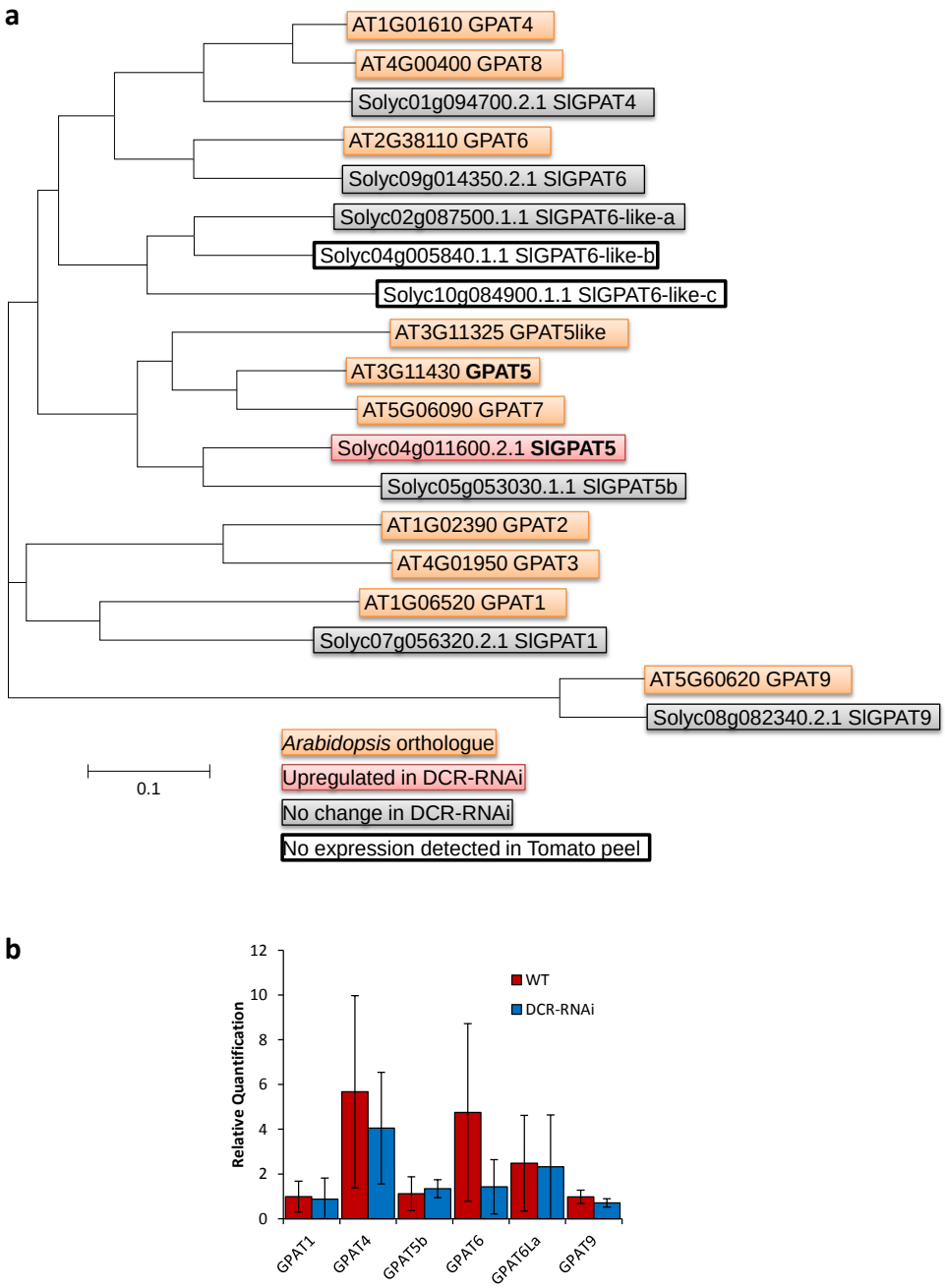

Supplementary Figure 5. Expression analysis of the *GPAT* gene family in tomato silenced for *SlDCR*. (**a**) Molecular phylogenetic analysis of the *Arabidopsis* GPAT protein clade is shown together with GPAT members from tomato analysed in this work. ClustalW and the MEGA6 software were used to align the proteins and compute the neighbor-joining tree. The scale bar represents the relative amino acid difference. Relevant information regarding functional annotation of some characterized proteins is also displayed. (**b**) qRT expression data for the *GPATs* in mature green stage tomato peel.

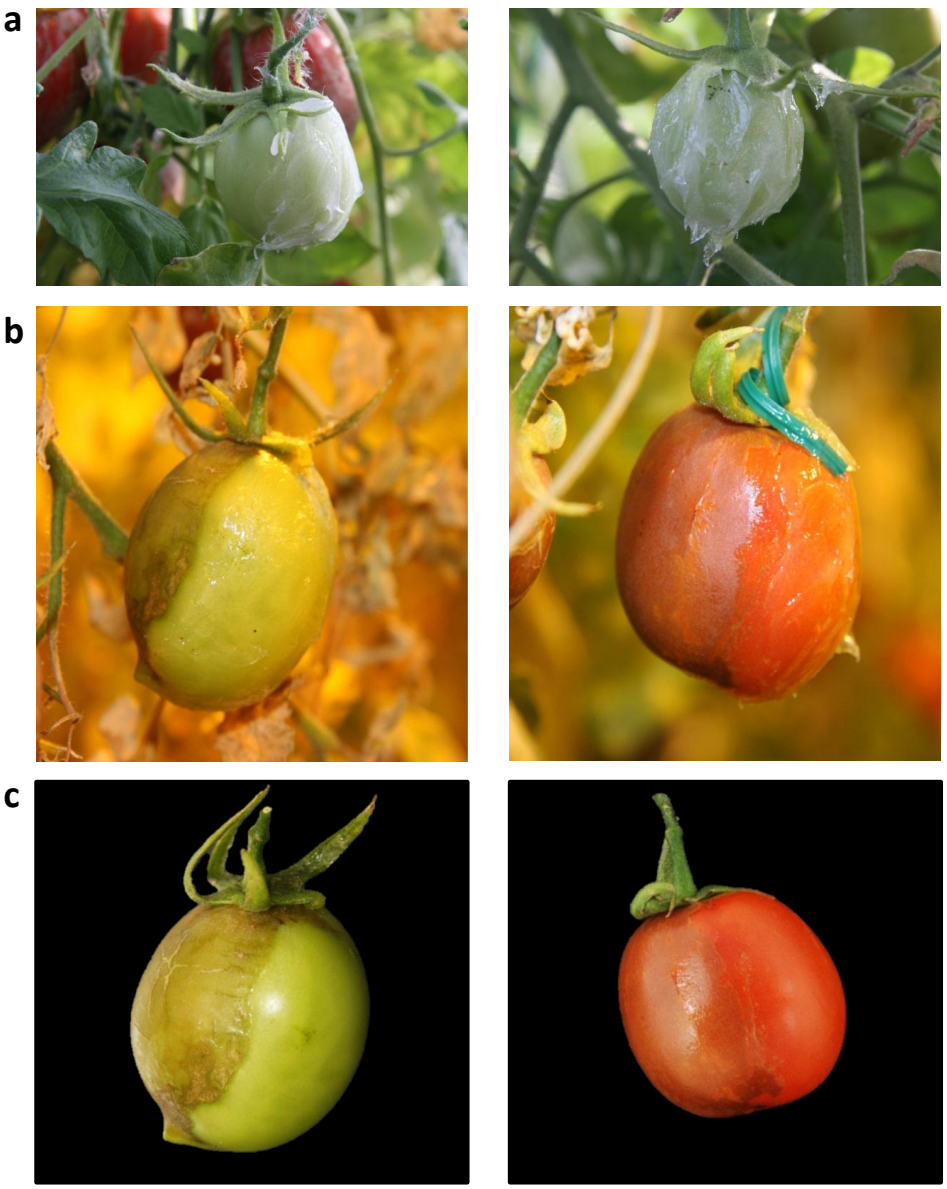

Supplementary Figure 6. Application of petroleum jelly to developing tomato fruit silenced for *SlDCR* expression. (**a**) Jelly was applied at the immature green stage of tomato development to half the tomato. (**b**) Tomatoes on the plant, still with jelly covering and (**c**) removed from the plant and jelly removed, showing absence of suberin formation in areas previously covered with jelly.

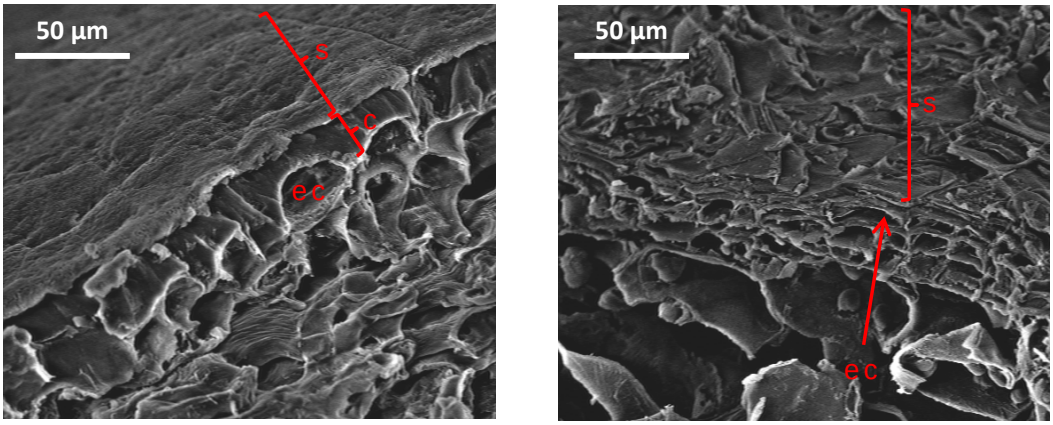

Supplementary Figure 7. SEM analysis of Apple surface. The normal skinned 'Renders' clone shows a thick cuticle layer, and a relatively smooth surface, while the cuticle layer of the russeted 'Rugiada' clone is not observable and the fruit surface is extremely rough. s, fruit surface; c, cuticle layer; ec, epidermal cell.

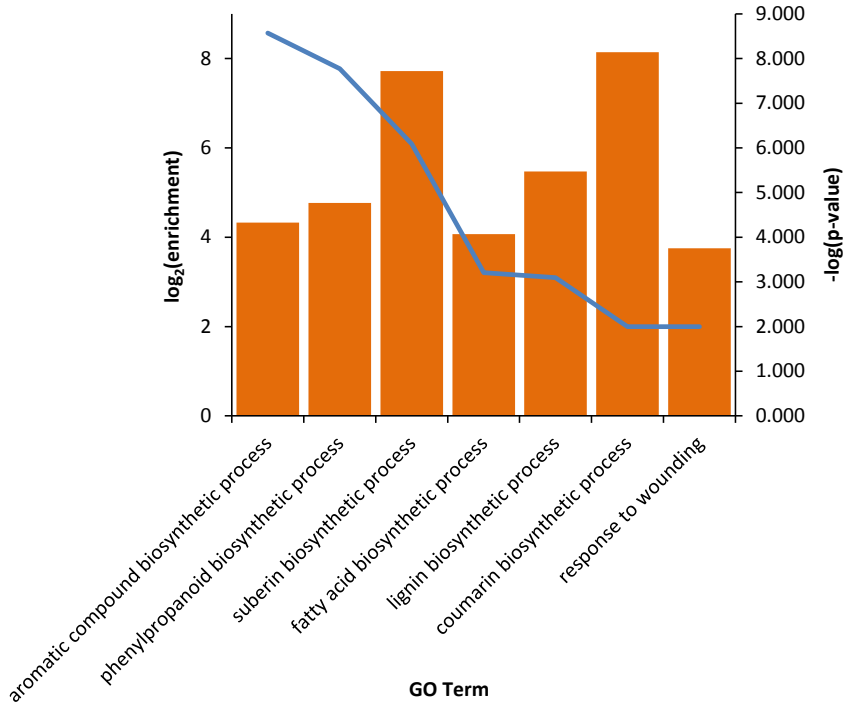

Supplementary Figure 8. GO enrichment analysis of orthologous genes found up regulated in suberized tomato and apple fruit surfaces.

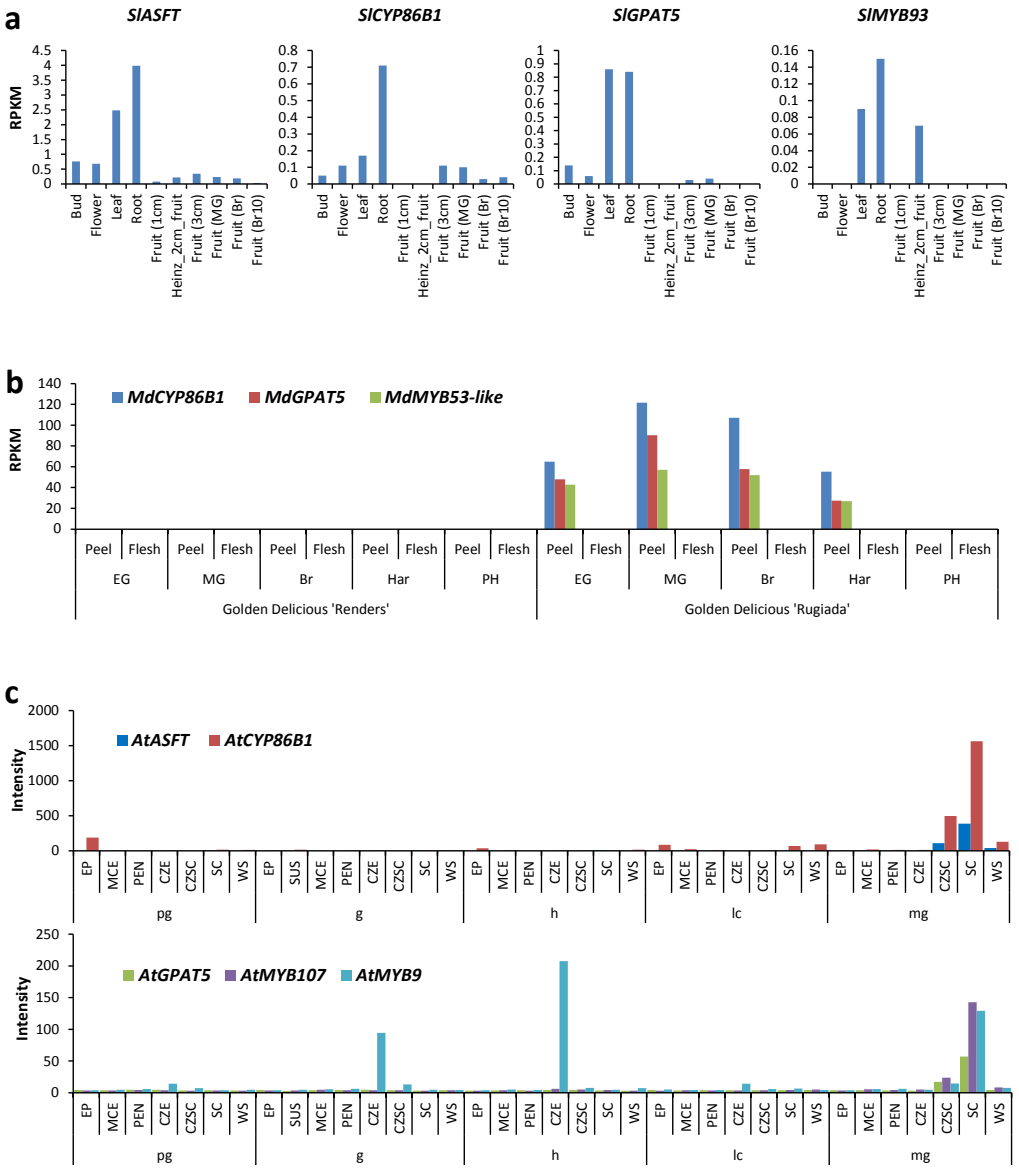

Supplementary Figure 9. Expression patterns of the co-expression 'baits' and the described MYB factors. Data was extracted from the relevant large scale expression experiments used in this work to perform the multi gene co-expression analysis. Data is shown for (**a**) tomato[33], (**b**) apple (See Supplementary Dataset 2), (**c**) *Arabidopsis*[31], (**d**) potato[34], (**e**) grape[32], (**f**) rice[35] and (**g**) *SlDCR*-RNAi tomato (See Supplementary Dataset 1). For full descriptions of samples see the referenced works.

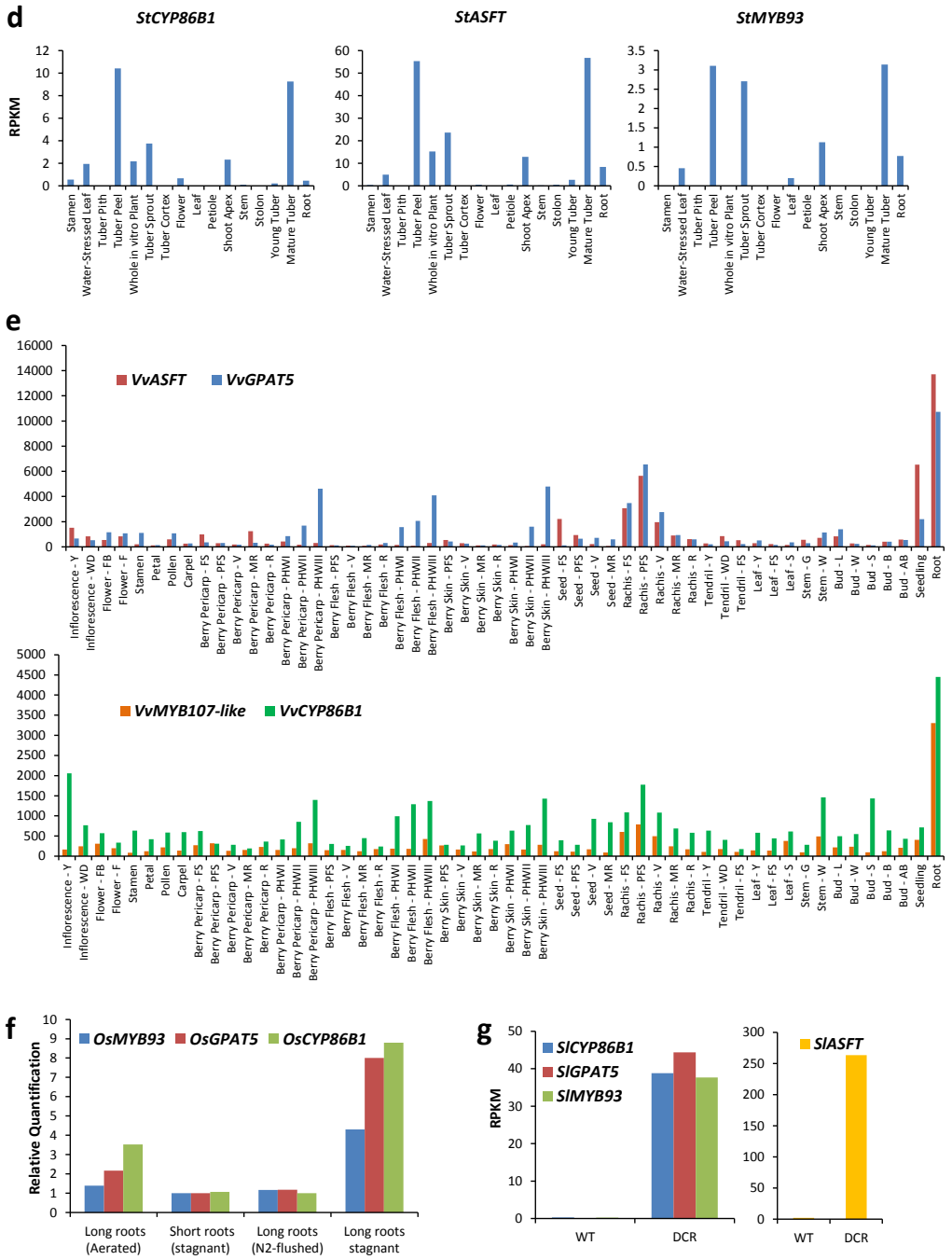

Supplementary Figure 9 (*cont.*). Expression patterns of the co-expression 'baits' and the described MYB factors. Data was extracted from the relevant large scale expression experiments used in this work to perform the multi gene co-expression analysis. Data is shown for (**a**) tomato[33], (**b**) apple (See Supplementary Dataset 2), (**c**) *Arabidopsis*[31], (**d**) potato[34], (**e**) grape[32], (**f**) rice[35] and (**g**) *SlDCR*-RNAi tomato (See Supplementary Dataset 1). For full descriptions of samples see the referenced works.

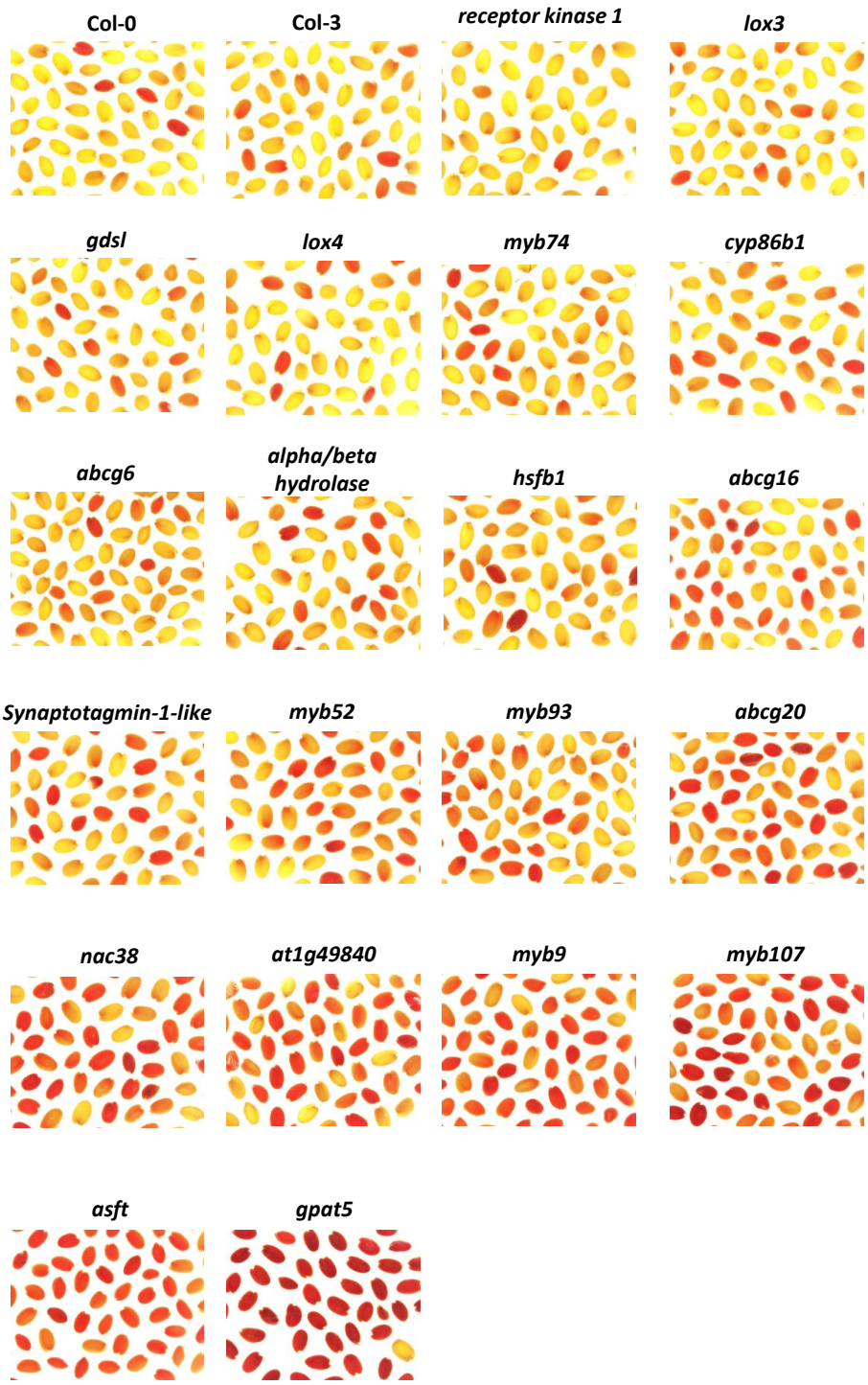

Supplementary Figure 10. Tetrazolium chloride staining assay. Tetrazolium chloride staining of *Arabidopsis* seeds from T-DNA insertion lines. Increase in red staining results from seed permeability. See Supplementary Table 4 for accessions.

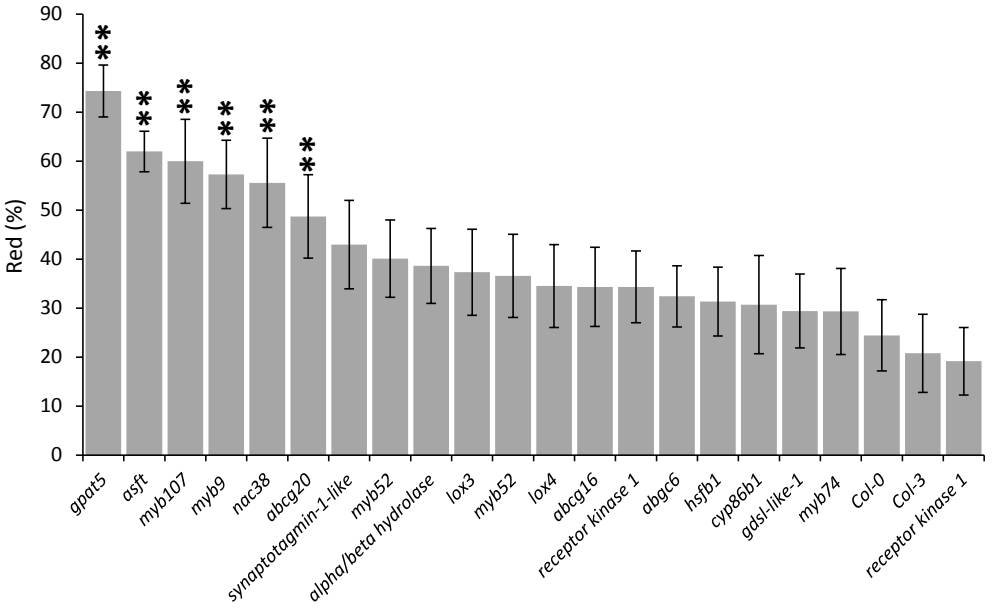

Supplementary Figure 11. Quantification of stain intensity in tetrazolium chloride staining assay. Data from images collected in Supplementary Figure 10 was quantified as a measure of red spectrum intensity. Significant increase in staining intensity is marked with ** (p-value < 0.005).

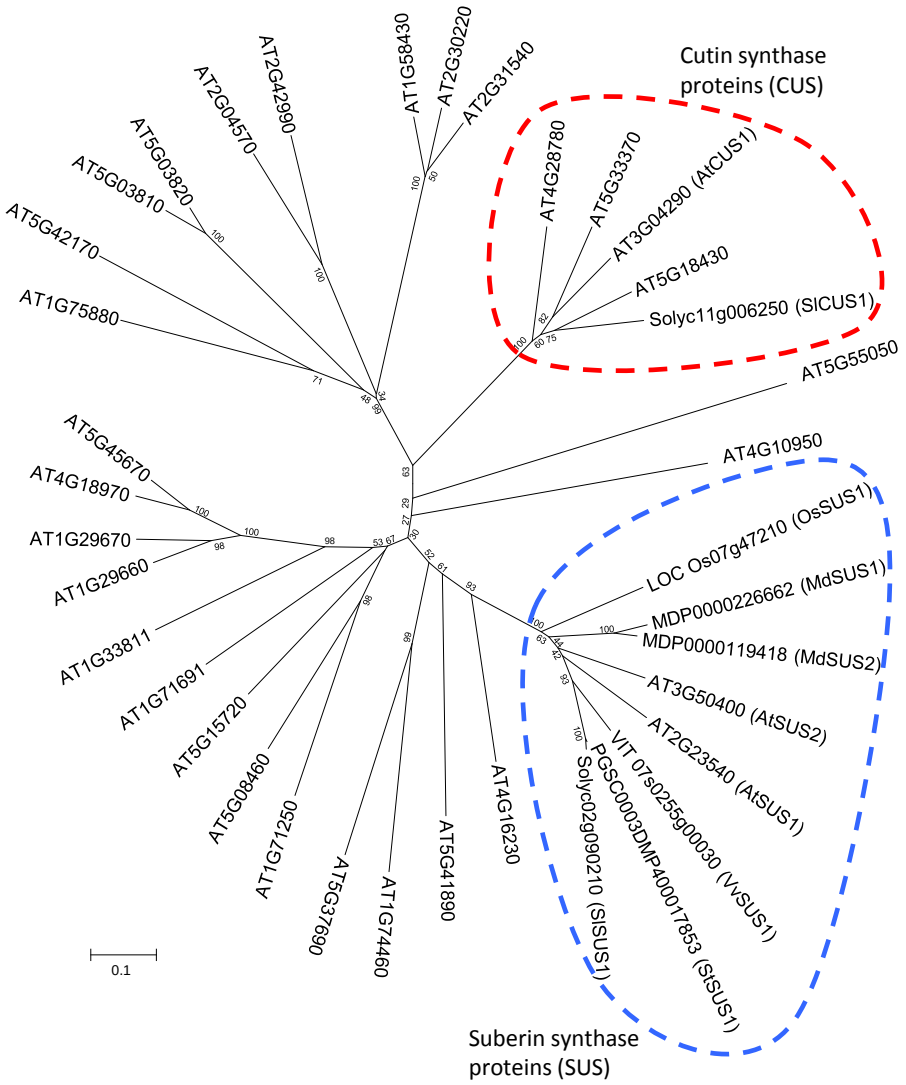

Supplementary Figure 12. Molecular phylogenetic analysis of cutin synthase (CUS) and suberin synthase (SUS) proteins. GDSL-motif esterases from *Arabidopsis* with the CUS clade highlighted. The proposed SUS clade is also shown. ClustalW and the MEGA6 software were used to align the proteins and compute the neighbor-joining tree with significance percentages (bootstrap values out of 1000). The scale bar represents the relative amino acid difference.

Supplementary Dataset 1. Supplementary Dataset 1. RNAseq analysis of mature green stage skin tissues of SlDCR-RNAi and Wild type tomato fruit. (Online resource: http://jmp.sh/vJrIUdx).

Supplementary Dataset 2. Supplementary Dataset 2. Large scale RNAseq expression analysis of skin and flesh tissue of developing apple. (Online resource: http://jmp.sh/vJrIUdx).

Supplementary Dataset 3. Genes identified in the multi-gene co-expression analysis from tomato, apple, *Arabidopsis*, potato and grape. (Online resource: http://jmp.sh/vJrIUdx).